UFES

Federal University of Espírito Santo
Department of Electrical Engineering
Electrical Engineering Postgraduate Program

Renato Santos Freire Ferraz

Optimization Approaches for Enhanced Operation and Planning of Distribution Systems: A Multi-objective Perspective

Vitória – ES

2025

Renato Santos Freire Ferraz

Optimization Approaches for Enhanced Operation and Planning of Distribution Systems: A Multi-objective Perspective

Ph.D. Thesis presented to the Electrical Engineering Postgraduate Program of the Federal University of Espírito Santo, as a requirement to obtain the degree of Doctor in Electrical Engineering in the concentration area: Energy Processing and Electrical Systems.

Advisor: Prof. Dr. Augusto César Rueda Medina

Vitória – ES

2025

Ficha catalográfica disponibilizada pelo Sistema Integrado de Bibliotecas - SIBI/UFES e elaborada pelo autor

---

Ferraz, Renato Santos Freire, 1996-
F368o Optimization approaches for enhanced operation and planning of distribution systems: a multi-objective perspective / Renato Santos Freire Ferraz. - 2025.
162 p. : il.

Orientador: Augusto César Rueda Medina.
Tese (Doutorado em Engenharia Elétrica) - Universidade Federal do Espírito Santo, Centro Tecnológico.

1. Energia elétrica - Distribuição. 2. Otimização combinatória. 3. Geração distribuida de energia elétrica. 4. Geração de energia fotovoltaica. 5. Sistemas de energia elétrica. 6. Planejamento. I. Rueda Medina, Augusto César. II. Universidade Federal do Espírito Santo. Centro Tecnológico. III. Título.

CDU: 621.3

Renato Santos Freire Ferraz

Optimization Approaches for Enhanced Operation and Planning of Distribution Systems: A Multi-objective Perspective

Ph.D. Thesis presented to the Electrical Engineering Postgraduate Program of the Federal University of Espírito Santo, as a requirement to obtain the degree of Doctor in Electrical Engineering in the concentration area: Energy Processing and Electrical Systems.

Approved on February 25th, 2025.

Prof. Dr. Augusto César Rueda Medina
Federal University of Espírito Santo

Documento assinado digitalmente
gov.br JUSSARA FARIAS FARDIN
Data: 19/03/2025 19:49:39-0300
Verifique em https://validar.iti.gov.br

Prof. Dr. Jussara Farias Fardin
Federal University of Espírito Santo

Documento assinado digitalmente
gov.br OURESTE ELIAS BATISTA
Data: 08/03/2025 07:34:38-0300
Verifique em https://validar.iti.gov.br

Prof. Dr. Oureste Elias Batista
Federal University of Espírito Santo

Prof. Dr. John Fredy Franco Baquero
São Paulo State University

Prof. Dr. Clainer Bravin Donadel
Federal Institute of Espírito Santo

Acknowledgements

First and foremost, I am deeply grateful to God, who granted me health, strength, and perseverance to overcome the challenges of this academic journey. Without His guidance and support, this achievement would not have been possible.

I extend my sincere gratitude to my advisor, Professor Augusto César Rueda Medina, for the opportunity to conduct this research and for his invaluable guidance and support throughout every stage of this work. His dedication, patience, and insightful advice were fundamental to the development of this thesis, as well as to my academic and professional growth.

To Brenda Leal Mota Santos, my life partner, who has been by my side from the admission process to the defense of this thesis, providing all the necessary support to ensure that this journey was successfully completed. Her patience, encouragement, unwavering support, and love have given me strength in the most challenging moments, and I am profoundly grateful for her presence throughout this path.

I am immensely thankful to my parents, Ana Cristina Santos Freire Ferraz and Roberto Francisco Freire Ferraz, for their unconditional love, unwavering support, and the values they have instilled in me. Their contributions to this achievement are immeasurable, and I am certain that none of this would have been possible without their constant encouragement and sacrifices. I also extend my gratitude to all my family members who, in various ways, have supported me along the way. In particular, I would like to thank my godmother, Adriana Sousa, and my aunt, Maria Edna, for always being there for me and offering their help whenever needed.

I would also like to express my heartfelt appreciation to my brother and dear friend, Rafael Santos Freire Ferraz, who was not only my classmate during my undergraduate studies but has also been a constant collaborator in all my academic projects. His intelligence, dedication, and valuable advice have been a source of inspiration and learning. His unwavering support and companionship have been essential in the development and completion of this thesis, and I am truly grateful to have him by my side throughout this journey.

Finally, this research was carried out with the support of the Fundação de Amparo à Pesquisa e Inovação do Espírito Santo (FAPES) – Brazil, through Grant 026/2021.

Abstract

Efficient planning and operation strategies are essential for modern electric power networks to ensure cost-effective electricity delivery while maintaining reliable performance. However, the ongoing transformation of traditional centralized distribution systems, driven by the integration of distributed energy resources (DERs) and the growing adoption of electric vehicles (EVs), has introduced new and complex challenges for distribution system operators (DSOs). To address these issues, this thesis proposes multi-objective optimization approaches aimed at enhancing the planning and operation of distribution networks from the DSO's perspective. The first approach focuses on the optimized allocation and sizing of DERs while ensuring recloser-fuse coordination to preserve the original network protection scheme. The second approach handles the static network reconfiguration problem, incorporating the allocation and sizing of DERs and capacitors. The third approach extends this to dynamic network reconfiguration, considering DERs, capacitors, and electric vehicle charging stations. Finally, the fourth approach explores the dynamic network reconfiguration, capacitors allocation, and on-load tap changer adjustment, while accounting for stochastic customer-owned DERs. The main objectives are to minimize investment and operational costs, improve the system's performance indicators–such as power losses and voltage deviation–and ensure the proper operation of the distribution system. Stochastic variations in DER generation, load profiles, and EV distribution throughout the day are modeled using the Monte Carlo Method. The multi-objective optimization problems are solved using the Non-dominated Sorting Genetic Algorithm II and the Multi-objective Cuckoo Search, with the final solution selected through the Fuzzy Decision-making Method. The results demonstrate significant improvements in the performance indicators of the distribution system, achieved while meeting all operational constraints.

Keywords: Capacitor, distributed energy resource, electric vehicle charging station, multi-objective optimization, network reconfiguration, radial distribution system.

Resumo

Estratégias eficientes de planejamento e operação são essenciais para as redes elétricas modernas, garantindo o fornecimento de energia de forma econômica e mantendo um desempenho confiável. No entanto, a transformação dos sistemas de distribuição centralizados tradicionais, impulsionada pela integração da geração distribuída (GD) e pela crescente adoção de veículos elétricos, introduziu novos e complexos desafios para os operadores de sistemas de distribuição. Para enfrentar esses desafios, esta tese propõe abordagens de otimização multiobjetivo voltadas para o aprimoramento do planejamento e operação das redes de distribuição sob a perspectiva dos operadores do sistema. A primeira abordagem trata da alocação e dimensionamento otimizados da GD, garantindo a coordenação entre religadores e fusíveis para preservar o esquema de proteção original da rede. A segunda abordagem resolve o problema da reconfiguração estática da rede, incorporando a alocação e o dimensionamento da GD e de bancos de capacitores. A terceira abordagem estende essa análise para a reconfiguração dinâmica da rede, considerando GD, capacitores e estações de recarga de veículos elétricos. Por fim, a quarta abordagem investiga a reconfiguração dinâmica da rede, a alocação de capacitores e o ajuste do transformador com tap sob carga, levando em conta a incerteza associada à GD instalada por consumidores. Os principais objetivos são minimizar os custos de investimento e operação, aprimorar os indicadores de desempenho do sistema–como perdas elétricas e desvio de tensão–e garantir o funcionamento adequado da rede de distribuição. As variações estocásticas da geração da GD, dos perfis de carga e da distribuição de veículos elétricos ao longo do dia são modeladas por meio do Método de Monte Carlo. Os problemas de otimização multiobjetivo são resolvidos utilizando o Algoritmo Genético de Ordenação Não Dominada II e o Método Busca do Cuco Multiobjetivo, com a solução final sendo selecionada pelo Método de Tomada de Decisão Fuzzy. Os resultados demonstram melhorias significativas nos indicadores de desempenho da rede de distribuição, garantindo o atendimento a todas as restrições operacionais.

Palavras-chave: Capacitor, geração distribuída, estação de recarga de veículos elétricos, otimização multiobjetivo, reconfiguração de rede, sistema de distribuição radial.

List of Figures

List of Tables

Nomenclature

Acronyms

CSA	Cuckoo Search Algorithm
DER	Distributed energy resource
DSO	Distribution system operator
EV	Electric vehicle
EVCS	Electric vehicle charging station
FCL	Fault current limiter
IEC	International Electrotechnical Commission
MOCS	Multi-objective Cuckoo Search
NSGA-II	Non-dominated Sorting Genetic Algorithm II
OLTC	On-load tap changer
PV	Photovoltaic
SoC	State of Charge
STC	Standard test condition
VCI	Voltage consistency indicator

Indexes

a	Objective function
f	Fault type
h	Time interval
i, j, k	Buses of the distribution system
ki, ij	Lines of the distribution system
m	Recloser
o	Lines connected downstream of bus j
s	Monte Carlo scenario

t	Fuse
v	Avaliable solution in the Pareto set approximation
z	Fault location

Matrices and vectors

$\dot{A}$	Adjacency matrix of graph $\mathcal{G}$
$\dot{B}_{ij}^{abc}$	Line current between buses i and j
$\dot{I}$	Current matrix
$\dot{I}_{inv}^{abc}$	Three-phase current vector of the inverter
$\dot{V}$	Voltage matrix
$\dot{V}_{inv}^{abc}$	Three-phase voltage vector of the inverter bus
$\dot{V}_{n}^{abc}$	Three-phase voltage vector of bus n
$\dot{V}_{n}^{pq}$	Voltage vector of bus n and phases pq
$\dot{V}_{n}^{p}$	Voltage vector of bus n and phase p
$\dot{Y}_{t}^{abc}$	Transformer admittance matrix
$\dot{Y}_{bus}$	Bus admittance matrix
$\dot{y}_{id}^{abc}$	Load admittance matrix at bus i
$\dot{y}_{ij}^{abc}$	Line admittance matrix between buses i and j
$\dot{Y}_{nn}^{abc}$	3×3 submatrix of $\dot{Y}_{bus}$ corresponding to bus n
$\dot{Z}_{l}$	Line impedance matrix
$\dot{Z}_{t}^{abc}$	Transformer impedance matrix
$\dot{z}_{ij}^{abc}$	Line impedance matrix between buses i and j

Parameters and variables

α	Significance level
$\bar{\chi}$, $\bar{\upsilon}$	Mean values of the datasets containing χ_ι and υ_ι
$\bar{x}_v$	Solutions in the Pareto front

χ_ι, υ_ι	Individual data points in the respective datasets
Δs^{dyn}	Maximum number of switching actions
ΔS_T	Sum of $\Delta S_{ja,jb,jc}$, $\forall j \in \Omega_b$
$\Delta S_{ja,jb,jc}$	Difference between the apparent power demanded by bus j and apparent power calculated using the voltage and current
δ	Coefficient related to wind speed
ε	Backward-forward Sweep iteration
η	Total number of data points in the datasets containing χ_ι and υ_ι
$\mathcal{G}$	Graph
μ	Mean of the sample
$\Phi_{f_a^v(x)}(\bar{x}_v)$	Membership function
ψ_t, λ_t	Fuse characteristic coefficients
σ	Standard deviation of the sample
σ_1, σ_2	Highest and lowest data points in the dataset, excluding any outliers
IQR	Interquartile range
$\widetilde{\Phi}_{f_a(x)}$	Level of desirability for objective function a
$\xi_{m,sm}$, $\xi_{m,fm}$, $\zeta_{m,fm}$, $\zeta_{m,fm}$	Constants according to the recloser type of curve
C^{DER}, C^{cap}, C^{OLTC}, C^{CS}	Investment cost of DER, capacitor, OLTC transformer, and EVCS
$C^{\max}$	Total available budget
C_c	Closeness centrality
CTI	Coordination time interval
ec^{DER}, ec^s	Energy cost for the DERs and substation
$f_a^v(x)$	Objective function value for solution v in the Pareto solution set
$f_a^{\max}(x)$, $f_a^{\max}(x)$	Maximum and minimum values of the objective function $f_a^v(x)$
G_h^c	Illumination intensity

gen, ite	Iteration counter of the NSGA-II and MOCS
I^{prot}	Current flowing through a protective device
$I_{h,ki}$, $I_{h,ij}$	Current flowing at time h and branches ki and ij
$I_{ij}^{\max}$	Maximum allowable branch current
I_i^p	Load current injected at bus i and phase p
$I_{ja,jb,jc}$	Load currents injected at bus j
I_{sc}^{inv}	Limit of short-circuit current of the inverter-based DER
$IF_{h,f,z}$	Short-circuit current
Ip_m	Pick-up current of recloser R_m
$Ip_m^{\min}$, $Ip_m^{\max}$	Minimum and maximum pick-up current of recloser R_m
$J_{la,lb,lc}$, $J_{oa,ob,oc}$	Currents flowing through line l and lines o
k^{PV}	Power temperature coefficient of the PV cells
n^{sample}	Sample size
$n_{\text{DER}}^{\max}$, $n_{\text{cap}}^{\max}$, $n_{\text{EVCS}}^{\max}$	Maximum allowable number of DERs, capacitors, and EVCSs
$n_{\text{EV}}^{\max}$	Number of EVs in the system
P^{STC}, G^{STC}, T^{STC}	STC output power, illumination intensity, and temperature
P_i^{rated}, S_i^{rated}	Rated active and apparent power of the DER at bus i
$P_{h,ij}$, $Q_{h,ij}$	Active and reactive power flows at time h and branch ij
$P_{h,i}^{\text{EVCS}}$	Active power consumed by the EVCS at time h and bus i
$P_{h,i}^d$, $Q_{h,i}^d$	Active and reactive power demands at time h and bus i
$P_{h,i}^s$, $Q_{h,i}^s$	Active and reactive power supplied by the substation at time h and bus i
$P_{h,i}^{\text{DER}}$, $Q_{h,i}^{\text{DER}}$	Active and reactive power generated by the DER at time h and bus i
$P_{h,i}^{PV}$	Output power of the photovoltaic system at time h and bus i
$P_{h,ki}$, $Q_{h.ki}$	Active and reactive power flows at time h and branch ki
P_h^s	Active power provided by the substation

$Pc_{h,i}^{\mathrm{DER}}$, $Qc_{h,i}^{\mathrm{DER}}$	Operating points of the DER
$Q_{h,i}^{\mathrm{cap}}$	Reactive power output of the capacitor at time h and bus i
r	Pearson correlation coefficient
$s_{h,ij}$	Binary variable representing the status of each switch
$S_{ja,jb,jc}$	Apparent power loads at bus j
T_h^c, T_h^a	Surface temperature of PV cells and environmental temperature
$T_{F_t,h,f,z}$	Operating time of the fuse
$T_{R_m,sm,h,f,z}$, $T_{R_m,fm,h,f,z}$	Operating time of the recloser in slow and fast mode
tap^{step}	Voltage adjustment per tap position
tap_h^{OLTC}	Tap position of the OLTC transformer at time h
$tap_{h,i}^{\mathrm{cap}}$	Tap position of the capacitor at time h and bus i
$TMS_{m,fm}^{\mathrm{min}}$, $TMS_{m,fm}^{\mathrm{max}}$	Minimum and maximum time multiplier setting of the recloser R_m in fast mode
$TMS_{m,sm}$, $TMS_{m,fm}$	Time multiplier setting of the recloser R_m in slow and fast mode
$TMS_{m,sm}^{\mathrm{min}}$, $TMS_{m,sm}^{\mathrm{max}}$	Minimum and maximum time multiplier setting of the recloser R_m in slow mode
V^{nom}	Nominal voltage of the distribution system
V_h^{pri}, V_h^{sec}	Voltage at the primary and secundary side of the OLTC transformer
V_i^{min}, V_i^{max}	Minimum and maximum allowable bus voltage
$V_{h,k}$, $V_{h,i}$, $V_{h,j}$	Voltage at buses k, i, and j
V_i^p	Pre-fault voltage at bus i and phase p
$V_{ja,jb,jc}$, $V_{ia,ib,ic}$	Phase voltages at buses j and i
y_{ff}	Fault admittance
y_{id}^p	Load admittance at bus i and phase p
$Y_{ja,jb,jc}$, $Y_{ia,ib,ic}$	Admittance at buses j and i

$z_{\alpha/2}$	Critical value from the standard normal distribution corresponding to the desired confidence level
z_{id}^{p}	Load impedance at bus i and phase p
Z_{ij}, R_{ij}, X_{ij}	Impedance, resistance, and reactance of branch ij
z_i, w_i, τ_i	Binary variables for the allocation of DER, capacitor, and EVCS at bus i
Z_{ki}, R_{ki}, X_{ki}	Impedance, resistance, and reactance of branch ki
$Q_{\max}^{\text{cap}}$	Total reactive power rating of the capacitor
$tap_{\max}^{\text{cap}}$	Total number of available tap positions of the capacitor
$tap_{\min}^{\text{OLTC}}$, $tap_{\max}^{\text{OLTC}}$	Lower and upper bounds of the OLTC tap position
Y_{ij}^{pq}, Y_{ii}^{pq}, Y_{ii}^{pp}, Y_{ij}^{pp}	Elements of $\dot{Y}_{bus}$ corresponding to buses i and j and phases p and q
CI	Confidence interval
VCI	Voltage consistency indicator

Sets

Ω_a	Set of objective functions
Ω_b	Set of buses in the system
Ω_o	Set of lines connected downstream of bus j
Ω_v	Set of avaliable solutions
Ω_f	Set of fault types
Ω_h	Set of time intervals
Ω_l	Set of lines in the system
Ω_m	Set of reclosers
Ω_p	Set of phases
Ω_s	Set of Monte Carlo scenarios
Ω_t	Set of fuses
Ω_z	Set of fault locations

Contents

Chapter 1

Introduction

In recent years, radial distribution systems have experienced a significant increase in the integration of distributed energy resources (DERs). This trend is driven by the growing demand for alternative energy sources that can mitigate the environmental impact associated with centralized power generation based on fossil fuels. Conventional fossil energy resources not only result in pollution and carbon dioxide emissions but also contribute to severe climatic disturbances on Earth [1]. Consequently, the traditional centralized power generation approach, based on fossil fuels, is considered unsustainable in long-term strategic plans.

To address these concerns and limitations, substantial efforts have been dedicated to promoting renewable energy sources in distribution systems. Government incentive policies and supportive regulatory frameworks have been important in facilitating the widespread integration of renewable energy sources, such as wind, solar photovoltaics (PVs), and hydropower, within distribution systems. These clean and sustainable DERs offer compelling alternatives to conventional fossil fuels, encouraging the development of environmentally sustainable and resilient energy networks.

The integration of large-scale dispersed generators provides several benefits to the network, including congestion relief, power loss reduction, voltage support, and improved power quality [2, 3]. Nevertheless, achieving these benefits requires a proper allocation and sizing of DERs along with an appropriate expansion of the network. Moreover, depending on the location and size of the DERs, the power system may not operate efficiently due to modifications in power flow directions, fault current magnitudes, and voltage profiles, which can result in adverse effects on the distribution system [1].

In addition to large-scale distributed generators, small-scale DERs have been extensively integrated into low-voltage networks by end-customers, as discussed in [4]. Although installed in low-voltage networks, they have significant impacts on medium-voltage systems, introducing challenges to operational efficiency and grid stability [1]. Consequently, effective planning and operation strategies are essential to ensure the safe and reliable integration of DERs into modern distribution networks [5]. Furthermore, the unpredictable nature of the quantity, sizes, and locations of customer-owned DERs–referred to as stochastic customer-owned DERs in this thesis–adds significant complexity to the system's planning, requiring robust methods to address their inherent uncertainty and variability.

In this context, the traditional protection scheme, which is primarily designed for con-

ventional power sources, is not optimized to accommodate the unique operating conditions and behaviors associated with DERs [6]. Therefore, it is important to evaluate and analyze the impact of DERs integration on the existing protection scheme to ensure the reliability and effectiveness of protective devices. This assessment is essential for identifying any necessary modifications or upgrades required to address potential issues and maintain the reliable operation of the network's protection system.

Furthermore, allocating and sizing capacitor banks in distribution systems, as a planning strategy, also brings benefits and challenges to the distribution systems. One of the key advantages is the power factor correction, which helps to reduce the reactive power demand and enhances the overall system efficiency. By installing capacitors at strategic locations, voltage levels can be regulated and maintained within acceptable limits, ensuring optimized performance of connected loads [7]. This leads to a reduction in power losses and improved voltage profile throughout the distribution network. Besides that, the deployment of capacitors can postpone or even eliminate the need for costly infrastructure upgrades, such as transformer replacements or conductor upgrades, by alleviating overloads and improving the overall system capacity.

In addition to the planning strategies, given by the DERs and capacitors allocation, network reconfiguration has emerged as a viable operation strategy for minimizing power losses and enhancing the performance of distribution systems. By intelligently adjusting the status of switches installed throughout the network, the topological arrangement of the distribution system can be optimized, resulting in reduced investment and operational costs. Network reconfiguration enables load balancing, alleviates overloads, and improves the voltage profile, enhancing the overall efficiency and stability of the distribution system. However, determining the optimized switch configuration that maintains a radial network structure while satisfying operational constraints poses a significant challenge due to the large number of possible network topologies. This complexity highlights the need for advanced optimization techniques and computational tools to effectively address the network reconfiguration process.

Lastly, it is important to note the rising prominence of electric vehicles (EVs) as a transportation tool due to their low impact on the environment, when compared to internal combustion engine vehicles. Consequently, the operation and planning strategies previously mentioned must account for the significant investment needed in electric vehicle charging stations (EVCSs) infrastructure to meet the growing demand for EVs. Improper EVCSs installation can have adverse effects on distribution systems, particularly with the increasing demand for EV charging. For this reason, the appropriate planning of EVCSs becomes necessary to minimize the issues caused by these devices, including line overload in the distribution system, increased power losses, and voltage regulation problems [8].

1.1 Justification for the Research

The efficient and reliable management of distribution systems is essential to ensure a sustainable and resilient energy network. Conversely, improper operation and planning can lead to various challenges that adversely impact the system's performance and reliability. Some of these problems include:

a) Voltage instabilities: Inadequate control of voltage levels can cause fluctuations in power supply and potential damage to sensitive electrical equipment.

b) Increased power losses: Improper distribution network planning may lead to overloaded lines and increased power losses, reducing the overall system's efficiency and raising operational costs.

c) Voltage regulation issues: Inadequate voltage regulation can result in high voltage deviations, leading to overvoltage or undervoltage problems.

d) Miscoordination between protective devices: The system's protection may not work as desired due to the modified load and short-circuit currents.

e) Escalating operational costs: Improper planning and operation can result in higher maintenance and repair expenses, leading to increased operational costs over time.

Based on these considerations, it can be concluded that the proper operation and planning of distribution networks are essential for ensuring the efficiency and reliability of distribution systems. Strategies that promote the integration of DERs, EVCSs, and capacitor banks, alongside network reconfiguration, can significantly enhance the system's performance while supporting the development of a sustainable and resilient grid. Furthermore, addressing the dynamic and stochastic nature of these resources is important to better prepare the system for emerging challenges and unforeseen conditions.

These strategies can be implemented through either static or dynamic approaches, each offering distinct advantages. Static methods rely on fixed operational variables, offering simplicity and ease of implementation. In contrast, dynamic strategies adjust these variables over time to reflect the system's evolving operational conditions, which is particularly advantageous given the variability in demand and DER generation throughout the day. However, the adaptability of dynamic strategies often comes with increased computational complexity, necessitating a careful evaluation of whether their benefits outweigh the additional intricacies compared to static methods.

1.2 Objectives

The main objective of this thesis is to develop operation and planning approaches considering DERs, capacitors, on-load tap changer (OLTC) transformer, and EVCSs with the

purpose of minimizing costs, voltage deviation, and power losses.

Furthermore, this thesis aims to accomplish the following specific objectives:

a) Optimize the allocation and sizing of DERs while ensuring the coordination of reclosers and fuses, to preserve the original protection scheme of the network and, consequently, avoid the need for adaptive protection schemes, application of fault current limiter (FCL) or modification of the protective device settings.

b) Develop a comprehensive framework for the simultaneous allocation and sizing of DERs and capacitors, integrated with static network reconfiguration to minimize power losses, voltage deviation, and overall costs.

c) Develop an integrated approach for the simultaneous allocation and sizing of DERs, capacitors, and EVCSs integrated with dynamic network reconfiguration to minimize power losses, voltage deviation, and overall costs.

d) Simultaneously address dynamic network reconfiguration, capacitors allocation, and dynamic adjustment of the OLTC transformer to minimize costs related to power losses and improve the system's voltage profile by minimizing a novel voltage consistency indicator (VCI).

e) Validate the optimization frameworks through case studies, ensuring robustness and applicability.

f) Achieve important insights from simulation results, providing essential guidance for optimizing electrical system operation and planning.

g) Contribute to intellectual production by authoring research papers for conferences and journals, promoting collaboration and knowledge exchange.

It is important to highlight that this thesis introduces four distinct approaches, with objectives **a**, **b**, **c**, and **d** associated with each of these approaches. Objectives **e**, **f**, and **g**, on the other hand, are considered common to all four approaches.

1.3 Contributions

Before outlining the contributions of this thesis, a brief description of the four proposed approaches is provided. Each of these approaches is independent, meaning that while they share some common elements, each formulation is distinct, and the results from one approach do not influence the others.

The first approach focuses on optimizing the allocation of DERs while ensuring recloser-fuse coordination to maintain the integrity of the original protection scheme. The second approach optimizes the allocation of DERs and capacitors in conjunction with static network reconfiguration. The third approach extends this optimization by also considering EVCSs and dynamic

network reconfiguration. Finally, the fourth approach optimizes the distribution system by dynamically reconfiguring the network, allocating and sizing capacitors, and adjusting the OLTC transformer at the substation, while accounting for DERs installed by end-customers. The main contributions of this thesis are summarized below:

a) Introduction of a novel cost-effective approach that includes the recloser-fuse coordination constraints in the formulation of the DERs allocation and sizing problem, which preserves the correct operation of the protection scheme, avoiding the need for adaptive protection schemes, the application of FCL, and the adjustment of the protective device settings considering the DERs integration in the system.

b) Proposal of an innovative approach simultaneously allocating DERs and capacitors, along with static network reconfiguration, to minimize overall cost, voltage deviation, and power losses.

c) Introduction of a novel two-stage multi-objective optimization approach for the allocation and sizing of EVCSs, DERs, and capacitors, alongside dynamic network reconfiguration. The proposed approach addresses both the planning and operation stages using a single mathematical formulation, incorporating constraints and objective functions within the same optimization model.

d) Formulation of a multi-objective planning approach simultaneously considering the dynamic reconfiguration of the network, the allocation and sizing of capacitors, and the dynamic adjustment of the OLTC transformer at the substation, incorporating stochastic customer-owned DERs.

e) Presentation of comprehensive and self-contained approaches that incorporate uncertainties and daily variations related to the generation of DERs, load fluctuations, and EVs traffic, along with the Fuzzy Decision-making Method for selecting the final solution based on the decision-maker's priorities.

f) A new metric, designated VCI, is proposed, considering not only the average deviation of voltage values from the nominal voltage but also the bounds of the voltage distribution, adjusted to exclude extreme outliers. The combination of these elements ensures that the VCI is sensitive to both average and extreme deviations, offering a more reliable evaluation of the system's performance.

g) A comparison between static and dynamic strategies is made to assess their relative performance. This comparison helps evaluate whether the added complexity of dynamic methods is justified by the improvements they offer over static approaches, particularly in the context of DERs integration.

1.4 Published Articles

The first approach undertaken in this work resulted in the publication of the following article in an international journal:

- **Ferraz, R. S. F.**; Ferraz, R. S. F.; Rueda-Medina, A. C. Multi-objective Optimization Approach for Allocation and Sizing of Distributed Energy Resources Preserving the Protection Scheme in Distribution Networks. Journal of Control, Automation and Electrical Systems, 2023 [9].

The implementation of the second approach outlined in this study led to the publication of the following article in an international journal:

- **Ferraz, R. S. F.**; Ferraz, R. S. F.; Rueda-Medina, A. C. A Comprehensive Multi-objective Optimization Framework for Balanced Distribution System Planning. Journal of Control, Automation and Electrical Systems, 2024 [10].

The third approach presented in this work resulted in the acceptance and presentation of one article at an international conference and the publication of one article in an international journal. These articles are presented as follows:

- **Ferraz, R. S. F.**; Ferraz, R. S. F.; Santos Júnior, V. F.; Rueda-Medina. Distributed Energy Resources, Capacitor Banks and Fast Charging Stations Allocation using a Multi-Objective Optimization Approach. In: Seminar on Power Electronics and Control. 2023 [11].
- **Ferraz, R. S. F.**; Ferraz, R. S. F.; Rueda-Medina, A. C. A novel two-stage multi-objective optimization strategy for enhanced network planning and operation. Electrical Engineering, 2024 [12].

The fourth approach introduced in this thesis led to the publication of the following article in an international journal:

- **Ferraz, R. S. F.**; Ferraz, R. S. F.; Santos Júnior, V. F.; Rueda-Medina, A. C. Multi-objective Approach for Distribution System Planning Considering Stochastic Customer-owned Distributed Energy Resources. IEEE Access, 2025 [13].

The research development also led to the acceptance and presentation of the following articles at an international conference:

- **Ferraz, R. S. F.**; Ferraz, R. S. F.; Rueda-Medina, A. C.; Paiva M. H. M. Power Flow and Fault analysis Using Graph Theory. In: 2021 IEEE URUCON. 2021, p. 6-11 [14].

- **Ferraz, R. S. F.**; Ferraz, R. S. F.; Rueda-Medina, A. C.; Paiva M. H. M. An Integer Linear Programming Approach for Phasor Measurement Unit Placement. In: 2021 IEEE URUCON. 2021, p. 108-112 [15].

Finally, in the course of developing this thesis, the author made contributions to the following articles:

- Ferraz, R. S. F.; **Ferraz, R. S. F.**; Rueda-Medina, A. C.; Fardin, J. F. Novel variable charging pricing strategy applied to the multi-objective planning of integrated fast and slow electric vehicle charging stations and distributed energy resources. Electric Power Systems Research, 2025 [16].
- Rueda-Medina, A. C.; Ferraz, R. S. F.; **Ferraz, R. S. F.**; Batista, O. E. A stochastic market-based clearing approach in active distribution networks by using interval optimization. Electric Power Systems Research, 2024 [17].
- Ferraz, R. S. F.; **Ferraz, R. S. F.**; Rueda-Medina, A. C.; Fardin, J. F. Integration of Slow and Fast Charging Modes in the Optimized Planning of Electric Vehicle Charging Station Using Multi-objective Optimization Approach. Journal of Control, Automation and Electrical Systems, 2024 [18].
- Ferraz, R. S. F.; **Ferraz, R. S. F.**; Rueda-Medina, A. C.; Fardin, J. F. Multi-objective Approach for Optimized Planning of Electric Vehicle Charging Stations and Distributed Energy Resources. Electrical Engineering, 2023 [19].
- Ferraz, R. S. F.; **Ferraz, R. S. F.**; Rueda-Medina, A. C.; Fardin, J. F. Multi-objective Optimization Approach for Allocation and Sizing of Distributed Energy Resources and Electric Vehicles Parking Lots with Smart Charging. Journal of Control, Automation and Electrical Systems, 2023 [20].
- Ferraz, R. S. F.; **Ferraz, R. S. F.**; Santos Júnior, V. F.; Rueda-Medina, A; Fardin, J. F. Distributed Energy Resources and Fast Charging Stations Allocation for Enhanced System Operation and Charging Infrastructure Coverage. In: Seminar on Power Electronics and Control. 2023 [21].
- Santos Júnior, V. F.; **Ferraz, R. S. F.**; Ferraz, R. S. F.; Rueda-Medina. Network Reconfiguration and Distributed Generators Allocation and Sizing Using Multi-objective Optimization Algorithms. In: Seminar on Power Electronics and Control. 2023 [22].
- Santos Júnior, V. F.; **Ferraz, R. S. F.**; Rueda-Medina. Allocation and Sizing of Distributed Generators in Distribution System Using Multi-Objective Optimization. In: Seminar on Power Electronics and Control. 2023 [23].
- Ferraz, R. S. F.; **Ferraz, R. S. F.**; Rueda-Medina, A. C.; Fardin, J. F. Multi-objective Optimization Approach for the Allocation of Fast Charging Stations and Distributed Energy Resources. In: IX Simpósio Brasileiro de Sistemas Elétricos. 2022. p. 1–7 [24].

- Ferraz, R. S. F.; **Ferraz, R. S. F.**; Rueda-Medina, A. C.; Fardin, J. F. Hybrid Model of Artificial Neural Network-Cuckoo Search for Irradiance and Load Forecasting. In: 2021 IEEE URUCON. 2021. p. 132-137 [25].
- Ferraz, R. S. F.; **Ferraz, R. S. F.**; Rueda-Medina, A. C.; Fardin, J. F.; Gomes, A. C. Optimized Allocation and Sizing of Distributed Energy Resource in Distribution Systems using Cuckoo Search Algorithm. In: XIX Conferência de Estudos em Engenharia Elétrica. 2021. p. 1–6 [26].

1.5 Outline of the Report

This thesis is divided into five chapters, organized in a similar manner to the research development. Initially, in this introductory chapter (Chapter 1), the contextualization of the topic, the main motivations and justifications for the development of this work, the general and specific objectives, and the main contributions of the study were presented.

Chapter 2 provides a comprehensive analysis of the existing research in this thesis' area, highlighting the main findings, methodologies, and results. It presents a literature review focusing on six aspects: protection schemes considering DERs integration; allocation of DERs and capacitors; allocation of EVCSs, operation of OLTC transformer, network reconfiguration, and planning of distribution system considering customer-owned DERs.

Chapter 3 presents a theory framework including concepts, methods, and algorithms that form the basis of the research outlined in this thesis. It discusses essential topics, including techniques for solving power flow equations and calculating short-circuit currents in the presence of DERs, as well as multi-objective optimization and a decision-making method. The chapter further presents the Monte Carlo Method, fundamental concepts of graph theory, and the Pearson correlation coefficient. Additionally, it includes a brief overview of the network reconfiguration process.

Chapter 4 details the mathematical formulation, methodology, and results of the four approaches proposed in this thesis. Although the approaches are related, they are independent, meaning the results of one do not influence the others. Since this thesis involves numerous variables and equations, each section presenting an optimization problem redefines the variables, even if they have been previously introduced. It is important to emphasize, however, that each variable retains a consistent meaning throughout the thesis; no variable is redefined with a different interpretation in another section. This strategy has been adopted to enhance readability and maintain clarity while ensuring consistency across the text.

Finally, Chapter 5 summarizes the main conclusions derived from the results and discusses potential directions for future work.

Chapter 2

Literature Review

Firstly, in the systematic literature review, it is essential to clearly define certain aspects of the research. As outlined in the introductory chapter (Chapter 1), four approaches have been proposed to enhance the operation and planning of distribution systems using multi-objective optimization algorithms. These approaches encompass six main topics, which are fundamental to understanding the development and contributions of this thesis. These topics are as follows:

- **Topic 1**: Planning and operation of distribution systems with a focus on protection schemes that account for the integration of DERs.
- **Topic 2**: Planning and operation of distribution systems considering the allocation and sizing of DERs and/or capacitor.
- **Topic 3**: Planning and operation of distribution systems involving the allocation and sizing of EVCSs alongside optimized DER integration.
- **Topic 4**: Planning and operation of distribution systems considering the adjustment of OLTC transformers.
- **Topic 5**: Planning and operation of distribution systems incorporating static or dynamic network reconfiguration.
- **Topic 6**: Planning and operation of distribution systems considering customer-owned DER.

To explore the six topics outlined, the following search platforms and digital libraries are utilized. These platforms have been selected for their critical importance in providing access to high-quality and peer-reviewed journals and conference proceedings. Leveraging these platforms ensures adherence to stringent criteria for identifying reputable and impactful publications, contributing to the advancement of knowledge in the field.

- IEEE Xplore.
- MDPI.
- ScienceDirect.
- Wiley Online Library.
- Springer Nature Link.

Journal available in these platforms with an impact factor exceeding one, as recorded on the date of article access, are deemed eligible. In the absence of journal articles on a specific topic, conference papers are considered as an alternative. The following national (Brazilian) conferences are eligible for sourcing articles:

- Brazilian Congress of Power Electronics *(Congresso Brasileiro de Eletrônica de Potência, COBEP)*.
- Brazilian Congress of Solar Energy *(Congresso Brasileiro de Energia Solar, CBENS)*.
- Brazilian Congress of Automation *(Congresso Brasileiro de Automática, CBA)*.
- Brazilian Conference on Electric Power Quality *(Conferência Brasileira sobre Qualidade da Energia Elétrica, CBQEE)*.
- Brazilian Symposium on Intelligent Automation *(Simpósio Brasileiro de Automação Inteligente, SBAI)*.
- Brazilian Symposium on Electrical Systems *(Simpósio Brasileiro de Sistemas Elétricos, SBSE)*.

The international conferences eligible for sourcing articles are as follows:

- IEEE International Conference on Electrical Machines and Systems (ICEMS).
- IEEE PES General Meeting.
- IEEE PES Innovative Smart Grid Technologies (ISGT).
- International Conference on Control, Decision and Information Technologies (CoDIT).
- International Conference on Electrical, Computer and Energy Technologies (ICECET).
- International Conference on Frontiers of Energy and Environment Engineering (CFEEE)
- International Conference on Intelligent System Application to Power Systems (ISAP).
- International Conference on Power Electronics, Intelligent Control and Energy Systems (ICPEICES).
- International Conference on Power Systems (ICPS).
- Power Systems Computation Conference (PSCC).
- Seminar on Power Electronics and Control (SEPOC).
- URUCON.
- Workshop on Communication Networks and Power Systems (WCNPS).

Furthermore, the search terms used during the literature review are presented below for each of the previously mentioned topics. It is worth noting that the search process followed

the order in which the terms are listed, starting with more restrictive searches and gradually expanding to broader ones.

- **Search terms for topic 1:** Protection coordination distributed energy resource; Protection scheme distributed energy resource; Adaptive protection distributed energy resource; Fault current limiter distributed energy resource.
- **Search terms for topic 2:** Distributed energy resource capacitor allocation; Multi-objective optimization distributed energy resource capacitor; Optimization distributed energy resource capacitor; Distributed energy resource allocation; Capacitor allocation.
- **Search terms for topic 3:** Electric vehicle charging station distributed energy resource allocation; Optimization electric vehicle charging station distributed energy resource; Electric vehicle charging station distributed energy resource; Fast charging station distributed energy resource.
- **Search terms for topic 4:** On-load tap changer transformer optimization; On-load tap changer operation; On-load tap changer transformer distribution system.
- **Search terms for Topic 5:** Optimization network reconfiguration; Optimization static network reconfiguration; Optimization dynamic network reconfiguration; Comparison static dynamic network reconfiguration.
- **Search terms for topic 6:** Customer-owned distributed energy resource; non-utility distributed energy resource; Low voltage distributed energy resource; Distributed energy resource non-optimal location.

To ensure the relevance of the systematic literature review, clear selection and elimination criteria are defined. These criteria guide the identification and evaluation of articles across the previously mentioned platforms and conferences. The process is given as follows:

1. **Initial screening**: Articles are first screened based on their titles, abstracts, and keywords. Studies that explicitly aligned with the defined topics are selected for further evaluation.
2. **Eligibility criteria**:
    - Articles must be published in journals with an impact factor greater than one, as recorded on the date of access.
    - Conference articles must originate from the eligible national and international conferences previously outlined.
    - Publications must be written in English or Portuguese, ensuring accessibility and comprehension.
    - Articles must have been published or presented within the last five years, counting from the start year of this research (2020).

3. **Exclusion criteria**:
    - Articles outside the scope of the six topics are excluded.
    - Duplicates across platforms or conferences are removed.
    - Studies lacking sufficient methodological detail, validation results, or peer-reviewed status are discarded.
4. **Full-text assessment**: For articles that passed the initial screening, a full-text assessment is conducted to evaluate their methodologies, results, and relevance to the research objectives.
5. **Final inclusion**: Articles that met all eligibility criteria and demonstrated a significant contribution to the understanding or advancement of the outlined topics are included in the final literature review.

Based on the previously defined criteria, including the selection and exclusion criteria for articles, a total of 66 studies were chosen to compose the literature review. These references are listed in [1–3, 6, 27–88] and are discussed in detail in Sections 2.1–2.6.

2.1 Articles Related to Topic 1

Currently, it is possible to notice the high integration of inverter-based DERs in distribution systems, which promotes several benefits in the network. Nevertheless, depending on the DER's location and size, the power system protection may not operate as desired, due to the modified load and short-circuit currents of the system [6]. For this reason, some studies have been carried out to evaluate the impacts caused by the DER integration in the protection schemes [1, 6, 27]. From the review performed in these papers, it is possible to notice that many methodologies have been proposed to mitigate the problems of the DERs on the power systems, with emphasis on the adaptive protection schemes, the application of FCLs, and the adjustment of the protective device settings considering the DER integration in the distribution system.

Adaptive protection consists of the modification of protective settings to address changes in the network through external control signals. In [28], a novel adaptive digital relaying scheme was introduced for distribution systems incorporating DERs to prevent miscoordination between recloser and fuse devices. The study conducted experiments on an Indian network, and the results indicated that the proposed scheme effectively ensures the appropriate coordination between the fuse and recloser for all fault types.

In [29], an adaptive protection scheme utilizing the Differential Evolution Algorithm was implemented to mitigate the impact of DERs on the coordination of directional overcurrent relays, while enhancing the overall sensitivity of the relays. The effectiveness of the proposed protection scheme was evaluated using interconnected 6-bus and IEEE 14-bus systems. The results demonstrated the ability of the adaptive scheme to effectively address the challenges

posed by DER integration, ensuring proper relay coordination and improved sensitivity in the presence of DERs.

A novel online adaptive protection coordination scheme was introduced in [30], employing numerical directional overcurrent relays within the IEEE 14-bus system. The scheme utilized A Mathematical Programming Language based on Interior Point Optimization solver to address the optimization problem associated with protection coordination. By dynamically adjusting the relay settings based on real-time system conditions, the proposed scheme aimed to enhance the coordination and performance of the protection system, even in the presence of DERs.

In [31], an adaptive protection scheme based on overcurrent relays was proposed to ensure the accurate operation of protective devices in the presence of multiple fault locations and types. The scheme aimed to dynamically adjust the settings of the overcurrent relays in response to changes in fault conditions, allowing for improved coordination and responsiveness. One notable feature of the proposed scheme is its local implementation within the relay, which enables autonomous operation and reduces the reliance on centralized control systems. The effectiveness of the scheme was assessed through tests conducted in a 15-bus distribution system with PV generators.

A centralized adaptive protection scheme was introduced in [32] to ensure the proper operation of protective devices under different operating conditions in distribution systems. The scheme aimed to provide optimized relay settings that adapt to the varying operating conditions of the DERs and the distribution system, resulting in fast, comprehensive, and self-adaptive protection. The results obtained from tests conducted on the IEEE 37-bus test feeder demonstrated the effectiveness of the proposed scheme in achieving optimized relay coordination for several operating conditions.

In [33], a superconductor device, known as FCL, was utilized to limit the magnitude of current during faults in distribution systems with high integration of DERs. The study focused on restoring the coordination between protective devices by allocating FCLs using the Multi-objective Particle Swarm Optimization. The proposed methodology was tested and evaluated on a modified 69-bus test system.

A Multi-objective Improved Bat Algorithm was adopted in [34] to allocate FCL devices. The objective was to simultaneously reduce costs and mitigate the effects of fault currents in power distribution systems. The study conducted experiments using both the 30 and 33-bus test systems to evaluate the performance of the proposed methodology. The results evidenced the higher efficiency of the Multi-objective Improved Bat Algorithm in finding optimized solutions for FCL allocation.

In [35], FCLs in conjunction with DERs were adopted to mitigate the negative effects of the DERs integration. The study proposed a comprehensive approach that employed the Non-dominated Sorting Genetic Algorithm II (NSGA-II) to determine the optimized location

and size of DERs, as well as the optimized size of FCLs. By strategically allocating DERs within the distribution network, the study achieved a significant reduction in the required size of FCLs. The effectiveness of the proposed approach was validated through experiments conducted on both the 33 and 69-bus test systems.

A novel framework was presented in [36] to address the simultaneous optimization of power quality and protection coordination in a microgrid incorporating DERs. The study proposed an approach that used Genetic Algorithms and Fuzzy optimization techniques to determine the optimized time and current settings of the overcurrent relays, in addition to the characteristics of the solid-state unidirectional FCL. By leveraging these optimization techniques, the framework aimed to enhance both the power quality and the coordination of protective devices within the microgrid.

In [37], an optimized allocation approach for different types of DERs in conjunction with FCLs was proposed. The study utilized a two-stage approach, combining the Coyote Optimization Algorithm and the Electrical Transient Analyzer program, to evaluate the system performance under normal and fault operating conditions. A Fuzzy-based multi-objective formulation was developed to enhance the distribution system performance in both scenarios. The proposed methodology was validated on the 33 and 69-bus test systems, as well as the Egyptian East Delta distribution network. The results presented significant improvements in power losses and fault level reduction.

Cuckoo Search Algorithm (CSA) and Linear Programming were combined in [38] as a new hybrid CSA-Linear Programming optimization algorithm in order to optimize the protection coordination of directional overcurrent relays in microgrids and find the optimized size of FCL at the point of common coupling. The proposed algorithm was applied to both the Canadian distribution benchmark and a modified IEEE 14-bus network. From the results, it was possible to conclude that the CSA-Linear Programming algorithm offers improved computational efficiency compared to Particle Swarm Optimization and Genetic Algorithm in terms of speed and total operating time of directional overcurrent relays.

In [39], the authors conducted a study focused on optimizing the size and location of DERs in a distribution feeder to reduce investment and operation costs. They also optimized the coordination between reclosers and fuses to minimize the actuation time of these protective devices under several operating conditions, including generation and load variations and different fault types. The study employed Genetic Algorithms as the optimization method and evaluated the proposed methodology using the IEEE 34-bus test feeder.

An offline solution was proposed in [40] to ensure the proper coordination of overcurrent relays for any penetration and location of DERs. By analyzing the conventional protection performance under different PV penetration levels and locations, the worst mis-coordination cases were identified. The characteristic curve of the backup relay was modified according to

relay standards to maintain coordination in all worst-case scenarios. The proposed methodology was applied to a practical power distribution network with multiple small-scale PV systems.

A multi-objective approach, based on NSGA-II, was adopted in [41] to obtain the optimized coordination of protective devices, through the minimization of the investment and power interruption costs. The operational constraints are based on practical rules of distribution companies and international technical standards, aiming to achieve coordination and selectivity of the protection devices installed in the network. The study utilized a real 135-bus system to evaluate the proposed approach.

In [42], an optimal recloser and fuse coordination scheme was proposed for distribution systems with DERs, utilizing the Interior Point Method. The scheme aimed to determine a single set of recloser and fuse settings that could effectively coordinate their operations, regardless of the presence of DERs in the system. The proposed approach was tested on the 33-bus test system, demonstrating its effectiveness in achieving proper coordination of protective devices.

An optimized and single protection scheme, based on overcurrent relays, was introduced in [43] for a microgrid to ensure effective handling of all operating modes and phase faults. The objective of the scheme was to minimize the operation time of the overcurrent relays. The protection scheme was developed using the Differential Evolution Algorithm and evaluated using the IEEE 9-bus test system.

The reviewed studies underscore the significant challenges posed by the integration of DERs into distribution systems, particularly concerning protection coordination. While these challenges arise primarily due to the variability in DER size, location, and penetration levels, the proposed methodologies, demonstrate promising solutions. By leveraging advanced optimization algorithms and probabilistic approaches, these methodologies ensure enhanced protection reliability and system performance under varying operating conditions. The findings emphasize the importance of adopting innovative and adaptable strategies to address the complexities introduced by DERs in modern distribution networks.

2.2 Articles Related to Topic 2

In recent years, the installation of DERs and capacitor banks within distribution systems has become increasingly prominent. The integration of these devices aims to address various challenges encountered by distribution system operators (DSOs), including congestion relief, reduction of power losses, voltage support, and enhancement of power quality [2, 3, 39]. By leveraging the capabilities of DERs and capacitors, DSOs can effectively mitigate these challenges, leading to more efficient and resilient network operation. Unlike the previous section, which placed emphasis on optimizing protection considering DERs, this section focuses on papers that allocate DERs and/or capacitors with the purpose of primarily enhancing the distribution system's performance and reducing overall costs.

An optimization approach was introduced in [44], featuring a Modified Gradient-based Optimization algorithm for the allocation and sizing of DERs and capacitors in distribution systems. The objective of this study is to enhance the performance of radial distribution networks by minimizing the power losses. The tests were conducted on a 59-bus Cairo distribution feeder in Egypt and a 135-bus distribution feeder.

In [45], DERs and capacitors were strategically allocated in distribution systems to minimize power losses using Genetic Algorithms. The simulations in this research were performed within a daily planning framework, considering the 24-hour load and generation curves. Furthermore, the study took into account the uncertainties associated with demand and generation by simulating many scenarios according to the hour of the day. The simulations were carried out on four distribution test feeders: IEEE 4, 13, 37, and 123-bus test feeders. Based on the results, it was possible to identify optimized zones in the test systems to properly integrate DERs and capacitors.

To optimize investment costs and reduce power losses, an enhanced Grey Wolf Algorithm was adopted in [46] for coordinated allocation of DERs, capacitor banks, and voltage regulators. The research utilized two Egyptian distribution systems as test cases to evaluate the proposed methodology. The results of the study demonstrated that significant savings could be achieved through individual allocations of capacitor banks or DERs. However, the greatest cost savings were observed when voltage regulators were simultaneously installed alongside capacitor banks and DERs to maintain an acceptable voltage profile.

In [47], a Mixed-integer Linear Programming model was proposed to determine the optimal short-term plan for distribution systems. The model considered several factors, including the siting and sizing of capacitors and DERs, conductor replacement for overloaded circuits, and allocation of voltage regulators. Additionally, the study took into account the uncertainties associated with load demand and DERs' generation; and, to evaluate the proposed approach, a 135-bus distribution system was used as a case study. The results demonstrated that the planning actions improve the efficiency of the distribution system and mitigate the pollutant emissions.

In [48], a novel approach using an Improved Manta Ray Foraging Optimizer was proposed for the optimized placement, sizing, and selection of distributed generation units to minimize active power losses in distribution networks. The proposed algorithm combined Manta Ray Foraging Optimizer with Genetic Algorithm to enhance global search capabilities. The method was evaluated using the 33 and 69-bus test systems, achieving substantial reductions in power losses, which demonstrated its effectiveness in enhancing power distribution network efficiency.

In [49], the authors proposed an effective approach combining distribution network reconfiguration with the allocation of DERs to reduce power losses under variable load conditions. The proposed model was simulated by A Mathematical Programming Language considering test

systems with 7, 12, 16, 28, 30, 33, and 49 buses, demonstrating its capability to minimize losses and improve the operational efficiency of distribution networks.

A multi-objective planning model for DERs was proposed in [50], aiming to balance carbon emissions and economic costs, which include both investment and operation stages. A novel Enhanced Adaptive Weighted-Sum Algorithm was introduced to generate an informative Pareto front, outperforming classical methods in effectiveness. The model evaluated the impacts of penetration levels of PV units and incorporated reactive power support to reduce power losses while accounting for carbon emissions. The methodology was tested on the 33, 69, and 141-bus systems, demonstrating satisfactory performance and convergence.

In [51], a short-term planning methodology was introduced for the allocation of DERs, capacitor banks, and protective devices, while incorporating branch reconductoring to optimize medium-voltage distribution networks. The study employed the NSGA-II to minimize multiple objectives, including investment costs, power losses, and non-supplied energy, along with improvements in system reliability. The proposed methodology was validated on a 135-bus distribution system, demonstrating its effectiveness in addressing these objectives.

In [52], the authors proposed a multi-objective optimization approach for the optimized allocation of DERs, capacitor banks, and FCL reactors in distribution feeders. The optimization aimed to minimize the short-circuit current, active power losses, and harmonic distortion rate. A Multi-objective Gray Wolf Optimization algorithm was employed to solve the problem, with its performance evaluated on the IEEE 13, 34, and 123-bus test systems. The results highlighted the efficiency of the proposed approach in achieving simultaneous reductions in the targeted parameters.

The reviewed studies highlight the growing importance of integrating DERs and capacitor banks into distribution systems to enhance network performance and efficiency. Through various optimization techniques, including metaheuristic algorithms, mathematical programming, and novel hybrid approaches, significant advancements have been achieved in minimizing power losses, improving voltage profile, and optimizing investment costs. Additionally, the incorporation of uncertainties related to load and generation, as well as multi-objective frameworks addressing economic and environmental considerations, underscores the comprehensive nature of these methodologies. Collectively, these contributions provide valuable insights and practical solutions for planning and operating modern distribution systems in an increasingly decentralized energy landscape.

2.3 Articles Related to Topic 3

Recent research efforts have focused on the allocation of EVCSs within distribution systems. With the increasing adoption of EVs, it has become essential to strategically plan the installation and placement of EVCSs to meet the growing charging demands. The research in

this area contributes to the development of strategies that enable the integration of EVCSs into distribution systems, promoting a sustainable and reliable transportation infrastructure.

A novel methodology for the optimized planning of EVCSs in conjunction with capacitors was presented in [53]. The Dragonfly Algorithm was employed for congestion management and reactive power compensation. The efficacy of this technique was evaluated on a modified IEEE 34-bus distribution network. Furthermore, the optimization algorithm was compared with the Biogeography-based Optimization and Particle Swarm Optimization.

In [54], the authors introduced a hybrid approach employing the Eurasian Oystercatcher Optimizer and Quantum Neural Network for the concurrent allocation of EVCS and capacitors in distribution systems. The primary goal of the proposed algorithm is to regulate the capacitors to improve the voltage profile and minimize active power losses. Comparative evaluations were conducted with Particle Swarm Optimization, Wild Horse Optimizer, and Scalp Swarm Algorithm.

In [55], an innovative planning model based on Mixed-integer Nonlinear Programming was presented. The objective of this model is to optimize the allocation and sizing of EVCSs and wind-based DERs while considering the dynamic variations in load and generation throughout the day. The study takes into account the stochastic nature of EVCSs, residential EV loads, and renewable generation. The results demonstrated the effectiveness of the proposed planning framework in strategically siting and sizing EVCSs and DERs, leading to several benefits, such as, maximizing profit, minimizing power losses, and deferring the need for distribution network upgrades.

A framework for the simultaneous planning of EVCSs and distribution network reconfiguration was proposed in [56] considering uncertainties of distribution system, EVCS load, and electricity price. The research used a Cooperative Coevolutionary Genetic Algorithm to minimize the initial investment and power loss costs. The tests conducted on the 33-bus test system demonstrated that the proposed scenario-based approach provides a more accurate solution compared to deterministic methods.

In [57], a Generalized Benders Decomposition Algorithm was employed to optimize the allocation and sizing of DERs and EVCSs in a distribution system consisting of 14 buses. This research considered the inherent uncertainty of future scenarios by incorporating a significant number of typical load, traffic flow, and PV generation curves. The numerical experiments conducted in the study revealed several benefits of investing in DERs with EVCSs. These benefits include the reduction of costs, promotion of renewable power integration, and alleviation of power congestion within the distribution system. Furthermore, the study highlighted that these benefits become more prominent when utilizing DER with reactive power control.

In [58], the authors proposed a methodology for the optimal placement of fast charging stations alongside solar-based distributed generators to address the challenges of increased energy

demand. The approach aimed to minimize power losses, reduce investment costs, and enhance system reliability. Six case studies were conducted to evaluate the impact of deploying fast charging stations with and without the integration of distributed generators. The methodology was tested on the Unified Egyptian Network with 30 buses, demonstrating the benefits of integrating renewable energy sources to support charging station deployment and improve distribution system performance.

A two-stage optimization approach was developed in [59] for the allocation of EVCSs in distribution networks, integrating electrical and road constraints. The first stage simulates the stochastic demand of EVs, incorporating uncertainties related to travel patterns and charging behavior. The second stage formulates a multi-objective optimization problem to minimize power losses, voltage deviation, and improve the system's reliability. The Galaxy Gravity Optimization technique was employed to solve the problem, with tests conducted on a 25-node transportation network connected to the 69-bus distribution system. The methodology illustrated the influence of charging station placement on reliability, power losses, and voltage profiles.

In [60], a hybrid Genetic Algorithm and Particle Swarm Optimization was proposed to allocate plug-in EVCSs within a distribution network integrated with DER. The study focused on the placement of PV systems, considering several penetration levels. The multi-objective optimization problem aimed to minimize both active and reactive power losses, as well as voltage deviation. The methodology was tested on the 33 and 69-bus distribution networks, demonstrating the effectiveness of the hybrid approach in ensuring voltage stability and improving the system's performance with the integration of EVCSs and DERs.

A planning framework was proposed in [61] to optimize the deployment of storage systems, EVs, and DERs within distribution networks. The study utilized a Genetic Algorithm-based Artificial Intelligence approach to identify the optimized locations for these resources, aiming to minimize power losses and incorporate peak load shaving strategies. The model considered both technical and operational constraints of the resources and the grid. The optimization approach was tested on the IEEE 34-bus distribution feeder.

The reviewed studies emphasize the importance of adopting advanced strategies for the allocation and sizing of EVCSs to address the growing demand for EV charging while maintaining the efficiency and reliability of distribution systems. These investigations highlight how optimization techniques can effectively minimize costs, mitigate power losses, and improve voltage regulation. Moreover, the coordinated integration of DERs and capacitors with EVCSs has demonstrated significant potential to enhance the overall network's performance, offering viable solutions to the challenges associated with high EV penetration. Together, these findings underscore the need for comprehensive planning approaches to modernize distribution systems in response to the rising adoption of EVs and renewable energy sources.

2.4 Articles Related to Topic 4

The optimized adjustment of OLTC transformers has emerged as a practical and effective solution for voltage regulation in distribution systems. By dynamically modifying the transformer tap positions in response to real-time variations in load demand and DER outputs, this approach ensures that voltage levels remain within acceptable limits throughout the network. This strategy not only improves power quality and system reliability but also increases the DER hosting capacity by mitigating voltage rise issues at points of common coupling. Furthermore, optimized OLTC operation reduces the reliance on other voltage control devices, such as capacitor banks, contributing to a more efficient and cost-effective management of the distribution network.

An enhanced Moth Search Optimization technique was developed in [62] to address DER integration challenges in distribution systems. The study optimized the placement of dispatchable DERs and shunt capacitors while simultaneously adjusting OLTC transformers to minimize annual energy loss costs and voltage deviations across multiple load levels. Tested on the 33 and 118-bus systems, the model efficiently utilized existing distribution resources, yielding greater benefits at lower DER penetration levels compared to conventional planning models that overlook such resources.

In [63], the authors proposed a comprehensive approach that integrates static network reconfiguration with the optimized operation of switchable capacitors and OLTC transformer to minimize power losses in distribution systems. The study specifically considered smart PV systems installed at fixed locations, focusing on their voltage regulation capabilities and extending the analysis to multi-period operations. Simulations conducted on 33 and 123-bus systems demonstrated significant reductions in power losses compared to scenarios without voltage control. These results highlighted the effectiveness of combining smart PV reactive power dispatch with network reconfiguration.

A two-stage real-time Volt-Var control method was proposed in [64] to address challenges associated with high penetration of intermittent renewable energy in active distribution networks. The first stage hourly adjusts OLTC transformers and capacitor banks using a Mixed-integer Second-order Cone Programming approach. The second stage employs a Multi-agent Deep Reinforcement Learning Method to dynamically regulate PV reactive power, mitigating fast voltage fluctuations. Tested on the 33-bus test system, the proposed approach effectively minimized power losses and enhanced voltage regulation.

In [65], a Bi-graph Neural Network modeling-based Deep Reinforcement Learning framework was proposed for the real-time coordination of dynamic network reconfiguration and Volt-Var control in active distribution networks. The Volt-Var control strategies involve the operation of capacitors and OLTC transformers. With the increasing integration of renewable energy sources, these techniques are becoming important for ensuring the secure and economic operation of distribution systems. The approach was tested on the modified 33 and 69-bus

systems, demonstrating its ability to effectively manage switching and tapping actions while reducing maintenance costs.

In [66], a two-stage voltage control scheme was proposed to coordinate OLTC transformer, capacitor banks, and DERs in distribution networks. The first stage optimizes OLTC tap positions using a Micro Genetic Algorithm, while the second stage applies a Recursive Genetic Algorithm to minimize power losses and optimize reactive power. The scheme, tested on the IEEE 37-node feeder with PV, wind, and dispatchable DERs, effectively addressed voltage regulation challenges caused by increasing DER integration.

A two-stage optimization strategy for Volt-Var coordination in distribution networks was proposed in [67] to address the challenges of renewable energy integration. The first stage addresses network reconfiguration to minimize power losses, using a Particle Swarm Optimization algorithm. The second stage optimizes the operation of capacitors and OLTC transformers to reduce voltage deviation and power losses. The approach was validated on the 33-bus test system, proving its effectiveness in improving the distribution network's performance under renewable energy variability.

In summary, the optimization of the OLTC transformer operation is important to ensure efficient voltage regulation and improve the overall performance of distribution systems. By dynamically adjusting tap positions in response to varying load and generation conditions, OLTC transformers help mitigate voltage deviations, reduce power losses, and increase the DER hosting capacity. Many studies explore the integration of OLTC transformers with other voltage control strategies, such as capacitor banks and DERs, to further enhance the system's reliability and economic performance. These advancements underscore the growing importance of advanced control strategies in managing increasingly complex distribution networks, particularly as the integration of DERs continues to rise.

2.5 Articles Related to Topic 5

Network reconfiguration has been the subject of extensive research in recent years, given its significant contribution in reducing power losses, improving voltage profile, and achieving load balancing within distribution systems [68]. The process of network reconfiguration involves intelligently adjusting the status of switches installed throughout the network to optimize the topological arrangement of the distribution system. These investigations aim to develop advanced optimization techniques and computational tools that can effectively address the complex task of determining the optimal switch configuration while maintaining a radial network structure and satisfying operational constraints.

A new approach was proposed in [69] to allocate and size DERs considering the distribution system reconfiguration. The Electromagnetism-like Mechanism was adopted to minimize the power loss and enhance the voltage stability. In this study, a novel encoding and decoding method

was presented to ensure the radial nature of the network. The effectiveness of the proposed methodology was demonstrated using the 33 and 69-bus test systems.

In [70], the authors utilized an Enhanced Marine Predators Algorithm for the concurrent tasks of distribution system reconfiguration and DERs allocation. The proposed algorithm was tested on both the 33-bus test system and a large-scale 137-bus distribution system, considering three distinct loading conditions. The primary objective of this study is to minimize power losses and enhance the voltage profile of the system. In [71], the Improved Heap-based Optimizer was adopted for a similar purpose, considering the 33-bus test system, the 59-bus Cairo distribution system, and the 84-bus Taiwan Power Company.

A Mixed Particle Swarm Optimization algorithm was applied in [72] to simultaneously optimize the network reconfiguration and DERs in distribution systems. The objective of the optimization approach was to minimize the active power losses. The proposed methodology was tested on both the 33 and 69-bus test systems. The results demonstrated that the application of the Mixed Particle Swarm Optimization promoted a significant reduction in power losses and an improvement in the voltage profile of the distribution network.

In [73], the Firefly Optimization Algorithm was used to simultaneously optimize network reconfiguration and DERs allocation in distribution systems. The objective is to minimize power losses and enhance reliability, considering the intermittent nature of DERs and load profiles. The results achieved on the 33-bus test system demonstrated significant cost reductions and improved voltage profiles through coordinated network reconfiguration and DERs allocation.

Grey Wolf Optimization technique was used in [74] to solve the problem of DERs allocation and static network reconfiguration, with an emphasis on minimizing power losses. To address the multi-objective nature of the problem, a weighted sum strategy was adopted to transform it into a single-objective optimization problem. The effectiveness of the proposed methodology was evaluated through case studies conducted on the 33-bus test system. The outcomes of the study emphasized the positive impact of network reconfiguration when combined with the optimized placement of DERs on enhancing the voltage stability margin of the system.

In [75], Mixed-integer Second-order Cone Programming formulation was employed to allocate capacitor banks and reconfigure the distribution network with the objective of minimizing the overall costs. The approach presented in this paper includes a voltage-dependent load representation, as well as a representation of the operation of capacitor banks, which is also voltage-dependent. The tests were performed using the 69-bus test system and a real 2313-bus distribution system.

In [76], the authors tackle the optimization, control, and operation of distribution systems by simultaneously addressing network reconfiguration and the allocation of DERs and capacitors. In this study, practical daily load profiles were employed to simulate the dynamic operation of automated distribution systems. To achieve these objectives, the Manta Ray Foraging Optimization

Algorithm was adopted, with evaluations conducted on the 33 and 69-bus test systems.

The Quasi-reflection-based Slime Mould Algorithm, introduced in [77], addresses the allocation of DERs and capacitors alongside network reconfiguration. It is noteworthy that this article takes into account the reactive power support provided by DERs. The effectiveness of the optimization algorithm was demonstrated through its application to distribution systems with 69, 85, and 118 buses.

In [78], a novel optimization approach called the Thief and Police Algorithm was introduced to simultaneously reconfigure the distribution system and allocate capacitors, PV generators, and wind turbine generators. The objective of this study is to minimize power losses, operational costs, and improve the voltage stability of the network. The proposed technique was evaluated using the 33-bus test system and compared with Symbiotic Organisms Search, Ant Colony Optimization, Particle Swarm Optimization, and Genetic Algorithm.

In [79], the authors proposed a novel optimization framework for the network reconfiguration problem in modern distribution networks, with the aim of minimizing power losses and enhancing the voltage profile. The article introduced a multiple-step resolution procedure, using the Harris Hawks Optimization algorithm, complemented with pre-processing and post-processing phases to improve search efficiency. The approach was validated on the 33, 85, and 295-bus test systems under varying distributed generation and load conditions. Results show that Harris Hawks Optimization algorithm outperforms other metaheuristics, such as Particle Swarm Optimization and Cuckoo Search, in minimizing power losses, improving voltage profile, and reducing computation time.

A multi-objective optimization model for network reconfiguration was proposed in [80] to improve the economic operation and power quality of distribution systems, particularly considering the fluctuating outputs from DERs and EVs. To solve this model efficiently, a Lévy Flight and Chaos Disturbed Beetle Antennae Search Algorithm was employed, which leverages grey target decision-making to enhance computational efficiency and identify optimized solutions. The study also analyzed the impact of varying EV penetration rates and charging/discharging modes on the load curve, considering uncertainties in loads and DER outputs. Simulation results on the modified 33-bus test system and the 118-bus radial distribution network demonstrated the effectiveness of the proposed method in improving operation economy, power quality, and supporting higher EV penetration in distribution systems.

In [81], a planning model for DERs in distribution networks was proposed, addressing the challenge of handling uncertainties and incorporating network reconfiguration. Using scenarios generated via Monte Carlo sampling, a chance-constrained planning model was developed. The model integrates dynamic network reconfiguration into the solution process, enhancing the performance of the distribution system compared to static reconfiguration. The Particle Swarm Optimization algorithm was employed to solve the model. Simulations were carried out on a

31-bus radial distribution network located in Tai'an City, Shandong Province, China.

In [82], a Chaotic Search Group Algorithm was proposed to solve the simultaneous network reconfiguration and DER allocation problem in radial distribution networks. The primary goal was to minimize real power losses while improving the voltage profile of the system. This optimization approach integrates a chaotic local search strategy into the standard Group Search Algorithm to enhance its search efficiency and solution quality. The methodology was tested on the 33, 69, 84, and 118-bus systems under three distinct load levels. Comparative analyses demonstrated that the Chaotic Search Group Algorithm outperformed the original Group Search Algorithm and other techniques reported in the literature, achieving superior results in reducing power losses and enhancing the voltage profile.

A novel approach was proposed in [83] to address the simultaneous optimization of network reconfiguration, capacitor placement, and DER allocation in distribution systems. This study aimed to reduce power losses, investment costs, and operational expenses while considering uncertain and dynamic load conditions. By integrating load uncertainty and dynamic variations into the optimization model, the authors demonstrated improved reliability and reduced computational time. The approach was validated on test systems with 7, 10, 12, 16, 28, and 30 buses.

The reviewed studies focus on optimizing distribution system operations through network reconfiguration. These efforts aim to minimize power losses, enhance voltage profile, and integrate renewable energy sources more effectively. Optimization techniques such as Particle Swarm Optimization, Genetic Algorithms, and Mixed-integer Programming are commonly employed to balance operational efficiency with system reliability. Furthermore, many studies consider the dynamic nature of modern loads and energy generation, highlighting the importance of adaptive reconfiguration strategies to accommodate variations in demand and renewable output. These findings underscore the potential of integrating reconfiguration and DER optimization to improve the overall distribution network's performance, supporting both economic and environmental goals.

2.6 Articles Related to Topic 6

According to the literature review presented in [4], the impacts of integrating DERs into distribution systems can be analyzed using either deterministic or stochastic approaches. Deterministic methods rely on fixed and known input data to evaluate the effects of DERs on the distribution grid. These methods assume that the size, location, and characteristics of all individual DER installations are precisely known for a given installed capacity. Conversely, stochastic methods account for the unpredictable and uncertain nature of distribution systems and DERs.

Furthermore, the authors in [4] noticed that the installation of DER in distribution

systems can take the form of either a single large installation or multiple smaller installations implemented by end-customers of the network. For a single large installation, deterministic methods are generally sufficient. However, for numerous small installations distributed across a wide geographical area, significant uncertainties arise–such as variations in size, location, and individual installation properties–rendering deterministic methods inadequate for accurately capturing the impacts of such systems.

For instance, in [84], a two-stage Volt-Var control strategy was proposed to coordinate utility-scale and customer-owned PVs for voltage regulation in active distribution networks. The optimization targets the tap position of the OLTC transformer, the step position of capacitors, and the reactive power of customer-owned DERs, assumed to be installed at fixed and predefined locations. In the first stage, a central controller performs optimal power flow based on day-ahead PV and load predictions to determine the hourly dispatch of OLTC and capacitor banks. In the second stage, the network is partitioned into zones based on PV and load types, with zone controllers, formulated using Deep Neural Networks, managing the reactive power of PV systems within each zone. Simulations on the 33-bus test system demonstrated the effectiveness of this approach in achieving voltage regulation with reduced power losses and fair participation of customers.

Additionally, a coordinated strategy integrating dynamic network reconfiguration and the allocation of switchable capacitor banks was proposed in [85] to mitigate voltage rise issues at points of common coupling caused by distributed generators. The approach features a capacitor sizing method to optimize hourly reactive power and employs a Particle Swarm Optimization algorithm to identify optimized switchable capacitor banks locations. The authors highlighted that DERs owned by customers are often not optimally located, as their installation is driven by the customer's preferences rather than the system's needs. Simulations on the 33-bus test system underscored the importance of dynamic network reconfiguration and switchable capacitor bank placement in maintaining a stable voltage profile.

It is important to notice that, while both [84] and [85] account for customer-owned DERs, they operate under the assumption that the locations of these DERs are fixed and predefined. However, this assumption deviates from real-world scenarios, where the placement and capacity of customer-installed DERs are inherently uncertain. Such unpredictability introduces significant challenges in developing and implementing effective operational strategies.

In [86], a probabilistic approach was employed to evaluate the impacts of customer-owned DER installations in distribution systems. The study incorporates various DER penetration levels and accounts for uncertainties related to their location, size, and operational behavior through Monte Carlo simulations. Additionally, residential load time-series were utilized to reflect customer behavior. Tests conducted on a real unbalanced distribution system revealed that overvoltage is the most prevalent issue associated with DER integration.

In [87], a Monte Carlo-based method was employed to evaluate the hosting capacity of customer-owned PV systems in distribution networks with high PV penetration. The approach assumes random PV locations and examines impacts such as overvoltage, undervoltage, and equipment loading. Applied to 50,000 real low-voltage systems, the analysis utilized a lognormal distribution to estimate DER hosting capacity. The findings identified overvoltage as the most critical issue. Additionally, sensitivity analyses underscored the influence of factors such as the number of PV systems, power factor, load levels, and conductor impedances on the performance of distribution systems.

A strategy combining network reconfiguration and the optimized Volt-Var curve setting of grid-tie inverters was proposed in [88] to maximize the hosting capacity of DERs and minimize power losses in distribution systems. The authors considered the stochastic nature of customer-owned DERs, where the quantity, sizes, and locations of DERs installed by end-customers are inherently unpredictable. By addressing uncertainties through the Monte Carlo Method and solving the multi-objective problem using NSGA-II, the approach was tested on the 33-bus test system utilizing Matlab and OpenDSS. The results emphasized the effectiveness of the proposed method, outperforming previous studies that addressed network reconfiguration and Volt-Var optimization separately. This underscores the importance of combining these strategies to expand the search space and, consequently, identify superior solutions.

The integration of customer-owned DERs into distribution systems introduces significant challenges due to the inherent uncertainties in their size, location, and operational behavior. While traditional methods often assume fixed and known DER characteristics, real-world scenarios involve dynamic and unpredictable factors that complicate the planning and operation of distribution networks. As a result, recent approaches have focused on probabilistic methods, such as Monte Carlo simulations, to better account for these uncertainties and assess the impacts of DERs on voltage stability and hosting capacity. Moreover, optimizing strategies that combine network reconfiguration, capacitor placement, and Volt-Var control have proven effective in addressing voltage rise issues and improving the overall system's performance. By incorporating stochastic elements into the decision-making process, these methods offer a more realistic and robust framework for managing the integration of customer-owned DERs, helping to maintain the stability and reliability of the system despite the unpredictability of DERs.

2.7 Literature Overview and Comparison

As presented in Chapter 1 of this thesis, four approaches are proposed during the course of this research. These approaches align with the six topics introduced in Chapter 2 as follows:

- Approach 1 $\rightarrow$ Topic 1.
- Approach 2 $\rightarrow$ Topics 2 and 5.
- Approach 3 $\rightarrow$ Topics 2, 3, and 5.

- Approach 4 → Topics 2, 4, 5, and 6.

To contextualize the proposed approaches within the landscape of recent research, they are compared with the studies referenced in the topics associated with each approach in Sections 2.7.1–2.7.4.

2.7.1 Approach 1: DERs Allocation Preserving the Original Protection Scheme

Table 1 provides a comparative review of the primary characteristics of the methodology introduced in Section 4.1 of this thesis, alongside the methodologies discussed in the literature review, specifically the references [28–43]. Columns 2 through 6 of Table 1 represent the following aspects, respectively:

- **Optimization**: Specifies whether the article employs multi-objective or single-objective optimization techniques.
- **DERs allocation**: Identifies whether the study includes the allocation of DERs as part of its methodology.
- **Recloser-fuse coordination**: Indicates whether the research addresses the coordination between recloser and fuse.
- **Uncertainty**: Refers to the consideration of uncertainties related to load fluctuations or renewable energy generation.
- **24-hour analysis**: Assesses whether the approach incorporates time-series or daily operational analysis to evaluate dynamic system behavior over a 24-hour period.

These aspects were chosen to highlight critical features and capabilities that distinguish different methodologies. They reflect the essential elements needed for a robust analysis of distribution systems, particularly in scenarios involving high penetration of DERs, optimization requirements, and protection challenges. By focusing on these aspects, the table ensures a clear and consistent comparison between the proposed approach and existing studies.

In [28–32], adaptive protection schemes are proposed to address the challenges arising from the integration of DERs in protection schemes. However, both online and offline adaptive protection methods have certain limitations. Online adaptive protection requires reliable and fast communication channels to update relay or recloser settings in real-time, which can be a drawback in terms of infrastructure requirements and potential communication delays. On the other hand, offline methods involve complex calculations to consider various system conditions, but they may fail to account for unexpected circumstances that may arise in real-time operation.

Table 1 – Approach 1 compared to other articles.

Article	Opt.	DERs allocation	Recloser-fuse coordination	Uncertainty	24-hour analysis
[28]	×	×	✓	×	×
[29]	SO	×	×	×	✓
[30]	SO	×	×	×	×
[31]	×	×	×	×	✓
[32]	SO	×	×	×	×
[33]	SO	×	✓	×	×
[34]	MO	×	×	✓	×
[35]	MO	✓	×	×	✓
[36]	SO	×	×	×	×
[37]	MO	✓	×	×	×
[38]	SO	×	×	×	×
[39]	SO	✓	✓	×	✓
[40]	×	×	✓	×	×
[41]	MO	×	✓	×	×
[42]	SO	×	✓	×	×
[43]	SO	×	×	×	×
Approach 1	MO	✓	✓	✓	✓

✓: Yes. ×: No. Opt.: Optimization. MO: Multi-objective optimization. SO: Single-objective optimization.

In [33–38], the mitigation of issues in protective devices' coordination is achieved using FCLs. Nevertheless, implementing FCLs in distribution systems with high DER penetration can lead to increased operating time when the DER is out of service [27]. When the DER is not in operation, the fault current tends to be lower due to reduced energy contribution from these sources. As a result, the fault current magnitude may fall below the tripping thresholds of protective devices, such as circuit breakers or relays, causing them to take longer to operate. This prolonged operating time reduces the sensitivity of the protection system, potentially leading to delayed fault detection and isolation. Furthermore, the prohibitive cost of FCL may limit the wide installation of this device in the networks.

The studies carried out in [39–43] considered the adjustment of the protective device settings after the integration of DER in the distribution system. Despite the benefits of resizing the protective devices, this method degrades the sensitivity of the protection scheme, mainly, when the DER is not operating; in addition to increasing the investment costs, through the replacement of reclosers, relays and fuses.

Furthermore, based on Table 1, it is possible to notice that most of the papers did not consider the uncertainties of the load and power generated by DERs. The stochastic characteristic of these variables interferes directly in the adjustment of protective devices. In addition, the 24-hour analysis of load and DER generation variation were not regarded in the majority of studies, which modifies the load and short-circuit current in the distribution feeder. Besides that, some studies only take the reclosers coordination into account, disregarding the coordination

of the reclosers, in fast and slow mode, with the fuses; however, it is essential to implement fuses in the problem formulation, to achieve greater protection selectivity and cost reduction. For this reason, the motivation of Approach 1 is to address certain gaps in the state of the art by adopting a multi-objective perspective for the allocation of DERs while maintaining the original recloser-fuse protection scheme. This approach considers uncertainties associated with both load and DERs generation.

2.7.2 Approach 2: Static approach for network operation and planning

Table 2 provides a comparative review of the primary characteristics of the methodology introduced in Section 4.2 of this thesis, alongside the methodologies discussed in the literature review, including references [39, 44–52, 69–82, 85, 88]. Columns 2 through 7 of Table 2 represent the following aspects:

- **Optimization**: Specifies whether the article employs multi-objective or single-objective optimization techniques.
- **DERs allocation**: Identifies whether the study includes the allocation of DERs as part of its methodology.
- **DERs' reactive power support**: Specifies whether the methodology accounts for the reactive power support provided by DERs, which is important for voltage regulation and system stability.
- **Capacitors allocation**: Identifies whether the study includes the allocation of capacitors as part of its methodology.
- **Network reconfiguration**: Highlights if the approach involves reconfiguring the distribution network to optimize its performance.
- **Uncertainty**: Refers to the consideration of uncertainties related to load fluctuations or renewable energy generation.

The selection of these aspects is justified by their importance in the evaluation and comparison of methodologies for the optimization of distribution systems. The allocation of DERs and capacitor banks, alongside network reconfiguration, is essential to enhance the efficiency and reliability of distribution systems. The inclusion of reactive power support from DERs is particularly relevant in modern networks, where these resources can provide essential ancillary services. Finally, the consideration of uncertainties is important to ensure the robustness and adaptability of the methodologies under real-world operating conditions. Together, these aspects provide a comprehensive and structured framework for comparative analysis.

Based on the comparative analysis presented in Table 2, it is evident that only a limited number of studies, such as [50–52, 80, 88], have considered the inherent multi-objective nature

Table 2 – Approach 2 compared to other articles.

Article	Opt.	DERs allocation	DERs' reactive power support	Capacitors allocation	Network reconfig.	Uncertainty
[39]	SO	✓	✓	×	×	×
[44]	SO	✓	×	✓	×	×
[45]	SO	✓	×	✓	×	✓
[46]	SO	✓	×	✓	×	×
[47]	SO	✓	✓	✓	×	✓
[48]	SO	✓	✓	✓	×	×
[49]	SO	✓	✓	×	✓	×
[50]	MO	✓	✓	×	×	✓
[51]	MO	✓	✓	✓	×	✓
[52]	MO	✓	✓	✓	×	×
[69]	SO	✓	×	×	✓	×
[70]	SO	✓	×	×	✓	×
[71]	SO	✓	×	×	✓	×
[72]	SO	✓	×	×	✓	×
[73]	SO	✓	×	×	✓	✓
[74]	SO	✓	✓	×	✓	×
[75]	SO	×	×	✓	✓	×
[76]	SO	✓	×	✓	✓	×
[77]	SO	✓	✓	✓	✓	×
[78]	SO	✓	✓	✓	✓	×
[79]	SO	×	×	×	✓	×
[80]	MO	×	×	×	✓	✓
[81]	SO	✓	×	×	✓	✓
[82]	SO	✓	✓	×	✓	×
[85]	SO	×	×	✓	✓	✓
[88]	MO	×	×	×	✓	✓
Approach 2	MO	✓	✓	✓	✓	✓

✓: Yes. ×: No. Opt.: Optimization. MO: Multi-objective optimization. SO: Single-objective optimization. Network reconfig.: Network reconfiguration.

and trade-offs involved in distribution system planning. Most of the reviewed works primarily employ single-objective optimization approaches, which may not adequately capture the complexities and conflicting objectives typical of real-world scenarios. Furthermore, while DERs have gained prominence in modern power systems, the potential of these resources to provide reactive power support–an essential ancillary services–remains unexplored in the majority of studies. Only a few references, including [39, 47–52, 74, 77, 78, 82], explicitly explored this capability. Regarding uncertainty modeling, although some works, such as [45, 47, 50, 51, 73, 80, 81, 85, 88], consider uncertainties related to load variations and the intermittent generation of DERs, many methodologies still fail to address these aspects comprehensively. Hence, the motivation behind Approach 2 is to fill some gaps in the state of the art by adopting a multi-objective perspective for DERs and capacitors allocation alongside distribution network reconfiguration, taking into account uncertainties and the reactive power support capability of DERs.

2.7.3 Approach 3: Dynamic approach for network operation and planning

Table 3 provides a comparative review of the key characteristics of the methodology presented in Section 4.3 of this thesis, in comparison with the articles discussed in the literature review, including references [39, 44–61, 69–83, 85, 88]. Columns 2 through 7 of Table 3 represent the following attributes:

- **Optimization**: Indicates whether the study adopts multi-objective or single-objective optimization techniques.
- **DERs allocation**: Refers to the inclusion of DER placement in the methodology.
- **EVCSs allocation**: Specifies whether the study considers the allocation of EVCSs.
- **Capacitors allocation**: Identifies if the approach includes the placement of capacitor banks.
- **Network reconfiguration (static and dynamic)**: Distinguishes whether static or dynamic network reconfiguration is incorporated.
- **Uncertainty**: Evaluates if the methodology addresses uncertainties in load behavior, renewable generation, or other stochastic variables.

The attributes selected for analysis are essential for evaluating the methodologies' ability to address the complex requirements of modern distribution systems. The optimization category highlights the scope of the problem-solving approach, while the inclusion of DERs, EVCSs, and capacitors reflects the ability to enhance the system's performance and reliability. The distinction between static and dynamic network reconfiguration is particularly relevant to the context of time-varying scenarios. Additionally, the consideration of uncertainty provides robustness and applicability to real-world conditions. Together, these aspects ensure a thorough and meaningful comparison.

Despite the efforts in [39, 44, 46–52, 69–83, 85, 88] to propose approaches for improving the distribution system's performance, these works did not consider planning and operation strategies for EVCSs in light of the current widespread adoption of EVs as a sustainable mode of transportation. Moreover, while some articles, including [49, 56, 69–83, 85, 88] have explored network reconfiguration, only a few studies, presented in [80, 81, 85] have implemented dynamic network reconfiguration, which adds substantial complexity to the optimization problem.

On the other hand, the simultaneous allocation of DERs, EVCSs, and capacitors has been considered exclusively in [45]. Despite the stochastic nature of the distribution system's operation and planning, only the articles in [45, 47, 50, 51, 55, 56, 73, 80, 81, 83, 85, 88] have addressed the uncertainties associated with EV user behavior, load variations, or DER generation. Additionally, multi-objective optimization methods have been employed only in [50–52, 54, 59, 80, 88], while the remaining studies either considered a single-objective framework or addressed

multiple objectives using a weighted sum approach, rather than utilizing concepts of dominance and Pareto optimality. Therefore, the motivation of Approach 3 is to address the gaps in the state of the art by proposing a comprehensive approach that takes into account all the characteristics presented in Table 3.

Table 3 – Approach 3 compared to other articles.

Article	Opt.	DERs allocation	EVCSs allocation	Capacitors allocation	Network reconfig.		Uncertainty
					Static	Dynamic	
[39]	SO	✓	×	×	×	×	×
[44]	SO	✓	×	✓	×	×	×
[45]	SO	✓	✓	✓	×	×	✓
[46]	SO	✓	×	✓	×	×	×
[47]	SO	✓	×	✓	×	×	✓
[48]	SO	✓	×	✓	×	×	×
[49]	SO	✓	×	✓	✓	×	×
[50]	MO	✓	×	×	×	×	✓
[51]	MO	✓	×	✓	×	×	✓
[52]	MO	✓	×	✓	×	×	×
[53]	SO	×	✓	✓	×	×	×
[54]	MO	×	✓	✓	×	×	×
[55]	SO	✓	✓	×	×	×	✓
[56]	SO	×	✓	×	✓	×	✓
[57]	SO	✓	✓	×	×	×	×
[58]	SO	✓	✓	×	×	×	×
[59]	MO	×	✓	✓	×	×	×
[60]	SO	✓	✓	×	×	×	×
[61]	SO	✓	✓	×	×	×	×
[69]	SO	✓	×	×	✓	×	×
[70]	SO	✓	×	×	✓	×	×
[71]	SO	✓	×	×	✓	×	×
[72]	SO	✓	×	×	✓	×	×
[73]	SO	✓	×	×	✓	×	✓
[74]	SO	✓	×	×	✓	×	×
[75]	SO	×	×	✓	✓	×	×
[76]	SO	✓	×	✓	✓	×	×
[77]	SO	✓	×	✓	✓	×	×
[78]	SO	✓	×	✓	✓	×	×
[79]	SO	×	×	×	✓	×	×
[80]	MO	×	×	×	×	✓	✓
[81]	SO	✓	×	×	×	✓	✓
[82]	SO	✓	×	✓	✓	×	×
[83]	SO	✓	×	✓	✓	×	✓
[85]	SO	×	×	✓	×	✓	✓
[88]	MO	×	×	×	✓	×	✓
Approach 3	MO	✓	✓	✓	×	✓	✓

✓: Yes. ×: No. Opt.: Optimization. MO: Multi-objective optimization. SO: Single-objective optimization. Network reconfig.: Network reconfiguration.

2.7.4 Approach 4: Network Operation and Planning Considering Stochastic Customer-owned DERs

Table 4 presents a comparative evaluation of the methodology proposed in Section 4.4 of this thesis, in relation to the articles discussed in the literature review, including references [44–52, 62–67, 69–88]. Columns 2 through 9 of Table 4 represent the following attributes:

- **Optimization**: Indicates whether the methodology applies single-objective or multi-objective optimization approaches.
- **Capacitors allocation**: Specifies whether the placement of capacitor banks is part of the approach.
- **OLTC adjustment**: Refers to the inclusion of OLTC adjustments in the methodology.
- **Customer-owned DERs**: Indicates whether the methodology incorporates customer-owned DERs in its analysis.
- **Network reconfiguration**: Identifies if reconfiguration of the network is considered.
- **Single-period vs. Multi-period analysis**: Differentiates between approaches that operate on a single-period or multi-period basis. In single-period analysis, the decision variables of the optimization problem remain constant over time. Conversely, in multi-period analysis, the decision variables can be adjusted at predefined intervals, enabling a dynamic response to temporal variations.
- **Uncertainty (load and DERs)**: Specifies whether the methodology accounts for uncertainties in load demand and DER behavior.

The selected attributes highlight the methodological distinctions and the innovative aspects of this approach. Capacitor allocation, OLTC adjustment, and network reconfiguration are important for improving the voltage profile and minimizing losses. The inclusion of customer-owned DERs emphasizes the integration of decentralized resources in modern networks by end-customers. Single-period and multi-period analyses address both static and dynamic scenarios, providing a more versatile planning framework. The explicit consideration of uncertainty in both load and DER behavior ensures the robustness and adaptability of the methodology.

Based on Table 4, the authors in [44–49, 62–66, 69–79, 81–85] adopted a single-objective framework or addressed multiple objectives using a weighted sum approach, despite the inherent multi-objective nature and trade-offs prevalent in the challenges addressed in this field. As highlighted in [89], a key strength of a posteriori methods, which leverage concepts of dominance and Pareto optimality, lies in their ability to generate the set of Pareto-optimal solutions set before presenting it to the decision-maker. This comprehensive overview enables the decision-maker to evaluate all possible solutions, facilitating a more informed and realistic selection of the most satisfactory option.

Table 4 – Approach 4 compared to other articles.

Article	Opt.	Capacitors allocation	OLTC adjustment	Customer-owned DERs	Network reconfig.	Single-period	Multi-period	Uncertainty	
								Load	DER
[44]	SO	✓	×	×	×	✓	×	×	×
[45]	SO	✓	×	×	×	×	×	✓	✓
[46]	SO	✓	×	×	×	✓	×	×	×
[47]	SO	✓	×	✓	×	✓	×	✓	✓
[48]	SO	✓	×	×	×	✓	×	×	×
[49]	SO	×	×	×	✓	×	✓	×	×
[50]	MO	×	×	×	×	×	✓	✓	✓
[51]	MO	✓	×	×	×	✓	×	✓	✓
[52]	MO	✓	×	×	×	✓	×	×	×
[62]	SO	×	✓	×	×	✓	×	×	×
[63]	SO	×	✓	×	✓	✓	×	×	×
[64]	SO	×	✓	×	×	×	✓	✓	✓
[65]	SO	×	✓	×	✓	×	✓	✓	✓
[66]	SO	×	✓	×	✓	×	✓	×	✓
[67]	MO	×	✓	×	✓	×	✓	×	✓
[69]	SO	×	×	×	✓	✓	×	×	×
[70]	SO	×	×	×	✓	×	×	×	×
[71]	SO	×	×	×	✓	✓	×	×	×
[72]	SO	×	×	×	✓	✓	×	×	×
[73]	SO	×	×	×	✓	×	✓	✓	✓
[74]	SO	×	×	×	✓	✓	×	×	×
[75]	SO	✓	×	×	✓	✓	×	×	×
[76]	SO	✓	×	×	✓	✓	×	×	×
[77]	SO	✓	×	×	✓	✓	×	×	×
[78]	SO	✓	×	×	✓	✓	×	×	×
[79]	SO	×	×	×	✓	✓	×	×	×
[80]	MO	×	×	×	✓	×	✓	✓	✓
[81]	SO	×	×	×	✓	×	✓	✓	✓
[82]	SO	×	×	×	✓	✓	×	×	×
[83]	SO	✓	×	×	✓	✓	×	✓	×
[84]	SO	×	✓	✓	×	×	✓	×	×
[85]	SO	✓	×	✓	✓	×	✓	✓	✓
[86]	×	×	×	×	✓	×	✓	×	✓	✓
[87]	×	×	×	×	✓	×	✓	×	✓	✓
[88]	MO	×	×	✓	✓	×	✓	✓	✓
Approach 4	MO	✓	✓	✓	✓	✓	✓	✓	✓

✓: Yes. ×: No. Opt.: Optimization. MO: Multi-objective optimization. SO: Single-objective optimization. Network reconfig.: Network reconfiguration.

Furthermore, only references [47, 84–88] considered customer-owned DERs, which adds complexity to the distribution system planning problem since it is not possible to optimally allocate and size DERs. Among these studies, only [86–88] accounted for stochastic customer-owned DERs, where the quantity, sizes, and locations of DERs installed by end-customers are inherently unpredictable. Some of the mentioned articles proposed single-period or multi-period approaches; nevertheless, none of them compared both approaches to determine whether the additional complexity of the multi-period approach is justified compared to the single-period approach. Regarding uncertainties, it is noted that some articles do not account for the

uncertainties in loads or DER generation, even though considering these uncertainties is essential to ensure the reliability and robustness of the proposed methodology. Therefore, the motivation behind Approach 4 is to fill some gaps in the state of the art by a comprehensive approach that takes into account all the characteristics presented in Table 4.

2.8 Chapter Conclusions

In this chapter, a systematic review of the literature was conducted to establish a solid foundation for the research presented in this thesis. The study focused on four main approaches aimed at improving the operation and planning of distribution systems. Key topics included protection schemes considering the integration of DERs, methodologies for allocating and sizing DERs, capacitors, and EVCSs, as well as challenges related to network reconfiguration. This comprehensive review not only highlights the state-of-the-art in these areas but also identifies research gaps that support the contributions of this thesis, setting the stage for the subsequent chapter.

Chapter 3

Theory Framework

This chapter provides the theoretical framework that supports the research presented in this thesis. It covers essential topics such as methods for solving power flow equations and calculating short-circuit currents, even in the presence of DERs. The chapter also explores multi-objective optimization and decision-making techniques, which are important for optimizing complex systems with competing goals. Additionally, it introduces a method for addressing uncertainties effectively, an important consideration for real-world applications. Fundamental concepts of graph theory are introduced in order to depict essential aspects of network representation and analysis. Finally, the chapter includes a brief overview of the network reconfiguration process.

3.1 Distribution System Modeling

This section presents the methods and equations necessary for modeling distribution systems. Figure 1 illustrates a representation of a distribution system, providing a clear visualization of the network structure and the key components involved in the system's operation. In Figure 1, Z_{ij}, R_{ij}, and X_{ij} represent the impedance, resistance, and reactance of branch ij, respectively; Z_{ki}, R_{ki}, and X_{ki} represent the impedance, resistance, and reactance of branch ki, respectively; and $V_{h,k}$, $V_{h,i}$, and $V_{h,j}$ are the voltage at time h and buses k, i, and j, respectively. Additionally, $P^s_{h,i}$ and $Q^s_{h,i}$ denote the active and reactive power supplied by the substation at bus i and time h; $P^d_{h,i}$ and $Q^d_{h,i}$ are the active and reactive power demands at bus i and time h; $P_{h,ki}$ and $Q_{h,ki}$ are the active and reactive power flows at branch ki and time h; and $P_{h,ij}$ and $Q_{h,ij}$ are the active and reactive power flows at time h and branch ij, respectively. Furthermore, $I_{h,ki}$ and $I_{h,ij}$ are the current flowing at time h and branches ki and ij, respectively.

Initially, it is essential to ensure the power balance of the system, which guarantees that the total power generated and supplied meets the total power demanded, including losses in the network. The active and reactive power balances at each bus are expressed as

$$\sum_{ki\in\Omega_l} P_{h,ki} - \sum_{ij\in\Omega_l} \left(P_{h,ij} + R_{ij}\cdot I^2_{h,ij}\right) + P^s_{h,i} = P^d_{h,i}, \quad \forall h \in \Omega_h, \forall i \in \Omega_b, \tag{3.1}$$

$$\sum_{ki\in\Omega_l} Q_{h,ki} - \sum_{ij\in\Omega_l} \left(Q_{h,ij} + X_{ij}\cdot I^2_{h,ij}\right) + Q^s_{h,i} = Q^d_{h,i}, \quad \forall h \in \Omega_h, \forall i \in \Omega_b, \tag{3.2}$$

where Ω_h, Ω_l, and Ω_b is the set of time intervals, branches, and buses of the system, respectively.

Figure 1 – Representation of a distribution system.

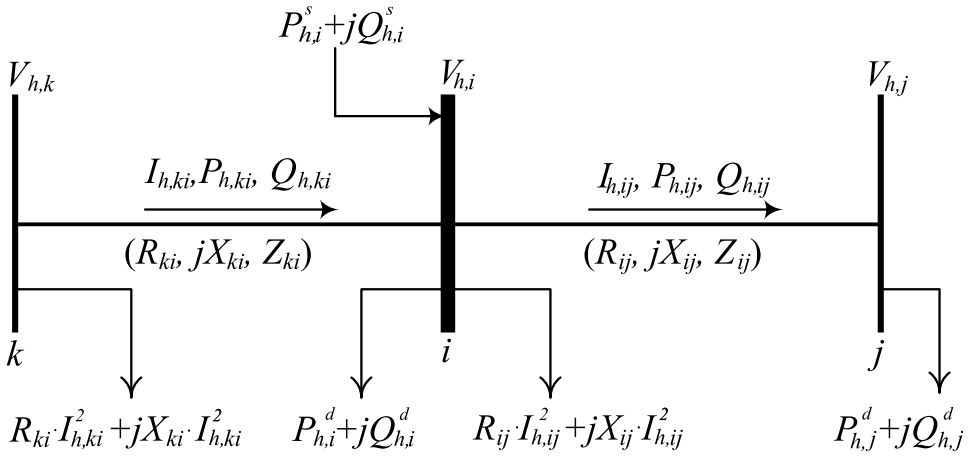

Source: Adapted from [90].

The voltage drop along branch ij is represented as

$$V^2_{h,i} - 2 \cdot \left(R_{ij} \cdot P_{h,ij} + X_{ij} \cdot Q_{h,ij}\right) - Z^2_{ij} \cdot I^2_{h,ij} - V^2_{h,j} = 0, \quad \forall h \in \Omega_h, \forall i \in \Omega_b, \forall j \in \Omega_b, \forall ij \in \Omega_l, \quad (3.3)$$

which takes into account both active and reactive power flows, as well as the impedance of the branch. This equation is important for accurately modeling voltage variations at different buses in the distribution network. The square of the voltage at bus i and current at branch ij are linked to the active and reactive power flows along the branch ij using

$$V^2_{h,j} \cdot I^2_{h,ij} = P^2_{h,ij} + Q^2_{h,ij}, \quad \forall h \in \Omega_h, \forall j \in \Omega_b, \forall ij \in \Omega_l. \quad (3.4)$$

Additionally, to ensure the proper operation of the distribution system, the current values in the branches and the voltage values at the buses must remain within specified limits, given by

$$I_{h,ij} \leq I^{\max}_{ij}, \quad \forall h \in \Omega_h, \forall ij \in \Omega_l, \quad (3.5)$$

$$V^{\min}_i \leq V_{h,i} \leq V^{\max}_i, \quad \forall h \in \Omega_h, \forall i \in \Omega_b, \quad (3.6)$$

where $I^{\max}_{ij}$ represents the maximum allowable current for branch ij, and $V^{\min}_i$ and $V^{\max}_i$ correspond to the minimum and maximum allowable voltage values at bus i, respectively.

To solve the power flow equations and analyze the behavior of the distribution system, the Backward-forward Sweep Power Flow Method is employed. This method is particularly suitable for radial distribution systems, which iteratively calculates the voltage magnitudes and phase angles at each bus, based on the power injections (active and reactive) and the network's impedance. The approach efficiently handles the non-linearities of the power flow equations and can incorporate the presence of DERs and other system components, providing valuable insights into the system's performance and stability. Further explanation of this method is presented in Section 3.1.1.

3.1.1 Backward-forward Sweep Power Flow Method

The Backward-forward Sweep Power Flow Method, proposed by Cheng and Shirmohammadi (1995) in [91], is a widely used technique for solving power flow problems in radial distribution systems. It operates in two distinct sweeps: a backward sweep, where currents are calculated from the loads to the source, and a forward sweep, where voltages are determined from the source to the loads. The Backward-forward Sweep is particularly advantageous for its simplicity, low computational effort, and high accuracy. This method can be summarized in three steps:

1. Calculation of load currents.
2. Calculation of distribution line currents.
3. Calculation of the voltages of the buses.

In Figure 2, a representation of two buses, i and j, in a distribution system is shown along with their respective loads. Additionally, the bus admittances, $Y_{ia,ib,ic}$ and $Y_{ja,jb,jc}$, as well as the line impedance, $\dot{Z}_l$, are depicted.

Figure 2 – Representation of two buses with loads in a distribution system.

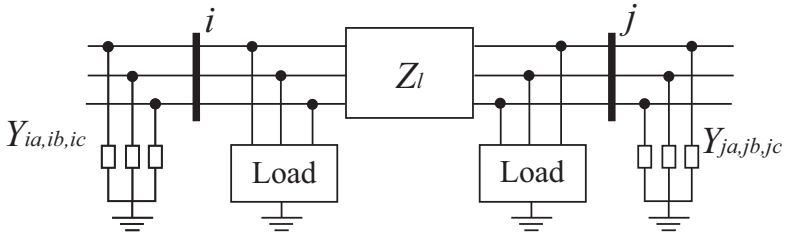

Source: Adapted from [91].

The Backward-forward Sweep Method starts by assigning the phase voltages to each bus of the system. To make the convergence faster, the voltage value of the slack bus is assigned to all buses. Iteration ε of the method begins with the calculation of load currents based on

$$\begin{bmatrix} I_{j,a} \\ I_{j,b} \\ I_{j,c} \end{bmatrix}^{(\varepsilon)} = \begin{bmatrix} \left(\frac{S^d_{j,a}}{V^{(\varepsilon-1)}_{j,a}}\right)^* \\ \left(\frac{S^d_{j,b}}{V^{(\varepsilon-1)}_{j,b}}\right)^* \\ \left(\frac{S^d_{j,c}}{V^{(\varepsilon-1)}_{j,c}}\right)^* \end{bmatrix} - \begin{bmatrix} Y^*_{j,aa} & Y^*_{j,ab} & Y^*_{j,ac} \\ Y^*_{j,ab} & Y^*_{j,bb} & Y^*_{j,bc} \\ Y^*_{j,ac} & Y^*_{j,bc} & Y^*_{j,cc} \end{bmatrix} \cdot \begin{bmatrix} V_{j,a} \\ V_{j,b} \\ V_{j,c} \end{bmatrix}^{(\varepsilon-1)}, \quad j \in \Omega_b, \tag{3.7}$$

where $I_{j,a}$, $I_{j,b}$, and $I_{j,c}$ are the currents injected at bus j; $S^d_{j,a}$, $S^d_{j,b}$, and $S^d_{j,c}$ are the apparent power of the loads at bus j; $V_{j,a}$, $V_{j,b}$, and $V_{j,c}$ are the phase voltages at bus j; and Ω_b is the set of buses.

Based on the values of load currents, it is possible to calculate the currents of the distribution lines in the system using

$$\begin{bmatrix} I_{ij,a} \\ I_{ij,b} \\ I_{ij,c} \end{bmatrix}^{(\varepsilon)} = -\begin{bmatrix} I_{j,a} \\ I_{j,b} \\ I_{j,c} \end{bmatrix}^{(\varepsilon)} + \sum_{o \in \Omega_o} \begin{bmatrix} I_{o,a} \\ I_{o,b} \\ I_{o,c} \end{bmatrix}^{(\varepsilon)}, \quad ij \in \Omega_l, j \in \Omega_b, o \in \Omega_o, \tag{3.8}$$

where $I_{ij,a}$, $I_{ij,b}$, and $I_{ij,c}$ are the currents flowing through line ij, and $I_{o,a}$, $I_{o,b}$, and $I_{o,c}$ are the currents flowing through the distribution lines connected downstream of bus j, in which these lines belong to the set Ω_o. This step must be performed from the farthest buses of the system towards the slack bus.

The next step of the method consists of calculating the voltage of the buses for each phase, starting from the slack bus to the farthest buses. This calculation is performed using

$$\begin{bmatrix} V_{j,a} \\ V_{j,b} \\ V_{j,c} \end{bmatrix}^{(\varepsilon)} = \begin{bmatrix} V_{i,a} \\ V_{i,b} \\ V_{i,c} \end{bmatrix}^{(\varepsilon)} - \begin{bmatrix} Z_{aa,ij} & Z_{ab,ij} & Z_{ac,ij} \\ Z_{ab,ij} & Z_{bb,ij} & Z_{bc,ij} \\ Z_{ac,ij} & Z_{bc,ij} & Z_{cc,ij} \end{bmatrix} \cdot \begin{bmatrix} I_{ij,a} \\ I_{ij,b} \\ I_{ij,c} \end{bmatrix}^{(\varepsilon)}, \quad ij \in \Omega_l, j \in \Omega_b, i \in \Omega_b, \tag{3.9}$$

where $V_{i,a}$, $V_{i,b}$, and $V_{i,c}$ are the phase voltages at bus i.

Finally, the stopping criterion of the method is represented as

$$\Delta S_{j,a}^{(\varepsilon)} = V_{j,a}^{(\varepsilon)} \cdot \left(I_{j,a}^{(\varepsilon)}\right)^* - Y_{j,a}^* \cdot \left|V_{j,a}^{(\varepsilon)}\right|^2 - S_{j,a}, \quad j \in \Omega_b, \tag{3.10}$$

$$\Delta S_{j,b}^{(\varepsilon)} = V_{j,b}^{(\varepsilon)} \cdot \left(I_{j,b}^{(\varepsilon)}\right)^* - Y_{j,b}^* \cdot \left|V_{j,b}^{(\varepsilon)}\right|^2 - S_{j,b}, \quad j \in \Omega_b, \tag{3.11}$$

$$\Delta S_{j,c}^{(\varepsilon)} = V_{j,c}^{(\varepsilon)} \cdot \left(I_{j,c}^{(\varepsilon)}\right)^* - Y_{j,c}^* \cdot \left|V_{j,c}^{(\varepsilon)}\right|^2 - S_{j,c}, \quad j \in \Omega_b. \tag{3.12}$$

In these equations, the power demanded by each bus is compared with the calculated power values based on the voltages and currents obtained in iteration ε. Thus, it is important to verify if the iterative process has converged considering

$$\Delta S_T = \sum_{j \in \Omega_b} \left(\Delta S_{j,a}^{(\varepsilon)} + \Delta S_{j,b}^{(\varepsilon)} + \Delta S_{j,c}^{(\varepsilon)}\right). \tag{3.13}$$

If the value of ΔS_T exceeds the tolerance, it is required to repeat the previous steps and assign $\varepsilon + 1 \rightarrow \varepsilon$; otherwise, the power flow solution has been obtained.

The PV-based DERs, capacitors, EVCSs, and loads adopted in this thesis operate with constant active and reactive power. This modeling approach is commonly used in studies where the focus is on broader system performance rather than on the dynamic control strategies of these devices, providing a practical and computationally efficient representation of their behavior under typical operating conditions in distribution networks. In this context, the DERs, capacitors, EVCSs, and loads can be integrated in the Backward-forward Sweep Power Flow Method using PQ buses, where positive power values correspond to consumption and negative values represent generation [91]. Therefore, the total power at each bus in Ω_b corresponds to the difference between the power consumed and the power generated.

3.1.2 DER Modeling

Regarding the dispersed generators, it is important to define the active and reactive power capability of the DER based on its rated powers. In this study, the active and reactive capability follows the guidelines of the IEEE 1547-2018 standard [92], which specifies reactive and active power control requirements for DER inverters based on their operating category (Category A or B). Category B performance covers all Category A requirements and includes additional capabilities for effective integration of DERs into distribution systems, particularly in high-penetration scenarios [92]. Therefore, this thesis exclusively considers DERs with Category B performance. Figure 3 depicts the DER capability curve for DERs operating in Category B.

Figure 3 – Active and reactive power capability of the DER operating in Category B based on the IEEE 1547-2018 standard.

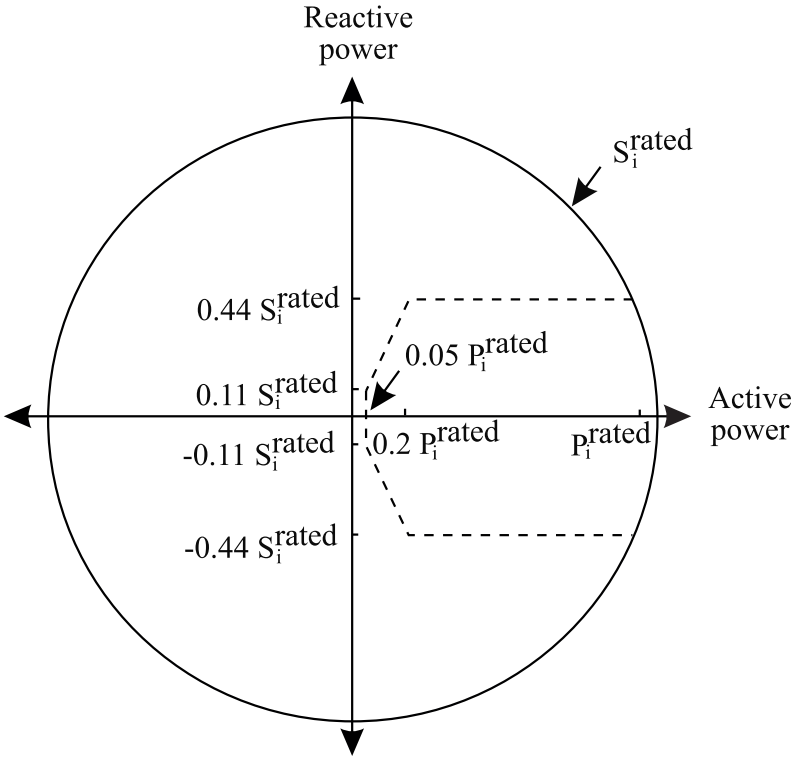

Source: Adapted from [92].

To incorporate these constraints into the problem formulations introduced in this thesis, they are modeled as

$$\left(P_{h,i}^{\mathrm{DER}}\right)^2 + \left(Q_{h,i}^{\mathrm{DER}}\right)^2 \leq \left(S_i^{\mathrm{rated}}\right)^2, \quad \forall h \in \Omega_h, \forall i \in \Omega_b, \tag{3.14}$$

$$P_{h,i}^{\mathrm{DER}} \geq 0.05 \cdot P_i^{\mathrm{rated}}, \quad \forall h \in \Omega_h, \forall i \in \Omega_b, \tag{3.15}$$

$$-0.44 \cdot S_i^{\mathrm{rated}} \leq Q_{h,i}^{\mathrm{DER}} \leq 0.44 \cdot S_i^{\mathrm{rated}}, \quad \forall h \in \Omega_h, \forall i \in \Omega_b, \tag{3.16}$$

$$-2.2 \cdot \frac{P_{h,i}^{\text{DER}} \cdot S_i^{\text{rated}}}{P_i^{\text{rated}}} \leq Q_{h,i}^{\text{DER}} \leq 2.2 \cdot \frac{P_{h,i}^{\text{DER}} \cdot S_i^{\text{rated}}}{P_i^{\text{rated}}}, \quad \forall h \in \Omega_h, \forall i \in \Omega_b, \tag{3.17}$$

where P_i^{rated} and S_i^{rated} are the rated active and apparent power of the DER located at bus i; while $P_{h,i}^{\text{DER}}$ and $Q_{h,i}^{\text{DER}}$ are the active and reactive power generated by each DER at bus i and time h.

In this study, only PV-based DERs are adopted, resulting in the DER's active power value varying according to the solar irradiance and temperature. Figure 4 illustrates a PV system, combining the PV generator, power electronic conversion, control, and monitoring. This figure also presents the DER's input variables (temperature and irradiance), the output power of the PV system ($P_{h,i}^{PV}$), the DER's output power ($P_{h,i}^{\text{DER}}$), and the DER operating points ($Pc_{h,i}^{\text{DER}}$ and $Qc_{h,i}^{\text{DER}}$). The PV system depicted in Figure 4 is modeled after the framework outlined in [1].

Figure 4 – Representation of the PV system.

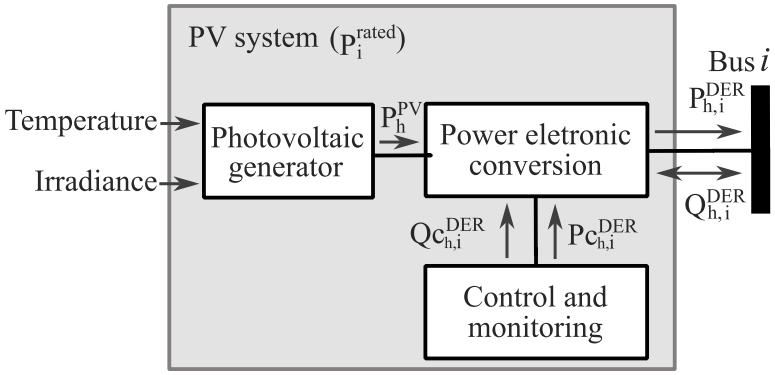

Source: Author.

The output power of the PV system is given by

$$P_h^{\text{PV}} = P^{\text{STC}} \cdot \frac{G_h^c}{G^{\text{STC}}} \left[1 + k \cdot (T_h^c - T^{\text{STC}})\right], \quad \forall h \in \Omega_h, \tag{3.18}$$

$$T_h^c = T_h^a + \delta \cdot G_h^c, \quad \forall h \in \Omega_h, \tag{3.19}$$

where T_h^c is the surface temperature of PV cells (in °C); G_h^c is the illumination intensity (in kW/m^2); k^{PV} is the power temperature coefficient; T_h^a is the environmental temperature; and δ is the coefficient related to wind speed. Moreover, P^{STC}, G^{STC}, and T^{STC} are the standard test conditions (STC): output power, illumination intensity (1 kW/m^2) and temperature (25 °C), respectively [93, 94].

The output active power of the DER according to the active power generated by the PV system and the DER's operating point is defined using

$$P_{h,i}^{\text{DER}} = \begin{cases} P_h^{PV}, & \text{if } P_h^{\text{PV}} < Pc_{h,i}^{\text{DER}} \\ Pc_{h,i}^{\text{DER}}, & \text{if } P_h^{\text{PV}} \geq Pc_{h,i}^{\text{DER}} \end{cases}, \quad \forall h \in \Omega_h, \forall i \in \Omega_b. \tag{3.20}$$

Meanwhile, the output DER reactive power matches the DER's operating point, i.e., $Q_{h,i}^{\text{DER}} = Qc_{h,i}^{\text{DER}}$, provided the latter falls within the limits outlined in Figure 4. Consequently, the

active and reactive power demands at bus i and time h, considering the DER installation, are depicted, respectively, as

$$P^d_{h,i} = \tilde{P}^d_{h,i} - P^{\text{DER}}_{h,i}, \quad \forall h \in \Omega_h, \forall i \in \Omega_b, \tag{3.21}$$

$$Q^d_{h,i} = \tilde{Q}^d_{h,i} - Q^{\text{DER}}_{h,i}, \quad \forall h \in \Omega_h, \forall i \in \Omega_b, \tag{3.22}$$

where $\tilde{P}^d_{h,i}$ and $\tilde{Q}^d_{h,i}$ are the active and reactive power demands at bus i and time h before the DER installation.

3.1.3 Switchable Capacitor Modeling

The reactive power output of the switchable capacitor depends on its capacitance and the selected tap position, with each tap corresponding to a discrete amount of reactive power. The reactive power output of the capacitor, $Q^{\text{cap}}_{h,i}$, at a specific tap position, $tap^{\text{cap}}_{h,i}$, is calculated using

$$Q^{\text{cap}}_{h,i} = Q^{\text{cap}}_{\text{max}} \cdot \frac{tap^{\text{cap}}_{h,i}}{tap^{\text{cap}}_{\text{max}}}, \quad \forall h \in \Omega_h, \forall i \in \Omega_b, \tag{3.23}$$

where $Q^{\text{cap}}_{\text{max}}$ represents the total reactive power rating of the capacitor and $tap^{\text{cap}}_{\text{max}}$ denotes the total number of available tap positions. Therefore, the reactive power demand at bus i and time h considering the capacitor installation is given by

$$Q^d_{h,i} = \tilde{Q}^d_{h,i} - Q^{\text{cap}}_{h,i} \quad \forall h \in \Omega_h, \forall i \in \Omega_b, \tag{3.24}$$

where $\tilde{Q}^d_{h,i}$ corresponds to the reactive power demands at bus i and time h before the capacitor installation.

3.1.4 EVCS Modeling

The integration of EVCSs in the distribution system is modeled by increasing the load at the bus where the EVCS is installed. This increment corresponds to the active power demand required for charging the EVs at a given time h in the corresponding EVCS. Thus, the total load at the respective bus is updated to reflect the additional active power consumed by the EVCS during the charging process, $P^{\text{EVCS}}_{h,i}$. This approach ensures that the impact of EV charging on the distribution system is accurately represented in the power flow analysis. The active power demand at bus i and time h considering the EVCS installation is depicted as

$$P^d_{h,i} = \tilde{P}^d_{h,i} + P^{\text{EVCS}}_{h,i}, \quad \forall h \in \Omega_h, \forall i \in \Omega_b, \tag{3.25}$$

where $\tilde{P}^d_{h,i}$ corresponds to the reactive power demands at bus i and time h before the EVCS installation.

3.1.5 OLTC Transformer Modeling

The modeling of the OLTC transformer is essential for considering voltage regulation in distribution networks. In the OLTC transformer, the tap settings are adjusted to regulate the voltage levels of the distribution system, ensuring they remain within acceptable limits [95]. The tap position is controlled dynamically, with the constraint that the tap must stay within a predefined minimum and maximum value, as given by the inequality

$$tap_{\min}^{\text{OLTC}} \leq tap_h^{\text{OLTC}} \leq tap_{\max}^{\text{OLTC}}, \quad \forall h \in \Omega_h, \tag{3.26}$$

where $tap_{\min}^{\text{OLTC}}$ and $tap_{\max}^{\text{OLTC}}$ represent the lower and upper bounds of the tap position, respectively, and tap_h^{OLTC} is the current tap setting. The voltage at the secondary side of the transformer, denoted as V_h^{sec}, in relation to the primary side voltage V_h^{pri}, is adjusted according to the tap position considering

$$V_h^{\text{sec}} = V_h^{\text{pri}} \cdot \left(1 + tap^{\text{step}} \cdot tap_h^{\text{OLTC}}\right), \quad \forall h \in \Omega_h, \tag{3.27}$$

where tap^{step} represents the voltage adjustment per tap position. This model allows the dynamic voltage regulation, ensuring that the voltage levels in the distribution network are maintained within operational limits, improving system stability and performance.

3.2 Short-circuit Analysis

Initially, the short-circuit analysis is performed in Section 3.2.1, considering the distribution system without the inclusion of DERs. Subsequently, in Section 3.2.2, the analysis is extended to account for the presence of DERs.

3.2.1 Short-circuit Analysis for the System without DER

For this analysis, the methodology introduced by Mathur et al. (2015) in [96] is employed. This approach takes into account the contribution of load current to accurately compute fault currents. For a more detailed explanation of this methodology, additional insights can be found in [96]. The main steps for calculating the short-circuit currents in the distribution system are outlined below:

Step 1 - *Execute the load flow algorithm:* In this step, the load flow algorithm (e.g., the Backward-forward Sweep Method detailed in Section 3.1.1) is performed to reach the voltage and the injected current values at each bus of the distribution system. In the event of a fault in the network, these values correspond to the pre-fault voltage, V_i^p, and the pre-fault load current, I_i^p.

Step 2 - *Determine the load admittance matrix at each bus:* The pre-fault voltage, V_i^p, and the pre-fault load current, I_i^p, are used to calculate the equivalent load impedance, z_{id}^p, and admittance, y_{id}^p, at bus i and phase p, as given, respectively, by

$$z_{id}^p = \frac{V_i^p}{I_i^p}, \quad \forall i \in \Omega_b, \tag{3.28}$$

$$y_{id}^{p} = \frac{1}{z_{id}^{p}}, \quad \forall i \in \Omega_b. \tag{3.29}$$

The load admittance matrix at bus i is then defined using

$$\dot{y}_{id}^{abc} = \begin{bmatrix} y_{id}^{a} & 0 & 0 \\ 0 & y_{id}^{b} & 0 \\ 0 & 0 & y_{id}^{c} \end{bmatrix}, \quad \forall i \in \Omega_b. \tag{3.30}$$

Step 3 - *Determine the line admittance matrix between buses i and j:* Considering the line impedance matrix, $\dot{z}_{ij}^{abc}$, represented by

$$\dot{z}_{ij}^{abc} = \begin{bmatrix} z_{ij}^{aa} & z_{ij}^{ab} & z_{ij}^{ac} \\ z_{ij}^{ba} & z_{ij}^{bb} & z_{ij}^{bc} \\ z_{ij}^{ca} & z_{ij}^{cb} & z_{ij}^{cc} \end{bmatrix}, \quad \forall ij \in \Omega_l, \tag{3.31}$$

it is possible to obtain the line admittance matrix, $\dot{y}_{ij}^{abc}$, expressed as

$$\dot{y}_{ij}^{abc} = \left(\dot{z}_{ij}^{abc}\right)^{-1} = \begin{bmatrix} y_{ij}^{aa} & y_{ij}^{ab} & y_{ij}^{ac} \\ y_{ij}^{ba} & y_{ij}^{bb} & y_{ij}^{bc} \\ y_{ij}^{ca} & y_{ij}^{cb} & y_{ij}^{cc} \end{bmatrix}, \quad \forall ij \in \Omega_l. \tag{3.32}$$

Step 4 - *Formulate the bus admittance matrix:* Using the load admittance matrix and the line admittance matrix, the bus admittance matrix $\dot{Y}_{bus}$ is expressed for a system consisting of n three-phase buses, m two-phase buses, and l single-phase buses as

$$\dot{Y}_{bus} = \begin{bmatrix} \dot{Y}_{22}^{abc} & \cdots & \dot{Y}_{2n}^{abc} & \dot{Y}_{2(n+1)}^{pq} & \cdots & \dot{Y}_{2(n+m)}^{pq} & \dot{Y}_{2(n+m+1)}^{p} & \cdots & \dot{Y}_{2(n+m+l)}^{p} \\ \vdots & \ddots & \vdots & \vdots & \vdots & \vdots & \vdots & \vdots & \vdots \\ \dot{Y}_{n2}^{abc} & \cdots & \dot{Y}_{nn}^{abc} & \dot{Y}_{n(n+1)}^{pq} & \cdots & \dot{Y}_{n(n+m)}^{pq} & \dot{Y}_{n(n+m+1)}^{p} & \cdots & \dot{Y}_{n(n+m+l)}^{p} \\ \dot{Y}_{(n+1)2}^{pq} & \cdots & \dot{Y}_{(n+1)n}^{pq} & \dot{Y}_{(n+1)(n+1)}^{pq} & \cdots & \dot{Y}_{(n+1)(n+m)}^{pq} & \dot{Y}_{(n+1)(n+m+1)}^{p} & \cdots & \dot{Y}_{(n+1)(n+m+l)}^{p} \\ \vdots & \vdots & \vdots & \vdots & \ddots & \vdots & \vdots & \vdots & \vdots \\ \dot{Y}_{(n+m)2}^{pq} & \cdots & \dot{Y}_{(n+m)n}^{pq} & \dot{Y}_{(n+m)(n+1)}^{pq} & \cdots & \dot{Y}_{(n+m)(n+m)}^{pq} & \dot{Y}_{(n+m)(n+m+1)}^{p} & \cdots & \dot{Y}_{(n+m)(n+m+l)}^{p} \\ \dot{Y}_{(n+m+1)2}^{p} & \cdots & \dot{Y}_{(n+m+1)n}^{p} & \dot{Y}_{(n+m+1)(n+1)}^{p} & \cdots & \dot{Y}_{(n+m+1)(n+m)}^{p} & \dot{Y}_{(n+m+1)(n+m+1)}^{p} & \cdots & \dot{Y}_{(n+m+1)(n+m+l)}^{p} \\ \vdots & \vdots & \vdots & \vdots & \vdots & \vdots & \vdots & \ddots & \vdots \\ \dot{Y}_{(n+m+l)2}^{p} & \cdots & \dot{Y}_{(n+m+l)n}^{p} & \dot{Y}_{(n+m+l)(n+1)}^{p} & \cdots & \dot{Y}_{(n+m+l)(n+m)}^{p} & \dot{Y}_{(n+m+l)(n+m+1)}^{p} & \cdots & \dot{Y}_{(n+m+l)(n+m+l)}^{p} \end{bmatrix}. \tag{3.33}$$

The elements of $\dot{Y}_{bus}$ can be calculated using

$$\begin{aligned} Y_{ii}^{pp} = y_{i1}^{pp} + y_{i2}^{pp} + \cdots + y_{in}^{pp} + y_{i(n+1)}^{pp} + \cdots + y_{i(n+m)}^{pp} + \\ y_{i(n+m+1)}^{pp} + \cdots + y_{i(n+m+1)}^{pp} + y_{i(n+m+l)}^{p} + y_{id}^{p}, \quad \forall i \in \Omega_b, \end{aligned} \tag{3.34}$$

$$Y_{ii}^{pq} = y_{i1}^{pq} + y_{i2}^{pq} + \cdots + y_{in}^{pq} + y_{i(n+1)}^{pq} + \cdots + y_{i(n+m)}^{pq}, \quad \forall i \in \Omega_b, \tag{3.35}$$

$$Y_{ij}^{pp} = -y_{ij}^{pp}, \quad \forall i \in \Omega_b, \forall j \in \Omega_b, \tag{3.36}$$

$$Y_{ij}^{pq} = -y_{ij}^{pq}, \quad \forall i \in \Omega_b, \forall j \in \Omega_b, \tag{3.37}$$

where:

- For three-phase buses: $i = 2,\ldots,n$; $j = 1,\ldots,n$; $j \neq i$; $p = a,b,c$; $q = a,b,c$; $p \neq q$.
- For two-phase buses: $i = (n+1),\ldots,(n+m)$; $j = (n+1),\ldots,(n+m)$; $j \neq i$; $p = a,b$ or b,c or c,a; $q = a,b$ or b,c or c,a; $p \neq q$.
- For single-phase buses: $i = (n+m+1),\ldots,(n+m+l)$; $j = (n+m+1),\ldots,(n+m+l)$; $j \neq i$; p and $q = a$ or b or c.

Step 5 - *Adjust the elements of the bus admittance matrix based on the specific fault type:* The bus admittance matrix, $\dot{Y}_{\text{bus}}$, is updated to account for the fault admittance, y_{ff}, in accordance with the type of fault, as described below:

- Single line-to-ground (phase p): $Y_{ii,new}^{pp} = Y_{ii}^{pp} + y_{ff}$.
- Double line-to-ground (phases pq): $Y_{ii,new}^{pp} = Y_{ii}^{pp} + y_{ff}$ and $Y_{ii,new}^{qq} = Y_{ii}^{qq} + y_{ff}$.
- Triple line-to-ground (phases abc): $Y_{ii,new}^{aa} = Y_{ii}^{aa} + y_{ff}$; $Y_{ii,new}^{bb} = Y_{ii}^{bb} + y_{ff}$; and $Y_{ii,new}^{cc} = Y_{ii}^{cc} + y_{ff}$.
- Line-to-line (phases pq): $Y_{ii,new}^{pp} = Y_{ii}^{pp} + y_{ff}$; $Y_{ii,new}^{qq} = Y_{ii}^{qq} + y_{ff}$; $Y_{ii,new}^{pq} = Y_{ii}^{pq} - y_{ff}$; and $Y_{ii,new}^{qp} = Y_{ii}^{qp} - y_{ff}$.

Step 6 - *Formulate the voltage and current matrices:* The voltage, $\dot{V}$, and current, $\dot{I}$, matrices are expressed, respectively, as

$$\dot{V} = \begin{bmatrix} \dot{V}_2^{abc} \\ \vdots \\ \dot{V}_n^{abc} \\ \dot{V}_{n+1}^{pq} \\ \vdots \\ \dot{V}_{n+m}^{pq} \\ \dot{V}_{n+m+1}^{p} \\ \vdots \\ \dot{V}_{n+m+l}^{p} \end{bmatrix}, \tag{3.38}$$

$$\dot{I} = \begin{bmatrix} \dot{y}_{12}^{abc} \cdot \dot{V}_s^{abc} \\ \vdots \\ 0 \\ 0 \\ \vdots \\ 0 \\ 0 \\ \vdots \\ 0 \end{bmatrix}. \tag{3.39}$$

Step 7 - *Compute the post-fault bus voltages:* The relationship between the bus admittance, $\dot{Y}_{bus}$, the voltage matrix, $\dot{V}$, and the current matrix, $\dot{I}$, is represented by

$$\dot{I} = \dot{Y}_{bus} \cdot \dot{V}, \tag{3.40}$$

which can be used to calculate the post-fault bus voltage.

Step 8 - *Compute the branch current between bus i and j:* The short-circuit current in each branch, $\dot{B}_{ij}^{abc}$, is calculated using

$$\dot{B}_{ij}^{abc} = \dot{y}_{ij}^{abc} \cdot (\dot{V}_i^{abc} - \dot{V}_j^{abc}), \quad \forall i \in \Omega_b, \forall j \in \Omega_b, \forall ij \in \Omega_l. \tag{3.41}$$

Recognizing the significance of accurately assessing fault currents in distribution systems, this study emphasizes the critical role of incorporating the current contribution from DERs in the fault analysis. DERs, as intermittent power sources, can cause a notable impact on fault currents, necessitating their comprehensive inclusion for precise fault calculations. To achieve this goal, this research adopts the insights introduced by Mathur et al. (2017) in [97], leveraging its methodologies to enhance fault analysis accuracy and, consequently, contribute to the overall reliability and effectiveness of distribution system protection strategies.

3.2.2 Short-circuit Analysis for the System with DER

The short-circuit analysis for the system with DER follows a similar approach to that presented in Section 3.2.1, with specific modifications detailed in this section. For the explanation, a DER is assumed to be installed at bus n, as illustrated in Figure 5.

To represent the DER connection, a new bus is introduced into the distribution system model, referred to as the inverter bus in Figure 5. A step-down transformer is installed between this new bus and bus n, with its impedance and admittance expressed, respectively, as

$$\dot{z}_t^{abc} = \begin{bmatrix} z_t^{aa} & z_t^{ab} & z_t^{ac} \\ z_t^{ba} & z_t^{bb} & z_t^{bc} \\ z_t^{ca} & z_t^{cb} & z_t^{cc} \end{bmatrix}, \tag{3.42}$$

$$\dot{y}_t^{abc} = \left(\dot{z}_t^{abc}\right)^{-1} = \begin{bmatrix} y_t^{aa} & y_t^{ab} & y_t^{ac} \\ y_t^{ba} & y_t^{bb} & y_t^{bc} \\ y_t^{ca} & y_t^{cb} & y_t^{cc} \end{bmatrix}. \tag{3.43}$$

Figure 5 – Representation of the distribution system with a DER installed at bus *n*.

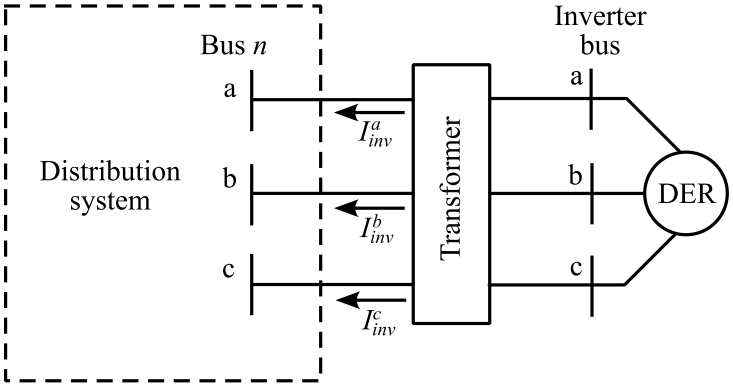

Source: Adapted from [97].

The main steps for calculating the short-circuit currents in the distribution system with DERs are outlined as follows:

Step 1 - *Execute the load flow algorithm considering the DER:* The load flow algorithm is applied to calculate the pre-fault voltages, V_i^p, and currents, I_i^p. Among these voltage values, the pre-fault voltage at the inverter bus, denoted as $\dot{V}_{inv}^{abc}$, is also calculated. During normal operating conditions (pre-fault period), the DER operates in constant active and reactive power mode. In this context, the DER is modeled as a PQ bus in the power flow analysis, where positive power values indicate consumption, and negative values represent generation.

Step 2 - *Determine the load admittance matrix at each bus:* This step is similar to the process used for systems without DER. The load admittance matrix is calculated based on the pre-fault voltage, V_i^p, and the pre-fault load current, I_i^p, using (3.28)–(3.30).

Step 3 - *Determine the line admittance matrix between buses i and j:* This step is also similar to the process used for systems without DERs, where the line admittance matrix is determined using (3.31) and (3.32).

Step 4 - *Formulate the bus admittance matrix:* The bus admittance matrix of the system is initially formulated considering the load admittance matrix and the line admittance matrix through (3.33). Thereafter, only the elements of $\dot{Y}_{bus}$ corresponding to bus n (location of DER) is modified considering the admittance of the step-down transformer, $\dot{y}_t^{abc}$, as represented by

$$\dot{Y}_{nn,new}^{abc} = \dot{Y}_{nn}^{abc} + \dot{y}_t^{abc}, \tag{3.44}$$

where $\dot{Y}_{nn}^{abc}$ is the 3×3 submatrix of $\dot{Y}_{bus}$ corresponding to bus n.

Step 5 - *Adjust the elements of the bus admittance matrix based on the specific fault type:* This step is similar to the process used for the systems without DERs, where the bus admittance, denoted as $\dot{Y}_{\text{bus}}$, is modified depending on the type of fault, as outlined below:

- Single line-to-ground (phase p): $Y^{pp}_{ii,new} = Y^{pp}_{ii} + y_{ff}$.
- Double line-to-ground (phases pq): $Y^{pp}_{ii,new} = Y^{pp}_{ii} + y_{ff}$ and $Y^{qq}_{ii,new} = Y^{qq}_{ii} + y_{ff}$.
- Triple line-to-ground (phases abc): $Y^{aa}_{ii,new} = Y^{aa}_{ii} + y_{ff}$; $Y^{bb}_{ii,new} = Y^{bb}_{ii} + y_{ff}$; and $Y^{cc}_{ii,new} = Y^{cc}_{ii} + y_{ff}$.
- Line-to-line (phases pq): $Y^{pp}_{ii,new} = Y^{pp}_{ii} + y_{ff}$; $Y^{qq}_{ii,new} = Y^{qq}_{ii} + y_{ff}$; $Y^{pq}_{ii,new} = Y^{pq}_{ii} - y_{ff}$; and $Y^{qp}_{ii,new} = Y^{qp}_{ii} - y_{ff}$.

Step 6 - *Formulate the voltage and current matrices:* Initially, the voltage, $\dot{V}$, and current, $\dot{I}$, matrices are formulated using (3.38) and (3.39), respectively. Subsequently, the current matrix is modified considering the current injected by the DER installed at bus n. This modification is given by

$$\dot{I}^{abc}_{n,new} = \dot{I}^{abc}_{n} + \left(\dot{y}^{abc}_{t} \cdot \dot{V}^{abc}_{inv} \right), \tag{3.45}$$

where V^{abc}_{inv} is the three-phase voltage vector of the inverter bus and $\dot{I}^{abc}_{n}$ is the 3×1 submatrix of $\dot{I}$ corresponding to bus n.

Step 7 - *Compute the post-fault bus voltages:* Following a similar procedure to that used for the system without DER, the post-fault bus voltages are determined using (3.40).

Step 8 - *Compute the inverter current:* Based on the post-fault voltages, the inverter current, $\dot{I}^{abc}_{inv}$, can be calculated using

$$\dot{I}^{abc}_{inv} = \dot{y}^{abc}_{t} \cdot (\dot{V}^{abc}_{inv} - \dot{V}^{abc}_{n}). \tag{3.46}$$

Step 9 - *Check whether $|\dot{I}^{abc}_{inv}| \leq I^{inv}_{sc}$ for all the DERs in the system:* In this approach, the short-circuit current contribution of inverter-based DERs is limited according to the constraints of the switching devices' short-circuit current capacity, denoted as I^{inv}_{sc}. This is achieved by maintaining the inverter in a consistent current mode during operation. Depending on the inverter current value, the following cases are considered:

- Case 1: If $|\dot{I}^{abc}_{inv}| \leq I^{inv}_{sc}$ for all DERs, then go to **Step 10**.
- Case 2: If $|\dot{I}^{abc}_{inv}| > I^{inv}_{sc}$ for all DERs, then set the inverter current of each DER to I^{inv}_{sc} and compute the post-fault bus voltages.
- Case 3: If $|\dot{I}^{abc}_{inv}| > I^{inv}_{sc}$ for ζ DERs and $|\dot{I}^{abc}_{inv}| \leq I^{inv}_{sc}$ for Γ DERs, then set the inverter current for each of the ζ DERs to I^{inv}_{sc}, set the inverter current for the remaining DERs to $\dot{I}^{abc}_{inv}$, and compute the post-fault bus voltages.

Step 10 - *Compute the post-fault inverter voltage:* Considering the post-fault voltage of each system's bus and the inverter current, the post-fault voltage value of the inverter can be calculated as

$$\dot{V}_{inv}^{abc} = \dot{V}_{n}^{abc} + \dot{I}_{inv}^{abc} \cdot \dot{z}_{t}^{abc}. \tag{3.47}$$

Step 11 - *Define the control mode of the inverter:* Depending on the voltage at the point of common coupling of the inverter-based DER, $\dot{V}_{inv}^{abc}$, the DER operates under one of the following control modes:

- Case 1: If $(min(|\dot{V}_{inv}^{abc}|) < 0.45)$ pu or $(max(|\dot{V}_{inv}^{abc}|) > 1.20)$ pu, then DER must be disconnected.
- Case 2: If $(0.45 \leq min(|\dot{V}_{inv}^{abc}|) < 0.88)$ pu and $(max(|\dot{V}_{inv}^{abc}|) \leq 1.0)$ pu, then the DER must operate providing reactive power to increase the bus voltage.
- Case 3: If $(min(|\dot{V}_{inv}^{abc}|) \geq 0.45)$ pu and $(max(|\dot{V}_{inv}^{abc}|) > 1.1)$ pu, then the DER must operate absorbing reactive power to decrease the bus voltage.
- Case 4: If $(0.45 \leq min(|\dot{V}_{inv}^{abc}|) < 0.88)$ pu and $(1.0 < max(|\dot{V}_{inv}^{abc}|) \leq 1.1)$ pu, then the DER must operate in the same control mode as in the previous iteration to avoid frequent changes between voltage control modes.
- Case 5: If $(min(|\dot{V}_{inv}^{abc}|) \geq 0.88)$ pu and $(max(|\dot{V}_{inv}^{abc}|) \leq 1.1)$ pu, then the DER must provide only active power.

These control modes are designed to assist the system's operation during fault conditions, aiming to maintain the bus voltage levels close to their nominal values.

Step 12 - *Compute the post-fault voltages:* Considering the previously defined control mode of the DER, the post-fault voltage values are calculated.

Step 13 - *Compute the branch current between buses i and j*: The short-circuit current in each branch, $\dot{B}_{ij}^{abc}$, is calculated using (3.41).

It is important to mention that the calculation of post-fault voltage, presented in steps **Step 9** and **Step 12**, requires a numerical method to solve non-linear equations. These non-linear equations and the corresponding solving procedure are available in [97].

3.3 Multi-objective optimization

Multi-objective optimization is a powerful approach that deals with decision-making in scenarios where multiple conflicting objectives need to be simultaneously optimized. This method is essential in several real-world applications, including engineering, economics, and other fields where complex decisions are influenced by multiple factors.

Distinct solution strategies are applied in multi-objective optimization. Among these, the weighted sum method stands out for its simplicity. However, the weighted sum approach, which combines multiple objectives into a single criterion, may not accurately represent the complexity of the original multi-objective problem. This is due to the arbitrary nature of the additional weighting coefficients, potentially resulting in a discrepancy between the transformed single objective and the true multi-objective nature of the problem [98]. A significant drawback of a priori approaches lies in the fact that decision makers may not have full awareness of the inherent possibilities and limitations of the multi-objective optimization problem. This can lead to a scenario where the information about the decision maker's preferences is either overly optimistic or overly pessimistic, impacting the quality of the optimization outcome [89].

To overcome this drawback, there are a posteriori approaches, which are established on the basis of finding the Pareto-optimal solution set and presenting it to the decision maker with the aim of choosing the final solution through the aforementioned set. A solution is considered Pareto-optimal if no other solution can improve one objective without worsening at least one other objective. In simpler terms, it represents the best possible trade-off among the multiple objectives. The set of all Pareto-optimal solutions forms the Pareto-optimal front, showcasing the trade-offs between the objectives. The main advantage of a posteriori approaches, in contrast to a priori methods, is that in the former, the Pareto-optimal solution set is generated independently of the decision maker's preferences. Consequently, the decision maker acquires a comprehensive view of all potential solutions, facilitating a more straightforward and realistic selection of the most satisfying solution [89].

Evolutionary algorithms have emerged as robust tools for tackling the complexities of multi-objective optimization problems. These algorithms simulate the natural evolution to generate a diverse set of candidate solutions. Therefore, this approach efficiently explores the Pareto-optimal front, providing a comprehensive view of the trade-offs. In this thesis, the NSGA-II and Multi-objective Cuckoo Search (MOCS) are adopted due to its proven efficacy in handling complex optimization tasks. These methods are briefly outlined in Sections 3.3.1 and 3.3.2.

3.3.1 Non-dominated Sorting Genetic Algorithm II

The NSGA-II operates by iteratively evolving a population of candidate solutions, aiming to enhance the distribution and convergence of the Pareto-optimal front. Based on [99], the primary steps of the NSGA-II can be summarized as follows:

Step 1 - *Initialization*: The algorithm starts by randomly initializing a population of candidate solutions. Each solution is represented as a chromosome in a genetic algorithm framework. The population size is a parameter defined by the user that affects the convergence and diversity of the algorithm.

Step 2 - *Fitness assignment*: In each iteration, the fitness of each candidate solution is

evaluated. Fitness assignment involves two main steps: non-dominated sorting and crowding distance calculation. Non-dominated sorting categorizes solutions into multiple fronts based on their dominance relationships. In this context, solutions in the first front are not dominated by any other solution. Crowding distance measures the density of solutions in each front to promote diversity among the Pareto-optimized solutions.

Step 3 - *Selection*: A binary tournament selection mechanism is adopted to select parents for reproduction. Two solutions are randomly chosen, and their dominance and crowding distances are compared to determine the better parent.

Step 4 - *Crossover and mutation*: Selected parents undergo crossover and mutation operations to create a new population of offspring solutions. Crossover combines genetic information from two parents, while mutation introduces small random changes to maintain the exploration. The crossover and mutation probabilities are defined by the user.

Step 5 - *Environmental selection*: The offspring population is combined with the previous one to form a larger population. NSGA-II performs non-dominated sorting and crowding distance calculation on this combined population to select the solution of the next generation. Elitism is introduced to ensure that the most promising solutions survive from one generation to the next by selecting the best solutions from each front.

Step 6 - *Stopping criterion*: The iterative process continues until the convergence criterion is met. In this case, the convergence criterion is defined as the maximum number of generations, which is previously specified by the user. If the stopping criterion has not been reached, the algorithm returns to **Step 2** to perform a new iteration, involving the steps of evaluation, selection, reproduction, and mutation. Otherwise, if the stopping criterion is satisfied, the algorithm is terminated.

NSGA-II has established itself as one of the most prominent algorithms in multi-objective optimization due to its ability to efficiently handle nonlinear and non-convex objective functions while identifying a diverse set of optimized solutions. Its continued application in recent studies, including [100–104], highlights its robustness and versatility in addressing diverse optimization challenges.

A key advantage of NSGA-II is its capacity to provide a comprehensive and well-distributed representation of the Pareto front, particularly in problems involving two or three conflicting objectives [103, 104]. This feature allows decision-makers to explore trade-offs effectively. Additionally, NSGA-II enables the adaptation to a wide range of problem contexts and ensures its applicability to diverse optimization challenges. Its ability to explore large solution spaces while maintaining diversity ensures high-quality solutions and thorough exploration of the Pareto front, making it well-suited for the objectives of this research.

In light of these advantages, NSGA-II is selected for this research to address the challenges posed by multi-objective optimization problems. Its demonstrated ability to deliver

high-quality solutions with an efficient trade-off between convergence and diversity aligns with the objectives of this study. Moreover, the algorithm's continued relevance in recent research highlight its robustness and effectiveness, further justifying its adoption in this context.

3.3.2 Multi-objective Cuckoo Search

The MOCS algorithm operates based on the principles of the CSA, enhancing its capability to handle multiple conflicting objectives. According to reference [105], the essential steps of the MOCS can be outlined as follows:

Step 1 - *Initialization*: The algorithm starts by initializing a population of candidate solutions, denoted as nests in MOCS. Each nest represents a potential solution in the optimization process.

Step 2 - *Objective function evaluation*: The fitness of each candidate solution is assessed based on the multiple conflicting objectives of the optimization problem. The goal is to explore and identify solutions that form a Pareto front, providing a trade-off between the different objectives. Fitness assignment involves non-dominated sorting and crowding distance calculation.

Step 3 - *Lévy flight*: Inspired by the Lévy flight behavior observed in some birds, the algorithm introduces randomness and exploration in the search space. Cuckoos lay eggs (new solutions) using a combination of their own solutions and solutions from other nests (candidates in the population).

Step 4 - *Stopping criterion*: The iterative process continues until the convergence criterion is met. In this case, the convergence criterion is defined as the maximum number of iterations, which is previously specified by the user. If the stopping criterion has not been reached, the algorithm returns to **Step 2** to perform a new iteration. Otherwise, if the stopping criterion is satisfied, the algorithm is terminated.

The CSA have demonstrated its efficacy as a robust optimization technique, particularly in addressing complex challenges within power distribution systems, as highlighted in recent studies, e.g., [106–110]. Building upon the foundational principles of the CSA, MOCS leverages its global search capabilities to efficiently navigate large solution spaces. The algorithm's search mechanism, inspired by Lévy flight random walk, enables it to avoid local optima while thoroughly exploring the search domain. These attributes make MOCS particularly effective for tackling optimization problems characterized by extensive and nonlinear search spaces. Moreover, this comprehensive exploration capability contributes to reducing computational costs and simulation times by efficiently converging toward high-quality solutions [111].

These advantageous features, combined with the algorithm's minimal parameter tuning requirements, underscore its suitability for the objectives of this thesis and its selection as the one of the optimization method of choice.

3.3.3 Fuzzy Decision-making Method

After completing the multi-objective optimization algorithm, it is important to select a realistic and flexible solution from the set of candidate solutions. In this research, the Fuzzy Decision-making Method is chosen due to its simplicity, flexibility, and alignment with human reasoning processes [89]. This method is particularly useful when dealing with multi-objective optimization problems where no single optimal solution exists, and trade-offs between competing objectives must be made.

The Fuzzy Decision-making Method works by defining membership functions for each objective function, which quantify the satisfaction level of the decision-maker for a given solution. These membership functions are denoted as $\Phi_{f_a^v(x)}(\bar{x}_v)$, where $f_a^v(x)$ represents the value of an objective function for the solution v in the Pareto solution set $\bar{x}_v$. The function assigns a satisfaction value between 0 and 1, with 1 indicating the highest degree of satisfaction and 0 indicating no satisfaction.

In this study, a linear membership function is adopted due to its simplicity and ability to provide a straightforward representation of the decision-maker's preferences. The linear membership function is expressed mathematically as

$$\Phi_{f_a^v(x)}(\bar{x}_v) = \begin{cases} 0 & \forall\{f_a^v(x) > f_a^{\max}(x)\} \\ \frac{f_a^{\max}(x) - f_a^v(x)}{f_a^{\max}(x) - f_a^{\min}(x)} & \forall\left\{f_a^{\min}(x) \le f_a^v(x) \le f_a^{\max}(x)\right\}, \\ 1 & \forall\left\{f_a^v(x) < f_a^{\min}(x)\right\} \end{cases} \quad \forall a \in \Omega_a, \forall v \in \Omega_v. \quad (3.48)$$

After calculating the membership functions for all objective functions, the next step is to determine the level of desirability, represented as $\widetilde{\Phi}_{f_a(x)}$, for each objective function. The final compromise solution, which aligns with the decision-maker's preferences, is then selected using

$$\min_{v \in \Omega_v} \left\{ \max_{a \in \Omega_a} \left\{ \left| \widetilde{\Phi}_{f_a(x)} - \Phi_{f_a^v(x)}(x_v) \right| \right\} \right\}, \quad (3.49)$$

where Ω_a and Ω_v represent the sets of objective functions and available solutions, and $f_a^{\max}(x)$ and $f_a^{\min}(x)$ are the maximum and minimum values of the objective function $f_a^v(x)$.

This method has been widely adopted in recent studies, including [88, 112–114], for its ability to effectively handle the complexity and subjectivity inherent in multi-objective decision-making processes, particularly when dealing with conflicting objectives. The flexibility of the Fuzzy Decision-making Method allows for the incorporation of decision-maker preferences, ensuring that the chosen solution is not only optimized but also aligned with practical considerations.

3.4 Monte Carlo Method

The distribution system operation involves several uncertainties, including load variations and renewable energy generation fluctuations. Conventional deterministic methods often overlook

these uncertainties, leading to suboptimal solutions or inaccurate performance evaluations. In this context, Monte Carlo Method is a powerful computational technique widely employed in various fields to model and analyze complex systems or processes with inherent uncertainties. The Monte Carlo Method consists of repeated random sampling to obtain numerical results, based on the law of large numbers and the central limit theorem. From this sampling, it is possible to estimate the behavior of a system or a process that involves stochastic variables [115].

The Monte Carlo Method offers significant advantages in addressing uncertainties, making it a widely adopted approach in several researches. It excels in capturing complex interactions, correlations, and non-linearities among multiple uncertain variables, providing a comprehensive perspective on how these uncertainties collectively influence outcomes. Additionally, its simplicity and ability to generate diverse scenarios contribute to its effectiveness as a tool for enhancing decision-making and understanding system behaviors under uncertain conditions. Its continued relevance is evidenced by its application in numerous recent studies, including [80, 81, 88, 112, 116, 117]. For these reasons, the Monte Carlo Method is adopted in this thesis.

The main steps of implementing the Monte Carlo Method involve [115]:

Step 1 - *Defining uncertain variables:* Identify the variables that introduce uncertainty into the problem, such as load demand and renewable energy generation.

Step 2 - *Scenario generation*: The process begins with the generation of multiple scenarios, each representing a distinct combination of uncertainties.

Step 3 - *Running the model:* For each scenario, execute the distribution system model. This involves solving the relevant equations and algorithms to obtain the system's response under the given conditions. In this study, the model includes the power flow and short-circuit algorithms.

Step 4 - *Statistical analysis:* By repeating the scenario generation process a considerable number of times, it is possible to perform statistical analysis, facilitating the extraction of meaningful patterns and trends. This step provides a detailed understanding of the system's behavior across different scenarios.

Several key concepts are essential for effectively analyzing the results obtained through the Monte Carlo Method. One of the most important of these is the significance level, a fundamental statistical concept used to evaluate the meaningfulness of an analysis. Denoted by α, the significance level sets a probability threshold below which the results are considered statistically significant. In essence, it quantifies the likelihood that the observed outcomes could have arisen by random chance [118]. The significance level is commonly set to values such as 0.05, 0.01, or 0.001, depending on the context of the study. A smaller value of α corresponds to stricter criteria for determining statistical significance, which reduces the chances of drawing incorrect conclusions and enhances the reliability of the results [118].

In the context of Monte Carlo simulations, the significance level is important to define the confidence level. This relationship is direct, as the confidence level is calculated as $1-\alpha$ [119]. The confidence level is then used to define the confidence interval, which represents a range of values within which the true parameter of interest is expected to lie. For instance, a confidence interval based on a 95% confidence level suggests that, if the experiment were repeated many times, the true parameter value would fall within this range in 95 out of 100 repetitions.

The confidence interval is given by

$$\mathrm{CI} = \mu \pm z_{\alpha/2} \cdot \frac{\sigma}{\sqrt{n^{\mathrm{sample}}}}, \tag{3.50}$$

where CI represents the confidence interval, μ is the sample mean; $z_{\alpha/2}$ is the critical value from the standard normal distribution corresponding to the desired confidence level, σ is the standard deviation of the sample, and n^{sample} is the sample size. The term $z_{\alpha/2} \cdot \frac{\sigma}{\sqrt{n^{\mathrm{sample}}}}$ represents the margin of error, which quantifies the uncertainty of the estimate. A larger margin of error indicates greater uncertainty about the true value, while a smaller margin suggests a more precise estimate. In Monte Carlo Method, confidence intervals are essential for assessing the variability of results and defining the proper number of Monte Carlo simulations.

3.4.1 Monte Carlo Method Convergence

The number of required simulations in the Monte Carlo Method is defined in this study based on an algorithm developed by the authors of this thesis in [10]. During the optimization process, the required number of simulations to ensure Monte Carlo convergence adjusts dynamically with each iteration of the optimization technique. Algorithm 1 outlines this procedure for one iteration.

Algorithm 1 starts by defining the confidence level, which in this thesis is set to 99%. This choice of a 99% confidence level indicates a high level of certainty in the accuracy of the results, providing a robust measure of the system's performance under various conditions. In Line 2, the variables s, $flag$, and *count* are initialized to 1, 0, and 0, respectively. The variable s represents the scenario counter, indicating the current iteration of the Monte Carlo Method. The variable $flag$ serves as a flag to control the end of the while loop, with a value of 0 indicating that the loop should continue iterating. The variable *count* is used to track the number of consecutive iterations where the confidence intervals, for all objective functions, have converged to a specified threshold.

The while loop, beginning at Line 3, continues until the variable $flag$ equals 0. Within this loop, a Monte Carlo scenario is generated and then, in Line 5, the power flow calculations are performed, considering both the random variables and the decision variables of the optimization problem. Based on the power flow solution, it is possible to verify the satisfaction of constraints in Line 6. It is important to guarantee compliance with these constraints for every Monte Carlo scenario to ensure proper system operation under diverse network conditions. In Line 7, the

objective functions are evaluated and stored in vectors f_a^s. Subsequently, in Line 8, the algorithm calculates the confidence interval CI_a^s considering all scenarios generated up to the current iteration.

The percentage changes between the current confidence intervals and those from the previous iteration are calculated in Line 9, resulting in $CI_{a\%}$. These percentage changes serve as indicators of convergence, informing the algorithm whether the confidence intervals are narrowing with each iteration. If the maximum of these percentage changes is less than 0.1%, as checked in Lines 10–17, the algorithm increments the *count* variable; otherwise, *count* is reset to 0. Once the count reaches 10, the loop terminates by setting the variable $flag$ to 1, indicating that the convergence criterion has been met. Finally, in Line 18, the Monte Carlo scenario counter s is incremented to move to the next iteration. This process continues until the convergence criterion is met, at which point the algorithm outputs the average value of the objective functions (Line 20), providing a comprehensive assessment of system performance under uncertainty.

Algorithm 1 Monte Carlo Method

1: Define the confidence level
2: $s \leftarrow 1$, $flag \leftarrow 0$, and $count \leftarrow 0$
3: **while** $flag == 0$ **do**
4: Generate a Monte Carlo scenario
5: Perform the power flow algorithm
6: Verify if the constraints of the optimization problem are met
7: Calculate the objective functions and store in f_a^s $(\forall a \in \Omega_a)$
8: Calculate the confidence intervals CI_a^s $(\forall a \in \Omega_a)$ considering all scenarios generated so far
9: Calculate the percentage changes between CI_a^s and CI_a^{s-1} $(\forall a \in \Omega_a)$
10: **if** $CI_{a\%} < 0.1\%$ $(\forall a \in \Omega_a)$ **then**
11: $count \leftarrow count + 1$ ▷ Increment count
12: **if** $count == 10$ **then** ▷ Check if count reaches 10
13: $flag \leftarrow 1$ ▷ Set flag to terminate loop
14: **end if**
15: **else**
16: $count \leftarrow 0$ ▷ Reset count if conditions are not met
17: **end if**
18: $s \leftarrow s + 1$ ▷ Increment scenario counter
19: **end while**
20: **Output:** Average value of the objective functions

3.5 Graph Theory

In this study, fundamental concepts of graph theory are employed in order to depict essential aspects of network representation and analysis. More specifically, these concepts are important to maintain the radial configuration of the system during the reconfiguration process,

determine the shortest path between EVs and EVCSs using the Dijkstra algorithm, and identify the central areas within the system using closeness centrality.

A graph $\mathcal{G} = (\Omega_b, \Omega_l)$ is a set of points called vertices or nodes, Ω_b, along with the set of connections known as edges or lines, Ω_l, that link these vertices. Each edge is formed by connecting two vertices, and these connections are represented as 2-element subsets of Ω_b. In a weighted graph, edges are assigned numerical values known as weights. Additionally, a graph $\mathcal{G}$ with κ vertices can be conveniently represented using an adjacency matrix $\dot{A} = [a_{i,j}]_{\kappa \times \kappa}$, where $a_{i,j}$ takes the value 1 if an edge exists between vertices i and j in $\mathcal{G}$, and 0 otherwise [120]. The degree of a vertex $i \in \Omega_b$ means the count of edges connected to that vertex.

A connected graph $\mathcal{G}$ is one where any two vertices are connected by at least one path. Such a graph that doesn't form any cycles is referred to as a tree. Within a tree structure, a vertex with only one connecting edge is called a pendant vertex. Based on [121], a graph $\mathcal{G}$ is classified as a tree when any two vertices within it are connected by just one path. Considering a connected weighted graph $\mathcal{G}$, the length of a path is the sum of the weights of its edges. A path with the smallest possible length between two vertices is known as the shortest path. To determine these shortest paths in a graph with non-negative edge weights, the Dijkstra algorithm [122] is commonly used.

According to [123], the initial step of the Dijkstra algorithm involves selecting a source vertex and assigning it a distance value of zero. For all other vertices, an initial distance value of infinity is assigned. This approach highlights that the cost of reaching any vertex from the source vertex is still unknown, except for the source vertex itself, which is assigned a cost of zero. Subsequently, the adjacent vertices to the source vertex are examined to identify the shortest distance to the next vertex to be explored. Additionally, along with the weight of the next vertex, the preceding vertex, in this case, the source vertex, is also recorded. Following this, the selected vertex is analyzed, and its unexplored adjacent vertices are visited. It is crucial to increment the weights accumulated up to that point with the weights of the adjacent vertices. If the total cost is lower than the current weight assigned to a specific adjacent vertex, its new weight value is assigned. This process continues until all vertices have been visited, or until the destination vertex is reached, resulting in the determination of the shortest path. Further details of this algorithm can be found in [123].

Another key concept of graph theory utilized in this research is the closeness centrality, a measure that quantifies how easily a vertex can be reached from other vertices within a graph. Closeness centrality is calculated by determining the average shortest path length from the vertex in question to all other vertices in the graph [124]. Vertices with higher closeness centrality values are more central and have a greater influence on the flow of information or resources within the network. Mathematically, the closeness centrality C_C of a vertex i is defined as the reciprocal of the sum of the shortest path lengths from that vertex to all other vertices in the

graph, defined as

$$C_C = \left(\sum_{j \in \Omega_b} d(i,j) \right)^{-1}. \tag{3.51}$$

This measure is particularly relevant for evaluating the efficiency of information dissemination or resource transfer in various real-world applications.

3.6 Network Reconfiguration

Network reconfiguration refers to the process of modifying the topology of the distribution network by opening and closing tie and sectionalizing switches. This operation is performed to achieve some operational goals, such as minimizing power losses, improving voltage profiles, or balancing load among feeders. This process is essential for the optimization of the distribution network, especially in a scenario of increasing energy demand and the need for greater network resilience.

Typically, optimization methods are employed to perform the optimized network reconfiguration. These methods aim to identify the best combination of switch status to meet predefined objectives while adhering to the technical constraints of the system. Commonly applied optimization techniques include metaheuristic algorithms, such as Genetic Algorithms, Particle Swarm Optimization, and Ant Colony Optimization, due to their efficiency in handling the complexity and non-linearity of the problem.

Network reconfiguration offers several advantages. It can significantly reduce active power losses, improve the voltage profile across the system, and enhance the reliability and resilience of the network. Additionally, it allows for better utilization of available infrastructure, postponing the need for costly upgrades or reinforcements. In systems with DERs, reconfiguration can also optimize their integration and enhance the overall system's performance.

The feasibility of network reconfiguration depends largely on the availability and functionality of tie and sectionalizing switches. These switches must be in good working condition and regularly maintained to enable the reconfiguration process effectively. Additionally, the reconfiguration must comply with safety and operational standards, ensuring that all protective devices, such as circuit breakers and relays, remain fully functional. Adhering to these requirements ensures that network reconfiguration can be performed reliably and safely, without compromising the system's ability to handle faults or other operational contingencies.

In this context, during the reconfiguration process, it is important to ensure the radial characteristic of the system due to its protection scheme coordination. According to [125], radial distribution feeders are characterized by having only one path for power to flow from the source, given by the substation bus, to each customer. Maintaining this radial structure not only reduces the costs associated with protection equipment compared to meshed networks but also simplifies fault detection and isolation, enhances operational reliability, and facilitates system restoration

after outages. Additionally, radial networks are easier to manage and require less complex control strategies.

Helmi et al. (2022) proposed in [79] a methodology to ensure the radiality of the distribution system during the reconfiguration process. This methodology is summarized in Algorithm 2.

Algorithm 2 Procedure to ensure the radiality of the distribution network

1: Model the distribution system as a graph $\mathcal{G}$.
2: Calculate the number of switches that must be opened to satisfy radiality conditions.
3: Identify the switches associated with each loop in the graph $\mathcal{G}$.
4: Remove duplicate switches that belong to multiple loops.
5: Open one switch per loop to ensure radial topology.

Firstly, in Line 1 of the algorithm, the distribution system is modeled as a graph $\mathcal{G}$, where buses are represented by vertices and line segments by edges. A radial topology corresponds to a tree structure in graph theory, which is defined as a connected and acyclic graph. For a graph with $|\Omega_b|$ vertices, a tree must have exactly $|\Omega_b|-1$ edges [121]. Therefore, in a system with $|\Omega_b|$ buses and $|\Omega_l|$ lines, $|\Omega_b|-1$ lines must remain closed, while the remaining $|\Omega_l|-|\Omega_b|+1$ line are opened (Line 2). This constraint is mathematically expressed as

$$\sum_{ij\in\Omega_l} s_{h,ij} = |\Omega_b|-1, \quad \forall h \in \Omega_h, \tag{3.52}$$

where Ω_h is the set of time interval and $s_{h,ij}$ corresponds to a binary variable indicating the status of each switch at line ij and time h.

While satisfying this condition is necessary, it does not ensure the elimination of loops in $\mathcal{G}$. To achieve a radial configuration, all loops in the graph must be identified (Line 3). This involves detecting the edges that form part of each loop when all switches are initially closed. Since some switches may belong to multiple loops, duplicate switches must be eliminated (Line 4). Furthermore, to prevent the isolation of buses, adjacent edges incident on a vertex of degree 2 should be grouped into the same loop. Finally, one switch per loop is opened to transform the graph $\mathcal{G}$ into a spanning tree, ensuring a radial topology (Line 5). Figure 6 illustrates a simplified distribution system for the reconfiguration process.

Figure 6 – Simplified representation of a distribution system for reconfiguration.

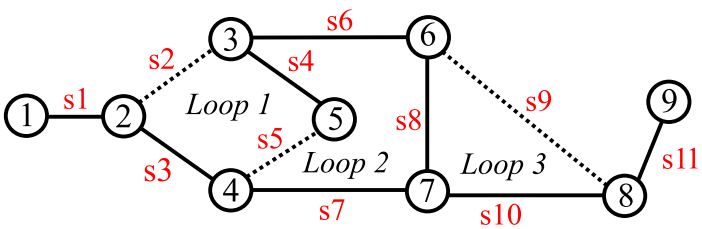

Source: Adapted from [79].

In this system, buses 1 to 9 are represented as vertices 1 to 9, and lines s_1 to s_9 are represented as edges s_1 to s_9. Initially, all switches, including sectionalizing and tie switches, are considered closed. To simplify the graph representation, pendent vertices (vertices connected by only one edge) are temporarily removed along with their incident edges. For example, in Figure 6, vertices 1 and 9 are pendent vertices.

Next, the loops in the system are identified. For the system in Figure 6, the loops are as follows:

- Loop 1: s_2, s_3, s_4, and s_5.
- Loop 2: s_4, s_5, s_6, s_7, and s_8.
- Loop 3: s_8, s_9, and s_{10}.

After identifying the loops, duplicate edges are removed. For instance, edges s_4 and s_5, which are part of both Loop 1 and Loop 2, must be assigned to only one loop. Furthermore, since these edges are incident on vertex 5, which has a degree of 2, they should remain grouped within the same loop to avoid isolating the connected bus during reconfiguration. After these adjustments, the resulting loops can be represented in several ways. One possible configuration is:

- Loop 1: s_2 and s_3.
- Loop 2: s_4, s_5, s_6, and s_7.
- Loop 3: s_8, s_9, and s_{10}.

Finally, a radial topology is achieved by opening one switch per loop. For example, opening switches s_2, s_4, and s_8 results in a radial configuration of the system. This ensures the elimination of all loops while maintaining the system's connectivity.

3.7 Pearson Correlation Coefficient

The Pearson correlation coefficient, often denoted as r, is a statistical measure that quantifies the strength and direction of a linear relationship between two variables. Mathematically, the Pearson correlation coefficient is defined as

$$r = \frac{\sum_{\iota=1}^{\eta}(\chi_\iota - \bar{\chi})(\upsilon_\iota - \bar{\upsilon})}{\sqrt{\sum_{\iota=1}^{\eta}(\chi_\iota - \bar{x})^2 \sum_{\iota=1}^{n}(\upsilon_\iota - \bar{\upsilon})^2}}, \tag{3.53}$$

where χ_ι and υ_ι represent individual data points, $\bar{\chi}$ and $\bar{\upsilon}$ are the means of the respective datasets, and η denotes the total number of data points [126].

The coefficient assumes values within the range -1 to 1, where:

- $r = 1$: Indicates a perfect positive linear relationship, meaning that as one variable increases, the other does so proportionally.
- $r = -1$: Reflects a perfect negative linear relationship, where one variable increases as the other decreases proportionally.
- $r = 0$: Suggests no linear relationship between the variables.

As outlined in [127], the interpretation of the Pearson correlation coefficient is presented in Table 5.

Table 5 – Interpretation of the Pearson correlation coefficient.

Coefficient Magnitude	Interpretation
0.00–0.10	Negligible correlation
0.10–0.39	Weak correlation
0.40–0.69	Moderate correlation
0.70–0.89	Strong correlation
0.90–1.00	Very strong correlation

3.8 Chapter Conclusions

In this chapter, theoretical concepts relevant to this research were thoroughly examined, providing the necessary basis for subsequent analyses and methodologies. The discussion on distribution system modeling highlighted the key principles required to represent and solve power flow equations and compute short-circuit currents, particularly in systems integrating DERs. The exploration of multi-objective optimization techniques and decision-making strategies underscored their significance in addressing complex engineering problems involving conflicting objectives. Furthermore, the incorporation of uncertainty modeling methods emphasized the importance of accounting for real-world variability to enhance the robustness of proposed solutions. The review of graph theory and network reconfiguration processes provided a solid framework for representing and optimizing distribution networks. Lastly, the introduction of the Pearson correlation coefficient offered a statistical tool for quantifying linear relationships between datasets. Collectively, these concepts provide the foundation for the advanced methodologies developed in the subsequent chapters.

Chapter 4

Multi-objective Optimization Approaches

This chapter presents the mathematical formulation, methodology, and results of the four multi-objective optimization approaches proposed in this thesis, organized as follows:

- **Section 4.1** presents the approach proposed to optimize the allocation and sizing of DERs while ensuring the coordination of reclosers and fuses, to preserve the original protection scheme of the network. This section is dedicated to discussing the problem formulation, methodology, and results outlined in the article titled *Multi-objective Optimization Approach for Allocation and Sizing of Distributed Energy Resources Preserving the Protection Scheme in Distribution Networks*, which was published in the *Journal of Control, Automation and Electrical Systems*.
- **Section 4.2** describes the approach proposed to solve the problem of static network reconfiguration, considering the allocation and sizing of inverter-based DERs and capacitors. This section presents the problem formulation, methodology, and results described in the article titled *A Comprehensive Multi-Objective Optimization Framework for Distribution System Planning*, which was published in the *Journal of Control, Automation and Electrical Systems*.
- **Section 4.3** introduces the approach proposed for the optimized allocation and sizing of EVCSs, DERs, and capacitors considering dynamic network reconfiguration. This section depicts the problem formulation, methodology, and results presented in the paper titled *A novel two-stage multi-objective optimization strategy for enhanced network planning and operation*, which was published in the *Electrical Engineering*.
- **Section 4.4** outlines the approach proposed to optimize the performance of the distribution system by simultaneously addressing dynamic network reconfiguration, capacitors allocation, and OLTC transformer adjustment. The approach incorporated stochastic customer-owned DERs and introduced a novel VCI to enhance voltage regulation while minimizing power loss costs. This section presents the problem formulation, methodology, and results outlined in the paper titled *Multi-objective Approach for Distribution System Planning Considering Stochastic Customer-owned Distributed Energy Resources*, which was published in the *IEEE Access*.

4.1 DERs Allocation Preserving the Protection Scheme

In this section, a multi-objective optimization approach is presented for the allocation and sizing of inverter-based DERs in distribution systems. The optimization objectives encompass minimizing investment and operation costs, voltage deviation, and short-circuit current. In addition to the operational constraints of the distribution system, this optimization problem includes the recloser-fuse coordination constraints, in order to preserve the original protection scheme of the network, avoiding the need for adaptive protection schemes, application of FCL or modification of the protective device settings. The recloser-fuse coordination scheme is also carried out using a multi-objective optimization approach to optimize the operating time of the reclosers in both fast and slow modes, as well as the operating time of the fuses.

It is worth noting that the analysis of this multi-objective optimization approach is conducted from the perspective of the DSO. In this context, the DSO assumes responsibility for the substation's operation and the management of DERs. It is also in the operator's interest to ensure the proper operation of the distribution system, even in the presence of DERs. Therefore, the objective functions and constraints of this multi-objective optimization problem are formulated to accurately reflect the operator's objectives. As suggested in [128], this approach is common in countries where the energy sector is showing increased interest in investing in DERs to diversify energy sources. This practice of considering the DSO's perspective, where they are responsible for the allocation and sizing of DERs within the system, has been widely addressed in recent studies, including [39, 44–52, 69–74, 76–79, 82, 83].

4.1.1 Problem Formulation

The problem formulations for the recloser-fuse coordination and DERs allocation are presented in Subsections 4.1.1.1 and 4.1.1.2, respectively.

4.1.1.1 Recloser-fuse Coordination

The multi-objective programming approach used to solve the optimized coordination of the protective devices consists of minimizing the operating time of the reclosers, in fast and slow mode, and the operating time of the fuses. The fuse saving scheme is adopted in this approach to avoid permanent outages during temporary faults, since the fuses require physical replacement after a fault clearing operation [39]. This protection scheme reduces the cost to replace the fuses and the outage time. The decision variables for this optimization problem are defined as follows:

- The time multiplier setting of the recloser R_m in slow mode, denoted by $TMS_{m,sm}$.
- The time multiplier setting of the recloser R_m in fast mode, denoted by $TMS_{m,fm}$.
- The pick-up current of the recloser R_m, represented by Ip_m.
- The fuse characteristic coefficients, denoted by ψ_t and λ_t.

Figure 7a illustrates an example of a distribution system protected by two reclosers and one fuse. It is important to note that the mathematical formulation provided in this section for recloser-fuse coordination is applicable to other system configurations. Figure 7b presents a flowchart outlining the sequence of recloser-fuse operation to ensure selective protection under the fuse saving scheme, where R_m represents the recloser and F_t the fuse. For simplicity, the reclosers are modeled to operate with a fast mode followed by a slow mode. This assumption, while important for analysis and visualization, represents a simplification of real-world operation, where reclosers may exhibit multiple stages of operation with varying timings and retries. Based on the operation sequence depicted in Figure 7, the recloser-fuse coordination constraints can be integrated into the problem formulation.

Figure 7 – (a) Distribution system example for the coordination of protective devices and (b) flowchart to demonstrate the protection scheme.

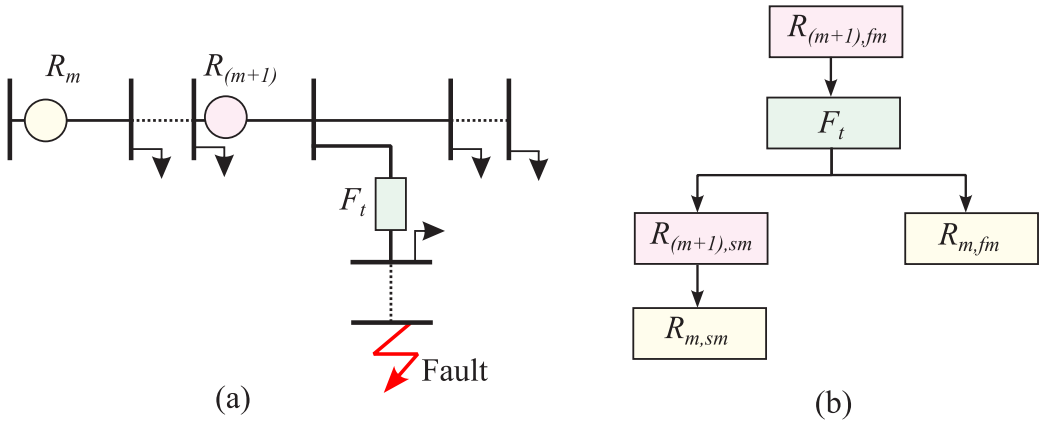

Source: Author.

The mathematical formulation for the recloser-fuse coordination problem is expressed as

$$\min \quad f_1 = \sum_{h\in\Omega_h}\sum_{f\in\Omega_f}\sum_{z\in\Omega_z}\sum_{n\in\Omega_n} T_{R_m,fm,h,f,z}, \tag{4.1}$$

$$\min \quad f_2 = \sum_{h\in\Omega_h}\sum_{f\in\Omega_f}\sum_{z\in\Omega_z}\sum_{n\in\Omega_n} T_{R_m,sm,h,f,z}, \tag{4.2}$$

$$\min \quad f_3 = \sum_{h\in\Omega_h}\sum_{f\in\Omega_f}\sum_{z\in\Omega_z}\sum_{t\in\Omega_t} T_{F_t,h,f,z}, \tag{4.3}$$

where Ω_h, Ω_f, Ω_z, Ω_m, and Ω_t are, respectively, sets of time intervals, fault types, fault locations, reclosers, and fuses; $T_{R_m,sm,h,f,z}$ and $T_{R_m,fm,h,f,z}$ are the operating time of the recloser in slow and fast mode, respectively; and $T_{F_t,h,f,z}$ is the operating time of the fuse.

This optimization problem is subject to

$$TMS^{\min}_{m,sm} \leq TMS_{m,sm} \leq TMS^{\max}_{m,sm}, \quad \forall m \in \Omega_m, \tag{4.4}$$

$$TMS^{\min}_{m,fm} \leq TMS_{m,fm} \leq TMS^{\max}_{m,fm}, \quad \forall m \in \Omega_m, \tag{4.5}$$

$$Ip_m^{\min} \leq Ip_m \leq Ip_m^{\max}, \quad \forall m \in \Omega_m, \tag{4.6}$$

$$T_{F_t} - T_{R_{(m+1),fm}} > CTI, \quad \forall t \in \Omega_t, \forall m \in \Omega_m, \tag{4.7}$$

$$T_{R_{m,fm}} - T_{F_t} > CTI, \quad \forall t \in \Omega_t, \forall m \in \Omega_m \tag{4.8}$$

$$T_{R_{(m+1),sm}} - T_{F_t} > CTI, \quad \forall t \in \Omega_t, \forall m \in \Omega_m, \tag{4.9}$$

$$T_{R_{m,sm}} - T_{R_{(m+1),sm}} > CTI, \quad \forall m \in \Omega_m, \tag{4.10}$$

where CTI is the coordination time interval; $TMS_{m,sm}^{\min}$ and $TMS_{m,sm}^{\max}$ are minimum and maximum time multiplier setting of the recloser R_m in slow mode, respectively; $TMS_{m,fm}^{\min}$ and $TMS_{m,fm}^{\max}$ are the minimum and maximum time multiplier setting of the recloser R_m in fast mode, respectively; and $Ip_m^{\min}$ and $Ip_m^{\max}$ are the minimum and maximum pick-up current of recloser R_m.

The objective functions in (4.1)–(4.3) correspond to the operating times of the reclosers in fast mode, the reclosers in slow mode, and the fuses, respectively. The constraints in (4.4)–(4.6) define the limits of the reclosers' setting parameters, while those in (4.7)–(4.9) address the recloser-fuse coordination based on the fuse saving scheme. Finally, constraint (4.10) specifies the coordination interval between reclosers $R_{(m+1)}$ and R_m.

Furthermore, the fuse characteristic curve, defined by the fuse coefficients ψ_t and λ_t [39, 42], is expressed using a $\log - \log$ function as

$$\log(T_{F_t}) = \psi_t \cdot \log(I^{\text{prot}}) + \lambda_t, \quad \forall t \in \Omega_t, \tag{4.11}$$

where I^{prot} is the current flowing through the protective device and T_{F_t} represents the operating time of the fuse. On the other hand, the inverse-time recloser, which can operate in either fast or slow mode, has its characteristic curve described, respectively, as

$$T_{R_m,fm} = TMS_{m,fm} \cdot \left[\frac{\xi_{m,fm}}{\left(\frac{I^{\text{prot}}}{Ip_m}\right)^{\zeta_{m,fm}} - 1} \right], \quad \forall m \in \Omega_m, \tag{4.12}$$

$$T_{R_m,sm} = TMS_{m,sm} \cdot \left[\frac{\xi_{m,sm}}{\left(\frac{I^{\text{prot}}}{Ip_m}\right)^{\zeta_{m,sm}} - 1} \right], \quad \forall m \in \Omega_m, \tag{4.13}$$

where $\xi_{m,fm}$, $\xi_{m,sm}$, $\zeta_{m,fm}$, and $\zeta_{m,sm}$ are constants specific to the recloser's characteristic curve type [129].

4.1.1.2 Allocation and Sizing of DERs

The multi-objective programming approach employed to optimize the size and location of DERs involves minimizing the system's annualized investment and operation costs, voltage deviation, and short-circuit current. The decision variables for this optimization problem are defined as follows:

- The placement of DERs, denoted by the binary variable z_i, which specifies whether a DER is installed at bus i.
- The operating points of the DERs, characterized by their active power, Pc_i^{DER}, and reactive power, Qc_i^{DER}.

Additionally, the objective functions are defined as

$$\min \quad f_4 = \sum_{i \in \Omega_b} z_i \cdot C^{\text{DER}} + 365 \cdot \sum_{h \in \Omega_h} \left(ec^s \cdot P_h^s + \sum_{i \in \Omega_b} ec^{\text{DER}} \cdot P_{h,i}^{\text{DER}} \right), \tag{4.14}$$

$$\min \quad f_5 = \sum_{h \in \Omega_h} \sum_{i \in \Omega_b} |V_{h,i} - V^{\text{nom}}|, \tag{4.15}$$

$$\min \quad f_6 = \sum_{h \in \Omega_h} \sum_{f \in \Omega_f} \sum_{z \in \Omega_z} IF_{h,f,z}, \tag{4.16}$$

where Ω_b is the set of buses; C^{DER} is the annualized installation cost of the DER; ec^{DER} and ec^s are, respectively, the energy cost for the DERs and substation; and $P_{h,i}^{DER}$ and P_h^s are, respectively, the active power provided by the DER and substation. The variable $V_{h,i}$ is the voltage at bus i and time h; V^{nom} is the nominal voltage of the distribution system; and $IF_{h,f,z}$ is the short-circuit current.

This optimization problem is subject to the following constraints: the distribution system constraints, defined in (3.1)–(3.6); the operational limits of the DER, presented in (3.14)–(3.22); and the recloser-fuse coordination constraints, outlined in (4.7)–(4.10). Additionally, the number of available DERs for allocation is limited by

$$\sum_{i \in \Omega_b} z_i \leq n_{\text{DER}}^{\max}, \tag{4.17}$$

where $n_{\text{DER}}^{\max}$ represents the maximum allowable number of DERs.

4.1.2 Methodology

In this section, the uncertainties related to load demand and the output power of DERs are modeled using the Monte Carlo Method. Specifically, each Monte Carlo scenario is created by randomly selecting load and DER generation profiles from a real-world database, containing records of load, irradiance, and temperature. The irradiance and temperature data are used to create generation profiles for PV-based DERs, following the DER model depicted in Section 3.1.2. It is noteworthy that the methodology outlined in Section 3.4.1 is employed to determine the number of simulations required to ensure the convergence of the Monte Carlo Method.

Figure 8a shows the methodology adopted to store the fault currents at the distribution lines of the system, considering all fault types and locations, hours of the day, and Monte Carlo scenarios. Similarly, Figure 8b shows the methodology adopted to store the load currents at the distribution lines of the system, considering all the Monte Carlo scenarios and hours of the

day. This approach enables the analysis of the system's performance under different stochastic conditions. The short-circuit currents are calculated using the methodology proposed in [96], as detailed in Section 3.2.1, which incorporates the contribution of load currents, given their potential impact on the operation of protective devices. The three-phase power flow solution method, used to achieve the load currents, is the Backward–forward Sweep (presented in Section 3.1.1), due to its simplicity, low computational effort, and high accuracy [91].

Figure 8 – Methodology adopted to store the (a) fault and (b) load currents.

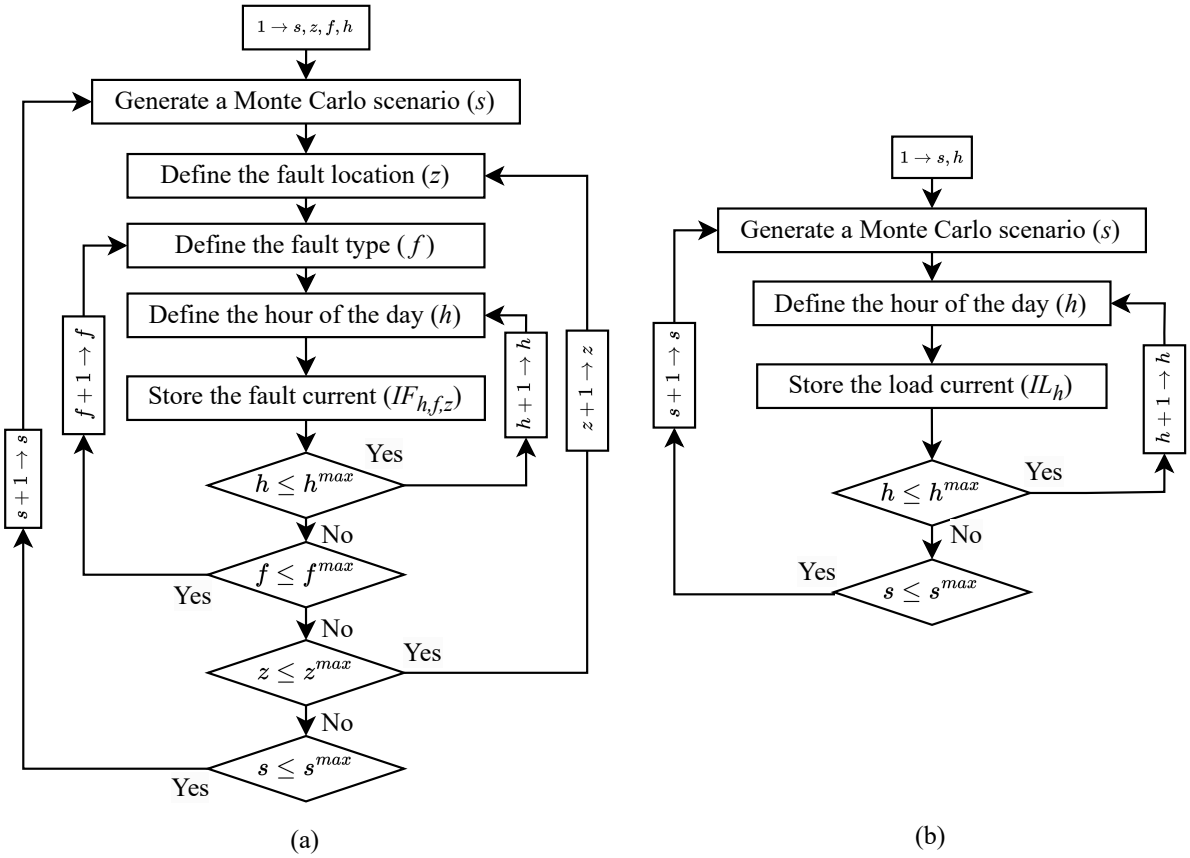

Source: Author.

Figure 9 illustrates the proposed methodology for solving the recloser-fuse coordination and DER allocation and sizing problems. Considering the multi-objective nature and inherent trade-offs of these optimization problems, they are addressed using the NSGA-II introduced by Deb et al. (2002) in [99]. However, the focus of this approach is on the proposed methodology rather than the optimization algorithm itself.

Before executing the algorithm depicted in Figure 9, the parameters of the multi-objective optimization algorithm must be defined. In the context of the NSGA-II utilized in this study, these parameters include the maximum number of individuals, crossover probability, mutation probability, and maximum number of generations [99].

Figure 9 – Methodology proposed to solve the problems of recloser-fuse coordination and DERs allocation and sizing.

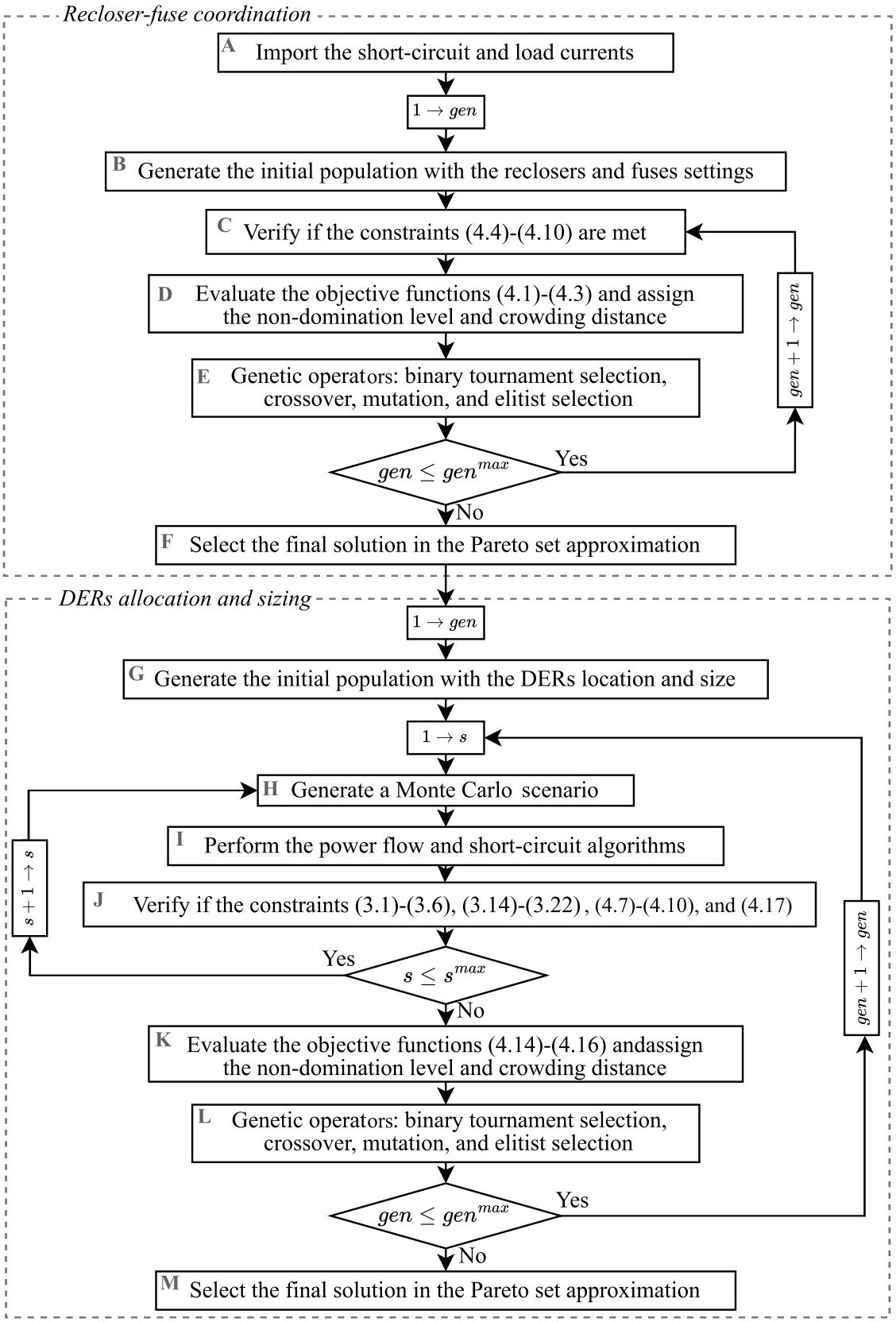

Source: Author.

In Block A, the fault and load currents are imported. In Block B, the initial population of NSGA-II is randomly generated. Each individual's codification in the recloser-fuse coordination problem is represented by the values of time multiplier settings and pick-up currents of the reclosers, as well as the characteristic coefficients of the fuses. Furthermore, the satisfaction of constraints (4.4)–(4.10) is verified in Block C. Then, the objective functions, presented in (4.1)–(4.3), are evaluated in Block D, in order to compute the non-domination levels and the crowding distance of each individual. In Block E, the genetic operators, including binary tournament selection, crossover, and mutation, are applied to generate the offspring population. After completing all generations of NSGA-II, the final solution in the Pareto set approximation is selected (Block F).

In Block G, the initial population, which represents the DERs location and size, is randomly generated. Then, in Block H, a Monte Carlo scenario is generated by selecting load and DERs generation profiles from a real database containing load, irradiance, and temperature data. For each Monte Carlo scenario and each individual in the population, the power flow calculations and short-circuit current computations are carried out (Block I). The fault current contribution of the inverter-based DER is computed based on the methodology proposed in [97], as presented in Section 3.2.2, which takes into account different voltage-dependent control modes, to improve the voltage profile of the system during fault conditions.

Considering these results, it is possible to verify the satisfaction of the constraints in (3.1)–(3.6), (3.14)–(3.22), (4.7)–(4.10), and (4.17) in Block J. Then, the objective functions, presented in (4.14)–(4.16), are evaluated in Block K, in order to compute the non-domination levels and the crowding distance of each individual. In Block L, the genetic operators, including binary tournament selection, crossover, and mutation, are applied to generate the offspring population. After completing all generations of NSGA-II, the final solution in the Pareto set approximation is selected in Block M.

4.1.3 Results and Discussion

This section presents the case study details related to the input data and simulation parameters, in addition to the simulation results regarding the proposed approach.

4.1.3.1 Case study

The four approaches introduced in Sections 4.1–4.4 of this thesis utilize the same dataset comprising irradiance, temperature, and load data, as depicted in Figure 10. In this figure, the load data were collected by Energisa [130], while the solar irradiance and temperaure data were collected by the National Institute of Meteorology [131], over a three-year period (2018–2020) in Campina Grande, Brazil. The irradiance and temperature data are employed to generate profiles for PV-based DERs, based on the output model described in Section 3.1.2.

Figure 10 – (a) Daily load profile, (b) solar irradiance, and (c) temperature data collected over three years (2018–2020) in Campina Grande, Brazil.

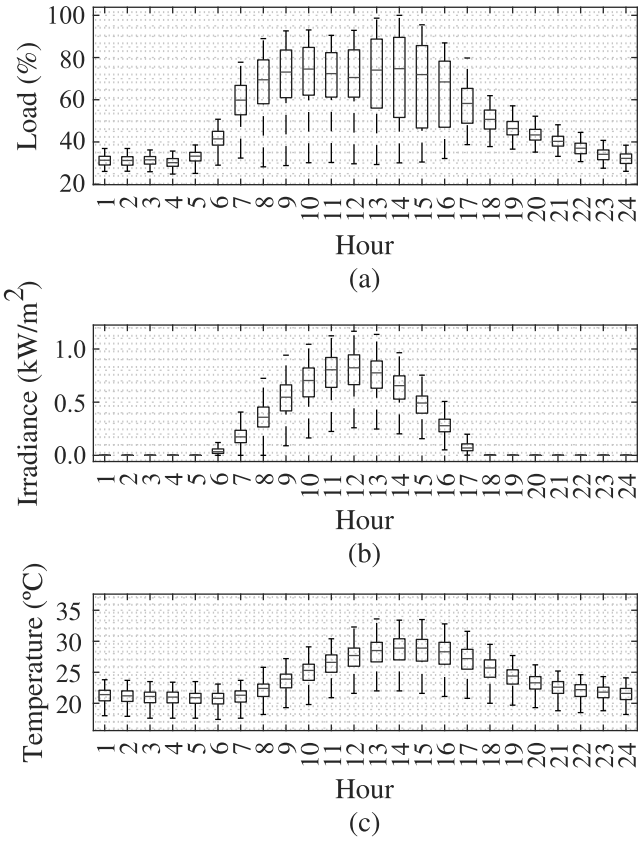

Source: Author.

Furthermore, in this approach, the coordination of protective devices is carried out in the first stage without considering the system's DERs. Only reclosers with very inverse curves, as defined by the International Electrotechnical Commission (IEC) [129], are utilized. Furthermore, in (4.6), Ip_m^{max} is determined by adjusting the smallest short-circuit current passing through the analyzed recloser, multiplied by a factor of 2/3 [39], while Ip_m^{min} is set based on the highest load current in the branch where recloser R_m is located, considering an overload factor of 25% [42]. In (4.4) and (4.5), the maximum and minimum time multiplier setting values are set to 0.05 s and 1.00 s, respectively [38]. It is assumed that the constant ψ_t in (4.11) is the same for all eight fuses, ensuring the use of a uniform fuse type throughout the system. The CTI value in (4.6)–(4.10) is set to 0.20 s [43].

In the second stage, the DERs are allocated while ensuring compliance with the recloser-fuse coordination constraints outlined in (4.6)–(4.10). For the system's operational limits, voltage is maintained in (3.6) between 0.88 and 1.10 pu [92], while current limits are defined by the configuration of the line sections in (3.5). Regarding the DER's constraints, the reactive power capability, presented in (3.14)–(3.17), is defined according to the IEEE 1547-2018 standard [92], and it is assumed in (4.17) that three PV systems are available for allocation. The DER and

substation energy costs expressed in (4.14) are US$ 0.03 and US$ 0.15 per kWh, respectively [132]. The DER's capacities of 50 kW and 100 kW are considered, with annualized investment costs of US$ 10,000 and US$ 20,000, respectively [132].

For the NSGA-II simulations, a population size of 60 individuals is used, with a crossover probability of 90%, a mutation probability of 10%, and a maximum of 400 generations. Additionally, the simulations are carried out using the unbalanced IEEE 34-bus test system, which is shown in Figure 11.

Figure 11 – Representation of the 34-bus test system.

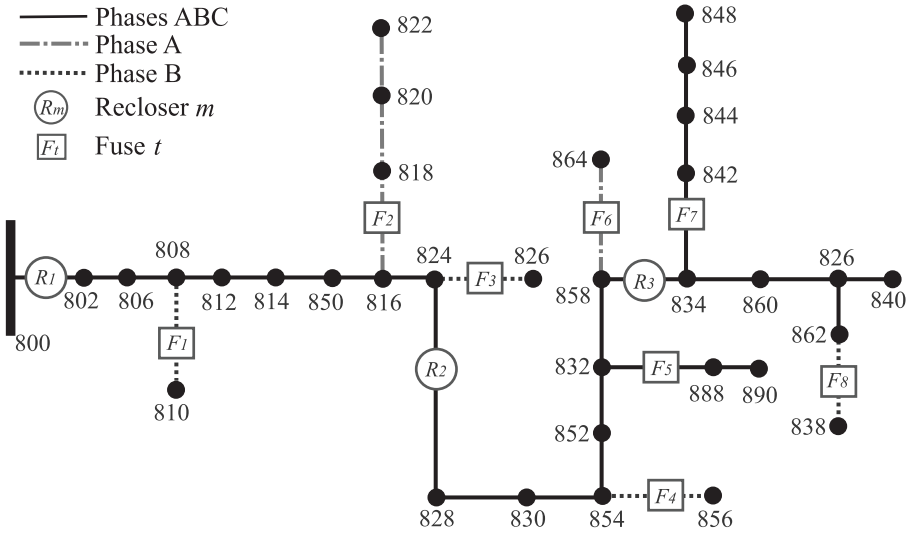

Source: Author.

This system consists of 34 buses and 33 branches, with a nominal voltage of 24.9 kV. However, the slack bus (bus 800) is set to 1.05 pu. The system is characterized by its considerable length and relatively light loading, leading to substantial voltage drops at distant buses due to line impedances. Furthermore, it is an unbalanced three-phase radial system, making it highly representative of real-world distribution systems and increasing the relevance of this study. To support voltage regulation, the system includes two capacitor banks located at buses 844 and 848. Additionally, it originally features two voltage regulators designed to maintain appropriate voltage levels throughout the feeder. However, these regulators are disregarded in the analysis to evaluate the capability of DERs in regulating the system's voltage. Further information regarding the IEEE 34-bus test system are provided in [133].

For providing selective protection based on the fuse-saving scheme, three reclosers in the primary branch and eight fuses in the branches derived from the primary branch are used, as shown in Figure 11. The reclosers protect the entire feeder from temporary faults and provide backup protection for any permanent fault that may occur in the distribution system. In the event of a fault in the primary branch, where there are no upstream fuses, the reclosers must handle both temporary and permanent faults to protect the feeder. Regarding the fuses, they serve as the primary protection against permanent faults occurring in the branch where they are installed. This

configuration allows for quick restoration in case of temporary faults, minimizing disruptions while balancing reliability with operational efficiency.

4.1.3.2 Stage 1: Recloser-fuse Coordination

Table 6 shows the minimum and maximum short-circuit currents passing through the protective devices considering 3-line-to-ground (3LG), Line-to-line (2L), 2-line-to-ground (2LG) and line-to-ground (LG) faults. The minimum and maximum short-circuit current values, for all fault types, are highlighted in bold for each protective device.

Table 6 – Fault minimum and maximum currents at the reclosers and fuses.

	3LG fault (A)		2L fault (A)		2LG fault (A)		LG fault (A)	
	Min	Max	Min	Max	Min	Max	Min	Max
R_1	118.41	644.67	**94.47**	554.84	112.71	652.24	105.55	**665.38**
R_2	117.48	**293.62**	**93.49**	263.71	110.81	280.77	102.50	252.10
R_3	195.41	**201.85**	163.36	181.32	178.21	187.94	**158.43**	173.95
F_1	-	-	-	-	-	-	**416.40**	**417.21**
F_2	-	-	-	-	-	-	**160.76**	**266.67**
F_3	-	-	-	-	-	-	**242.39**	**246.21**
F_4	-	-	-	-	-	-	**180.59**	**182.45**
F_5	113.77	**120.44**	**97.24**	106.03	108.21	115.33	100.75	108.01
F_6	-	-	-	-	-	-	**166.71**	**170.76**
F_7	195.17	**201.58**	164.57	181.29	178.14	187.66	**158.64**	170.14
F_8	195.92	**197.12**	170.59	178.85	178.84	182.84	**158.27**	165.89

3LG: 3-Line-to-ground. 2L: Line-to-line. 2LG: 2-Line-to-ground. LG: Line-to-ground.

Additionally, Tables 7 and 8 present the minimum and maximum load currents passing through the protective devices. These values are considered to set $Ip_m^{\min}$ and $Ip_m^{\max}$.

Table 7 – Load minimum and maximum currents at the reclosers.

		R_1	R_2	R_3
Load current (A)	Min	13.22	9.40	5.76
	Max	45.42	31.92	19.81

Table 8 – Load minimum and maximum currents at the fuses.

		F_1	F_2	F_3	F_4	F_5	F_6	F_7	F_8
Load current (A)	Min	0.14	3.25	0.37	0.03	2.42	0.02	3.81	0.51
	Max	0.58	12.65	1.47	0.14	11.25	0.07	14.41	1.97

Tables 9 and 10 present the optimized parameters of the protective devices that are achieved considering the mathematical formulation of the recloser-fuse coordination problem.

Table 9 – Solution of the NSGA-II regarding the recloser parameters.

Setting	**Recloser**		
	R_1	R_2	R_3
TMS_{sm} (s)	0.90	0.45	0.80
TMS_{fm} (s)	0.20	0.10	0.05
Ip (A)	60.00	54.00	25.00

Table 10 – Solution of the NSGA-II regarding the fuse parameters.

Setting	**Fuse**							
	F_1	F_2	F_3	F_4	F_5	F_6	F_7	F_8
ψ	-1.26	-1.26	-1.26	-1.26	-1.26	-1.26	-1.26	-1.26
λ	7.26	7.01	6.99	6.46	6.44	6.32	5.51	5.49

Based on the determination of the characteristic coefficients ψ and λ for each fuse, it becomes feasible to define commercially available fuses that effectively integrate the proposed protection scheme. For fuses F_1–F_8, the Bussmann series 5.5 kV E-Rated medium voltage fuses for feeder circuits, specifically the MV055 model, are adopted with the following current ratings: 50 A, 30 A, 40 A, 25 A, 20 A, 20 A, 20 A, and 20 A, respectively [134]. Then, using the optimized parameters in (4.12) and (4.13), in addition to the characteristic curve of the fuses previously mentioned, it is possible to reach the coordination between each fuse and its nearest upstream recloser, depicted in Figure 12. The minimum and maximum short-circuit current values for each fuse, presented in Table 6, are highlighted in red in the graphs of Figure 12. Furthermore, the difference in operation time of the protective devices for the aforementioned short-circuit current values is also presented in Figure 12, aiming to demonstrate that the constraints (4.7)–(4.10) are met, since the coordination intervals are higher than CTI.

From Figure 12, it is possible to notice that the reclosers in fast mode will operate for temporary faults, in order to preserve the fuse saving scheme. The fuses will actuate for permanent faults and, for backup protection, the recloser in slow mode shall operate. For this reason, the fuses curves lie well inside the operating times of the reclosers, as shown in Figure 12. Nevertheless, for the faults that occur in the primary branch, where there are no upstream fuses, the reclosers will protect the feeder from permanent and temporary faults. Therefore, based on the coordination curves, presented in Figure 12, it is concluded that for all possible fault types and locations, the protection scheme will work properly according to the sequence of recloser-fuse operation depicted in Figure 7.

Figure 12 – Coordination between the reclosers and fuses: (a) F_1, (b) F_2, (c) F_3, (d) F_4, (e) F_5, (f) F_6, (g) F_7, and (h) F_8.

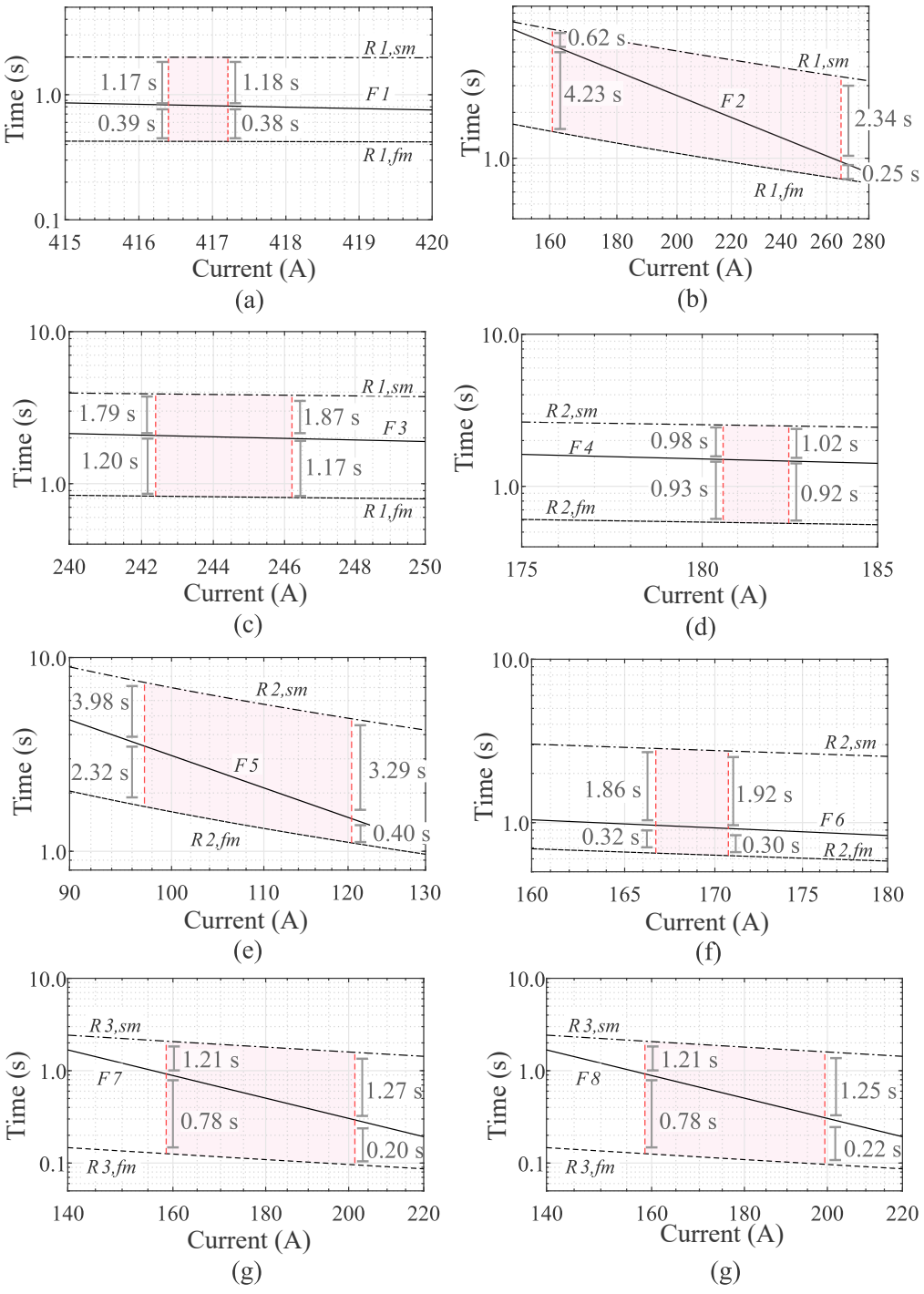

Source: Author.

4.1.3.3 Stage 2: Allocation and Sizing of DERs

The optimized allocation and sizing of DERs in the IEEE 34-bus test feeder is carried out considering the recloser-fuse coordination constraints in order to preserve the protection scheme proposed in Subsection 4.1.3.2. Considering the mathematical formulation of the DERs

allocation and sizing problem, it is possible to reach the Pareto set approximation, shown in Figure 13. In the graphs of Figure 13, the value of 100%, present in the short-circuit and voltage deviation axis, corresponds to the system without DERs.

Figure 13 – Pareto set approximation for the problem of DERs sizing and allocation: (a) three-dimensional chart, (b) vertical view, (c) left view, and (d) front view.

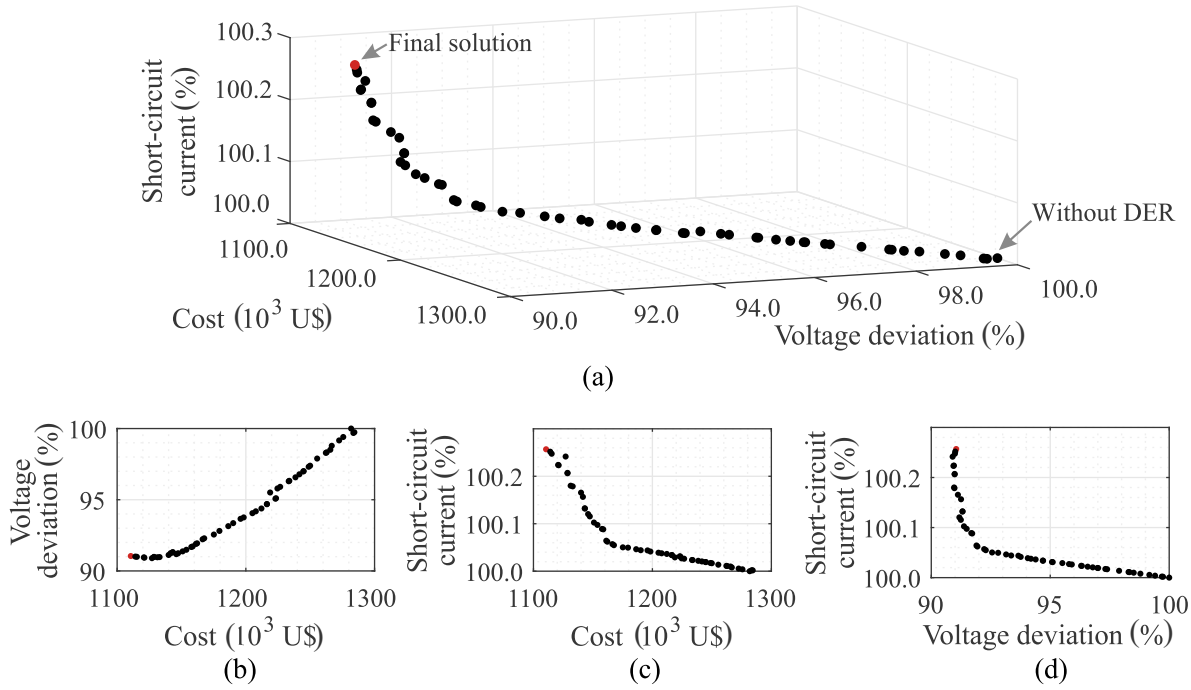

Source: Author.

Based on Figure 13b, it is noticed that the objective functions f_4 (investment cost) and f_5 (voltage deviation) are non-conflicting objectives; consequently, it is possible to achieve the optimized solution considering only f_4 and f_5. Nevertheless, the objective functions f_6 (short-circuit current) and f_4, presented in Figure 13c, are conflicting objectives; thus, the attenuation of the costs promotes an increase in the short-circuit current, due to the fault current contribution of the inverter-based DER. The same behavior can be observed from the analysis of the objective functions f_6 and f_5, which are shown in Figure 13d. All the solutions, present in the Pareto set approximation, are equally valid from the point of view of multi-objective optimization. Therefore, the DSO can choose any of these solutions depending on the decision maker's preferences.

In this study, the solution which mutually minimizes f_4 and f_5, highlighted in red in Figure 13a, is chosen, since the fault current increased by only 0.26%. From this solution, it is possible to achieve a 15.61% and 10.01% reduction of the overall cost and voltage deviation, respectively, when compared to the system without DER. The slight short-circuit current variation, observed in the Pareto set approximation, is due to the DER locations selected by the NSGA-II

combined with the voltage-dependent control modes adopted in this study, which limit the fault current contribution of the DER. The chosen solution presents DERs in buses 852, 888, and 846, with active power of 100, 100, and 100 kW, and reactive power of 26, 22, and 12 kVAr, respectively. From the probabilistic scenarios generated by the Monte Carlo Method, it is possible to obtain the voltage in each bus of the feeder, considering the system without and with DERs. These statistical results are exposed in Figure 14 using a boxplot. It is important to mention that the voltage and current data are plotted between 8 and 16 h, since this time interval presents the highest generation levels.

Figure 14 – Voltage profile considering the system (a) without DER and (b) with DER.

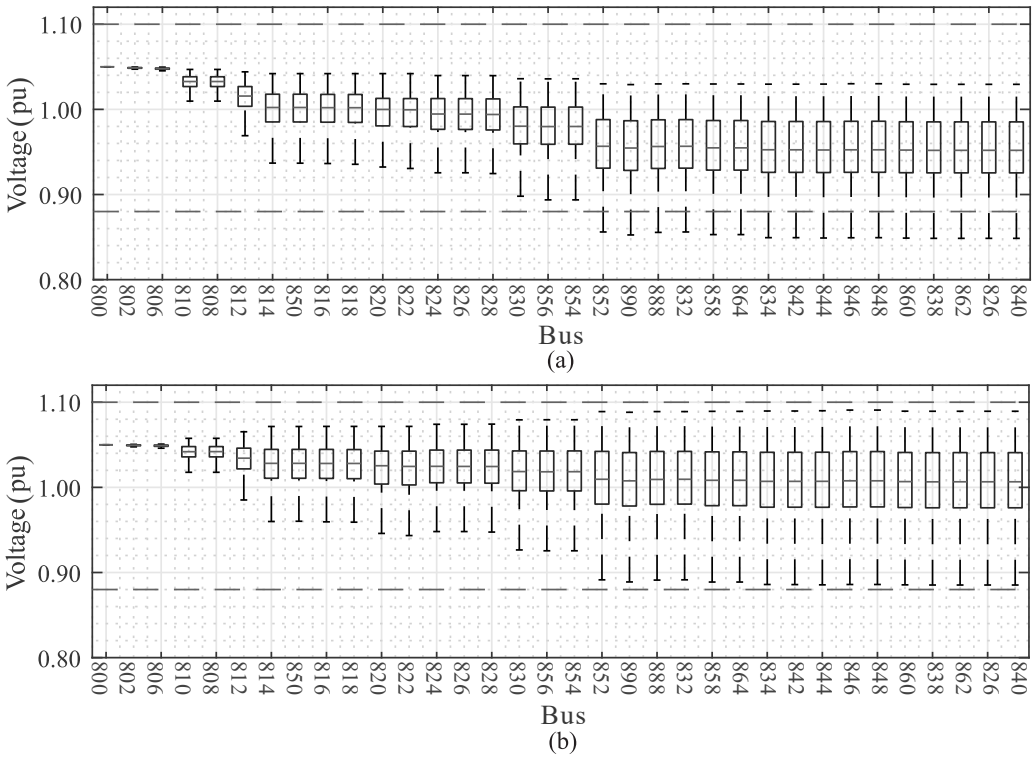

Source: Author.

By comparing Figures 14a and 14b, it can be observed that the DERs integration promoted an improvement in the voltage profile. In this context, the minimum and maximum values (disregarding the outliers), and the lower and upper quartile of the voltage values shifted up. In addition, the variation of the voltage magnitude median along the distribution system is reduced when considering the optimized solution. This reduction is due to the objective function f_2, which minimized by 10.01% the voltage deviation of the system.

The load current of the IEEE 34-bus test feeder is presented in Figure 15, considering the system without and with DERs. From Figures 15a and 15b, it can be noted that the system with DERs presents lower load current values compared to the system without DER. The study conducted in [135] provides supporting evidence for the observed reduction, demonstrating that the allocation of DERs contributes to the minimization of the distribution network currents. The

research findings emphasize the significant influence of DERs location and size on the load current; consequently, the proper allocation and sizing of DERs in the system become important for optimizing the overall system's performance, since the load current decrease leads to the minimization of the network power losses [136].

Figure 15 – Load current considering the system (a) without DER and (b) with DER.

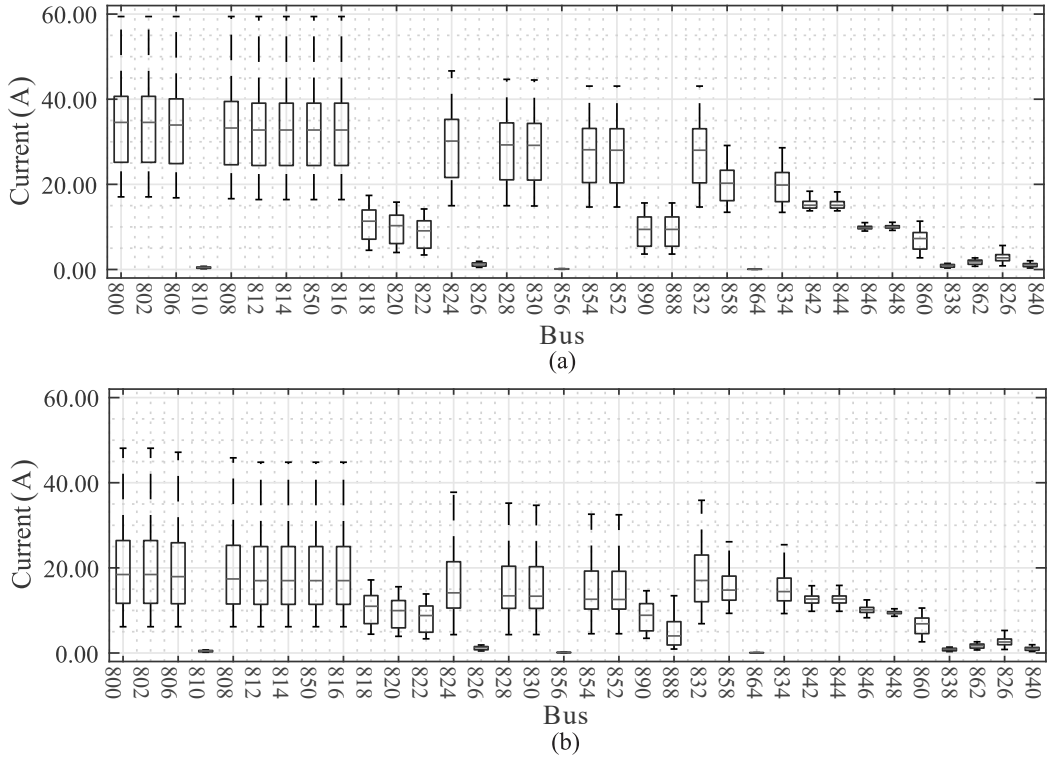

Source: Author.

The fault current is exposed only for the scenario with the DERs allocated in the distribution system, since the short-circuit currents are not substantially modified by the DERs integration, as depicted in Figure 13. Figure 16 shows a boxplot of these currents considering all fault types (3-line, three line-to-ground, line-to-ground, line-to-line and line-to-line-to-ground faults) and the probabilistic scenarios generated by the Monte Carlo Method. It is important to highlight that the x-axis corresponds to the bus in which the fault is applied and calculated. From Figure 16, it is possible to observe the substantial variation of the short-circuit current considering all the fault types and the stochastic nature of the generation and load profile. Furthermore, the fault current reduces as far as the fault moves away from the substation, due to the increase in the line section impedance.

Taking Figures 15 and 16 into account, it is noticed the importance of considering all fault types and the generation and load uncertainties in both mathematical formulations (coordination of protective devices and DERs allocation), since these variables interfere directly in the adjustment of protective devices. Therefore, through the proposed methodology, it is possible to ensure the minimization of the objective functions present in (4.1)–(4.3) and (4.14)–

(4.16), and the correct coordination of reclosers and fuses, regardless of the fault type and location, for the system with and without DERs.

Figure 16 – Short-circuit current at the faulted bus considering a fault application in each bus of the system.

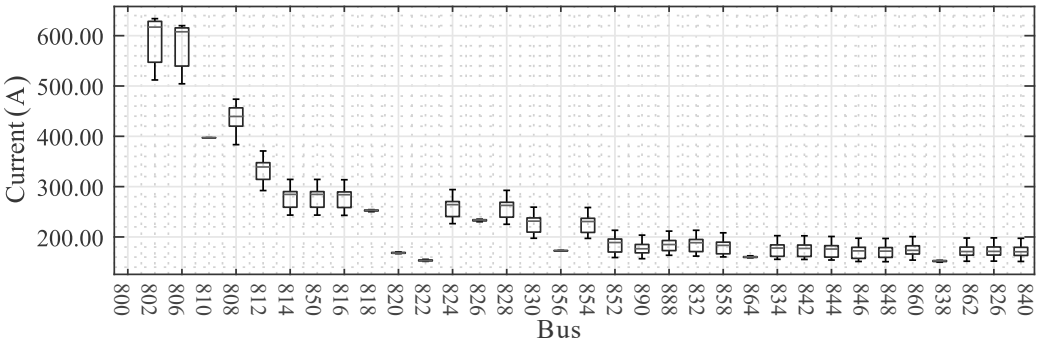

Source: Author.

4.2 Static Approach for Network Operation and Planning

In this section, a multi-objective optimization approach is presented to solve the problem of static network reconfiguration considering the allocation and sizing of inverter-based DERs and capacitors. The objectives of this optimization problem consist of minimizing investment and operation costs, voltage deviation, and power losses.

In line with the previous section, the analysis of the multi-objective optimization approach is conducted taking into account the perspective of the DSO [128]. In this context, the operator manages the costs related to both the substation's and DERs' energy requirements. Additionally, the operator is responsible for carefully determining the optimized placement of DERs and capacitors, in addition to their associated operational and investment costs. It is also in the operator's interest to ensure the proper operation of the distribution system; therefore, it is important to enhance some performance indicators of the distribution system, including power losses and voltage deviation.

4.2.1 Problem Formulation

The static approach for network operation and planning aims to minimize the annualized investment and operation costs, as well as reducing voltage deviation and power losses within the system. This optimization is accomplished through the combination of network reconfiguration and the strategic allocation of DERs and capacitors. The decision variables of this optimization problem are:

- The placement of DERs, denoted by the binary variable z_i, which specifies whether a DER is installed at bus i.

- The placement of capacitors, denoted by the binary variable w_i, which specifies whether a capacitor is installed at bus i.
- The operating points of the DERs, characterized by their active power, $Pc_{h,i}^{\text{DER}}$, and reactive power, $Qc_{h,i}^{\text{DER}}$.
- Nominal reactive power of the capacitors, represented by $Q_{\text{max}}^{\text{cap}}$.
- The status of each tie and sectionalizing switch, given by the binary variable $s_{h,ij}$.

Given the static nature of the proposed approach, the decision variables $Pc_{h,i}^{\text{DER}}$, $Qc_{h,i}^{\text{DER}}$, and $s_{h,ij}$ remain constant for all h in Ω_h.

The objective functions are defined as

$$\min \quad f_1 = 365 \cdot \sum_{h \in \Omega_h} \left(ec^s \cdot P_h^s + \sum_{i \in \Omega_b} ec^{\text{DER}} \cdot P_{h,i}^{\text{DER}} \right) + \sum_{i \in \Omega_b} \left(z_i \cdot C^{\text{DER}} + w_i \cdot C^{\text{cap}} \right), \tag{4.18}$$

$$\min \quad f_2 = \sum_{h \in \Omega_h} \sum_{i \in \Omega_b} |V_{h,i} - V^{\text{nom}}|, \tag{4.19}$$

$$\min \quad f_3 = \sum_{h \in \Omega_h} \sum_{ij \in \Omega_l} P_{h,ij}^{\text{loss}}, \tag{4.20}$$

where Ω_h, Ω_b, and Ω_l are, respectively, sets of time intervals, buses, and branches of the system; C^{DER} and C^{cap} are the annualized installation cost of DER and capacitor, respectively; ec^{DER} and ec^s are, respectively, the energy cost for the DERs and substation; and $P_{h,i}^{\text{DER}}$ and P_h^s are, respectively, the active power provided by the DER and substation. The variable $V_{h,i}$ is the voltage at bus i and time h; V^{nom} is the nominal voltage of the distribution system; and $P_{h,ij}^{\text{loss}}$ is the active power losses in branch ij at time h.

This optimization problem is subject to the following constraints: the distribution system constraints specified in (3.1)–(3.6); the operational limits of DERs described in (3.14)–(3.22); the operational limits of capacitors, depicted in (3.23) and (3.24); the radiality constraint outlined in (3.52); and the number of DERs and capacitors available for allocation, expressed as

$$\sum_{i \in \Omega_b} z_i \leq n_{\text{DER}}^{\text{max}}, \tag{4.21}$$

$$\sum_{i \in \Omega_b} w_i \leq n_{\text{cap}}^{\text{max}}, \tag{4.22}$$

where $n_{\text{DER}}^{\text{max}}$ and $n_{\text{cap}}^{\text{max}}$ are the maximum permissible number of DERs and capacitors, respectively.

To ensure a feasible configuration during the reconfiguration process, this approach applies the methodology proposed in [79], which is elaborated in Section 3.6 of Chapter 3.

4.2.2 Methodology

The inherent multi-objective nature and trade-offs involved in the optimized planning of distribution systems underscore the significance of adopting a multi-objective optimization algorithm. Consequently, the problem of network reconfiguration, combined with the allocation of DERs and capacitors, is addressed using the MOCS method introduced by Yang and Deb (2013) in [105]. Nevertheless, the emphasis of this research is on the proposed methodology rather than the optimization method itself.

Figure 17 shows the flowchart which summarizes the MOCS algorithm adapted to the problem of network reconfiguration considering the allocation and sizing of DERs and capacitors presented in this section. In this flowchart, s is the Monte Carlo simulation and ite is the iteration of the multi-objective optimization.

Figure 17 – Flowchart of the static approach for network operation and planning.

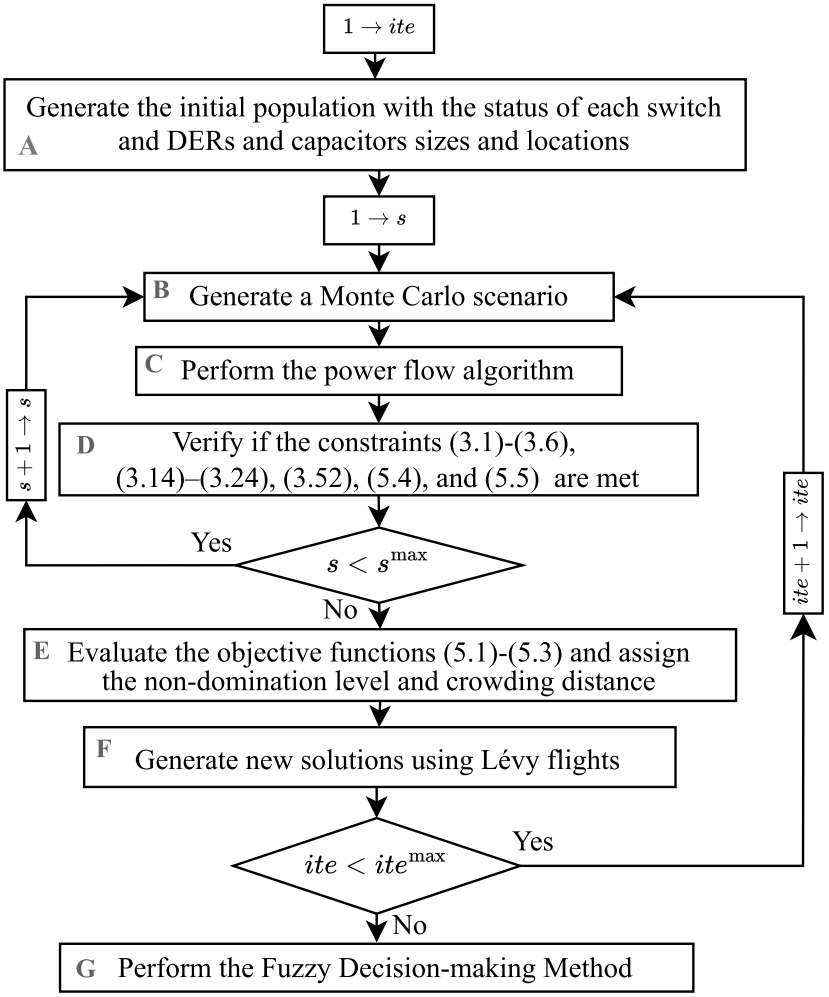

Source: Author.

Before executing the methodology outlined in Figure 17, a real historical database is imported, containing records of load, irradiance, and temperature. The irradiance and temperature

data are used to create generation profiles for PV-based DERs, considering the output model detailed in Section 3.1.2. Additionally, the parameters of the multi-objective optimization algorithm are defined. In the context of the MOCS approach utilized in this study, these parameters include the maximum number of iterations, the discovery probability for outlier solutions, and the number of nests [105].

In Block A of the flowchart presented in Figure 17, the initial population is randomly generated. Then, in Block B, a Monte Carlo scenario is generated by randomly selecting load and DERs generation profiles. It is important to mention the methodology outlined in Section 3.4.1 is employed to determine the number of Monte Carlo simulations required to ensure the convergence of the Monte Carlo Method. For each simulation and each solution in the population, the power flow calculations are carried out in Block C using the Backward–forward Sweep (presented in Section 3.1.1), due to its simplicity, low computational effort, and high accuracy [91]. Considering these results, it is possible to verify the satisfaction of constraints in (3.1)–(3.6), (3.14)–(3.24), (3.52), (4.21), and (4.22) in Block D. In Block E, the objective functions in (4.18)–(4.20) are evaluated with the purpose of computing the non-domination levels and the crowding distance of each solution. In addition, new solutions are generated using Lévy flights in block F. After obtaining the Pareto set approximation in the optimization stage, the Fuzzy Decision-making Method is utilized to determine the compromise solution. This method takes into account the decision maker's preferences, following the framework outlined in Section 3.3.3 (Block G).

4.2.3 Results and Discussion

This section presents the case study details related to the input data and simulation parameters. Additionally, the simulation results regarding the proposed approach are outlined, followed by a comparative analysis with other papers.

4.2.3.1 Case study

The balanced 33, 69, and 136-bus test systems are adopted to evaluate the proposed approach. These systems are predominantly employed in studies addressing network reconfiguration due to the presence of tie and sectionalizing switches, as observed in [49, 56, 63, 65, 67, 69, 70, 72–80, 82, 85, 88]. The 33-bus test system, depicted in Figure 18, consists of 33 buses and 37 branches, including 32 sectionalizing switches and 5 tie switches. The 69-bus test system, shown in Figure 19, comprises 69 buses and 73 branches, with 68 sectionalizing switches and 5 tie switches. The 136-bus test system, illustrated in Figure 20, includes 136 buses and 156 branches, of which 135 are sectionalizing switches and 21 are tie switches. The nominal voltages of the 33, 69, and 136-bus test systems are 12.66 kV, 12.66 kV, and 13.80 kV, respectively. Additional details regarding the loads and lines of these systems are available in [90].

Furthermore, the voltage limits in (3.6) are 0.88 and 1.10 pu, based on IEEE 1547 standard [92]; while the current limits are defined in (3.5) according to the line section configuration. In the 33 and 69-bus test systems, it is assumed in (4.22) that four DERs are available for allocation, considering a nominal active power of 300 kW. These DERs limits are chosen to obtain a penetration level of, approximately, 30% (considering that the penetration level is the ratio between the total DER installed capacity and the total network load). Additionally, in (4.27), four capacitors are available for allocation in these systems. In the 136-bus distribution system, it is assumed that sixteen DERs are available for allocation, considering a nominal active power of 300 kW, to achieve the same DER penetration level of 30%; while sixteen capacitors are available for allocation. The capacitors present five different levels of nominal reactive power: 50, 75, 100, 125, 150 and 175 kVAr, where the investment cost is US$ 30 per kVAr [137]. The investment cost of the DERs is US$ 20,000 per generator [39, 132]. The DERs and substation energy costs employed in (4.18) are US$ 0.03 and US$ 0.15 per kWh, respectively [132].

Figure 18 – Representation of the 33-bus test system.

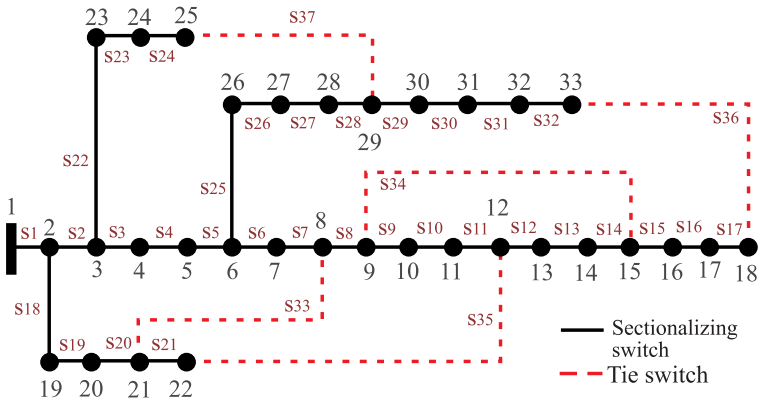

Source: Author.

Figure 19 – Representation of the 69-bus test system.

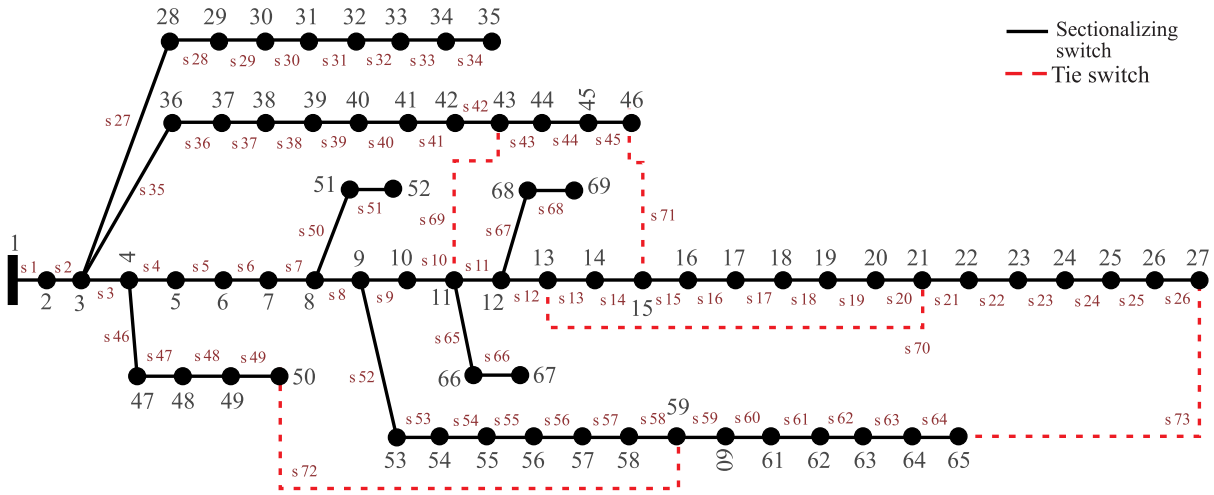

Source: Author.

Figure 20 – Representation of the 136-bus test system.

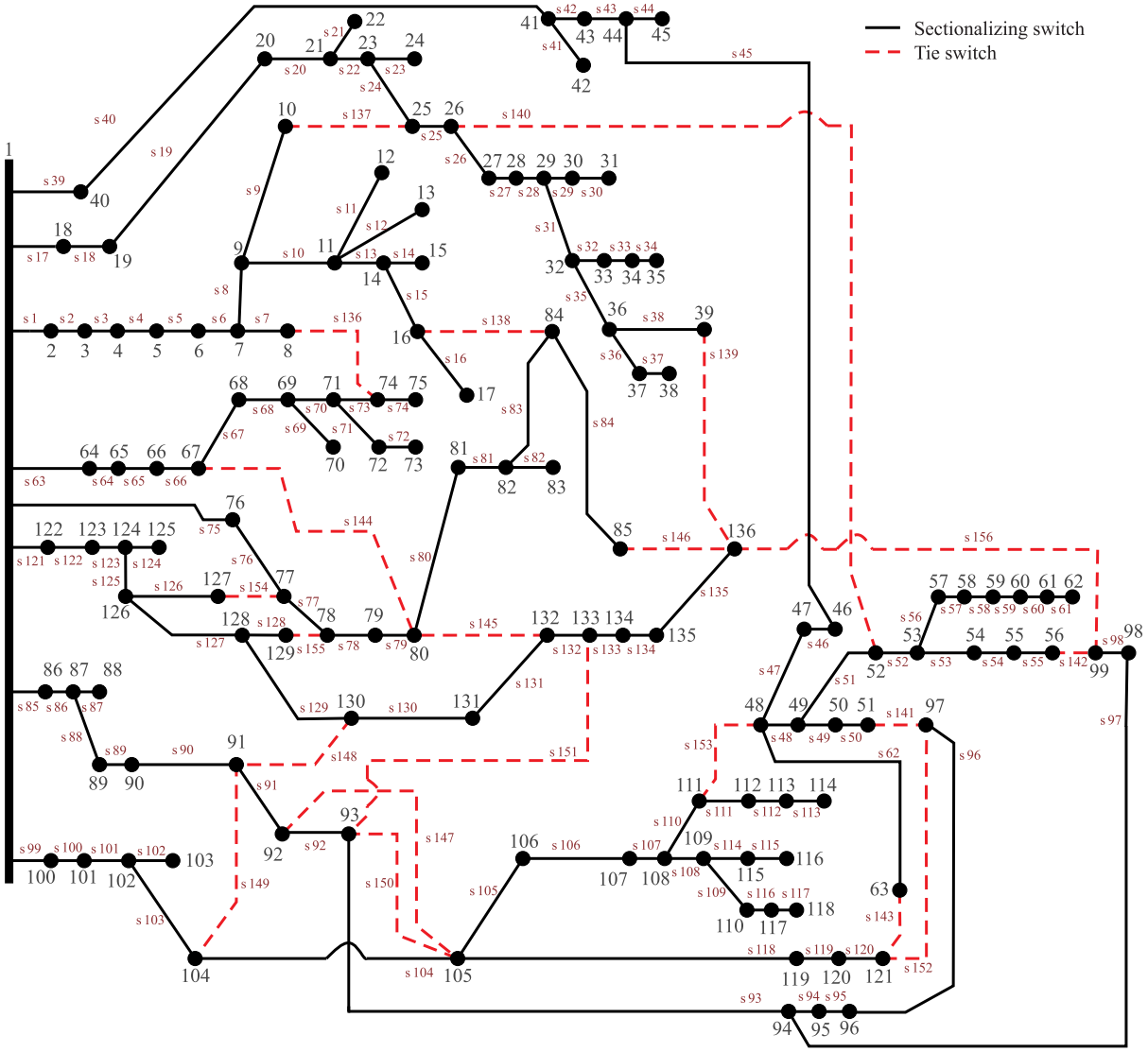

Source: Author.

The MOCS simulations are conducted with 200 nests, a discovery probability of 25%, and a maximum of 100 iterations. In this approach, the Fuzzy Decision-making Method is employed to select the final solution, aiming to equally maximize satisfaction across all objective functions. This is achieved by setting $\widetilde{\Phi}_{f_1(x)}$, $\widetilde{\Phi}_{f_2(x)}$, and $\widetilde{\Phi}_{f_3(x)}$ to 1 in (3.49).

4.2.3.2 Simulation Results

Considering the mathematical formulation proposed in Section 4.2.1, it is possible to reach the Pareto set approximations, as demonstrated in Figure 21 for the 33, 69, and 136-bus distribution systems. Additionally, the Fuzzy Decision-making Method is adopted to obtain the final solution, using (3.48) and (3.49); and this solution is highlighted as $\min(f_1, f_2, f_3)$ in Figure 21. The CSA is also employed to minimize each objective function individually, highlighted as $\min(f_1)$, $\min(f_2)$, and $\min(f_3)$. To ensure consistency, the CSA is executed with the same

parameters of nests and discovery probability as the MOCS, enhancing the comparability of results. This comparative analysis is crucial for comprehending the inherent trade-offs within the objective functions.

From the analysis of Figure 21, it is evident that the three evaluated objective functions are conflicting; therefore, it is not possible to find a solution that minimizes all three objective functions simultaneously. Through the Pareto front approximation, the system operator gains a complete understanding of the inherent possibilities and limitations of the multi-objective optimization problem. As a result, the decision maker acquires a comprehensive view of all potential solutions, facilitating a more straightforward and realistic selection of the most satisfying solution.

Figure 21 – Pareto set approximations for the (a) 33, (b) 69, and (c) 136-bus distribution systems.

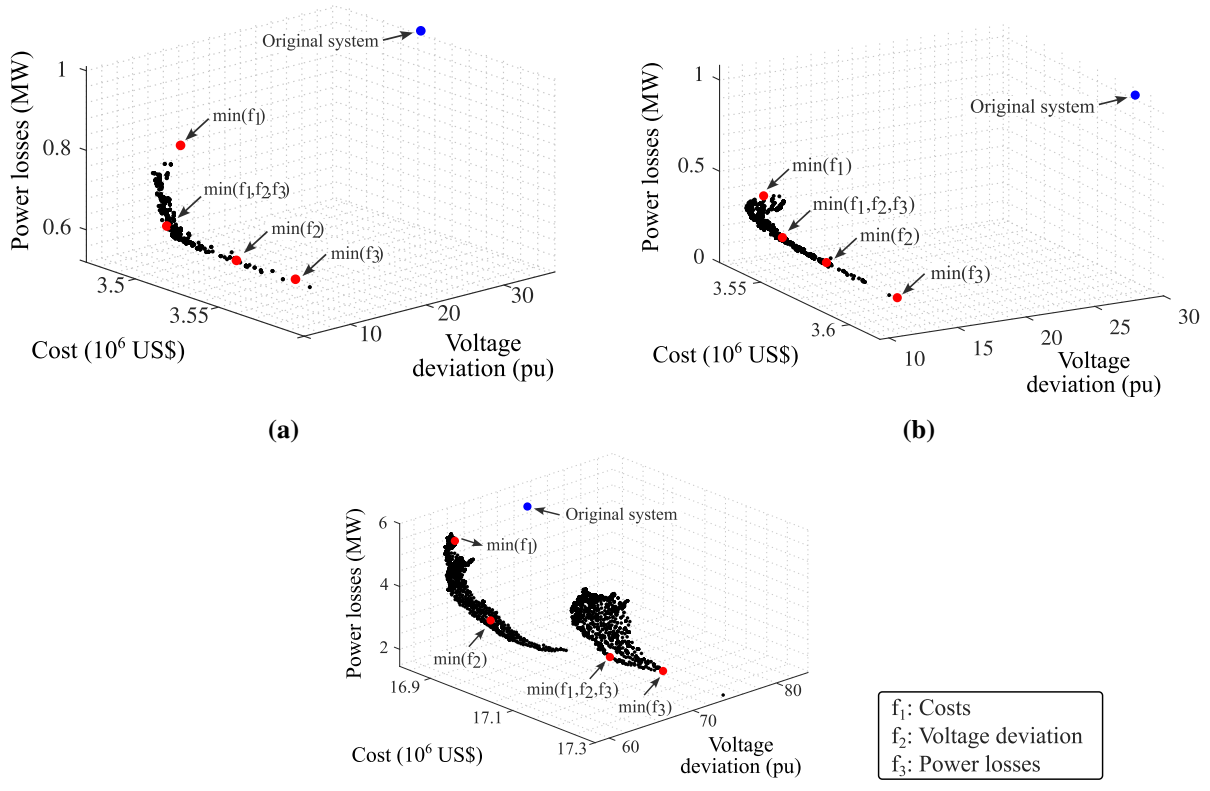

Source: Author.

Table 11 presents the sizes and locations of DERs and capacitors, along with the switches that need to be opened during the reconfiguration process for the 33, 69, and 136-bus distribution systems considering the solutions highlighted in Figure 21. Overall, the DERs and capacitors are strategically placed in buses situated farther from the substation. This allocation aims to minimize power losses within the network by leveraging the proximity of loads to generation units. Furthermore, these specific buses commonly face undervoltage challenges attributed to the

increased equivalent impedance between the substation and the buses. The installation of DERs and capacitors serves to minimize these undervoltage issues effectively.

Table 11 – Solutions of the MOCS and CSA.

System	f_1	f_2	f_3	Opened switch	DER location (size)[1]	Capacitor location (size)[1]
33-bus	✓	✓	✓	33, 34, 10, 36, 28	33(108, 25), 33(123, 17) 30(115, 0)	29(175), 32(175) 32(175), 17(125)
	✓			6, 14, 9, 32, 37	-	30(175), 32(125)
		✓		33, 34, 10, 32, 28	33(161, 44), 32(149, 2) 33(188, 9), 17(233, 21)	31(175), 15(175) 31(175), 30(175)
			✓	33, 34, 9, 17, 27	33(188, 44), 33(232, 24) 33(172, 7), 33(253, 44)	30(175), 29(175) 31(175), 11(175)
69-bus	✓	✓	✓	69, 19, 12, 58, 64	20(113, 4), 64(125, 6)	21(175), 61(150) 62(175), 69(100)
	✓			69, 15, 12, 57, 61	-	61(175)
		✓		69, 20, 12, 58, 61	24(169, 2), 46(99, 30) 45(118, -21), 62(245, -2)	69(175), 60(175) 41(150), 65(175)
			✓	69, 19, 12, 58, 64	60(300, -10), 61(157, 6) 63(138, -9), 69(240, -23)	64(175), 60(175) 69(150), 62(150)
136-bus	✓	✓	✓	1, 8, 13, 139, 140 141, 53, 120, 144 145, 84, 147, 148 149, 150, 151, 152 107, 126, 128, 156	60(99, 43), 93(113, -2) 37(224, 30), 3(165, 13) 81(15, 31), 53(143, 13) 108(185, 40), 56(176, 44) 31(94, 44), 13(167, 33) 28(117, -37), 65(95, 25) 136(155, -28), 47(66, 20)	22 (50), 81(75), 2(175) 42(100), 67(150), 2(175) 84(125), 22(125), 13(125) 128(100), 136(125) 112(150), 131(150) 132(100), 97(100)
	✓			136, 137, 53, 38, 51, 106, 141, 138, 143, 144, 126, 145, 146, 147, 148, 155, 149, 150, 151, 152, 156	-	-
		✓		50, 53, 62, 136, 98, 138, 139, 140, 144 145, 146, 147, 148 149, 150, 151, 152, 107, 126, 155, 137	136(199, 2), 60(241, 44) 61(130, 35), 38(185, -3) 72(153, -40), 24(160, 25) 17(102, 40), 126(89, 31) 104(108, -44), 136(146, 33) 106(169, 1), 113(189, -11) 136(92, 31), 136(114, 44) 97(74, 24), 113(62, -39)	8(100), 67(150), 53(125) 28(50), 97(100), 50(150) 64(75), 91(150), 74(125) 30(175), 136(100) 126(125), 116(175) 120(125), 45(125)
			✓	1, 84, 137, 10, 139 140, 141, 142, 120 144, 145, 147, 148 149, 150, 151, 152 107, 154, 155, 97	82(197, 44), 79(116, -44) 121(174, -27), 136(15, -34) 57(15, 8), 47(15, -44) 39(160, 14), 136(116, 43) 11(179, -12), 10(80, 8) 136(177, -29), 7(182, 17) 108(135, -44), 55(130, -42) 117(110, 17), 136(15, -44)	136(175), 19(175), 2(175) 34(125), 72(175), 33(175) 59(150), 105(75), 2(175) 21(175), 79(125), 136(175) 115(175), 136(175) 121(100), 56(175)

[1]DER size corresponds to active (kW) and reactive power (kVAr), while capacitor size corresponds to reactive power (kVAr).

When the objective was to minimize total costs (f_1) exclusively, no DERs were allocated to avoid the associated investment costs. In the solution where the goal was to minimize only voltage deviation (f_2) or power losses (f_3), the maximum number of DERs and capacitors were

installed in the distribution system. Meanwhile, in the case where the Fuzzy Decision-making Method was applied to simultaneously minimize f_1, f_2, and f_3, an intermediate quantity between 0 and $n_{\text{DER}}^{\max}$ or $n_{\text{cap}}^{\max}$ was allocated. This illustrates the effort to achieve balance between the objective functions.

Figure 22 illustrates the objective functions for the 33, 69, and 136-bus distribution systems. The solutions along the horizontal axis of the graphs represent:

- Solution 1: Baseline case considering the original system.
- Solution 2: Solution minimizing f_1, f_2, and f_3 simultaneously.
- Solution 3: Solution minimizing f_1 only.
- Solution 4: Solution minimizing f_2 only.
- Solution 5: Solution minimizing f_3 only.

Figure 22 – Objective functions considering the (a) 33, (b) 69, and (c) 136-bus distribution systems.

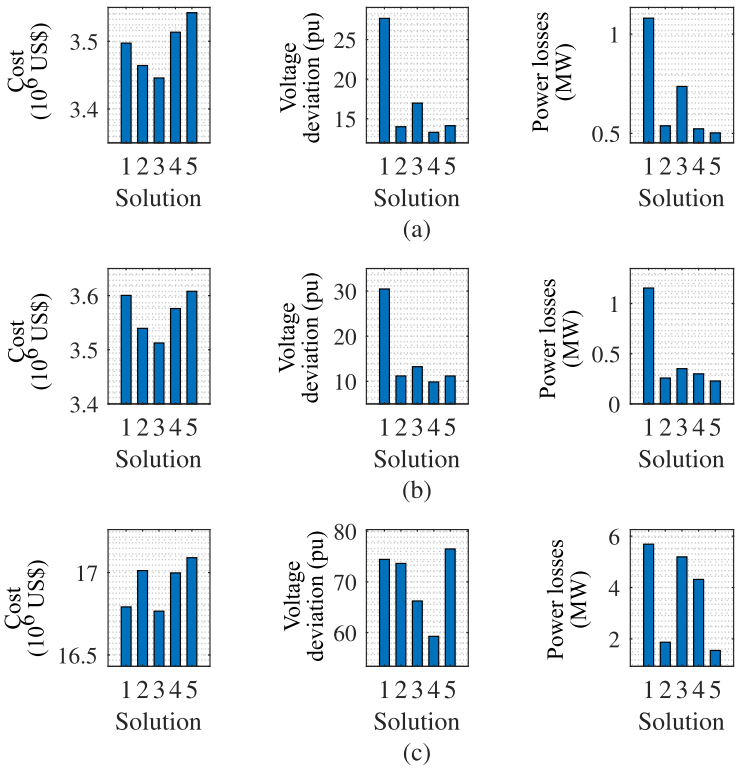

Source: Author.

Initially, it is noticeable that the solutions that only minimized f_3 exhibited the highest total cost values. However, the percentage increase in costs compared to the original system was not significant, representing a percentage change of 1.28%, 0.20%, and 1.77% for the 33, 69, and 136-bus systems, respectively. Subsequently, the solutions that only minimized f_2 presented

the second-highest cost values, with percentage changes, in relation to the original system, of 0.46%, -0.67%, and 1.22%, respectively. This result is attributed to the installation of DERs and capacitors in the system, necessary to minimize voltage deviation and power losses, which escalates investment costs.

As expected, when minimizing only one objective through the CSA, the optimization process achieves the best solution for that specific objective at the expense of the deterioration of the other two objective functions not under consideration. This result arises from the inherent conflicts among these objectives, emphasizing the suitability of multi-objective algorithms in effectively managing such conflicting optimization scenarios. In this regard, the solution obtained through MOCS and the Fuzzy Decision-making Method demonstrates a more balanced outcome across all objective functions.

Considering the 33-bus test system, the MOCS solution resulted in reductions of 0.94% in costs, 49.48% in voltage deviation, and 50.16% in power losses compared to the original system. For the 69-bus test system, the MOCS solution achieved reductions of 1.69% in costs, 63.24% in voltage deviation, and 77.64% in power losses. In the 136-bus distribution system, a significant reduction of 67.08% in power losses was observed, with slight variations in costs (an increase of 1.31%) and voltage deviation (a decrease of 1.07%).

Despite opting for this solution to evaluate the performance of the distribution systems, it is worth noting that other solutions could also be considered, since all of them are equally valid from a multi-objective optimization perspective. Figures 23–25 shows the voltage profile and power losses of the 33, 69, and 136-bus distribution systems, respectively, considering the original and MOCS solution.

Figure 23 – Voltage profile of the 33-bus test system, considering the (a) original and (b) MOCS solution; and power losses, considering the (c) original and (d) MOCS solution.

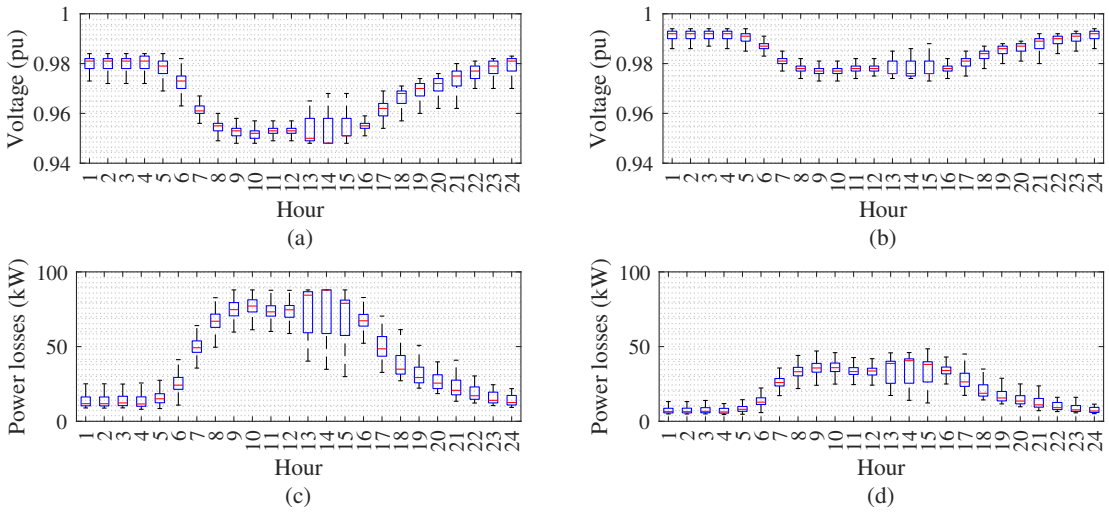

Source: Author.

Figure 24 – Voltage profile of the 69-bus test system, considering the (a) original and (b) MOCS solution; and power losses, considering the (c) original and (d) MOCS solution.

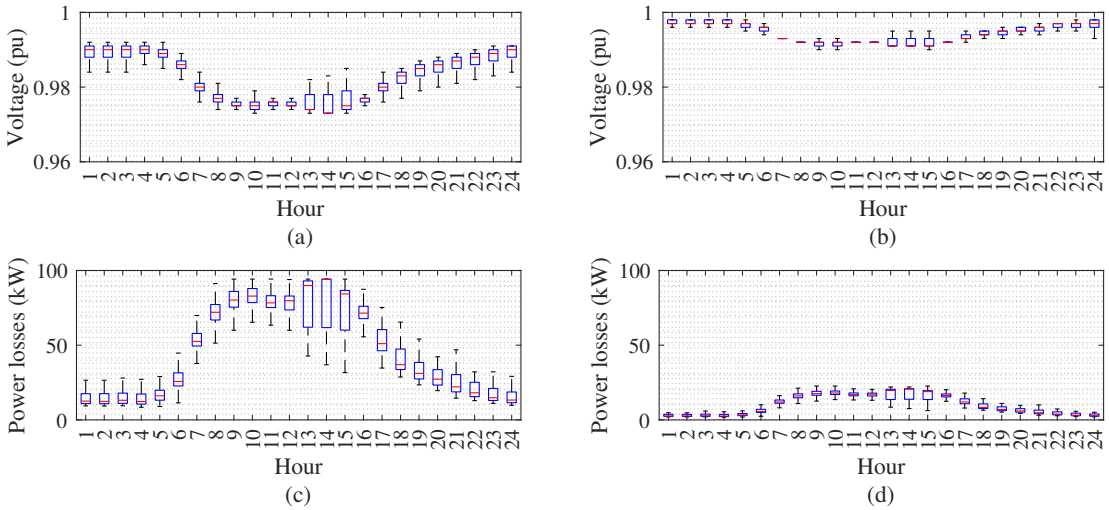

Source: Author.

Figure 25 – Voltage profile of the 136-bus test system, considering the (a) original and (b) MOCS solution; and power losses, considering the (c) original and (d) MOCS solution.

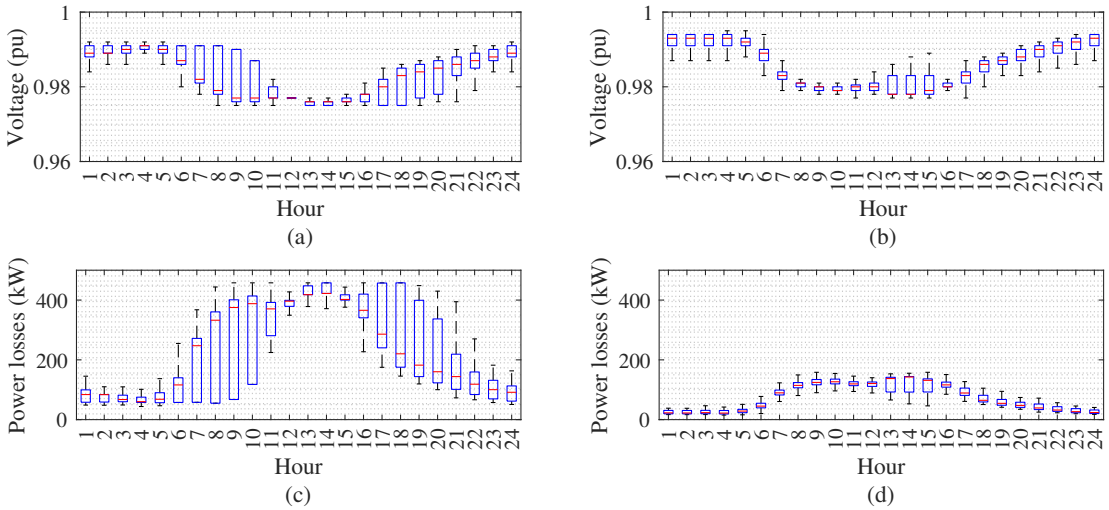

Source: Author.

In general, the optimized solution enhanced the voltage profile of the analyzed distribution systems throughout the day. The support of reactive power, provided by DERs and capacitors, effectively stabilized voltage levels and minimized voltage fluctuations, ensuring consistent and reliable power supply to consumers. The optimized solution also minimized the power losses of the distribution systems, particularly during hours of high load demand. This was achieved by strategically allocating DERs and capacitors to buses close to the highest loads of the system. Additionally, the network reconfiguration also contributes to this reduction in losses by optimizing the distribution network topology.

4.2.3.3 Comparative Analysis

To demonstrate the effectiveness of the multi-objective optimization approach introduced in this section, a comparative analysis is conducted against the strategies introduced in recent articles, outlined as follows:

- Strategy 1: Baseline case considering the original system.
- Strategy 2: Network reconfiguration [79].
- Strategy 3: DERs allocation [39].
- Strategy 4: Capacitors allocation [138].
- Strategy 5: Network reconfiguration and DERs allocation [69, 70, 72–74, 82].
- Strategy 6: Network reconfiguration and capacitors allocation [75, 85].
- Strategy 7: DERs and capacitors allocation [44–47, 51, 52].
- Strategy 8: DERs and capacitors allocation along with static network reconfiguration (proposed in this section).

It is important to note that the articles referenced for each strategy do not utilize the same input parameters and are not evaluated across the same distribution systems. Thus, in this work, these strategies are tested using the same parameters and distribution systems outlined in Section 4.2.3.1, ensuring a direct comparison of the outcomes. Figure 26 shows the objective function results for the 33, 69, and 136-bus distribution systems, taking into account the previously described strategies.

Initially, it is possible to observe slight variations in total costs of the 33, 69, and 136-bus distribution systems compared to the original systems. In this regard, the percentage changes observed when implementing Strategies 2–8 are, respectively, -1.22%, 0.24%, -0.55%, -0.57%, -1.37%, -0.02%, and -0.94% for the 33-bus test system; -2.36%, 0.96%, -0.48%, -1.72%, -2.30%, 0.01%, and -1.69% for the 69-bus test system; and -0.14%, 0.50%, 0.15%, 0.46%, 0.21%, 0.43%, and 1.31% for the 136-bus distribution system. This occurs because, while costs increase with the installation of new devices in the network, they also decrease due to the minimization of power losses in the systems, resulting in low variations in f_1.

Analyzing voltage deviation and power losses in the 33 and 69-bus test systems, a significant reduction is achieved, particularly in strategies involving network reconfiguration (Strategies 2, 5, 6, and 8). Despite the lower impact of DERs and capacitors allocation, it is observed that these strategies enhance the positive impacts of network reconfiguration in minimizing voltage deviation and power losses. Considering the approach proposed in this work (Strategy 8 in the graphs of Figure 26), a substantial reduction in voltage deviation and power losses of 49.48% and 50.16%, respectively, was observed for the 33-bus test system, and 63.24% and 77.64% for the 69-bus test system.

From the analysis of the 136-bus distribution system, it can be concluded that the proposed approach presented a moderate reduction in voltage deviation compared to Strategies 2–7, of only 1.07% when compared to the original system. Regarding power losses, reductions of 24.47%, 8.73%, 7.72%, 7.81%, 31.76%, 11.79%, and 67.08% are observed for Strategies 2–8, respectively, when compared to the original system. Thus, the proposed approach achieved a considerable reduction in this objective function.

It is important to highlight that the favorable results achieved by the proposed approach result from the expansion of the optimization problem search space. This expansion occurs as a result of increasing the flexibility of the distribution system's operation and planning, enabling the exploration of a larger set of non-dominated solutions. Therefore, different solutions can be obtained depending on the priorities and preferences of the DSO. Additionally, the solutions presented in Strategies 2–7 are also part of the search space of the proposed approach, since the optimization model allows the allocation of a number of DERs that is less than or equal to $n_{\text{DER}}^{\text{max}}$ and a number of capacitors that is less than or equal to $n_{\text{cap}}^{\text{max}}$.

Figure 26 – Comparative analysis of the objective functions considering the (a) 33, (b) 69, and (c) 136-bus distribution systems.

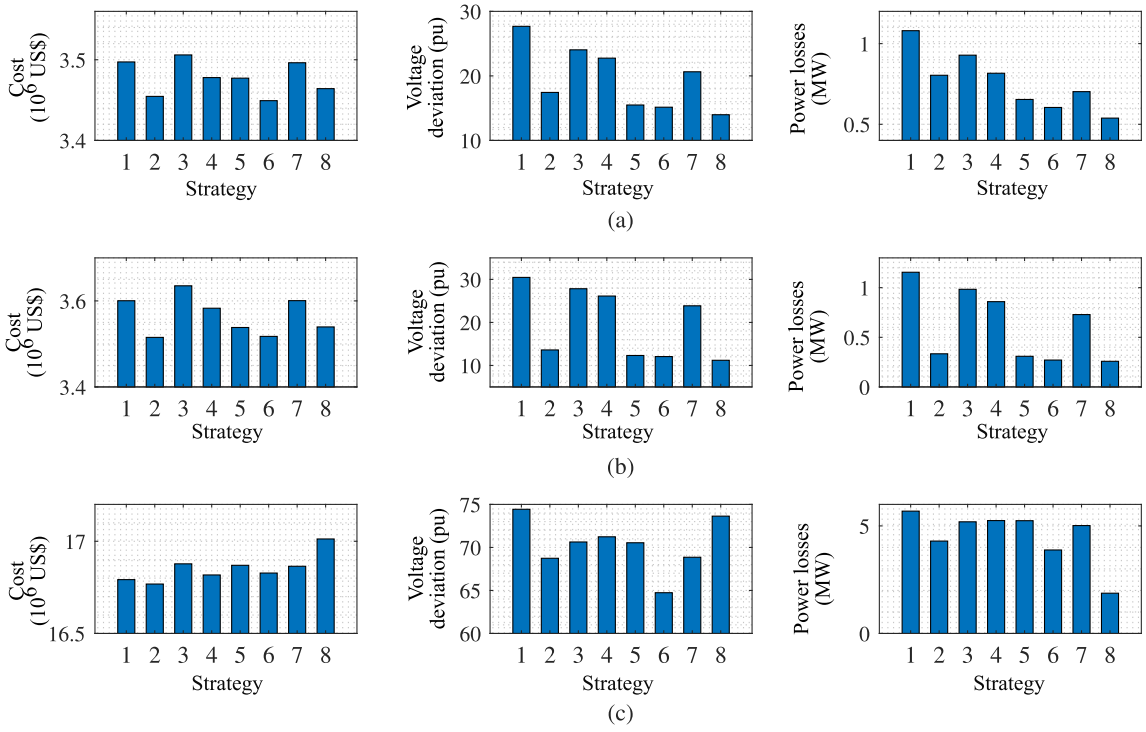

Source: Author.

4.3 Dynamic Approach for Network Operation and Planning

In this section, a multi-objective optimization approach is introduced for the optimized allocation and sizing of EVCSs, DERs, and capacitors considering dynamic network reconfiguration. The objective is to simultaneously minimize investment and operational costs, voltage

deviation, and power losses within the network. In alignment with the preceding sections, the multi-objective optimization approach takes into consideration the perspective of the DSO [128]. Consequently, the operator assumes responsibility for various critical aspects, including the costs associated with the substation, DERs, capacitors, and EVCSs, as well as the overall operation and planning of the distribution system.

4.3.1 Problem Formulation

This section presents the problem formulation of dynamic network reconfiguration combined with the EVCSs, DERs and capacitors allocation. The objectives of this multi-objective optimization problem consist of minimizing the annualized investment and operational costs, voltage deviation, and power losses of the system. The decision variables of this optimization approach are outlined as follows:

- The placement of DERs, denoted by the binary variable z_i, which specifies whether a DER is installed at bus i.
- The placement of capacitors, denoted by the binary variable w_i, which specifies whether a capacitor is installed at bus i.
- The placement of EVCSs, denoted by the binary variable τ_i, which specifies whether a EVCS is installed at bus i.
- The operating points of the DERs, characterized by their active power, Pc_i^{DER}, and reactive power, Qc_i^{DER}.
- The tap positions of the capacitors, represented by $tap_{h,i}^{\mathrm{cap}}$.
- The status of each tie and sectionalizing switch, given by the binary variable $s_{h,ij}$.

The mathematical formulation regarding the proposed dynamic multi-objective optimization approach is expressed as

$$\min \quad f_1 = \sum_{i\in\Omega_b}\left(\tau_i\cdot C^{\mathrm{CS}} + z_i\cdot C^{\mathrm{DER}} + w_i\cdot C^{\mathrm{cap}}\right) + 365\cdot\sum_{h\in\Omega_h}\left(ec^s\cdot P_h^s + \sum_{i\in\Omega_b} ec^{\mathrm{DER}}\cdot P_{h,i}^{\mathrm{DER}} + \sum_{ij\in\Omega_l}|s_{h,ij}-s_{h-1,ij}|\cdot c^s\right), \quad (4.23)$$

$$\min \quad f_2 = \sum_{h\in\Omega_h}\sum_{i\in\Omega_b}|V_{h,i}-V^{\mathrm{nom}}|, \quad (4.24)$$

$$\min \quad f_3 = \sum_{h\in\Omega_h}\sum_{ij\in\Omega_l} P_{h,ij}^{\mathrm{loss}}, \quad (4.25)$$

where Ω_h, Ω_l, and Ω_b are sets of time intervals, branches, and buses, respectively; C^{CS}, C^{DER}, and C^{cap} are the annualized installation cost of EVCSs, DERs, and capacitors, respectively; ec^{DER} and ec^s are, respectively, the energy cost for the DERs and substation; $P_{h,i}^{\mathrm{DER}}$ and P_h^s are

the active power provided by the DERs and substation, respectively; c^s is the switching cost; $V_{h,i}$ is the voltage at bus i and time h; V^{nom} is the nominal voltage of the distribution system; and $P^{\text{loss}}_{h,ij}$ is the active power losses at branch ij and time h.

This optimization problem is subject to the following constraints: the distribution system constraints specified in (3.1)–(3.6); the operational limits of DERs described in (3.14)–(3.22); the operational limits of capacitors, depicted in (3.23) and (3.24); and the radiality constraint outlined in (3.52). Furthermore, the maximum number of DERs, capacitors and EVCSs available for allocation are expressed as

$$\sum_{i \in \Omega_b} z_i \leq n^{\max}_{\text{DER}}, \tag{4.26}$$

$$\sum_{i \in \Omega_b} w_i \leq n^{\max}_{\text{cap}}, \tag{4.27}$$

$$\sum_{i \in \Omega_b} \tau_i \leq n^{\max}_{\text{EVCS}}, \tag{4.28}$$

where $n^{\max}_{\text{DER}}$, $n^{\max}_{\text{cap}}$, and $n^{\max}_{\text{EVCS}}$ denote the maximum permissible number of DERs, capacitors, and EVCSs, respectively.

The maximum number of switching actions (Δs^{dyn}) required to transfer from one state to another is given by

$$\sum_{ij \in \Omega_l} |s_{h,ij} - s_{h-1,ij}| \leq \Delta s^{dyn}, \quad \forall h \in \Omega_h, \tag{4.29}$$

since frequent switching can not only compromise the system's stability but also shorten the lifespan of these devices, as discussed in [139, 140].

4.3.2 Methodology

Figure 27 shows the proposed methodology in this section, which is divided into two stages to separate decision variables that remain constant over time (e.g., location of DERs, EVCSs, and capacitors) from those that can be adjusted in real-time (e.g., network configuration, capacitors taps, and DERs operating points). In this figure, s is the Monte Carlo simulation, ite is the iteration of the multi-objective optimization, and h is the time of the day. The first stage of the approach addresses a planning problem, focusing on the allocation and sizing of EVCSs, DERs, and capacitors. In contrast, the second stage covers an operation problem, concentrating on the dynamic network reconfiguration and the adjustment of capacitor taps and DERs operating points.

Given the multi-objective nature and trade-offs inherent in optimizing distribution systems, the MOCS method and the NSGA-II are employed to solve the optimization problem. These methods are compared to determine the most suitable approach for this context. However, the primary focus of this study lies in the proposed methodology rather than the specific optimization algorithm used.

Figure 27 – Flowchart of the dynamic approach for network operation and planning.

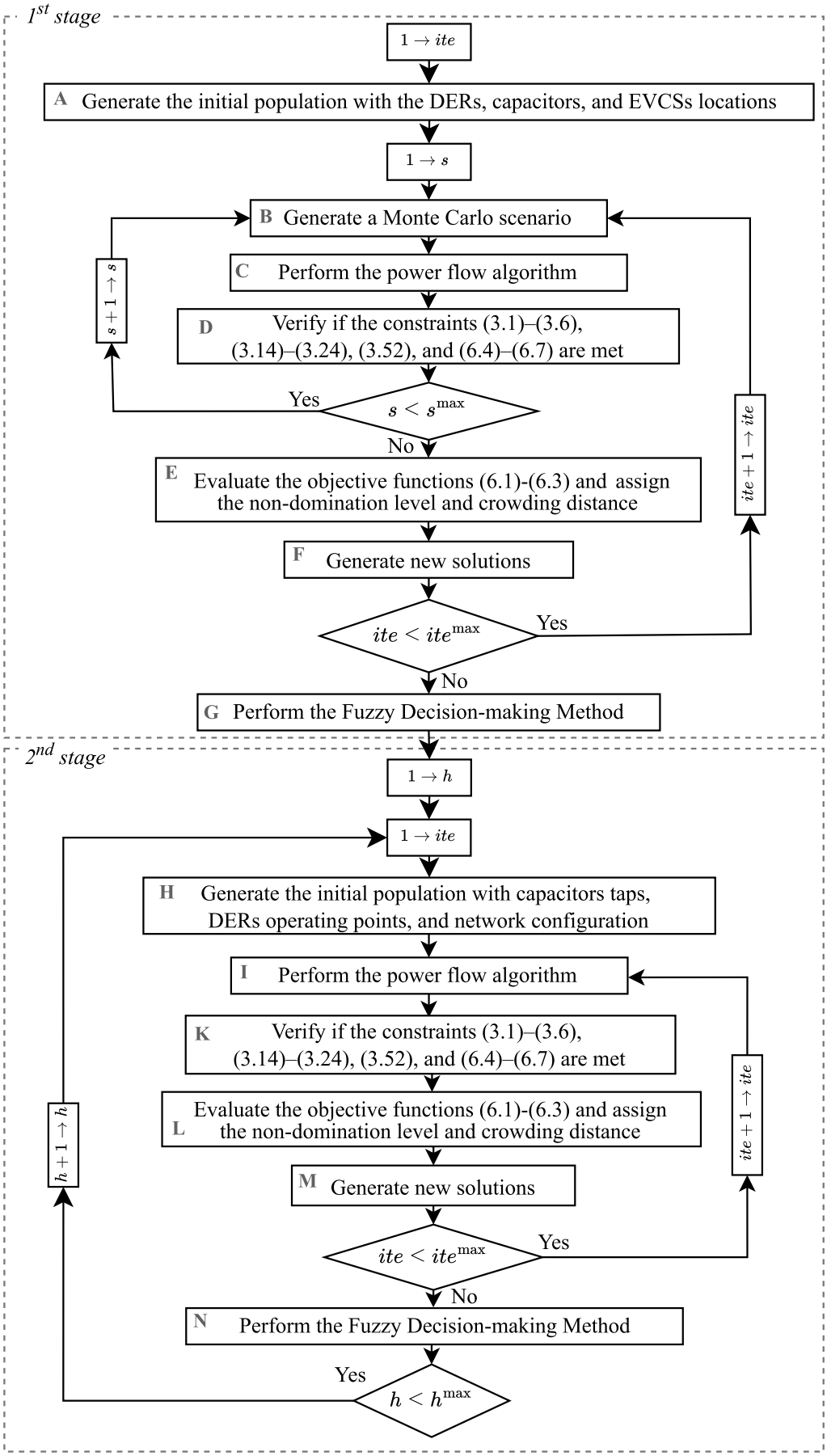

Source: Author.

Before implementing the methodology outlined in Figure 27, a real historical database is imported, containing records of load, irradiance, and temperature. The irradiance and temperature data are utilized to generate profiles for PV-based DERs, considering the output model described in Section 3.1.2. Additionally, the parameters for the multi-objective optimization algorithms are defined. For the MOCS method, these parameters include the maximum number of iterations, the discovery probability for outlier solutions, and the number of nests [105]. Conversely, the NSGA-II requires parameters such as the maximum number of individuals, crossover probability, mutation probability, and maximum number of generations [99].

The first stage of Figure 27 starts at Block A, where the initial population is randomly generated, encompassing the locations of EVCSs, DERs, and capacitors. Subsequently, a probabilistic approach, utilizing Monte Carlo Method, is employed in Block B to address the uncertainties related to load, power generation from each DER unit, and the distribution of EVs. In this context, the methodology outlined in Section 3.4.1 is employed to determine the number of Monte Carlo simulations required to ensure the convergence of the Monte Carlo Method. The procedure for obtaining the stochastic EVs distribution throughout the day is outlined in Algorithm 3.

Algorithm 3 EVs distribution during the day

1: Define the number EVs, $n_{\text{EV}}^{\max}$, in the distribution system
2: **for** $n_{\text{EV}}, \ldots, n_{\text{EV}}^{\max}$ **do**
3: Distribute the EV in the system according to the buses' closeness centrality
4: Define the time that the EV will travel - Figure 28
5: Define the EV SoC - Figure 29a
6: Verify if the EV will be recharged - Figure 29b
7: Define the EVCS that will recharge the EV based on the shortest path between the EVCSs and the EV
8: **end for**

Source: Author.

In Line 1 of Algorithm 3, the number of EVs present in the system is determined. Subsequently, the closeness centrality of each bus is calculated using (3.51) to assess the probability of allocating an EV at a particular bus (Line 3). This approach ensures that EVs are primarily allocated to central buses within the distribution network. The traffic probability, shown in Figure 28, obtained from the mass probability function detailed in [141], is employed in Line 4 to determine the time of day when the EVs will be travelling.

Additionally, the State of Charge (SoC) probability mass, depicted in Figure 29a, is adopted in Line 5 to determine the SoC of the EVs. Taking into consideration the EVs' SoC, the EVs recharging probability presented in Figure 29b is considered in Line 6 to determine if an EV will recharge. To establish the most suitable EVCS for recharging, the algorithm utilizes the

Dijkstra algorithm to compute the shortest paths between the EV and the available EVCSs. The EV will be directed to the nearest EVCS that has at least one available charger. In the event that the closest EVCS is fully occupied, the EV will be directed to the next closest EVCS, and so forth.

Figure 28 – Daily traffic probability of EVs.

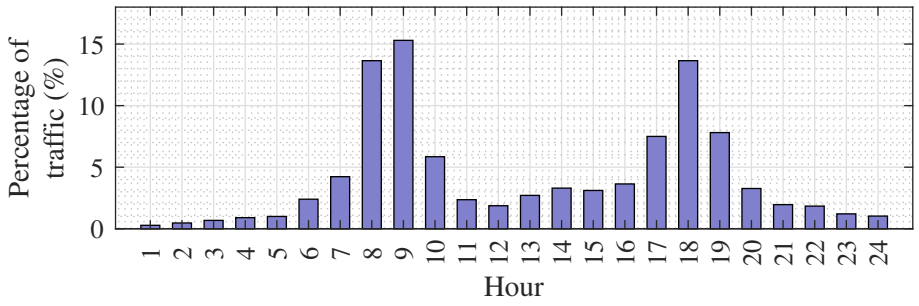

Source: Adapted from [141].

Figure 29 – State of Charge probabilities: (a) probability mass function and (b) EVs recharging probability.

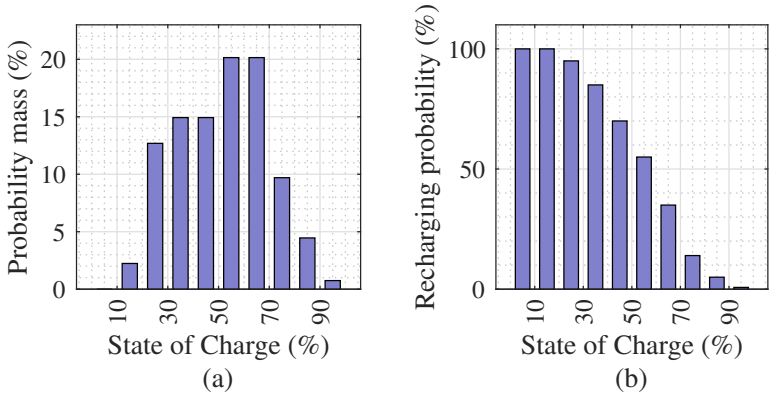

Source: Adapted from [142].

The Backward-forward Sweep Method, detailed in Section 3.1.1, is utilized in Block C of Figure 27 to solve the power flow equations [91]. In Blocks E and D, the objective functions (4.23)–(4.25) and constraints (3.1)–(3.6), (3.14)–(3.24), (3.52), and (4.26)–(4.29) are evaluated to determine the non-domination levels and crowding distances for each individual. Subsequently, new solutions are generated in Block F using exploration and exploitation mechanisms. In NSGA-II, genetic operators such as crossover and mutation are used to generate new solutions, whereas in MOCS, new solutions are generated using Lévy flights. After obtaining the Pareto set approximation in the first stage, the Fuzzy Decision-making Method, presented in Section 3.3.3, is applied to find the compromise solution based on the decision maker's preferences.

The second stage starts at Block H, where the initial population is initialized with the status of tie and sectionalizing switches, the capacitors taps, and the DERs operating points. In

Blocks L and K, the solutions are evaluated, considering the objective functions (4.23)–(4.25) and the constraints (3.1)–(3.6), (3.14)–(3.24), (3.52), and (4.26)–(4.29). Subsequently, new solutions are generated, evaluated, and combined with the previous solutions in Block M. Finally, the Fuzzy Decision-making Method is employed to determine the compromise solution.

4.3.3 Results and Discussion

This section presents the case study details, the simulation results of the proposed approach, and a comparative analysis with other approaches.

4.3.3.1 Case Study

In this approach, DERs, capacitors, and EVCSs are allocated in the 33-bus test system (Figure 18) along with the dynamic network reconfiguration. In the context of EVs, there are two EVCSs in (4.28) available for allocation, each with an investment cost of US$ 70,000 per station [143, 144]. Each EVCS can accommodate up to 20 chargers, and the investment cost per charger is US$ 10,416.50 [143, 144]. The strategic allocation of these EVCSs and chargers is essential to avoid queues and enhance the service for EV users. This study considers a total of 100 EVs, each equipped with a battery having a capacity of 24 kWh [113]. For the allocation of DERs, it is assumed in (4.26) that two generators are available, each with a nominal active power of 100 kW and an investment cost of US$ 20,000 per generator [132]. The energy costs for the DERs and the substation employed in (4.23) are US$ 0.08 and US$ 0.15 per kWh, respectively [132].

Additionally, there are two capacitors available in (4.27) for allocation, offering five distinct levels of reactive power: 50, 75, 100, 125, and 150 kVAr, according to the tap position. The investment cost for each kVAr of the capacitors is US$ 30 [137]. Concerning the operational limits of the distribution system, the voltage limits in (3.6) are set at 0.88 and 1.10 pu [92], while the current limits in (3.5) are defined according to the configuration of the line sections. The maximum number of switching actions to transfer from one state to another in (4.29) is limited to 4 [139], with a cost of US$ 5 per each switching operation [145].

The MOCS simulations are conducted with 100 nests, incorporating a 25% discovery probability and a maximum of 100 iterations. Additionally, the NSGA-II simulations are carried out considering 100 individuals across 100 generations, with a crossover probability of 90% and a mutation probability of 10%. The Fuzzy Decision-making Method is employed in this approach to select the final solution, aiming to equally maximize satisfaction across all objective functions. This is achieved by setting $\widetilde{\Phi}_{f_1(x)}$, $\widetilde{\Phi}_{f_2(x)}$, and $\widetilde{\Phi}_{f_3(x)}$ to 1 in (3.49).

4.3.3.2 Simulation Results

Firstly, the MOCS is employed to solve the problem formulation presented in Section 4.3.1 for the planning stage outlined in Figure 27. In this stage, the decision variables are the

locations of the DERs, capacitors, and EVCSs, which remain constant over time. The Pareto front approximation for this planning stage, obtained through the MOCS, is presented in Figure 30.

In the final solution, achieved through the Fuzzy Decision-making Method, the EVCSs are installed at buses 2 and 19, with 14 and 3 charger units, respectively. The DERs are installed at buses 17 and 18, and the capacitors are installed at buses 18 and 31. Considering this solution, the overall cost, voltage deviation, and power losses are US$ 3.74×10^6, 23.44 pu, and 1.07 MW, respectively. In the original system, without EVCSs, DERs, and capacitors, the overall cost, voltage deviation, and power losses are US$ 3.32×10^6, 26.28 pu, and 1.25 MW, respectively. Therefore, the planning stage increased the overall cost by 12.85%, while reducing the voltage deviation and power losses by 10.83% and 14.17%, respectively.

Figure 30 – Pareto set approximation for the planning stage.

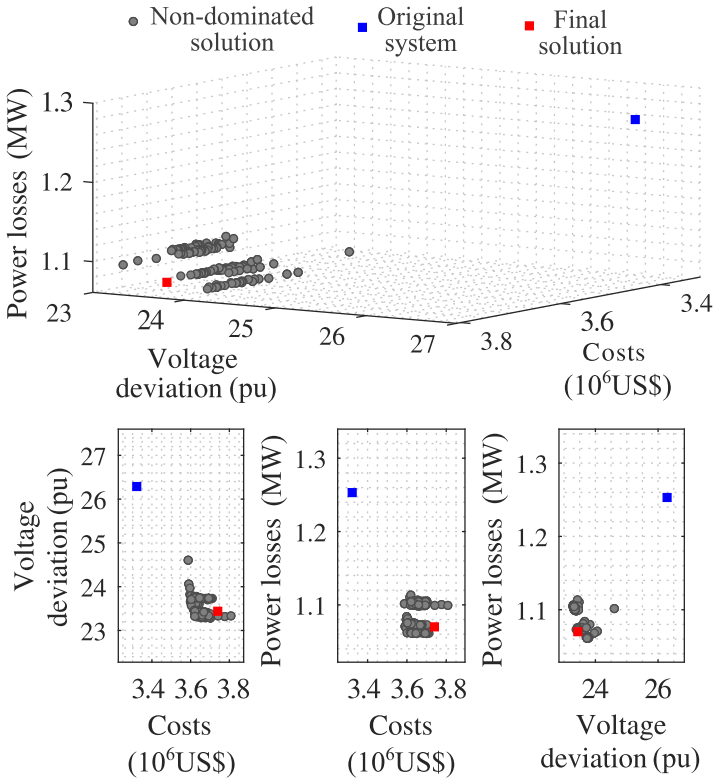

Source: Author.

It is important to highlight that the increased cost is primarily caused by the investment expenses associated with EVCSs, which are required to meet the increasing load demand from EVs. Despite the additional load demand from EVs, the proposed solution effectively reduced both f_2 (voltage deviation) and f_3 (power losses), demonstrating the efficiency of the planning stage in enhancing the overall performance of the distribution system.

Subsequently, considering the final solution of the planning stage, the MOCS is employed to solve the problem formulation presented in Section 4.3.1 for the operation stage outlined

in Figure 27. With the solution of the operation stage, the overall cost, voltage deviation, and power losses are US$ 3.70×10^6, 14.32 pu, and 0.58 MW, respectively. Consequently, in the operation stage, where dynamic network reconfiguration and adjustments of capacitor taps and DER operating points are carried out, it is possible to reduce the overall cost, voltage deviation, and power losses by 0.95%, 38.88%, and 53.05%, respectively, compared to the first stage solution. This emphasizes the importance of implementing an operational strategy, in addition to planning, to improve the overall performance of the system.

Although a historical database covering a period of three years is considered, the following results correspond to one day, as the variables exhibit similar behavior over different days. Figure 31 shows the reactive power output of the DERs, the tap positions of the capacitors, and the switch status for the dynamic network reconfiguration.

Figure 31 – Hourly (a) DERs reactive power, (b) capacitors tap, and (c) switch status obtained for the proposed approach.

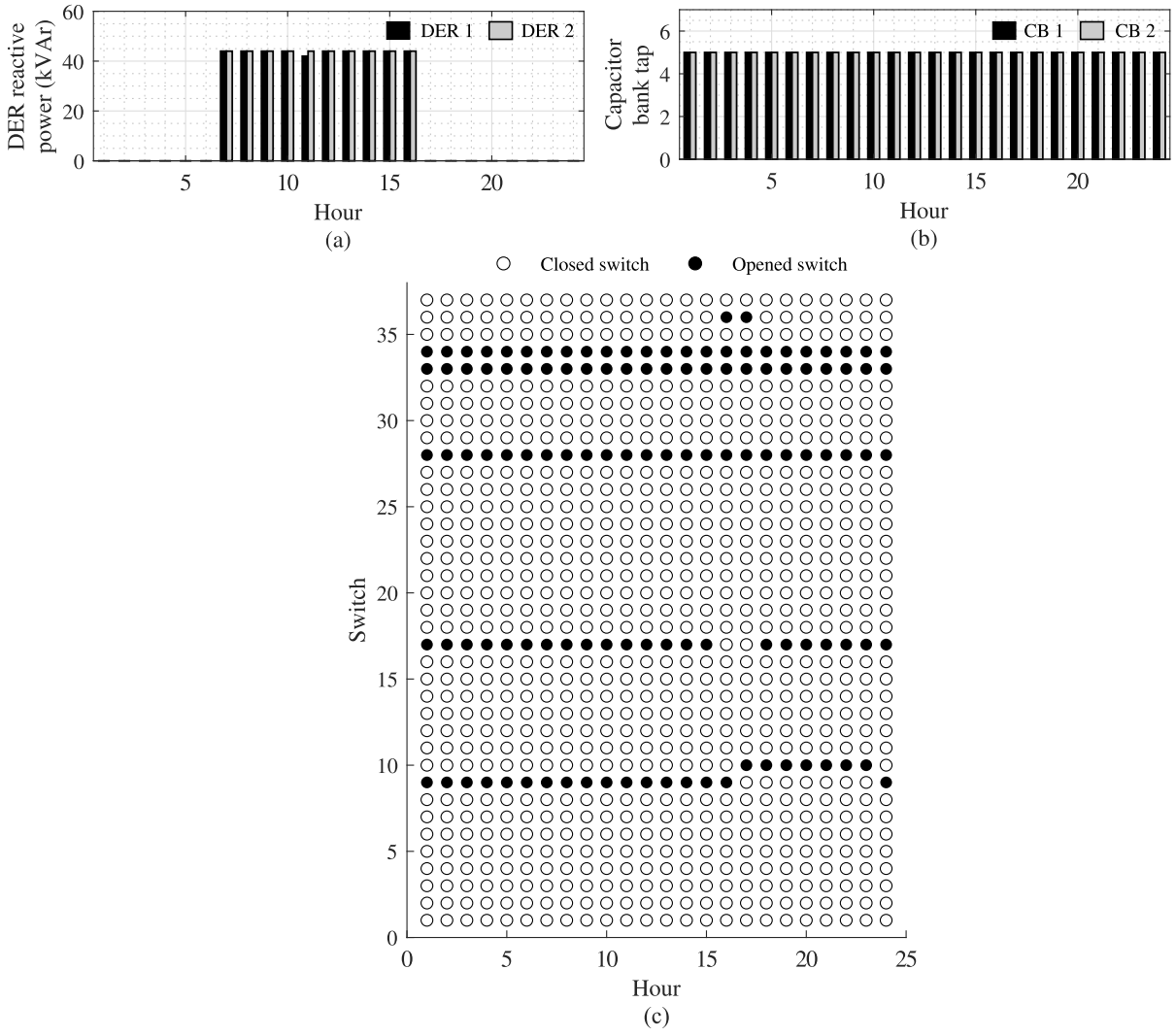

Source: Author

Analyzing Figure 31, it can be observed that the optimization algorithm set the DERs and capacitors to operate at their maximum reactive power capacity. The reactive power support helps maintain voltage levels and reduce power losses. More details and discussions on the results shown in Figure 31 will be presented in the comparative analysis in Section 4.3.3.3.

4.3.3.3 Comparative Analysis

To demonstrate the effectiveness of the multi-objective optimization approach proposed in this section, a comparative analysis is conducted against the methodologies introduced in recent articles, outlined as follows:

- Strategy 1: EVCSs allocation [8, 113].
- Strategy 2: EVCSs and DERs allocation [55].
- Strategy 3: EVCSs and capacitors allocation [53, 54].
- Strategy 4: EVCSs, DERs, and capacitors allocation [11][1].
- Strategy 5: EVCSs allocation and dynamic network reconfiguration [56][2].
- Strategy 6: EVCSs, DERs, capacitors allocation and dynamic network reconfiguration (proposed in this section).

It is important to mention that the same parameters outlined in Section 4.3.3.1 are employed in the tests conducted for each one of these strategies, ensuring a direct comparison of the outcomes. Figure 32 presents the values of the objective functions (4.23)–(4.25) for the original system and the six approaches previously mentioned, considering both the MOCS and the NSGA-II, to compare the two optimization algorithms.

It is possible to observe that the MOCS demonstrates more favorable outcomes compared to the NSGA-II, indicating its greater suitability for this particular application. For this reason, the upcoming results are based on the solutions obtained through MOCS and selected using Fuzzy Decision-making Method. The percentage change in the overall cost, voltage deviation, and power losses for each strategy compared to the original system is shown in Figure 33. It is important to note that a positive percentage change indicates an increase in the variable's value, while a negative percentage change indicates a decrease.

Based on Figure 33a, it is possible to notice that the addition of devices to the distribution system tends to increase the overall system costs, primarily due to investment expenditures. Despite this trend, the proposed approach (Strategy 6) demonstrates lower costs compared to Strategies 2 and 4, even with the addition of dynamic reconfiguration, which incurs switching

[1] The referenced article was authored by the writer of this thesis as part of the research conducted during the development of this work.

[2] The referenced article addresses EVCSs allocation and static network reconfiguration; however, it is cited in this item due to the absence of references covering EVCSs allocation and dynamic network reconfiguration.

costs. The cost reduction in the proposed approach can be attributed to the more efficient operation of the system, leading to a decrease in energy-related expenses. Furthermore, the cost variation is below 3% when comparing all six strategies.

Figure 32 – (a) Overall cost, (b) voltage deviation, and (c) power losses for each strategy.

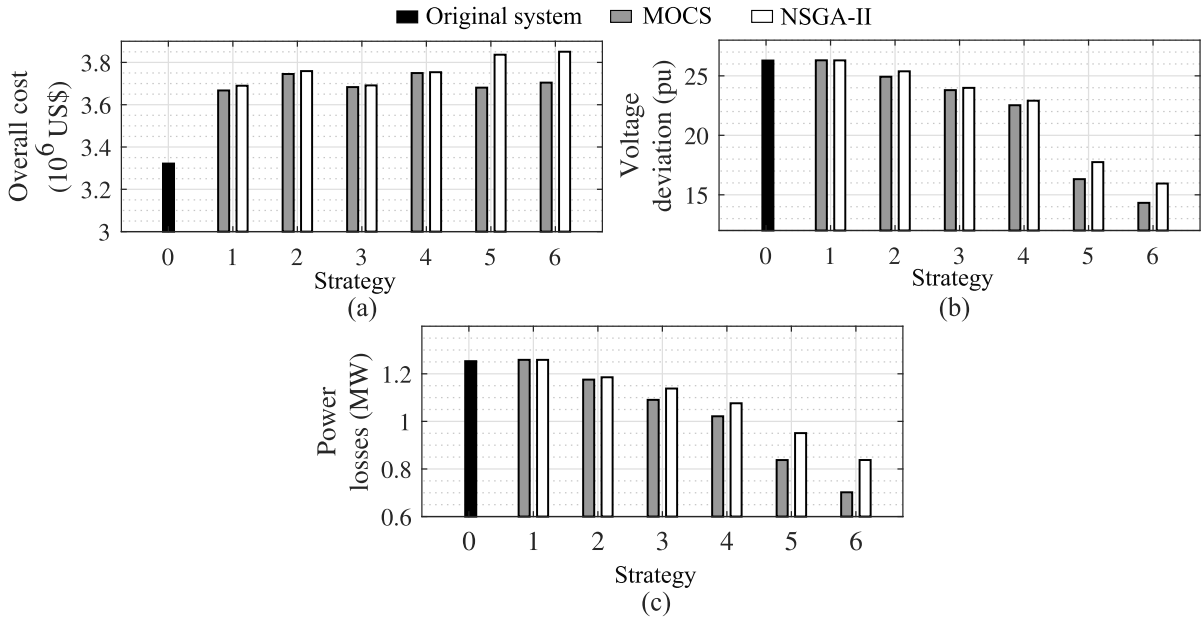

Source: Author.

Figure 33 – Percentage change of the (a) overall cost, (b) voltage deviation, and (c) power losses compared to the original system.

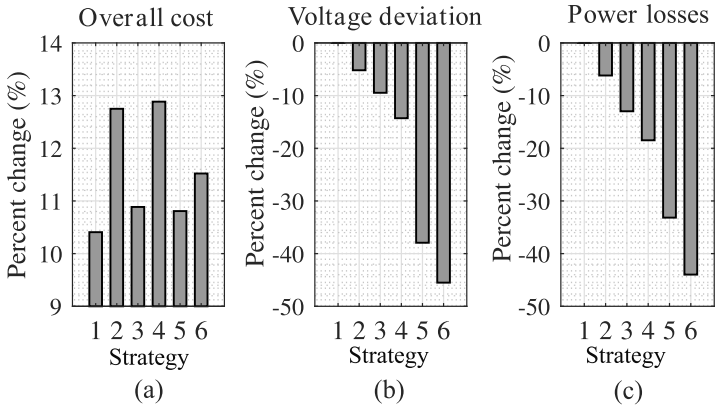

Source: Author.

In Figure 33b, the proposed methodology showcases the lowest voltage deviation, indicating a substantial reduction of 45.50% compared to the original system. In addition, Strategy 5, involving the allocation of EVCSs and dynamic system reconfiguration, also demonstrates noteworthy performance with a low voltage deviation. It is important to emphasize that both methodologies (Strategies 5 and 6) have not been explored in prior studies, as identified through

the literature review conducted in this thesis. Concerning Strategies 2–4, with DERs and/or capacitors allocated in the distribution system, they promote a moderate decrease in voltage deviation, primarily due to reactive support, leading to an enhanced system voltage profile.

From the analysis of Figure 33c, the proposed methodology exhibits the lowest power losses, showcasing a reduction of 43.97% compared to the original system. Similarly to the previous analysis, Strategy 5 presents the second-best result, with a reduction of 33.16%. Despite the decrease in power losses observed in Strategies 2–4, it is not as substantial as those presented in Strategies 5 and 6.

Therefore, despite the slight increase in costs associated with the proposed methodology, it is essential to emphasize that this rise is minimal compared to the substantial improvements in voltage deviation and power losses. These advancements underscore the effectiveness and viability of the proposed approach in achieving a favorable balance between operational efficiency and cost-effectiveness.

Table 12 presents the results corresponding to the planning stage of all six strategies evaluated in this section. Based on the results regarding the EVCSs installation locations, it is evident that the multi-objective optimization algorithm favored buses close to the substation (e.g., buses 2, 19, 21, 22, and 25). Furthermore, the majority of chargers installed in the distribution system are concentrated in the bus closest to the substation, which is bus 2. The addition of EVCS loads in these locations significantly reduces their impacts on voltage profile, due to the approximation to the slack bus. On the other hand, the incremental current caused by EV charging, flowing between the substation and EVCSs, takes a shorter path when the charging stations are closer to the slack bus, resulting in reduced power losses. In contrast, DERs and capacitors are allocated in buses farther away from the substation in order to minimize power losses in the network, leveraging the proximity of loads to generation units. Additionally, these buses often exhibit undervoltage issues due to the higher equivalent impedance between the substation and the buses.

Table 12 – MOCS solutions for the planning stage regarding the locations of EVCSs, DERs, and capacitors for each strategy.

Strategy	EVCSs locations (No. of chargers)	DERs locations	capacitors locations
1	2 (7), 22 (9)	-	-
2	2 (9), 25 (7)	16, 17	-
3	2 (14), 21 (5)	-	17, 33
4	2 (14), 19 (3)	17, 18	18, 31
5	2 (7), 22 (9)	-	-
6	2 (14), 19 (3)	17, 18	18, 31

The graphs presented in Figures 34–37 correspond to the operation stage of the evaluated strategies. In Strategy 1, there are no variables that can be adjusted in real-time; thus, none of

the following operation stage results pertain to this strategy. Figure 34 shows the reactive power provided by each DER for each hour of the day in Strategy 2.

Figure 34 – Hourly reactive power provided by each DER obtained in Strategy 2.

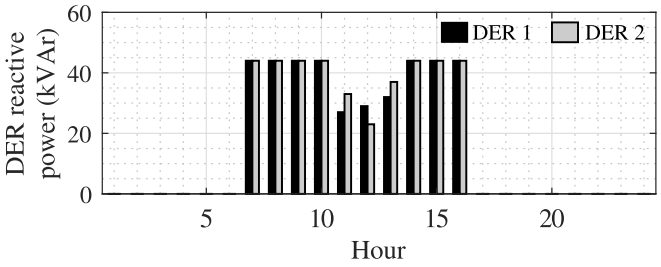

Source: Author.

The reactive support from each DER takes place only between 7 and 16 h, as a consequence of the irradiance curve presented in Figure 10b, as well as the requirements established in the IEEE 1547 standard. In this context, around 7 and 16 h, the supply of reactive power approaches the maximum value established in (3.16), while around 12 h, this supplied power tends to decrease. This behavior is a consequence of the irradiance curve presented in Figure 10b. In moments of high active power supply, the voltage at buses near the DER rises; therefore, the additional supply of reactive power during these hours can lead to overvoltage issues in the system, especially when the total system load is lower.

The tap positions for each capacitor allocated in Strategy 3 are illustrated in Figure 35. In tap 1, the capacitor provides 50 kVAr; in tap 2, it provides 75 kVAr, and so forth. Unlike what occurred in Strategy 2 with the DERs, the capacitors are adjusted to supply the maximum reactive power throughout the day. Thus, the high supply of reactive power by the capacitors, properly allocated in the distribution system, enhances the voltage profile and reduces power losses.

Figure 35 – Hourly tap position for each capacitors obtained in Strategy 3.

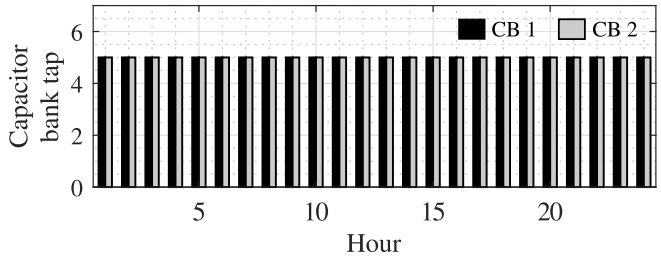

Source: Author.

In addition, the reactive power output of the DERs and the tap positions of the CBs, defined in Strategy 4, are presented in Figure 36.

Figure 36 – Hourly (a) DERs reactive power and (b) capacitors tap position obtained in Strategy 4.

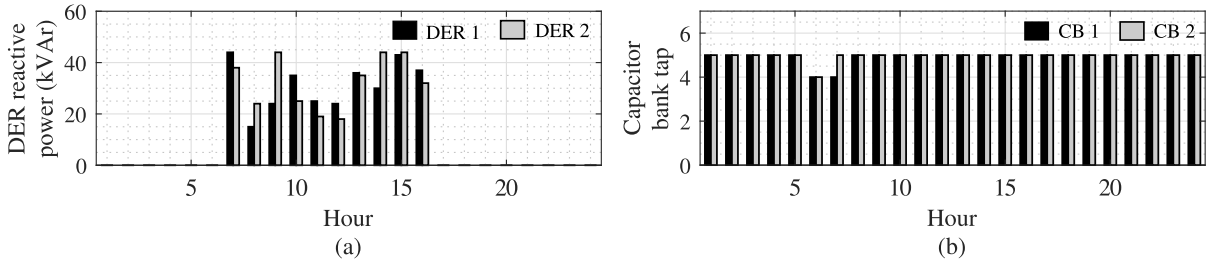

Source: Author.

Firstly, a similar behavior to that observed in Figure 34 can be identified in the graph of Figure 36a, in which an increase in active power provided by the DERs is accompanied by a reduction in reactive power output. Regarding Figure 36b, there is a slight decrease in the reactive power provided by the capacitors between 6 and 7 h, corresponding to periods of lower demand, as indicated in Figure 10a. Thus, the optimization method reduces the supply of reactive power to control the system's voltage during these low-demand hours.

Figure 37 displays the switch status for the dynamic network reconfiguration performed in Strategy 5.

Figure 37 – Hourly switch status for network reconfiguration performed in Strategy 5.

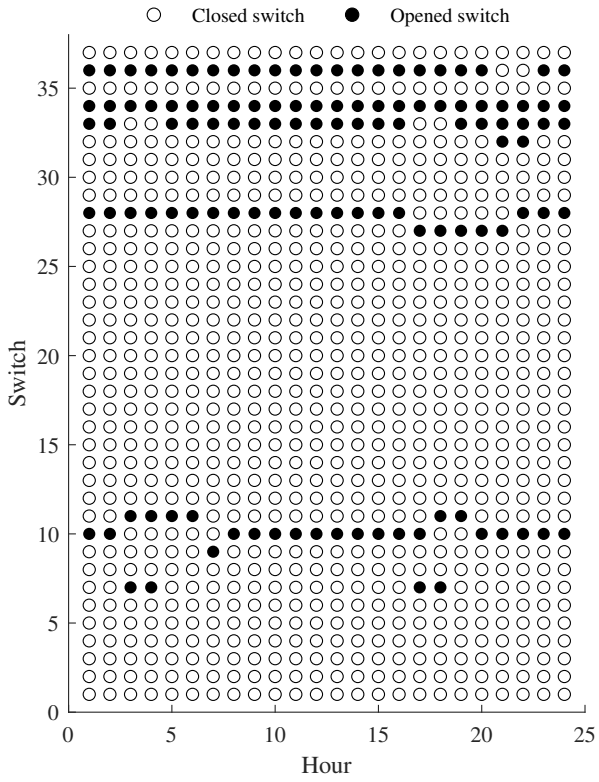

Source: Author.

It is possible to notice that at each time interval, only a few switching operations are performed in order to maintain the system's stability and reliability while minimizing switching costs. Furthermore, in this reconfiguration process, the switch s_{34} remains open throughout the day due to the high impedance of line 34, which would lead to an increase in power losses in the system. The hourly changes in the network topology, as depicted in Figure 37, guarantee adherence to the operational limits of the network while simultaneously minimizing the objective functions based on the current system condition.

It is important to mention that the solution achieved through the methodology proposed in this thesis (Strategy 6), shown in Figure 31, offers some advantages over Strategies 2 and 4. Unlike these strategies, the multi-objective optimization algorithm used Strategy 6 does not need to curtail the reactive power supplied by the DERs. This is made possible by dynamically reconfiguring the network topology to meet the system's operational constraints. Furthermore, the capacitors are set to provide maximum reactive power throughout the day. This strategy, which simultaneously allocates DERs, capacitors, and EVCSs along with dynamic network reconfiguration, effectively leverages the full capacity of each device, thereby enhancing the system's operation.

The voltage profile of the 33-bus test system is depicted in Figure 38 for the six strategies evaluated in this section. Each data point in this graph represents the average of the Monte Carlo simulations for each hour of the day, with the red line indicating the overall average value across all hours.

Figure 38 – Voltage profile considering the solutions provided by the MOCS for Strategies (a) 1, (b) 2, (c) 3, (d) 4, (e) 5, and (f) 6.

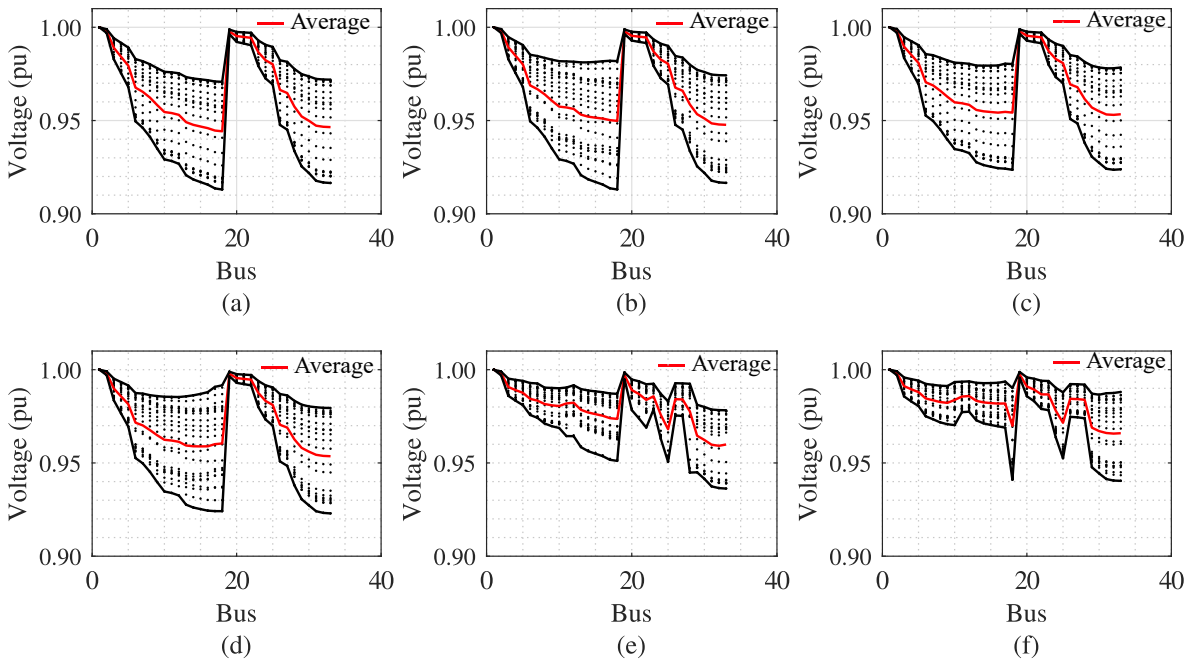

Source: Author.

Figure 38a indicates that when the system operates under Strategy 1, it experiences high voltage deviation, with voltage values dropping below 0.92 pu during specific hours and at particular buses. This observation suggests that the allocation of EVCSs may lead to undervoltage issues in the system, due to the increasing load demand from EVs. In addition, considering Figure 38b, it is evident that the allocation of DERs in Strategy 2 does not effectively mitigate the high voltage deviation issue, despite the improvement in the average voltage profile compared to Strategy 1. It is worth noting that the installation of PV-based DERs is effective in enhancing the voltage profile, but within a specific time interval determined by the irradiance curve. Consequently, if the distribution system presents voltage regulation challenges beyond this interval, relying only on DER installation may not be enough to address this issue.

From the analysis of Figures 38c and 38d, it is possible to notice that the installation of capacitors, carried out in Strategies 3 and 4, effectively regulated the voltage profile by providing reactive power support, which is an essential aspect of ancillary services. On the other hand, the dynamic network reconfiguration also proved capable of improving the voltage profile, as presented in Figure 38e. According to Figure 38f, the combination of DERs and capacitors with the dynamic network reconfiguration, implemented in Strategy 6, emerged as the most effective strategy for enhancing the voltage profile, demonstrating the lowest voltage deviation when compared to the other strategies.

Figure 39 illustrates the average power losses of the system for each hour of the day. The power losses curve aligns with the load profile from the adopted database, as increased power demand amplifies the current flow through distribution lines, subsequently elevating the overall system's losses. Among the six strategies, the strategy exclusively allocating EVCSs (Strategy 1) presented the highest power losses. In contrast, the strategy combining DERs and capacitors with dynamic system reconfiguration (Strategy 6) showcases the lowest power losses, indicating reductions throughout the entire day. This highlights the significance of integrating planning and operation strategies to optimize the advantages of DERs, capacitors, and dynamic system reconfiguration based on the system's operational conditions at each time of the day.

Overall, Strategy 6 demonstrated the most favorable results. In this strategy, the total costs increased minimally (less than a 2% compared to the strategy that allocated only EVCSs), while significantly reducing voltage deviation and power losses. These improvements not only enhance operational efficiency for the DSO but also translate to improved reliability and cost savings for end consumers. By mitigating power losses, the overall energy efficiency of the distribution system is increased, leading to a more economically viable solution for both stakeholders. Additionally, the reduction in voltage deviation ensures a stable and consistent supply, contributing to enhanced performance and longevity of connected devices for end consumers.

Figure 39 – Active power losses considering the solutions provided by the MOCS for Strategies 1–6.

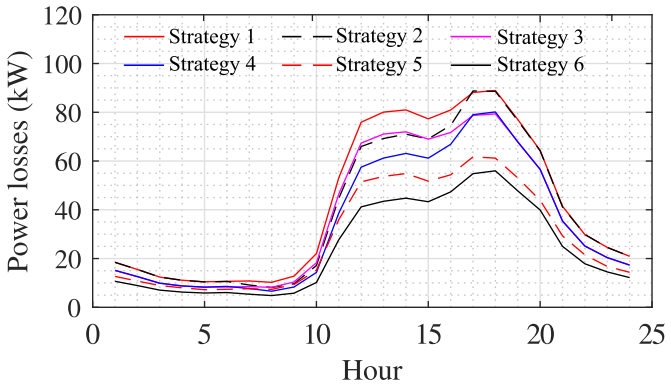

Source: Author.

4.4 Network Operation and Planning Considering Stochastic Customer-owned DERs

This section introduces a multi-objective operation and planning approach aimed at optimizing the performance of the distribution system by simultaneously addressing dynamic network reconfiguration, capacitor placement, and OLTC transformer adjustments. The primary goals are to minimize power loss costs and enhance the system's voltage profile by reducing a novel VCI, introduced herein.

Aligned with the methodologies presented in the preceding sections, this multi-objective optimization approach adopts the perspective of the DSO. However, unlike the strategies outlined in Sections 4.1–4.3, the DSO is not responsible for optimizing the allocation and sizing of DERs. In this case, the DERs integrated into the distribution system are independently installed by end customers, with their quantity, sizes, and locations considered as unpredictable variables.

Under these circumstances, the DSO relies on three primary operational resources: capacitor placement, OLTC transformer adjustments at the substation, and network reconfiguration. By employing these strategies, the DSO aims to improve the system's performance, reduce operational costs, and maintain adherence to both operational and physical constraints.

4.4.1 Problem Formulation

In this section, the mathematical formulation of the multi-objective optimization problem is presented, encompassing the dynamic reconfiguration of the network, the allocation and sizing of capacitors, and the dynamic adjustment of the OLTC transformer at the substation. The decision variables of this optimization problem are presented as follows:

- The placement of capacitors, denoted by the binary variable w_i, which specifies whether a capacitor is installed at bus i.

- The tap positions of the capacitors, represented by $tap_{h,i}^{\text{cap}}$.
- The tap position of the OLTC transformer, represented by tap_{h}^{OLTC}.
- The status of each tie and sectionalizing switch, given by the binary variable $s_{h,ij}$.

The objective functions of this optimization problem are expressed as

$$\min \quad f_1 = \sum_{h\in\Omega_h}\sum_{ij\in\Omega_l} s_{h,ij}\cdot ec^s \cdot P_{h,ij}^{\text{loss}}, \tag{4.30}$$

$$\min \quad f_2 = \text{VCI}, \tag{4.31}$$

where

$$\text{VCI} = \sqrt{\frac{(|\sigma_1 - V^n| + |\sigma_2 - V^n|)\cdot \sum_{h\in\Omega_h}\sum_{i\in\Omega_b}\left|V_{h,i} - V^n\right|}{|\Omega_h|\cdot|\Omega_b|}}, \tag{4.32}$$

$$\sigma_1 = \min\left\{V_{h,i}^{\max}, \left(\text{quartile}(V_{h,i}, 0.75) + 1.5\cdot\text{IQR}\right)\right\}, \tag{4.33}$$

$$\sigma_2 = \max\left\{V_{h,i}^{\min}, \left(\text{quartile}(V_{h,i}, 0.25) - 1.5\cdot\text{IQR}\right)\right\}, \tag{4.34}$$

$$\text{IQR} = \text{quartile}(V_{h,i}, 0.75) - \text{quartile}(V_{h,i}, 0.25). \tag{4.35}$$

In these equations, the sets of time intervals, branches, and buses are represented by Ω_h, Ω_l, and Ω_b, respectively. Accordingly, h, ij, and i correspond to the evaluated time, branch, and bus, respectively. The total number of buses in the network is represented by $|\Omega_b|$, while $|\Omega_h|$ denotes the total time horizon considered for the optimization process. The active power losses in branch ij at time h is given by $P_{h,ij}^{\text{loss}}$. Additionally, ec^s is the energy cost associated with the substation; V^{nom} denotes the nominal voltage of the distribution system; $V_{h,i}$ is the voltage value at time h and bus i. The interquartile range (IQR) represents the distance between the 75th percentile, quartile$(V_{h,i}, 0.75)$, and the 25th percentile, quartile$(V_{h,i}, 0.25)$, of the voltage dataset. σ_1 represents the minimum between the largest observation in the dataset and the 75th percentile plus 1.5 times the interquartile range. Similarly, σ_2 is defined as the maximum between the smallest observation in the dataset and the 25th percentile minus 1.5 times the interquartile range.

The first objective function, shown in (4.30), focuses on minimizing active power loss costs to enhance the overall cost efficiency of the distribution system. The second objective function, introduced in (4.31), aims to improve the voltage profile across the distribution network. The proposed VCI metric goes beyond the traditional approach of simply analyzing the average voltage across all buses and time periods. Instead, it incorporates both the deviation of voltage values from the nominal voltage (V^n) and the bounds of the voltage distribution, adjusted to exclude outliers.

The numerator in (4.32) is composed of two main components. The first term, given by $(|\sigma_1 - V^n| + |\sigma_2 - V^n|)$, quantifies the deviation of σ_1 and σ_2 from the nominal voltage. This term is designed to minimize voltage variations across the system's buses and throughout the

evaluated time horizon. By bringing σ_1 and σ_2 closer to the nominal voltage, the system's reliability is enhanced, maintaining voltage levels within safe operating limits even under adverse conditions. The second term, $\left|V_{h,i} - V^n\right|$, represents the deviation of the voltage at bus i and time h from the nominal voltage, ensuring that the VCI metric accurately reflects the proximity of the system's overall voltage to the reference value. The combination of these terms makes the VCI sensitive to both average and boundary voltage deviations (excluding outliers), providing a more comprehensive and reliable evaluation of the system's performance.

The optimization problem is constrained by several factors, including: the distribution system constraints outlined in (3.1)–(3.6); the operational boundaries of DERs described in (3.14)–(3.22); the capacitor operational limits specified in (3.23) and (3.24); the OLTC transformer operational limits detailed in (3.26) and (3.27); and the radiality constraint presented in (3.52).

Additionally, the maximum allowable number of switching actions, Δs^{dyn}, required to transition between states is expressed as

$$\sum_{ij \in \Omega_l} |s_{h,ij} - s_{h-1,ij}| \leq \Delta s^{dyn}, \quad \forall h \in \Omega_h, \tag{4.36}$$

to ensure the system's stability and prevent excessive wear on the devices, as highlighted in [139, 140].

The total investment cost is further constrained by the available budget, represented as

$$\sum_{i \in \Omega_b} (w_i \cdot C^{\text{cap}}) + C^{\text{OLTC}} \leq C^{\max}, \tag{4.37}$$

where C^{cap} and C^{OLTC} denote the investment costs of capacitors and the OLTC transformer, respectively, and $C^{\max}$ represents the total available budget.

4.4.2 Methodology

In this approach, the MOCS is adopted to solve the multi-objective optimization problem involving network reconfiguration, the allocation and sizing of capacitors, and the adjustment of the OLTC transformer at the substation. Nevertheless, the emphasis of this research is on the proposed methodology rather than the optimization method itself. Figure 40 illustrates the detailed steps of the proposed methodology for solving this multi-objective optimization problem, incorporating the MOCS, the Monte Carlo Method, and the Fuzzy Decision-making Method. In Figure 40, ite denotes the iteration counter of the MOCS, h represents the time counter, s refers to the scenario generated by the Monte Carlo Method, and t^{int} indicates the multi-period time interval of the multi-period analysis. The maximum values for these counters are $ite^{\max}$, $h^{\max}$, and $s^{\max}$, respectively.

Figure 40 – Flowchart of the proposed approach considering stochastic customer-owned DERs.

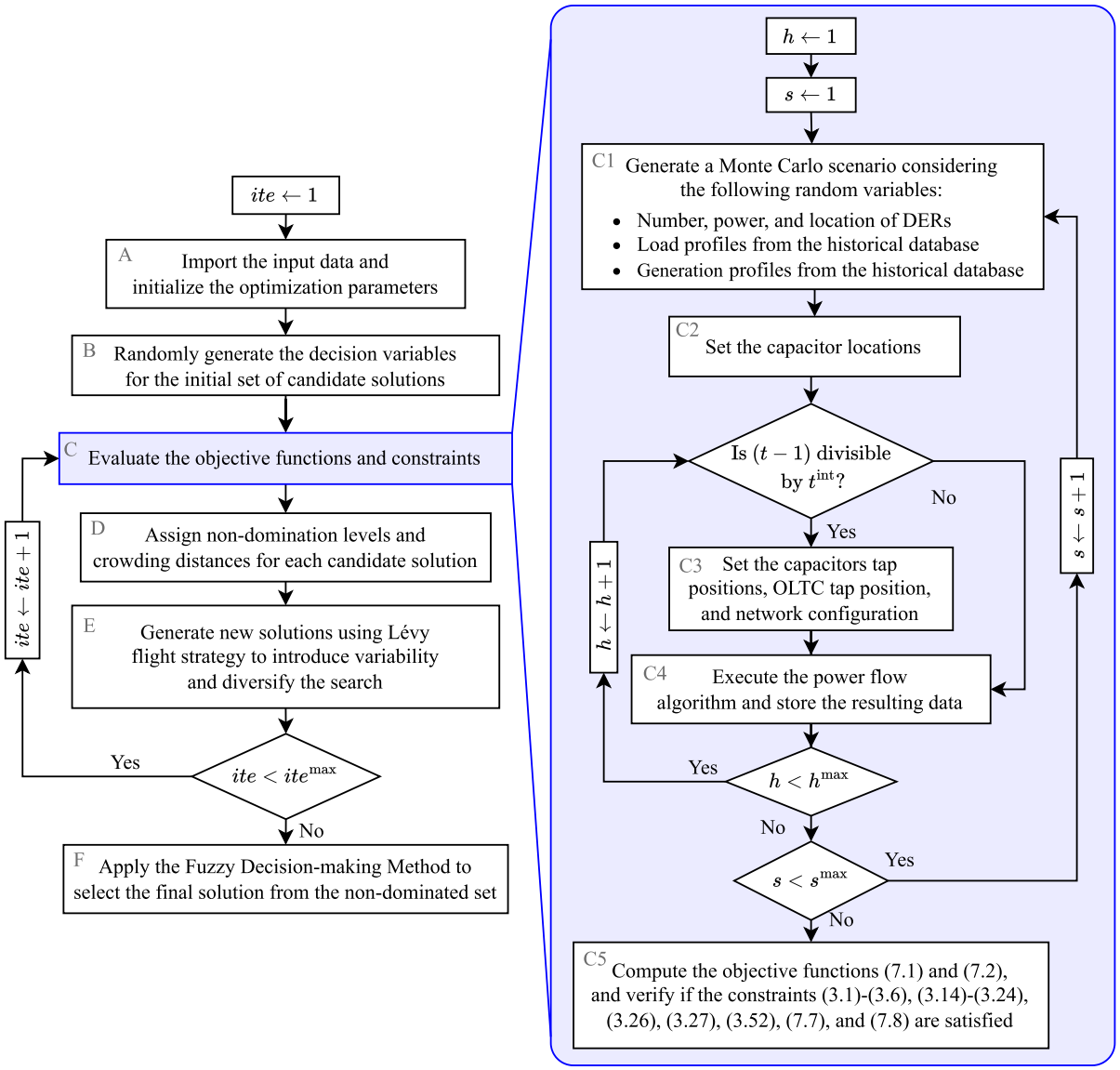

Source: Author.

The iteration counter of the MOCS is initially set to 1. Thereafter, in Block A, the input data, which includes historical irradiance, temperature, and load profiles, is imported. The irradiance and temperature data are utilized to generate profiles for PV-based DERs, considering the output model described in Section 3.1.2. To ensure the methodology's reliability, the irradiance and temperature data should cover a sufficiently long time span to capture the seasonal variations throughout the year, reflecting the full range of DER power generation. Regarding the MOCS, the parameters initialized are: number of nests, discovery probability for outlier solutions, and maximum number of iterations.

In Block B, the decision variables–comprising the capacitors locations, the status of sectionalizing and tie switches, the capacitors tap positions, and the OLTC transformer tap

position–are randomly generated to form the initial solution. Furthermore, Block C handles the evaluation of the objective functions and constraints, beginning with the initialization of the time and Monte Carlo scenario counters. In Block C1, a Monte Carlo scenario is randomly generated considering the number, location, and power of DERs, alongside load and generation profiles from the historical database. Regarding the DERs, the number of generators ranges from 0 to the number of customers of the system, their sizes range from 0% to 100% of the respective customers' power consumption, and their locations are randomly distributed across the distribution system. The methodology outlined in Section 3.4.1 is considered to determine the number of Monte Carlo simulations required to ensure the convergence of the Monte Carlo Method.

Considering the decision variables defined by the optimization algorithm, the capacitor locations are configured in Block C2. Then, for specific multi-period intervals, the capacitor tap positions, OLTC tap settings, and network configuration are updated in Block C3 according to the decision variables. For instance, if the multi-period interval is set to 4 h ($t^{\text{int}} = 4\,\text{h}$), these settings will be updated six times throughout the day, specifically at 1 h, 5 h, 9 h, 13 h, 17 h, and 21 h. After performing the power flow analysis for each time of the day and each Monte Carlo scenario using the Backward–forward Sweep method (described in Section 3.1.1), the objective functions (4.30) and (4.31) are calculated in Block C5, under the constraints outlined in (3.1)–(3.6), (3.14)–(3.24), (3.26), (3.27), (3.52), (4.36), and (4.37), ensuring compliance with operational and physical limits of the distribution system. The compliance of these constraints is verified across all random scenarios generated through the Monte Carlo Method, ensuring the proper operation of the system under varying conditions. In Block D, the non-domination level and crowding distance are assigned to each candidate solution. Furthermore, new solutions are generated using Lévy flights in Block E. After completing all iterations of the MOCS, the Fuzzy Decision-making Method, detailed in Section 3.3.3, is performed in Block F.

4.4.3 Results and Discussion

This section presents an overview of the case study, detailing the input data, and simulation parameters. It then evaluates the impacts of stochastic customer-owned DERs and discusses the optimization results obtained through the proposed approach.

4.4.3.1 Case Study

The voltage lower and upper limits considered in (3.6) are 0.88 and 1.10 pu, respectively, based on the IEEE 1547-2018 standard [92]; while the current limits are defined in (3.5) according to each line section. The OLTC transformer, modeled in (3.26) and (3.27), has a voltage step of 1.8% per tap and 19 operating positions (±9 from the neutral position) with an investment cost of US$ 7,000 [95]. The capacitors available for allocation feature a nominal reactive power of 175 kVAr, equally divided into 7 switchable taps, with an investment cost of US$ 30 per kVAr [137].

The total available investment budget in (4.37) is US$ 35,000. Additionally, the energy cost in (4.30) is US$ 0.13 per kWh [137]. The maximum number of switching operations, represented by Δs^{dyn} in (4.36), is 6.

For the MOCS, simulations are executed with 100 nests, incorporating a 25% discovery probability and a maximum of 100 iterations. Regarding the Fuzzy Decision-making Method, the desirability levels $\widetilde{\Phi}_{f_1(x)}$ and $\widetilde{\Phi}_{f_2(x)}$ are set to 0.5 and 1.0, respectively, with the purpose of prioritizing the improvement of the system's voltage profile. Additionally, the proposed methodology is evaluated using the 69-bus test system (Figure 19).

The proposed approach integrates the allocation and sizing of capacitors, the operation of the OLTC transformer, and network reconfiguration. To assess the individual impact of each strategy on the objective functions, the following strategies are tested:

- Strategy 1: Capacitors allocation and sizing.
- Strategy 2: OLTC transformer operation.
- Strategy 3: Network reconfiguration.
- Strategy 4: Capacitors allocation and sizing combined with OLTC transformer operation.
- Strategy 5: Capacitors allocation and sizing combined with network reconfiguration.
- Strategy 6: Network reconfiguration combined with OLTC transformer operation.
- Strategy 7: Capacitors allocation and sizing, OLTC transformer operation, and network reconfiguration (proposed in this section).

To evaluate and compare the performance of static and dynamic strategies, five configurations with different multi-period time intervals are analyzed: one static evaluation ($t^{\text{int}} = h^{\text{max}}$) and four dynamic evaluations with multi-period time intervals of 8, 4, 2, and 1 h.

4.4.3.2 Impacts of Stochastic Customer-owned DERs

Figures 41 and 42 present the voltage profile and power losses of the original system with and without stochastic customer-owned DERs, respectively. These figures are provided to illustrate the impacts of DERs integration on the system's performance. In Figures 41a and 42a, each point represents a voltage value at each bus of the system for every random scenario generated using the Monte Carlo Method. Similarly, in Figures 41b and 42b, each point corresponds to a power loss value at each line of the system under the same set of random scenarios. It is important to note that the points in the graphs are plotted with 2% opacity to allow for a clear visualization of the density and distribution of data points in each region. This approach effectively highlights areas where voltage or power loss values are more concentrated, facilitating an in-depth understanding of the variability introduced by the stochastic nature of DERs.

Figure 41 – (a) Voltage profile at each bus and (b) power losses at each line considering the original system without stochastic customer-owned DERs.

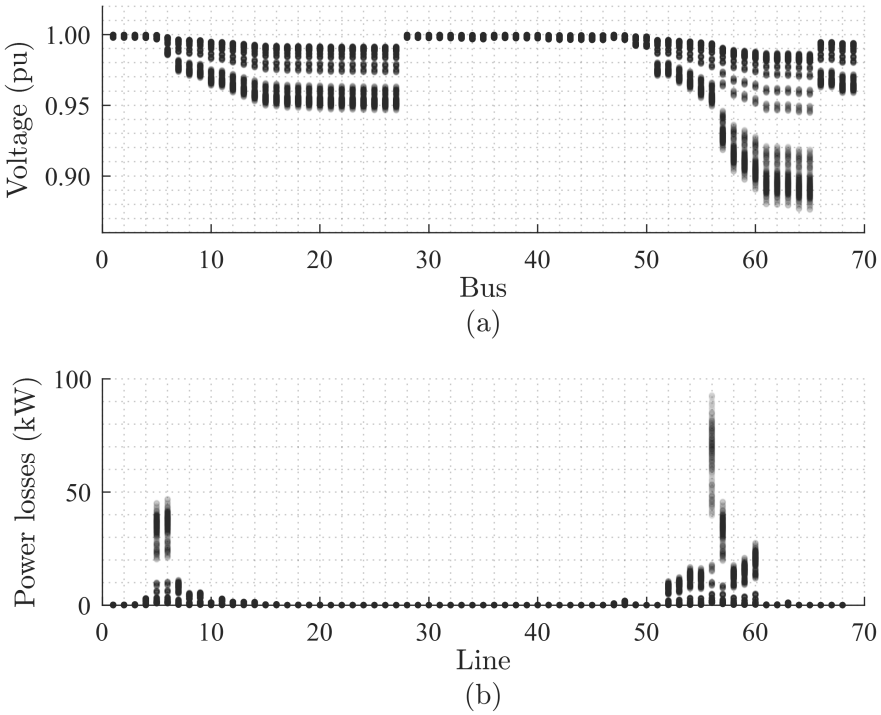

Source: Author.

Figure 42 – (a) Voltage profile at each bus and (b) power losses at each line considering the original system with stochastic customer-owned DERs.

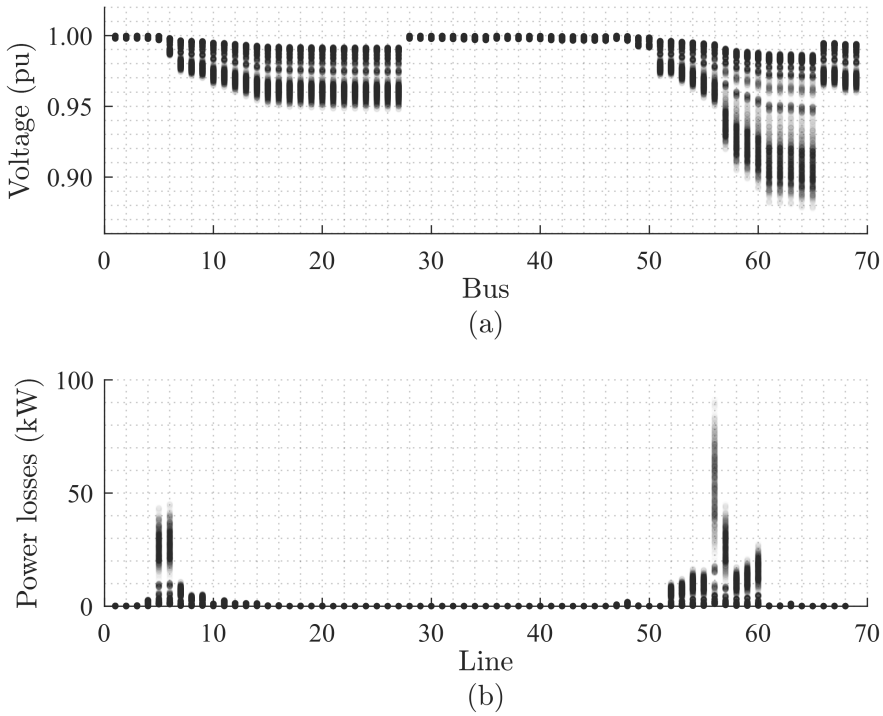

Source: Author.

When comparing the voltage profiles and power losses in Figures 41 and 42, it is possible to notice that the minimum voltage values and maximum power losses change only slightly with the integration of stochastic DERs. This subtle variation occurs because DERs are randomly distributed in terms of quantity, location, and capacity. As a result, certain scenarios may arise where few or no DERs are installed, leaving the system's performance in these cases similar to the original configuration without DERs.

Despite that, an improvement can be observed in other regions of the graphs. Many points in the voltage profile (Figures 41a and 42a) shift upward, driven by scenarios where higher DER capacities are installed, leading to an increase in the average voltage across the system. Similarly, reductions in power losses are evident in several points of the loss distribution (Figures 41b and 42b), corresponding to scenarios where DERs effectively supply local demand or inject power into the grid. This results in a lower average for power losses after DER integration.

Furthermore, the distribution of points in both voltage and power loss graphs becomes more dispersed when considering DERs. This increased spread reflects the expanded operational possibilities introduced by DERs, which adds variability to the system's performance. Consequently, this variability highlights the increased complexity of the system's analysis, requiring a more thorough consideration of uncertainties in operational conditions.

4.4.3.3 Optimization Results

Figures 43a–43c illustrate the Pareto front approximation obtained by executing each strategy individually, including capacitors allocation and sizing, OLTC transformer operation, and network reconfiguration, respectively. To enhance visualization and address the overlapping of multiple points, each Pareto front approximation was shifted along the third axis of the graph. This adjustment was also applied to the graphs in Figs. **??** and **??**. It is important to note that the objective function values f_1 and f_2 for the original system considering customer-owned DERs are 319.92 US$ and 0.0287 pu, respectively.

Regarding the allocation of capacitors, shown in Figure 43a, capacitors are primarily placed at buses with high load demand and those located farther from the substation. This allocation pattern is supported by a positive correlation (Pearson coefficient of 0.74) between the installed capacitor power and the total load at each bus of the distribution network. Additionally, a positive correlation (Pearson coefficient of 0.37) is also observed between the installed capacitor power and the total impedance separating each bus from the substation.

Furthermore, in the multi-period configurations, capacitors are adjusted to higher tap positions during periods of increased load demand, when reactive power support is essential for maintaining the system's voltage profile. In this context, a positive correlation (Pearson coefficient of 0.85) is observed between the capacitor tap position and the total system load. Similarly, for the OLTC transformer operation, shown in Figure 43b, a very strong positive

correlation (Pearson coefficient of 0.91) exists between the OLTC tap position and the overall system load demand.

Figure 43 – Pareto front approximation considering Strategies (a) 1, (b) 2, and (c) 3.

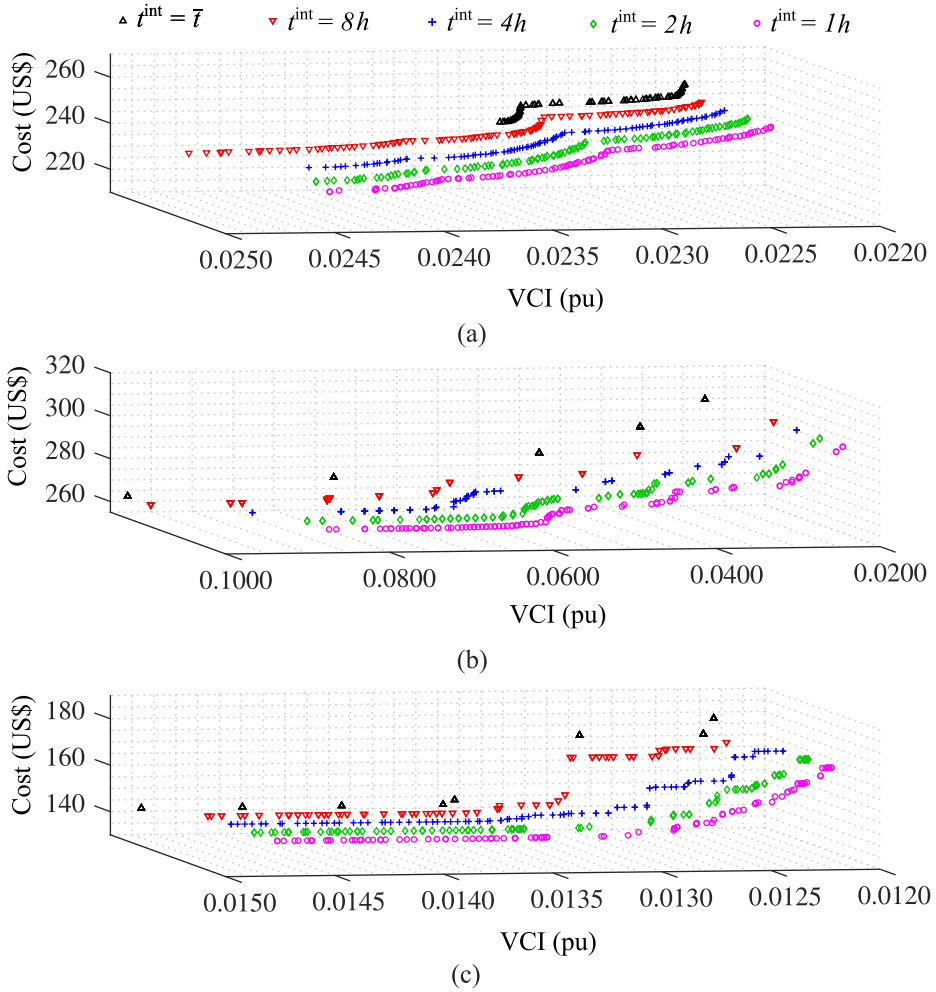

Source: Author.

During network reconfiguration, it is observed that the multi-objective optimization algorithm defines topologies that strategically reduce the total distance between buses with heavier loads and the substation, while increasing the distance for buses with lighter loads. These changes are measured relative to the original configuration, in which switches s_{69}, s_{70}, s_{71}, s_{72}, and s_{73}, presented in Figure 19, are open. A negative correlation (Pearson coefficient of -0.36) was calculated between each bus's load and its distance variation to the substation, where a negative distance variation indicates a reduction and a positive variation represents an increase compared to the original system's configuration. By minimizing the distance between heavier loads and the substation, the power losses are decreased, since the current travels shorter paths to reach high-demand buses, consequently improving the system's voltage profile.

The results presented in Figure 43 highlight that subdividing the multi-period time intervals increases the diversity of solutions and improves the quality of the results by expanding

the search space. However, this improvement diminishes progressively as the number of intervals increases. This trend aligns with the load and irradiance patterns shown in Figure 10, where significant variations in average values are observed when comparing the entire day (1–24 h) to three equally divided periods (1–8 h, 9–16 h, and 17–24 h). In contrast, further subdividing these three intervals does not substantially affect the average load and irradiance values. In other words, the variation in these averages decreases as the number of intervals grows, meaning that additional subdivisions primarily serve to enhance solution diversity by further expanding the search space of the optimization problem.

Figure 44 shows the Pareto front approximation considering the OLTC transformer operation combined with capacitors allocation and sizing (Strategy 4); network reconfiguration combined with capacitors allocation and sizing (Strategy 5); and network reconfiguration combined with OLTC transformer operation (Strategy 6). Furthermore, Figure 45 illustrates the Pareto front approximation considering the combination of network reconfiguration, OLTC transformer operation, and capacitors allocation and sizing (Strategy 7).

Figure 44 – Pareto front approximation considering Strategies (a) 4, (b) 5, and (c) 6.

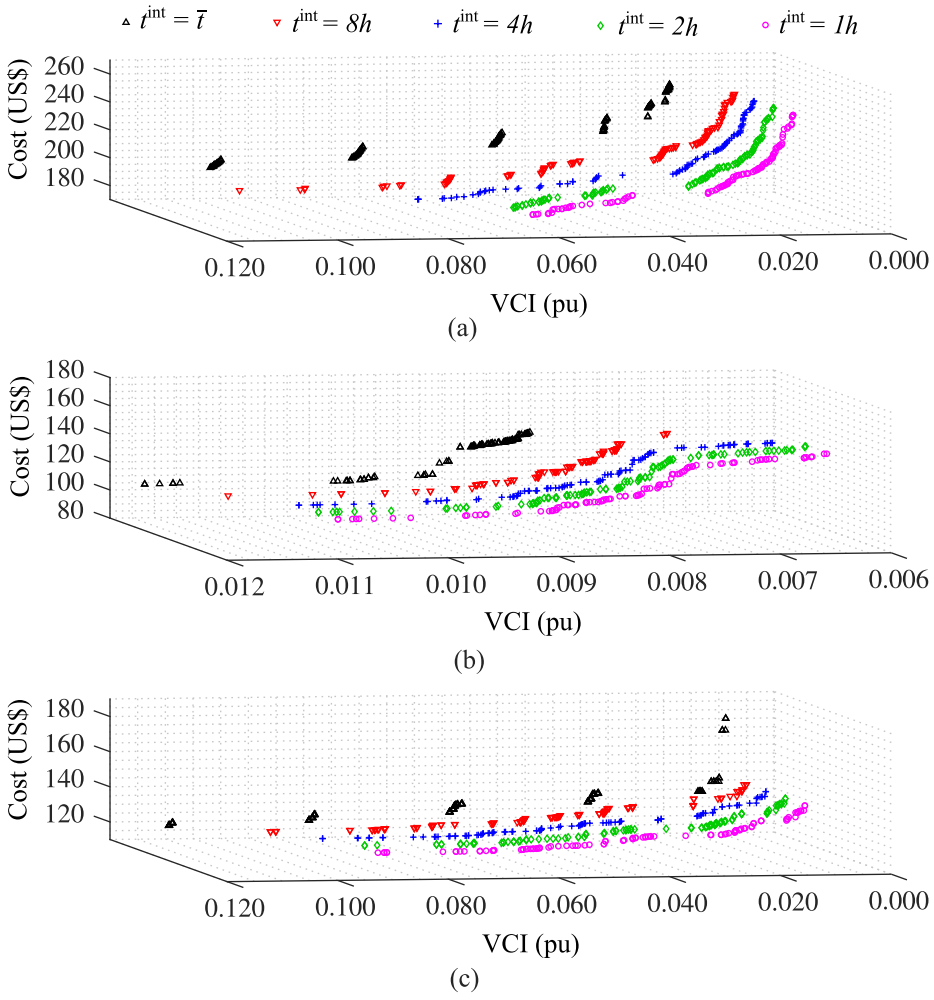

Source: Author.

Figure 45 – Pareto front approximation considering the combination of network reconfiguration, OLTC transformer operation, and capacitors allocation and sizing (Strategy 7).

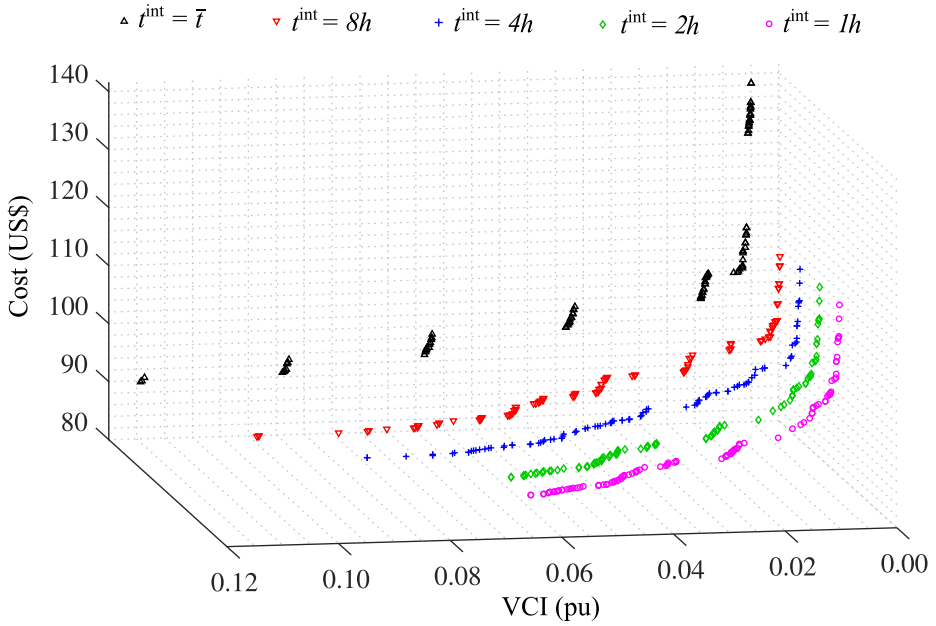

Source: Author.

As expected, integrating the strategies into a multi-objective optimization problem significantly expands the search space, resulting in higher-quality solutions. From Figures 43b, 44a, 44c, and 45, it can be observed that the operation of the OLTC transformer has a substantial impact on the objective function f_2. In other words, while adjusting the OLTC transformer tap can improve the system's voltage profile, it can also degrade it, potentially making the system more unstable and less reliable. Therefore, properly incorporating this operational aspect into system planning is essential to ensure both stability and reliability.

Conversely, as illustrated in Figures 43a, 44a, 44b, and 45, the allocation of capacitors has a limited impact on the objective function f_2. However, it is highly effective in reducing costs associated with power losses. Consequently, the optimized allocation, sizing, and operation of capacitors in the distribution system enhance the overall efficiency while providing modest improvements to the voltage profile. With respect to network reconfiguration, as shown in Figures 43c, 44b, 44c, and 45, this strategy has the potential to significantly reduce both objective functions. It demonstrates notable improvements in the voltage profile of the system, as well as reductions in costs associated with power losses.

Similarly to what is depicted in Figure 43, the results shown in Figures 44 and 45 reveal diminishing returns as the multi-period time intervals t^{int} are further subdivided. Despite that, the most significant reductions are observed when the multi-period time interval is set to 1 h. For this reason, the Pareto front approximations of the seven evaluated strategies are presented in Figure 46, considering a multi-period time interval of 1 h.

Figure 46 – Pareto front approximation considering the evaluated strategies and $t^{\text{int}} = 1$ h.

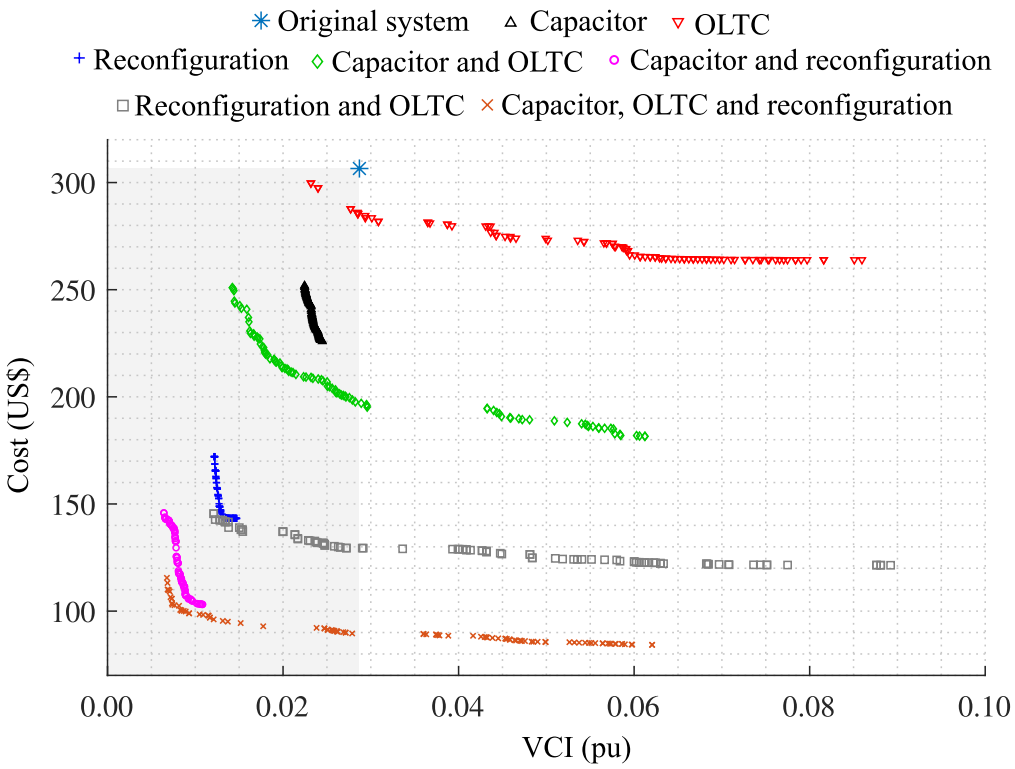

Source: Author.

Figure 46 demonstrates that all the identified solutions achieve lower costs associated with power losses compared to the original system configuration. Additionally, when analyzing the three individual strategies, it is evident that all solutions obtained through the operation of the OLTC transformer are dominated by at least one solution derived from the allocation of capacitors. Similarly, all solutions resulting from the allocation of capacitors are dominated by at least one solution obtained through the dynamic network reconfiguration. Therefore, in the case study analyzed, dynamic network reconfiguration proves to be the most effective strategy for minimizing power loss costs and enhancing the system's voltage profile, while the OLTC transformer operation is the least effective.

A similar observation can be made for the combined approaches. The combination of capacitors allocation and dynamic network reconfiguration stands out as the most effective strategy for minimizing both f_1 and f_2, whereas the combination of capacitors allocation with OLTC transformer operation is the least effective. Moreover, the integration of all three strategies–capacitors allocation, OLTC transformer operation, and dynamic network reconfiguration–yields the best overall results.

Subsequently, the Fuzzy Decision-making Method is employed to determine the final solution for each approach, considering a multi-period time interval of 1 h. Figure 47 presents a histogram of the voltage profile of the distribution system, where the frequency values are

normalized such that the highest frequency value reaches 1. Additionally, a boxplot is overlaid to illustrate the interquartile range as well as the highest and lowest data points, excluding any outliers, of the voltage profile dataset. It is important to mention that the results presented in Figures 47 and 48 account for the integration of customer-owned DERs.

Figure 47 – Voltage profile considering the (a) original system, and Strategies (b) 1, (c) 2, (d) 3, (e) 4, (f) 5, (g) 6, and (h) 7.

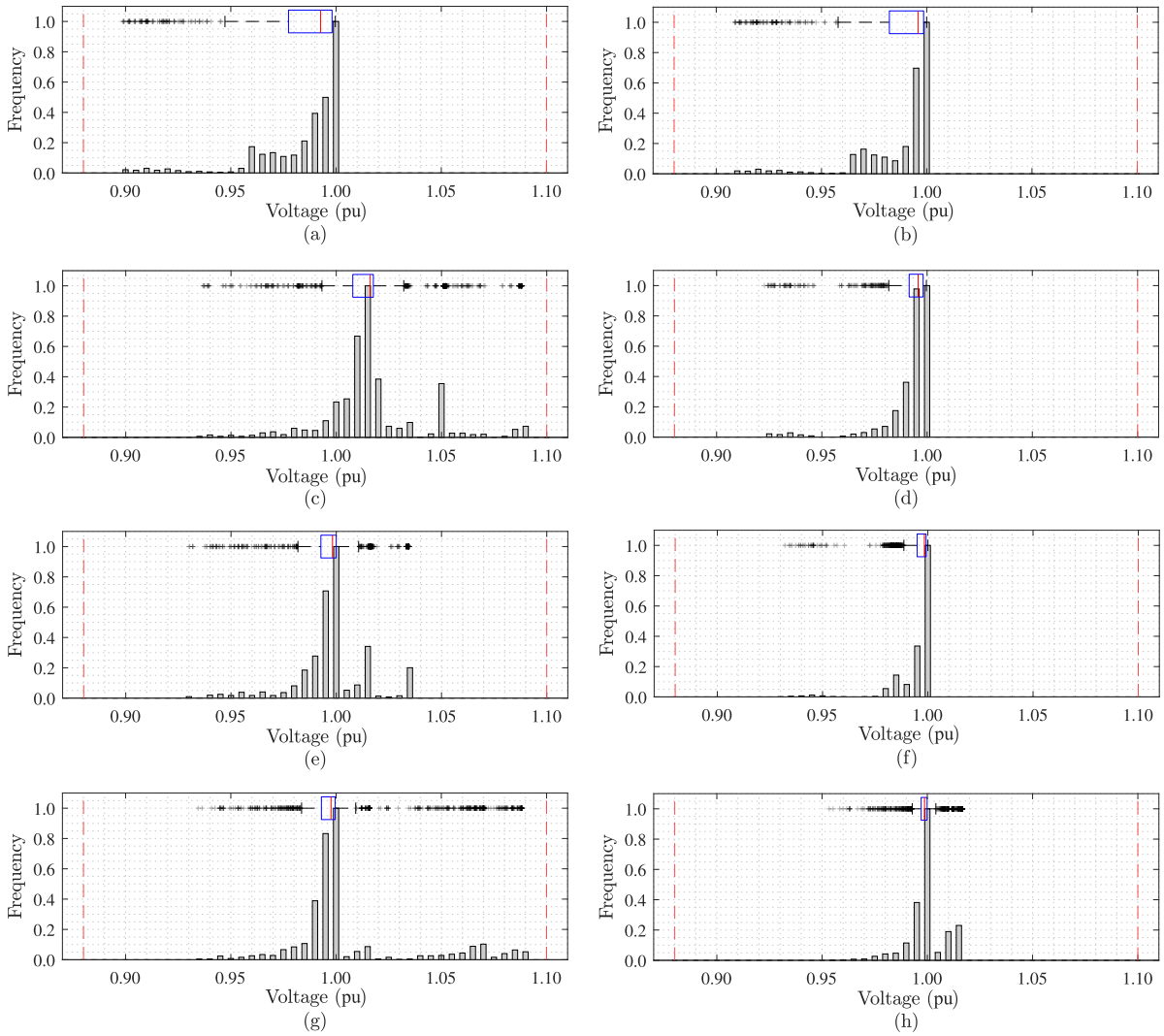

Source: Author.

In Figure 47a, which corresponds to the original system, the voltage profile shows a high concentration of values near the lower acceptable limit, reflecting improper voltage regulation and a lack of reliability in the system. This serves as a baseline for evaluating the impact of the proposed optimization strategies. It is important to mention that the wide variation in voltage values arises from uncertainties related to load, DER generation, and the quantity, sizes, and locations of customer-owned DERs. In Figure 47b, where only capacitors allocation and sizing are considered, there is a shift of the voltage values closer to the nominal voltage, resulting in

an improved profile. However, this approach still exhibits high variability, suggesting limited effectiveness when employed as a standalone solution.

Figure 47c, representing OLTC transformer operation, shows a slight improvement in the voltage profile compared to the original system. The adjustment of the OLTC transformer results in voltage values shifting closer to the upper acceptable limit. While this indicates better regulation compared to the baseline, the method remains insufficient when applied alone, given the proximity of some voltage values to the acceptable bounds. Conversely, Figure 47d, which reflects the results of network reconfiguration, achieves substantial improvements, with voltage values more concentrated near the nominal voltage. This demonstrates the superior impact of reconfiguration compared to the isolated application of OLTC operation or capacitors allocation.

In Figure 47e, the combination of OLTC operation and capacitors allocation achieves better voltage regulation than their individual applications. However, this approach is still outperformed by the results obtained through network reconfiguration. Figure 47f, which integrates network reconfiguration with capacitors allocation, demonstrates a significant improvement, presenting a tighter distribution of voltage values near the nominal voltage and minimizing extreme deviations. On the other hand, Figure 47g, which combines network reconfiguration with OLTC operation, also enhances the voltage profile but falls slightly short compared to Figure 47f. This comparison highlights that the inclusion of capacitors has a greater impact on improving voltage regulation than OLTC operation when paired with network reconfiguration. Finally, Figure 47h, which integrates all three strategies, achieves the most optimized voltage profile. However, while this comprehensive approach produces the best results, the improvement over Figure 47f is relatively marginal, suggesting diminishing returns from adding OLTC operation to the combination of reconfiguration and capacitors, when considering only the VCI.

Figure 48 shows the average power losses for each line and hour, considering the original system and the seven strategies evaluated in this section. In Figure 48a, which represents the power losses in the original system, the losses are concentrated along specific lines with higher impedance and close to heavier loads, with notable peaks in time period when the load is higher, as shown in Figure 10a. These high peaks highlight inefficiencies in the system under the baseline configuration, with no interventions applied. Figure 48b, showing the effect of the allocation and sizing of capacitors, illustrates a reduction in power losses compared to the original system. While the peaks remain in the same regions, their magnitudes are reduced, indicating an improvement in the system's efficiency due to reactive power compensation. In Figure 48c, where OLTC transformer operation is implemented, a slight improvement in power loss reduction is observed. However, the effect is less pronounced than in Figure 48b, as the OLTC operation alone is not as effective in reducing losses across the network. The distribution of losses remains similar to the original system, although the magnitude of some peaks is diminished.

Figure 48 – Power losses considering the (a) original system, and Strategies (b) 1, (c) 2, (d) 3, (e) 4, (f) 5, (g) 6, and (h) 7.

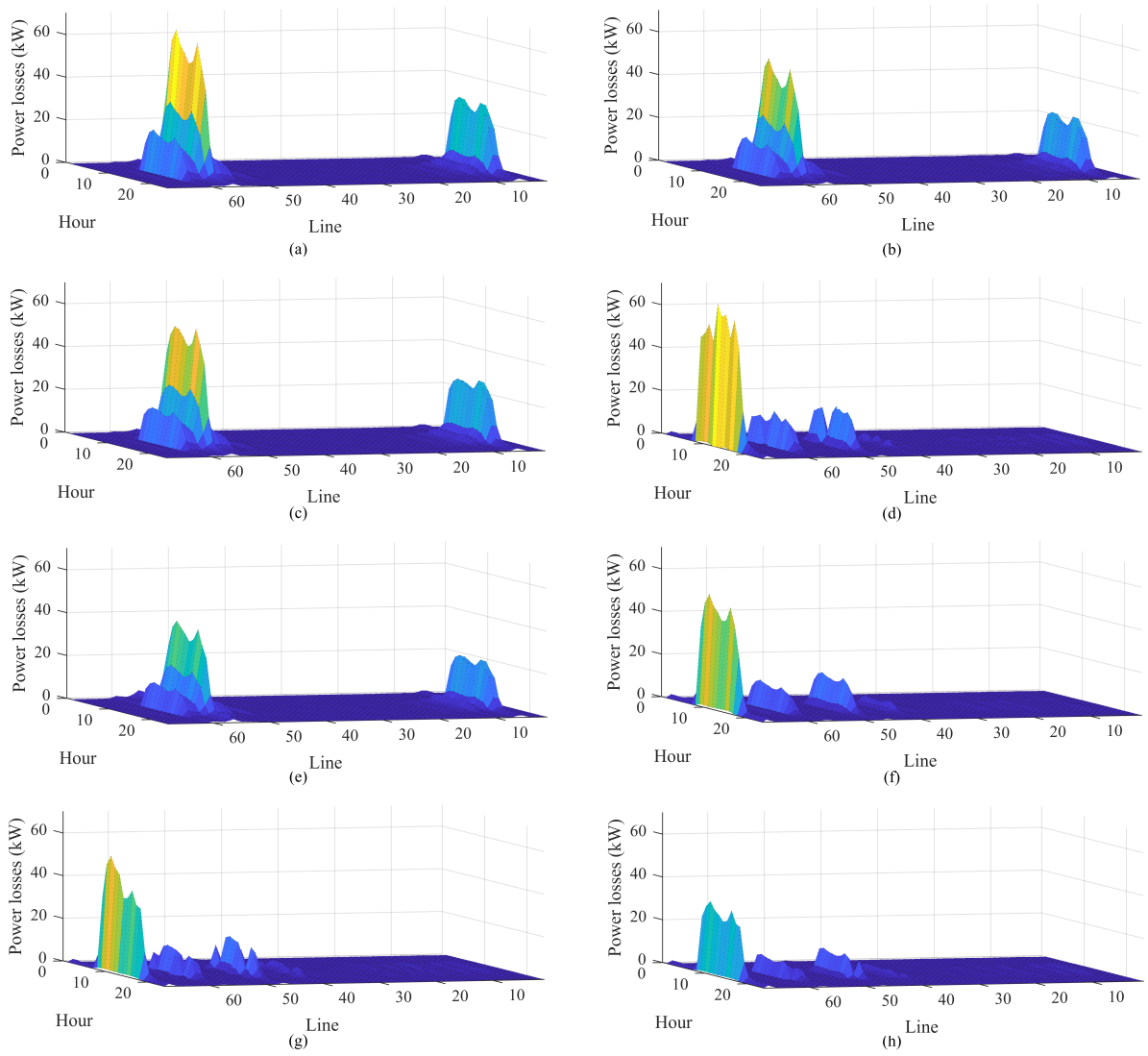

Source: Author.

Figure 48d highlights the performance of network reconfiguration, where power losses are minimized compared to Figure 48b and 48c. Unlike the original system or the other individual strategies, the losses become more concentrated along a specific line rather than being distributed across multiple lines. This shift indicates a reallocation of power flows in the network. Despite the overall minimization of losses, concentrating them on fewer lines may not be ideal in the long term, as it could necessitate network expansion to accommodate increased load demands. Over time, this could result in higher infrastructure costs and operational challenges, making a more balanced distribution of power losses a potentially more sustainable approach.

On the other hand, Figure 48e combines OLTC operation with capacitors allocation and sizing, yielding a more prominent reduction in power losses compared to their individual effects. The peaks are further suppressed, but they still remain in the same lines as the original system.

Figures 48f and 48g, which combine network reconfiguration with capacitors allocation and OLTC operation, respectively, present similar behaviors in reducing power losses across the system. Both strategies achieve notable improvements, with the lines experiencing higher losses now concentrated in different areas compared to the original system, due to the reconfiguration process. However, the combination with capacitors allocation (Figure 48f) results in slightly more effective loss reduction than the combination with OLTC operation (Figure 48g). Finally, Figure 48h, representing the combined application of all three strategies, achieves the lowest power losses among all configurations, indicating that the integration of all methods offers significant benefits. Additionally, this approach significantly reduces the peak of the losses, which may contribute to greater long-term efficiency by potentially delaying or minimizing the need for future network expansion investments.

Table 13 presents the objective function values for each approach evaluated in this study, considering $t^{\text{int}} = 1$ h. The results in Table 13 support the insights derived from the analyses of Figures 47 and 48, emphasizing the effectiveness of network reconfiguration, both individually and when combined with other strategies. Notably, network reconfiguration alone achieves a 49.99% reduction in f_1 compared to the original system, highlighting its significant impact on reducing power loss costs. When combined with capacitors allocation, f_1 is further reduced by 14.56%, while its combination with OLTC transformer operation results in a further reduction of 15.11%. The comprehensive strategy that combines capacitors allocation, OLTC operation, and network reconfiguration achieves the lowest f_1, representing a 37.13% reduction compared to network reconfiguration alone and a 68.56% reduction compared to the original system.

Table 13 – Values of the objective functions for each strategy considering $t^{\text{int}} = 1$ h.

Approach	f_1 (US$)	f_2 (pu)
Original system	319.92	0.029
Capacitors allocation and sizing	244.61	0.023
OLTC transformer operation	284.56	0.029
Network reconfiguration	159.97	0.012
Capacitors allocation and sizing combined with OLTC transformer operation	220.89	0.018
Capacitors allocation and sizing combined with network reconfiguration	136.67	0.008
Network reconfiguration combined with OLTC transformer operation	135.79	0.021
Capacitors allocation and sizing, OLTC transformer operation, and network reconfiguration	100.57	0.008

In terms of f_2, network reconfiguration results in a 58.62% reduction compared to the original system, while the comprehensive approach achieves a total reduction of 72.41%. It can be observed that, although the OLTC transformer operation directly influences the voltage profile, this strategy alone is not effective in minimizing f_2, as it produced a VCI value nearly

identical to that of the original system. This is because the strategy only adjusts the voltage at the substation, whereas the critical issue lies in the voltage variation throughout the network. As the impedance between the substation and the bus increases, the voltage decreases, approaching the lower acceptable limit.

Furthermore, it is essential to assess the practical implications for utility operators when implementing the proposed methodology. In the approach where capacitors are allocated and sized, an OLTC transformer is installed and operated, and the system is reconfigured, the total investment cost is 33,250 US$, which remains within the available investment budget. Conversely, in the original system, since no expansion is carried out, there are no investment costs. However, the original system incurs an active power loss cost of 319.92 US$ per day, whereas the proposed approach, incorporating capacitors, the OLTC transformer, and system reconfiguration, results in a significantly lower active power loss cost of 100.57 US$ per day. Based on these values, the payback period for the investment in network expansion is approximately 152 days, given the substantial reduction in active power loss costs.

Beyond the financial aspects, feasibility must also be considered when deploying these strategies in real-world distribution networks. The integration of OLTC transformers and capacitors requires careful planning to ensure compatibility with existing infrastructure and compliance with regulatory standards. Additionally, system reconfiguration may introduce operational challenges, such as switching constraints and reliability concerns, which must be addressed through proper coordination and monitoring. Despite these challenges, the relatively short payback period and long-term cost savings indicate that the proposed approach is a viable and economically attractive solution for improving distribution system performance. Moreover, these strategies are already widely adopted in practical distribution networks, further reinforcing their feasibility.

4.5 Chapter Conclusions

The results presented in this chapter demonstrate the effectiveness of the proposed methodologies in optimizing the planning and operation of distribution networks. The multi-objective optimization approaches effectively addressed the conflicting objectives of minimizing power losses, voltage deviation, and operational costs, while ensuring the proper integration of DERs, capacitors, and EVCSs. Furthermore, the results highlight the significance of accounting for stochastic variations in uncertain variables to guarantee robust and reliable performance under unforeseen network conditions. These outcomes underscore the practical applicability and relevance of the proposed strategies in modern distribution systems.

Chapter 5

Conclusions

This thesis introduced multi-objective optimization approaches with the aim of enhancing the operation and planning of distribution networks, focusing on the DSO's perspective. In the first approach, a protection scheme composed of reclosers and fuses was proposed, considering the NSGA-II to mutually minimize the operating time of each protective device. The NSGA-II was also used to optimize the size and location of DERs in the IEEE 34-bus test feeder. The objectives of this allocation problem consisted of the minimization of the investment and operational costs, voltage deviation, and short-circuit current. The addition of the short-circuit current in the mathematical formulation assisted in the maintenance of the original protection scheme, since the fault current increased by only 0.26% when considering the DERs allocated in the distribution system.

Another important contribution of this first approach is the inclusion of the recloser-fuse coordination constraints in the formulation of the DERs allocation and sizing problem, which preserved the correct operation of the protection scheme proposed in this study. Taking this novel approach into account, it is possible to avoid the need for adaptive protection schemes, the application of FCLs, and the adjustment of the protective device settings considering the DERs integration in the system, which are the most adopted solutions in recent papers. Regarding the DERs allocation results, it was observed a 15.61% reduction of the overall cost, due to the lower DER energy cost when compared to the substation energy cost. In addition, the voltage deviation of the system was reduced by 10.01%, caused by the minimization of the current of each branch, which decreases the power losses of the network.

In the second approach, a novel multi-objective optimization framework for balanced three-phase distribution system planning was introduced, incorporating the allocation and sizing of DERs and capacitors, along with static network reconfiguration. Each individual strategy, encompassing DERs, capacitors, and static network reconfiguration, was systematically performed and compared across all possible combinations. Initially, it became evident that strategies exclusively focused on DERs and/or capacitors do not effectively mitigate the high voltage deviation issue. Nevertheless, these components, contributing reactive power support to the distribution system, enhanced the benefits of the static network reconfiguration.

When comparing the solutions derived from the multi-objective optimization method, MOCS, with those from the single-objective optimization method, CSA, a greater balance in the MOCS solutions concerning the objective functions was observed, attributed to the

application of dominance concepts inherent in multi-objective optimization. Another advantage of employing the multi-objective method lies in the potential to explore other non-dominated solutions by adjusting the parameters of the Fuzzy Decision-making Method, while single-objective optimization restricts the result to a single final solution. Finally, the proposed approach demonstrated superior results compared to the other strategies introduced in previous articles, due to the enhanced flexibility of the distribution system's operation and planning, enabling the exploration of a larger set of non-dominated solutions.

In the third approach, a multi-objective optimization strategy was proposed for the allocation and sizing of EVCSs, DERs, and capacitors, combined with dynamic network reconfiguration. The effectiveness of this methodology was demonstrated through comprehensive comparisons with prior studies in the field, employing the 33-bus test system as a case study. The novel two-stage approach introduced in this approach, which optimized planning and operation separately, demonstrated the most favorable outcome, achieving an effective balance by minimizing overall costs, improving the voltage profile, and reducing power losses. This approach not only ensures operational efficiency for the DSO but also enhances reliability and cost-effectiveness for end customer, providing a sustainable and economically viable solution for modern distribution systems. In this context, notable improvements were achieved, resulting in a remarkable reduction of power losses by 45.50% and voltage deviation by 43.97% when compared to the original system.

In the forth approach, a multi-objective planning framework was proposed to optimize the performance of the distribution system by simultaneously addressing dynamic network reconfiguration, capacitors allocation, and OLTC transformer adjustment. The approach incorporated stochastic customer-owned DERs and introduced a novel VCI to enhance voltage regulation while minimizing power loss costs. The results highlighted the effectiveness of the dynamic network reconfiguration, both as a standalone strategy and when combined with other methods, particularly capacitors allocation and OLTC transformer adjustment.

Based on the results of this approach, the significant expansion of the search space achieved by integrating the strategies resulted in higher-quality solutions. In this context, the integrated framework, combining all three strategies, yielded the best results, reducing power losses by 68.56% and significantly improving the voltage profile, with a 72.41% reduction in the VCI compared to the original system. It is also noteworthy that this approach resulted in a reduction in the peaks of power losses, contributing to improved long-term efficiency by potentially postponing or reducing the need for future network expansion investments.

In summary, this thesis presents a comprehensive and innovative set of methodologies to address the critical challenges encountered by DSOs in modern distribution networks. By integrating advanced multi-objective optimization techniques with practical considerations, the proposed approaches provide well-balanced solutions that effectively enhance the operational efficiency and reliability of distribution systems. These methodologies equip DSOs with the

necessary tools to manage the increasing complexity of modern grids, characterized by high DER penetration and growing sustainability demands, ensuring optimized performance while adhering to technical, economic, and regulatory requirements.

5.1 Future Work

Regarding the evaluation of the protection scheme, carried out in the approach outlined in Section 4.1, the following directions can be explored in future research:

- Integrate the methodology outlined in Section 4.1 with those presented in Sections 4.2–4.4. This integration aims to incorporate constraints related to the coordination of protective devices into the optimization process. By doing so, the planning and operation of the distribution system can be optimized while ensuring that the original protection scheme of the system continues to operate correctly after the optimization.
- In addition to preserving the coordination of protective devices, it is essential to assess other impacts that DER integration may have on the protection scheme, such as sympathetic tripping, blind protection, reduced reach of distance protection, among others.
- Include other types of DERs since they present distinct behaviors under fault conditions, which can significantly impact the proper operation of protective devices. Each DER technology may introduce unique challenges and considerations regarding fault response and protective devices' coordination.

For the allocation of EVCSs, as in the approach described in Section 4.3, the following aspects should be considered:

- Incorporate various EV models into the analysis, considering different battery storage capacities, maximum charging power, and driving ranges.
- Incorporate user behavior patterns, as well as cost and land availability considerations, into the objective function evaluation to achieve a solution that benefits both EV users and the entity responsible for infrastructure deployment.
- Assess the impact of EVCS integration on grid stability and reliability, considering factors such as charging demand fluctuations and peak load contributions.

In terms of network reconfiguration, the following aspects can be incorporated into the approaches detailed in Sections 4.2–4.4:

- Assess the availability and functionality of sectionalizing devices to enable network reconfiguration.

- Consider the impact of switching operations on system reliability and power quality, including potential transient effects.

Finally, considering aspects common to all approaches proposed in this thesis, future research directions also include:

- Evaluate the priorities and requirements of utility companies to refine the mathematical formulation of the optimization problem.
- Assess the applicability and scalability of the proposed approaches by testing them on larger and real-world systems.
- Implement additional stochastic techniques for comparison with the Monte Carlo Method to further enhance the efficiency of the proposed methodologies.
- Employ several optimization methods with distinct characteristics to compare the results obtained in this thesis. Additionally, given the stochastic nature of some optimization methods, perform a predefined number of simulations to evaluate the consistency of the results through a statistical analysis.
- Implement a self-tuning framework to properly configure the optimization algorithms, ensuring more reliable and consistent results.

References

[1] F. Blaabjerg, Y. Yang, D. Yang, and X. Wang, "Distributed power-generation systems and protection", *Proceedings of the IEEE*, vol. 105, no. 7, pp. 1311–1331, 2017. DOI: 10.1109/JPROC.2017.2696878 (cited on pages 20, 31, 60).

[2] B. R. Pereira, G. R. M. da Costa, J. Contreras, and J. R. S. Mantovani, "Optimal distributed generation and reactive power allocation in electrical distribution systems", *IEEE Transactions on Sustainable Energy*, vol. 7, no. 3, pp. 975–984, 2016. DOI: 10.1109/TSTE.2015.2512819 (cited on pages 20, 31, 34).

[3] J. Qiu, Z. Xu, Y. Zheng, D. Wang, and Z. Y. Dong, "Distributed generation and energy storage system planning for a distribution system operator", *IET Renewable Power Generation*, vol. 12, no. 12, pp. 1345–1353, 2018. DOI: 10.1049/iet-rpg.2018.5115 (cited on pages 20, 31, 34).

[4] E. Mulenga, M. H. Bollen, and N. Etherden, "A review of hosting capacity quantification methods for photovoltaics in low-voltage distribution grids", *International Journal of Electrical Power & Energy Systems*, vol. 115, p. 105 445, 2020, ISSN: 0142-0615. DOI: 10.1016/j.ijepes.2019.105445 (cited on pages 20, 43).

[5] P. Chaudhary and M. Rizwan, "Voltage regulation mitigation techniques in distribution system with high PV penetration: A review", *Renewable and Sustainable Energy Reviews*, vol. 82, pp. 3279–3287, 2018, ISSN: 1364-0321. DOI: 10.1016/j.rser.2017.10.017 (cited on page 20).

[6] M. Usama *et al.*, "A comprehensive review on protection strategies to mitigate the impact of renewable energy sources on interconnected distribution networks", *IEEE Access*, vol. 9, pp. 35 740–35 765, 2021. DOI: 10.1109/ACCESS.2021.3061919 (cited on pages 21, 31).

[7] K. Mahmoud and M. Lehtonen, "Direct approach for optimal allocation of multiple capacitors in distribution systems using novel analytical closed-form expressions", *Electrical Engineering*, vol. 103, no. 1, pp. 245–256, 2021, ISSN: 1432-0487. DOI: 10.1007/s00202-020-01073-9 (cited on page 21).

[8] M. Asna, H. Shareef, and A. Prasanthi, "Planning of fast charging stations with consideration of EV user, distribution network and station operation", *Energy Reports*, vol. 9, pp. 455–462, 2023, ISSN: 2352-4847. DOI: 10.1016/j.egyr.2023.01.063 (cited on pages 21, 118).

[9] R. S. F. Ferraz, R. S. F. Ferraz, and A. C. Rueda-Medina, "Multi-objective optimization approach for allocation and sizing of distributed energy resources preserving the protection scheme in distribution networks", *Journal of Control, Automation and Electrical Sys-*

tems, vol. 34, no. 5, pp. 1080–1092, Oct. 2023, ISSN: 2195-3899. DOI: 10.1007/s40313-023-01030-4 (cited on page 25).

[10] R. S. F. Ferraz, R. S. F. Ferraz, and A. C. Rueda-Medina, "A comprehensive multi-objective optimization framework for balanced distribution system planning", *Journal of Control, Automation and Electrical Systems*, vol. 36, no. 1, pp. 117–133, Feb. 2025, ISSN: 2195-3899. DOI: 10.1007/s40313-024-01134-5 (cited on pages 25, 74).

[11] R. S. F. Ferraz, R. S. F. Ferraz, V. F. S. Júnior, and A. C. Rueda-Medina, "Distributed energy resources, capacitor banks and fast charging stations allocation using a multi-objective optimization approach", in *2023 15th Seminar on Power Electronics and Control (SEPOC)*, 2023, pp. 1–6. DOI: 10.1109/SEPOC58810.2023.10322585 (cited on pages 25, 118).

[12] R. S. F. Ferraz, R. S. F. Ferraz, and A. C. Rueda-Medina, "A novel two-stage multi-objective optimization strategy for enhanced network planning and operation", *Electrical Engineering*, Sep. 2024, ISSN: 1432-0487. DOI: 10.1007/s00202-024-02675-3 (cited on page 25).

[13] R. S. F. Ferraz, R. S. F. Ferraz, V. F. S. Júnior, and A. C. Rueda-Medina, "Multi-objective approach for distribution system planning considering stochastic customer-owned distributed energy resources", *IEEE Access*, 2025. DOI: 10.1109/ACCESS.2025.3547277 (cited on page 25).

[14] R. S. F. Ferraz, R. S. F. Ferraz, A. C. Rueda-Medina, and M. H. M. Paiva, "Power flow and fault analysis using graph theory", in *2021 IEEE URUCON*, 2021, pp. 6–11. DOI: 10.1109/URUCON53396.2021.9647053 (cited on page 25).

[15] R. S. F. Ferraz, R. S. F. Ferraz, A. C. Rueda-Medina, and M. H. M. Paiva, "An integer linear programming approach for phasor measurement unit placement", in *2021 IEEE URUCON*, 2021, pp. 108–112. DOI: 10.1109/URUCON53396.2021.9647377 (cited on page 26).

[16] R. S. Ferraz, R. S. Ferraz, A. C. Rueda-Medina, and J. F. Fardin, "Novel variable charging pricing strategy applied to the multi-objective planning of integrated fast and slow electric vehicle charging stations and distributed energy resources", *Electric Power Systems Research*, vol. 241, p. 111 293, 2025, ISSN: 0378-7796. DOI: 10.1016/j.epsr.2024.111293 (cited on page 26).

[17] A. C. Rueda-Medina, R. S. Ferraz, R. S. Ferraz, and O. E. Batista, "A stochastic market-based clearing approach in active distribution networks by using interval optimization", *Electric Power Systems Research*, vol. 235, p. 110 621, 2024, ISSN: 0378-7796. DOI: 10.1016/j.epsr.2024.110621 (cited on page 26).

[18] R. S. F. Ferraz, R. S. F. Ferraz, A. C. Rueda-Medina, and J. F. Fardin, "Integration of slow and fast charging modes in the optimized planning of electric vehicle charging station using multi-objective optimization approach", *Journal of Control, Automation and Electrical Systems*, vol. 36, no. 1, pp. 165–180, Feb. 2025, ISSN: 2195-3899. DOI: 10.1007/s40313-024-01142-5 (cited on page 26).

[19] R. S. F. Ferraz, R. S. F. Ferraz, A. C. Rueda-Medina, and J. F. Fardin, "Multi-objective approach for optimized planning of electric vehicle charging stations and distributed energy resources", *Electrical Engineering*, vol. 105, no. 6, pp. 4105–4117, Dec. 2023, ISSN: 1432-0487. DOI: 10.1007/s00202-023-01942-z (cited on page 26).

[20] R. S. F. Ferraz, R. S. F. Ferraz, A. C. Rueda-Medina, and J. F. Fardin, "Multi-objective optimization approach for allocation of electric vehicles parking lots and smart charging with distributed energy resource", *Journal of Control, Automation and Electrical Systems*, vol. 34, no. 5, pp. 1070–1079, Oct. 2023, ISSN: 2195-3899. DOI: 10.1007/s40313-023-01027-z (cited on page 26).

[21] R. S. F. Ferraz, R. S. F. Ferraz, V. F. S. Júnior, A. C. Rueda-Medina, and J. F. Fardin, "Distributed energy resources and fast charging stations allocation for enhanced system operation and charging infrastructure coverage", in *2023 15th Seminar on Power Electronics and Control (SEPOC)*, 2023, pp. 1–6. DOI: 10.1109/SEPOC58810.2023.10322598 (cited on page 26).

[22] V. F. S. Júnior, R. S. F. Ferraz, R. S. F. Ferraz, and A. C. Rueda-Medina, "Network reconfiguration and distributed generators allocation and sizing using multi-objective optimization algorithms", in *2023 15th Seminar on Power Electronics and Control (SEPOC)*, 2023, pp. 1–6. DOI: 10.1109/SEPOC58810.2023.10322616 (cited on page 26).

[23] V. F. Dos Santos Júnior, R. Santos Freire Ferraz, and A. C. Rueda-Medina, "Allocation and sizing of distributed generators in distribution system using multi-objective optimization", in *2023 15th Seminar on Power Electronics and Control (SEPOC)*, 2023, pp. 1–6. DOI: 10.1109/SEPOC58810.2023.10322617 (cited on page 26).

[24] R. S. F. Ferraz, R. S. F. Ferraz, A. C. Rueda-Medina, and J. F. Fardin, "Multi-objective optimization approach for the allocation of fast charging stations and distributed energy resources", in *VI Simpósio Brasileiro de Sistemas Elétricos*, Santa Maria, Rio Grande do Sul, Brasil: SBA Sociedade Brasileira de Automática, 2022 (cited on page 26).

[25] R. S. F. Ferraz, R. S. F. Ferraz, A. C. Rueda-Medina, and J. F. Fardin, "Hybrid model of artificial neural network-cuckoo search for irradiance and load forecasting", in *2021 IEEE URUCON*, 2021, pp. 132–137. DOI: 10.1109/URUCON53396.2021.9647366 (cited on page 27).

[26] R. S. F. Ferraz, R. S. F. Ferraz, A. C. Rueda-Medina, J. Farias F., and A. Custódio G., "Optimized allocation and sizing of distributed energy resource in distribution systems using cuckoo search algorithm", in *XIX Conferência de Estudos em Engenharia Elétrica*, Universidade Federal de Uberlândia, Nov. 2021 (cited on page 27).

[27] M. Meskin, A. Domijan, and I. Grinberg, "Impact of distributed generation on the protection systems of distribution networks: Analysis and remedies – review paper", *IET Generation, Transmission & Distribution*, vol. 14, no. 24, pp. 5944–5960, 2020. DOI: 10.1049/iet-gtd.2019.1652 (cited on pages 31, 47).

[28] P. H. Shah and B. R. Bhalja, "New adaptive digital relaying scheme to tackle recloser–fuse miscoordination during distributed generation interconnections", *IET Generation, Transmission & Distribution*, vol. 8, pp. 682–688, 2014. DOI: 10.1049/iet-gtd.2013.0222 (cited on pages 31, 46, 47).

[29] M. Y. Shih, A. Conde, Z. Leonowicz, and L. Martirano, "An adaptive overcurrent coordination scheme to improve relay sensitivity and overcome drawbacks due to distributed generation in smart grids", *IEEE Transactions on Industry Applications*, vol. 53, pp. 5217–5228, 2017. DOI: 10.1109/TIA.2017.2717880 (cited on pages 31, 46, 47).

[30] M. N. Alam, "Adaptive protection coordination scheme using numerical directional overcurrent relays", *IEEE Transactions on Industrial Informatics*, vol. 15, pp. 64–73, 2019. DOI: 10.1109/TII.2018.2834474 (cited on pages 31, 32, 46, 47).

[31] R. Jain, D. L. Lubkeman, and S. M. Lukic, "Dynamic adaptive protection for distribution systems in grid-connected and islanded modes", *IEEE Transactions on Power Delivery*, vol. 34, pp. 281–289, 2019. DOI: 10.1109/TPWRD.2018.2884705 (cited on pages 31, 32, 46, 47).

[32] E. Purwar, S. P. Singh, and D. N. Vishwakarma, "A robust protection scheme based on hybrid pick-up and optimal hierarchy selection of relays in the variable DGs-distribution system", *IEEE Transactions on Power Delivery*, vol. 35, pp. 150–159, 2020. DOI: 10.1109/TPWRD.2019.2929755 (cited on pages 31, 32, 46, 47).

[33] A. Elmitwally, E. Gouda, and S. Eladawy, "Restoring recloser-fuse coordination by optimal fault current limiters planning in DG-integrated distribution systems", *International Journal of Electrical Power & Energy Systems*, vol. 77, pp. 9–18, 2016, ISSN: 0142-0615. DOI: 10.1016/j.ijepes.2015.11.021 (cited on pages 31, 32, 46, 47).

[34] Z. Shu, Y. Chen, C. Deng, F. Zheng, and H. Zhong, "Pareto optimal allocation of flexible fault current limiter based on multi-objective improved bat algorithm", *IEEE Access*, vol. 9, pp. 12 762–12 778, 2021. DOI: 10.1109/ACCESS.2021.3050795 (cited on pages 31, 32, 46, 47).

[35] M. E. Hamidi and R. M. Chabanloo, "Optimal allocation of distributed generation with optimal sizing of fault current limiter to reduce the impact on distribution networks using NSGA-II", *IEEE Systems Journal*, vol. 13, pp. 1714–1724, 2019. DOI: 10.1109/JSYST.2018.2867910 (cited on pages 31, 32, 46, 47).

[36] A. E. Dahej, S. Esmaeili, and H. Hojabri, "Co-optimization of protection coordination and power quality in microgrids using unidirectional fault current limiters", *IEEE Transactions on Smart Grid*, vol. 9, pp. 5080–5091, 2018. DOI: 10.1109/TSG.2017.2679281 (cited on pages 31, 33, 46, 47).

[37] A. A. A. El-Ela, R. A. El-Sehiemy, A. M. Shaheen, and A. R. Ellien, "Optimal allocation of distributed generation units correlated with fault current limiter sites in distribution systems", *IEEE Systems Journal*, vol. 15, pp. 2148–2155, 2021. DOI: 10.1109/JSYST.2020.3009028 (cited on pages 31, 33, 46, 47).

[38] E. Dehghanpour, H. Kazemi Karegar, R. Kheirollahi, and T. Soleymani, "Optimal coordination of directional overcurrent relays in microgrids by using cuckoo-linear optimization algorithm and fault current limiter", *IEEE Transactions on Smart Grid*, vol. 9, pp. 1365–1375, 2018. DOI: 10.1109/TSG.2016.2587725 (cited on pages 31, 33, 46, 47, 89).

[39] R. S. F. Ferraz, R. S. F. Ferraz, A. C. Rueda-Medina, and O. E. Batista, "Genetic optimisation-based distributed energy resource allocation and recloser-fuse coordination", *IET Generation, Transmission & Distribution*, vol. 14, no. 20, pp. 4501–4508, 2020. DOI: 10.1049/iet-gtd.2020.0664 (cited on pages 31, 33, 34, 46–51, 82, 84, 89, 101, 108).

[40] B. Fani, H. Bisheh, and A. Karami-Horestani, "An offline penetration-free protection scheme for PV-dominated distribution systems", *Electric Power Systems Research*, vol. 157, pp. 1–9, 2018, ISSN: 0378-7796. DOI: 10.1016/j.epsr.2017.11.020 (cited on pages 31, 33, 46, 47).

[41] K. Pereira, B. R. Pereira, J. Contreras, and J. R. S. Mantovani, "A multiobjective optimization technique to develop protection systems of distribution networks with distributed generation", *IEEE Transactions on Power Systems*, vol. 33, pp. 7064–7075, 2018. DOI: 10.1109/TPWRS.2018.2842648 (cited on pages 31, 34, 46, 47).

[42] M. N. Alam, B. Das, and V. Pant, "Optimum recloser–fuse coordination for radial distribution systems in the presence of multiple distributed generations", *IET Generation, Transmission & Distribution*, vol. 12, pp. 2585–2594, 2018. DOI: 10.1049/iet-gtd.2017.1532 (cited on pages 31, 34, 46, 47, 84, 89).

[43] A. Sharma and B. K. Panigrahi, "Phase fault protection scheme for reliable operation of microgrids", *IEEE Transactions on Industry Applications*, vol. 54, pp. 2646–2655, 2018. DOI: 10.1109/TIA.2017.2787691 (cited on pages 31, 34, 46, 47, 89).

[44] A. M. El-Rifaie *et al.*, "Modified gradient-based algorithm for distributed generation and capacitors integration in radial distribution networks", *IEEE Access*, vol. 11, pp. 120 899–120 917, 2023. DOI: 10.1109/ACCESS.2023.3326758 (cited on pages 31, 35, 48–53, 82, 108).

[45] A. S. C. Martins, L. R. de Araujo, and D. R. R. Penido, "Sensibility analysis with genetic algorithm to allocate distributed generation and capacitor banks in unbalanced distribution systems", *Electric Power Systems Research*, vol. 209, p. 107 962, 2022, ISSN: 0378-7796. DOI: 10.1016/j.epsr.2022.107962 (cited on pages 31, 35, 48–53, 82, 108).

[46] A. M. Shaheen and R. A. El-Sehiemy, "Optimal coordinated allocation of distributed generation units/ capacitor banks/ voltage regulators by EGWA", *IEEE Systems Journal*, vol. 15, no. 1, pp. 257–264, 2021. DOI: 10.1109/JSYST.2020.2986647 (cited on pages 31, 35, 48–53, 82, 108).

[47] O. D. Melgar-Dominguez, M. Pourakbari-Kasmaei, and J. R. S. Mantovani, "Adaptive robust short-term planning of electrical distribution systems considering siting and sizing of renewable energy based DG units", *IEEE Transactions on Sustainable Energy*, vol. 10, no. 1, pp. 158–169, 2019. DOI: 10.1109/TSTE.2018.2828778 (cited on pages 31, 35, 48–53, 82, 108).

[48] H. A. Khattab, A. S. Aljumah, A. M. Shaheen, and H. A. Omar, "Improved manta ray foraging algorithm for optimal allocation strategies to power delivery capabilities in active distribution networks", *IEEE Access*, vol. 12, pp. 157 699–157 715, 2024. DOI: 10.1109/ACCESS.2024.3486743 (cited on pages 31, 35, 48–53, 82).

[49] M. Mahdavi, K. Schmitt, F. Jurado, A. Awaafo, and M. Chamana, "An efficient framework for optimal allocation of renewable energy sources in reconfigurable distribution systems with variable loads", *IEEE Transactions on Industry Applications*, vol. 60, no. 2, pp. 2431–2442, 2024. DOI: 10.1109/TIA.2023.3341876 (cited on pages 31, 35, 48–53, 82, 100).

[50] Y. Wang, Y. Xu, and H. Sun, "Multi-objective planning of distributed energy resources based on enhanced adaptive weighted-sum algorithm", *IEEE Transactions on Power Systems*, vol. 39, no. 2, pp. 4624–4637, 2024. DOI: 10.1109/TPWRS.2023.3317782 (cited on pages 31, 36, 48–53, 82).

[51] R. R. C. Paiva, A. C. Rueda-Medina, and J. R. S. Mantovani, "Short-term electrical distribution systems planning considering distributed generation and reliability", *Journal of Control, Automation and Electrical Systems*, vol. 28, no. 4, pp. 552–566, 2017, ISSN: 2195-3899. DOI: 10.1007/s40313-017-0323-1 (cited on pages 31, 36, 48–53, 82, 108).

[52] L. F. Azeredo, I. Yahyaoui, R. Fiorotti, J. F. Fardin, H. Garcia-Pereira, and H. R. Rocha, "Study of reducing losses, short-circuit currents and harmonics by allocation of distributed generation, capacitor banks and fault current limiters in distribution grids", *Applied*

Energy, vol. 350, p. 121 760, 2023, ISSN: 0306-2619. DOI: 10.1016/j.apenergy.2023.121760 (cited on pages 31, 36, 48–53, 82, 108).

[53] P. Rajesh and F. H. Shajin, "Optimal allocation of EV charging spots and capacitors in distribution network improving voltage and power loss by quantum-behaved and gaussian mutational dragonfly algorithm (QGDA)", *Electric Power Systems Research*, vol. 194, p. 107 049, 2021, ISSN: 0378-7796. DOI: 10.1016/j.epsr.2021.107049 (cited on pages 31, 37, 50, 51, 118).

[54] B. Geetha, P. A., S. Jeyasudha, and K. Dinakaran, "Hybrid approach based combined allocation of electric vehicle charging stations and capacitors in distribution systems", *Journal of Energy Storage*, vol. 72, p. 108 273, 2023, ISSN: 2352-152X. DOI: 10.1016/j.est.2023.108273 (cited on pages 31, 37, 50, 51, 118).

[55] A. Amer, M. A. Azzouz, A. Azab, and A. S. A. Awad, "Stochastic planning for optimal allocation of fast charging stations and wind-based DGs", *IEEE Systems Journal*, vol. 15, no. 3, pp. 4589–4599, 2021. DOI: 10.1109/JSYST.2020.3012939 (cited on pages 31, 37, 50, 51, 118).

[56] A. Pahlavanhoseini and M. S. Sepasian, "Scenario-based planning of fast charging stations considering network reconfiguration using cooperative coevolutionary approach", *Journal of Energy Storage*, vol. 23, pp. 544–557, 2019, ISSN: 2352-152X. DOI: 10.1016/j.est.2019.04.024 (cited on pages 31, 37, 50, 51, 100, 118).

[57] H. Zhang, S. J. Moura, Z. Hu, W. Qi, and Y. Song, "Joint PEV charging network and distributed PV generation planning based on accelerated generalized benders decomposition", *IEEE Transactions on Transportation Electrification*, vol. 4, no. 3, pp. 789–803, 2018. DOI: 10.1109/TTE.2018.2847244 (cited on pages 31, 37, 50, 51).

[58] F. Ahmad, I. Ashraf, A. Iqbal, M. Marzband, and I. Khan, "A novel AI approach for optimal deployment of EV fast charging station and reliability analysis with solar based DGs in distribution network", *Energy Reports*, vol. 8, pp. 11 646–11 660, 2022, ISSN: 2352-4847. DOI: 10.1016/j.egyr.2022.09.058 (cited on pages 31, 37, 50, 51).

[59] M. Abdelaziz, A. Ali, R. Swief, and R. Elazab, "A reliable optimal electric vehicle charging stations allocation", *Ain Shams Engineering Journal*, vol. 15, no. 7, p. 102 763, 2024, ISSN: 2090-4479. DOI: 10.1016/j.asej.2024.102763 (cited on pages 31, 38, 50, 51).

[60] E. A. Rene, W. S. Tounsi Fokui, and P. K. Nembou Kouonchie, "Optimal allocation of plug-in electric vehicle charging stations in the distribution network with distributed generation", *Green Energy and Intelligent Transportation*, vol. 2, no. 3, p. 100 094, 2023, ISSN: 2773-1537. DOI: 10.1016/j.geits.2023.100094 (cited on pages 31, 38, 50, 51).

[61] J. J. Saldanha, A. Nied, R. Trentini, and R. Kutzner, "AI-based optimal allocation of bess, EV charging station and DG in distribution network for losses reduction and peak load shaving", *Electric Power Systems Research*, vol. 234, p. 110 554, 2024, ISSN: 0378-7796. DOI: 10.1016/j.epsr.2024.110554 (cited on pages 31, 38, 50, 51).

[62] P. Singh, S. K. Bishnoi, and N. K. Meena, "Moth search optimization for optimal DERs integration in conjunction to OLTC tap operations in distribution systems", *IEEE Systems Journal*, vol. 14, no. 1, pp. 880–888, 2020. DOI: 10.1109/JSYST.2019.2911534 (cited on pages 31, 39, 52, 53).

[63] W. Zhang, W. Sheng, K. Liu, T. Kang, and H. Zhan, "Toward optimal voltage/var control with smart PVs in active distribution networks", *Electric Power Systems Research*, vol. 228, p. 110 076, 2024, ISSN: 0378-7796. DOI: 10.1016/j.epsr.2023.110076 (cited on pages 31, 39, 52, 53, 100).

[64] X. Sun and J. Qiu, "Two-stage volt/var control in active distribution networks with multi-agent deep reinforcement learning method", *IEEE Transactions on Smart Grid*, vol. 12, no. 4, pp. 2903–2912, 2021. DOI: 10.1109/TSG.2021.3052998 (cited on pages 31, 39, 52, 53).

[65] R. Wang, X. Bi, and S. Bu, "Real-time coordination of dynamic network reconfiguration and volt-var control in active distribution network: A graph-aware deep reinforcement learning approach", *IEEE Transactions on Smart Grid*, vol. 15, no. 3, pp. 3288–3302, 2024. DOI: 10.1109/TSG.2023.3324474 (cited on pages 31, 39, 52, 53, 100).

[66] K. K. Mehmood, S. U. Khan, S.-J. Lee, Z. M. Haider, M. K. Rafique, and C.-H. Kim, "A real-time optimal coordination scheme for the voltage regulation of a distribution network including an OLTC, capacitor banks, and multiple distributed energy resources", *International Journal of Electrical Power & Energy Systems*, vol. 94, pp. 1–14, 2018, ISSN: 0142-0615. DOI: 10.1016/j.ijepes.2017.06.024 (cited on pages 31, 40, 52, 53).

[67] H. Quan, Z. Li, T. Zhou, and J. Yin, "Two-stage optimization strategy of multi-objective volt/var coordination in electric distribution network considering renewable uncertainties", *Energy Reports*, vol. 9, pp. 155–166, 2023, ISSN: 2352-4847. DOI: 10.1016/j.egyr.2023.04.089 (cited on pages 31, 40, 52, 53, 100).

[68] M. Mahdavi, H. H. Alhelou, N. D. Hatziargyriou, and F. Jurado, "Reconfiguration of electric power distribution systems: Comprehensive review and classification", *IEEE Access*, vol. 9, pp. 118 502–118 527, 2021. DOI: 10.1109/ACCESS.2021.3107475 (cited on pages 31, 40).

[69] Z. Gong, Q. Chen, and K. Sun, "Novel methodology solving distribution network reconfiguration with DG placement", *The Journal of Engineering*, vol. 2019, no. 16, pp. 1668–1674, 2019. DOI: 10.1049/joe.2018.8521 (cited on pages 31, 40, 48–53, 82, 100, 108).

[70] A. M. Shaheen, R. A. El-Sehiemy, S. Kamel, E. E. Elattar, and A. M. Elsayed, "Improving distribution networks' consistency by optimal distribution system reconfiguration and distributed generations", *IEEE Access*, vol. 9, pp. 67 186–67 200, 2021. DOI: 10.1109/ACCESS.2021.3076670 (cited on pages 31, 41, 48–53, 82, 100, 108).

[71] A. M. Shaheen, A. M. Elsayed, A. R. Ginidi, R. A. El-Sehiemy, and E. E. Elattar, "Improved heap-based optimizer for DG allocation in reconfigured radial feeder distribution systems", *IEEE Systems Journal*, vol. 16, no. 4, pp. 6371–6380, 2022. DOI: 10.1109/JSYST.2021.3136778 (cited on pages 31, 41, 48–53, 82).

[72] S. Essallah and A. Khedher, "Optimization of distribution system operation by network reconfiguration and DG integration using MPSO algorithm", *Renewable Energy Focus*, vol. 34, pp. 37–46, 2020, ISSN: 1755-0084. DOI: 10.1016/j.ref.2020.04.002 (cited on pages 31, 41, 48–53, 82, 100, 108).

[73] M. Naguib, W. A. Omran, and H. E. A. Talaat, "Performance enhancement of distribution systems via distribution network reconfiguration and distributed generator allocation considering uncertain environment", *Journal of Modern Power Systems and Clean Energy*, vol. 10, no. 3, pp. 647–655, 2022. DOI: 10.35833/MPCE.2020.000333 (cited on pages 31, 41, 48–53, 82, 100, 108).

[74] A. K. Barnwal, L. K. Yadav, and M. K. Verma, "A multi-objective approach for voltage stability enhancement and loss reduction under PQV and P buses through reconfiguration and distributed generation allocation", *IEEE Access*, vol. 10, pp. 16 609–16 623, 2022. DOI: 10.1109/ACCESS.2022.3146333 (cited on pages 31, 41, 48–53, 82, 100, 108).

[75] J. M. Home-Ortiz, R. Vargas, L. H. Macedo, and R. Romero, "Joint reconfiguration of feeders and allocation of capacitor banks in radial distribution systems considering voltage-dependent models", *International Journal of Electrical Power & Energy Systems*, vol. 107, pp. 298–310, 2019, ISSN: 0142-0615. DOI: 10.1016/j.ijepes.2018.11.035 (cited on pages 31, 41, 48–53, 100, 108).

[76] E. E. Elattar, A. M. Shaheen, A. M. El-Sayed, R. A. El-Sehiemy, and A. R. Ginidi, "Optimal operation of automated distribution networks based-MRFO algorithm", *IEEE Access*, vol. 9, pp. 19 586–19 601, 2021. DOI: 10.1109/ACCESS.2021.3053479 (cited on pages 31, 41, 48–53, 82, 100).

[77] S. R. Biswal, G. Shankar, R. M. Elavarasan, and L. Mihet-Popa, "Optimal allocation/sizing of DGs/capacitors in reconfigured radial distribution system using quasi-reflected slime mould algorithm", *IEEE Access*, vol. 9, pp. 125 658–125 677, 2021. DOI: 10.1109/ACCESS.2021.3111027 (cited on pages 31, 42, 48–53, 82, 100).

[78] H. Tolabi, A. L. Ara, and R. Hosseini, "A new thief and police algorithm and its application in simultaneous reconfiguration with optimal allocation of capacitor and distributed generation units", *Energy*, vol. 203, p. 117 911, 2020, ISSN: 0360-5442. DOI: 10.1016/j.energy.2020.117911 (cited on pages 31, 42, 48–53, 82, 100).

[79] A. M. Helmi, R. Carli, M. Dotoli, and H. S. Ramadan, "Efficient and sustainable reconfiguration of distribution networks via metaheuristic optimization", *IEEE Transactions on Automation Science and Engineering*, vol. 19, no. 1, pp. 82–98, 2022. DOI: 10.1109/TASE.2021.3072862 (cited on pages 31, 42, 48–53, 78, 82, 98, 100, 108).

[80] J. Wang, W. Wang, H. Wang, and H. Zuo, "Dynamic reconfiguration of multiobjective distribution networks considering DG and EVs based on a novel LDBAS algorithm", *IEEE Access*, vol. 8, pp. 216 873–216 893, 2020. DOI: 10.1109/ACCESS.2020.3041398 (cited on pages 31, 42, 48–53, 73, 100).

[81] W. Wang, Y. Huang, M. Yang, C. Chen, Y. Zhang, and X. Xu, "Renewable energy sources planning considering approximate dynamic network reconfiguration and nonlinear correlations of uncertainties in distribution network", *International Journal of Electrical Power & Energy Systems*, vol. 139, p. 107 791, 2022, ISSN: 0142-0615. DOI: 10.1016/j.ijepes.2021.107791 (cited on pages 31, 42, 48–53, 73).

[82] T. H. B. Huy, T. V. Tran, D. Ngoc Vo, and H. T. T. Nguyen, "An improved metaheuristic method for simultaneous network reconfiguration and distributed generation allocation", *Alexandria Engineering Journal*, vol. 61, no. 10, pp. 8069–8088, 2022, ISSN: 1110-0168. DOI: 10.1016/j.aej.2022.01.056 (cited on pages 31, 43, 48–53, 82, 100, 108).

[83] M. Mahdavi, A. Awaafo, S. Z. Djokic, and F. Jurado, "An innovative power loss and cost minimization framework for distribution networks with uncertain variable loads by coordinating reconfiguration, capacitor installation and renewable generators placement", *IEEE Transactions on Industry Applications*, vol. 60, no. 5, pp. 7500–7510, 2024. DOI: 10.1109/TIA.2024.3403958 (cited on pages 31, 43, 50–53, 82).

[84] X. Sun, J. Qiu, Y. Tao, and J. Zhao, "Data-driven combined central and distributed volt/var control in active distribution networks", *IEEE Transactions on Smart Grid*, vol. 14, no. 3, pp. 1855–1867, 2023. DOI: 10.1109/TSG.2022.3213587 (cited on pages 31, 44, 52, 53).

[85] R. B. Navesi, D. Nazarpour, R. Ghanizadeh, and P. Alemi, "Switchable capacitor bank coordination and dynamic network reconfiguration for improving operation of distribution network integrated with renewable energy resources", *Journal of Modern Power Systems and Clean Energy*, vol. 10, no. 3, pp. 637–646, 2022 (cited on pages 31, 44, 48–53, 100, 108).

[86] A. Navarro-Espinosa and L. F. Ochoa, "Probabilistic impact assessment of low carbon technologies in LV distribution systems", *IEEE Transactions on Power Systems*, vol. 31, no. 3, pp. 2192–2203, 2016. DOI: 10.1109/TPWRS.2015.2448663 (cited on pages 31, 44, 52, 53).

[87] R. Torquato, D. Salles, C. Oriente Pereira, P. C. M. Meira, and W. Freitas, "A comprehensive assessment of PV hosting capacity on low-voltage distribution systems", *IEEE Transactions on Power Delivery*, vol. 33, no. 2, pp. 1002–1012, 2018. DOI: 10.1109/TPWRD.2018.2798707 (cited on pages 31, 45, 52, 53).

[88] B. L. M. Santos, L. S. Barros, F. A. Moreira, and D. Barbosa, "Hosting capacity maximization of distributed energy resources through simultaneous optimized volt–var curve and network reconfiguration", *Electric Power Systems Research*, vol. 234, p. 110 743, 2024, ISSN: 0378-7796. DOI: 10.1016/j.epsr.2024.110743 (cited on pages 31, 45, 48–53, 72, 73, 100).

[89] M. Kiani-Moghaddam, M. Shivaie, and P. D. Weinsier, *Introduction to Multi-objective Optimization and Decision-Making Analysis*. Springer International Publishing, 2019, pp. 21–45, ISBN: 978-3-030-12044-3. DOI: 10.1007/978-3-030-12044-3_2 (cited on pages 52, 69, 72).

[90] L. A. Gallego Pareja, J. M. López-Lezama, and O. Gómez Carmona, "A mixed-integer linear programming model for the simultaneous optimal distribution network reconfiguration and optimal placement of distributed generation", *Energies*, vol. 15, no. 9, pp. 1–26, 2022, ISSN: 1996-1073. DOI: 10.3390/en15093063 (cited on pages 56, 100).

[91] C. S. Cheng and D. Shirmohammadi, "A three-phase power flow method for real-time distribution system analysis", *IEEE Transactions on Power Systems*, vol. 10, no. 2, pp. 671–679, 1995. DOI: 10.1109/59.387902 (cited on pages 57, 58, 86, 100, 114).

[92] IEEE, "IEEE standard for interconnection and interoperability of distributed energy resources with associated electric power systems interfaces", *IEEE Std 1547-2018*, pp. 1–138, 2018. DOI: 10.1109/IEEESTD.2018.8332112 (cited on pages 59, 89, 101, 115, 129).

[93] P. Wang, W. Wang, and D. Xu, "Optimal sizing of distributed generations in DC microgrids with comprehensive consideration of system operation modes and operation targets", *IEEE Access*, vol. 6, pp. 31 129–31 140, 2018. DOI: 10.1109/ACCESS.2018.2842119 (cited on page 60).

[94] B. Zhao, X. Zhang, J. Chen, C. Wang, and L. Guo, "Operation optimization of standalone microgrids considering lifetime characteristics of battery energy storage system", *IEEE Transactions on Sustainable Energy*, vol. 4, no. 4, pp. 934–943, 2013. DOI: 10.1109/TSTE.2013.2248400 (cited on page 60).

[95] N. Efkarpidis, T. De Rybel, and J. Driesen, "Optimization control scheme utilizing small-scale distributed generators and oltc distribution transformers", *Sustainable Energy, Grids and Networks*, vol. 8, pp. 74–84, 2016, ISSN: 2352-4677. DOI: 10.1016/j.segan.2016.09.002 (cited on pages 62, 129).

[96] A. Mathur, V. Pant, and B. Das, "Unsymmetrical short-circuit analysis for distribution system considering loads", *International Journal of Electrical Power & Energy Systems*, vol. 70, pp. 27–38, 2015, ISSN: 0142-0615. DOI: 10.1016/j.ijepes.2015.02.003 (cited on pages 62, 86).

[97] A. Mathur, B. Das, and V. Pant, "Fault analysis of unbalanced radial and meshed distribution system with inverter based distributed generation (IBDG)", *International Journal of Electrical Power & Energy Systems*, vol. 85, pp. 164–177, 2017, ISSN: 0142-0615. DOI: 10.1016/j.ijepes.2016.09.003 (cited on pages 65, 66, 68, 88).

[98] X.-S. Yang, "Chapter 14 - multi-objective optimization", in *Nature-Inspired Optimization Algorithms*, X.-S. Yang, Ed., Oxford: Elsevier, 2014, pp. 197–211, ISBN: 978-0-12-416743-8. DOI: 10.1016/B978-0-12-416743-8.00014-2 (cited on page 69).

[99] K. Deb, A. Pratap, S. Agarwal, and T. Meyarivan, "A fast and elitist multiobjective genetic algorithm: NSGA-II", *IEEE Transactions on Evolutionary Computation*, vol. 6, no. 2, pp. 182–197, 2002. DOI: 10.1109/4235.996017 (cited on pages 69, 86, 113).

[100] B. S. Mahdi, N. Sulaiman, M. A. Shehab, S. Shafie, H. Hizam, and S. L. B. M. Hassan, "Optimization of operating cost and energy consumption in a smart grid", *IEEE Access*, vol. 12, pp. 18 837–18 850, 2024. DOI: 10.1109/ACCESS.2024.3354065 (cited on page 70).

[101] R. Hu, X. Zhang, F. Du, J. Yu, J. Luo, and F. Fan, "Coordinated dispatch for power grid and pumped storage hydropower plants with embedded market game model", in *2024 IEEE 2nd International Conference on Power Science and Technology (ICPST)*, 2024, pp. 2184–2188. DOI: 10.1109/ICPST61417.2024.10601934 (cited on page 70).

[102] C. Zhou, X. Yang, Y. Wang, Q. Duan, T. Tang, and S. Ke, "A multi-objective two-layer collaborative optimal configuration method for ship hybrid energy storage system based on NSGA II", in *2024 IEEE 7th International Electrical and Energy Conference (CIEEC)*, 2024, pp. 3803–3808. DOI: 10.1109/CIEEC60922.2024.10583386 (cited on page 70).

[103] C. Guerrero, I. Lera, and C. Juiz, "Distributed genetic algorithm for application placement in the compute continuum leveraging infrastructure nodes for optimization", *Future Generation Computer Systems*, vol. 160, pp. 154–170, 2024, ISSN: 0167-739X. DOI: 10.1016/j.future.2024.05.044 (cited on page 70).

[104] M. Cordeiro-Costas, H. Labandeira-Pérez, D. Villanueva, R. Pérez-Orozco, and P. Eguía-Oller, "NSGA-II based short-term building energy management using optimal lstm-mlp forecasts", *International Journal of Electrical Power & Energy Systems*, vol. 159, p. 110 070, 2024, ISSN: 0142-0615. DOI: 10.1016/j.ijepes.2024.110070 (cited on page 70).

[105] X.-S. Yang and S. Deb, "Multiobjective cuckoo search for design optimization", *Computers & Operations Research*, vol. 40, no. 6, pp. 1616–1624, 2013, ISSN: 0305-0548. DOI: 10.1016/j.cor.2011.09.026 (cited on pages 71, 99, 100, 113).

[106] M. I. Zainal, Z. M. Yasin, and Z. Zakaria, "Optimizing voltage profile and loss minimization using multi objective cuckoo search algorithm", in *2021 IEEE 11th IEEE Symposium on Computer Applications & Industrial Electronics (ISCAIE)*, 2021, pp. 116–122. DOI: 10.1109/ISCAIE51753.2021.9431835 (cited on page 71).

[107] S. Makhloufi, S. Khennas, S. Bouchaib, and A. H. Arab, "Multi-objective cuckoo search algorithm for optimized pathways for 75% renewable electricity mix by 2050 in algeria", *Renewable Energy*, vol. 185, pp. 1410–1424, 2022, ISSN: 0960-1481. DOI: 10.1016/j.renene.2021.10.088 (cited on page 71).

[108] S. B. Thanikanti, T. Yuvaraj, R. Hemalatha, B. Aljafari, and N. I. Nwulu, "Optimizing radial distribution system with distributed generation and EV charging: A spotted hyena approach", *IEEE Access*, vol. 12, pp. 113 422–113 441, 2024. DOI: 10.1109/ACCESS.2024.3438456 (cited on page 71).

[109] F. B. Dantas, D. Fernandes, W. L. A. Neves, A. K. X. B. Branco, and F. B. Costa, "Optimal inverter-based resource installation to minimize technical energy losses in distribution systems", *IEEE Access*, vol. 11, pp. 123 961–123 976, 2023. DOI: 10.1109/ACCESS.2023.3330083 (cited on page 71).

[110] M. Guindi and R. M. Kamel, "Optimal location and sizing of renewable distributed generations and electric vehicle charging stations", *Renewable Energy*, vol. 235, p. 121 272, 2024, ISSN: 0960-1481. DOI: 10.1016/j.renene.2024.121272 (cited on page 71).

[111] X.-S. Yang, "Chapter 9 - cuckoo search", in *Nature-Inspired Optimization Algorithms*, X.-S. Yang, Ed., Oxford: Elsevier, 2014, pp. 129–139, ISBN: 978-0-12-416743-8. DOI: 10.1016/B978-0-12-416743-8.00009-9 (cited on page 71).

[112] S.-M. Razavi, H.-R. Momeni, M.-R. Haghifam, and S. Bolouki, "Multi-objective optimization of distribution networks via daily reconfiguration", *IEEE Transactions on Power Delivery*, vol. 37, no. 2, pp. 775–785, 2022. DOI: 10.1109/TPWRD.2021.3070796 (cited on pages 72, 73).

[113] M. Asna, H. Shareef, P. Achikkulath, H. Mokhlis, R. Errouissi, and A. Wahyudie, "Analysis of an optimal planning model for electric vehicle fast-charging stations in Al Ain City, United Arab Emirates", *IEEE Access*, vol. 9, pp. 73 678–73 694, 2021. DOI: 10.1109/ACCESS.2021.3081020 (cited on pages 72, 115, 118).

[114] S. R. Biswal and G. Shankar, "Simultaneous optimal allocation and sizing of DGs and capacitors in radial distribution systems using SPEA2 considering load uncertainty", *IET Generation, Transmission & Distribution*, vol. 14, no. 3, pp. 494–505, 2020. DOI: 10.1049/iet-gtd.2018.5896 (cited on page 72).

[115] R. Billinton and W. Li, *Reliability Assessment of Electric Power Systems Using Monte Carlo Methods*. Springer US, 1994. DOI: 10.1007/978-1-4899-1346-3 (cited on page 73).

[116] L. D. Pereira *et al.*, "Optimal allocation of distributed generation and capacitor banks using probabilistic generation models with correlations", *Applied Energy*, vol. 307, p. 118 097, 2022, ISSN: 0306-2619. DOI: 10.1016/j.apenergy.2021.118097 (cited on page 73).

[117] F. Sheidaei, A. Ahmarinejad, M. Tabrizian, and M. Babaei, "A stochastic multi-objective optimization framework for distribution feeder reconfiguration in the presence of renewable energy sources and energy storages", *Journal of Energy Storage*, vol. 40, p. 102 775, 2021, ISSN: 2352-152X. DOI: /10.1016/j.est.2021.102775 (cited on page 73).

[118] A. E. Doan, "Type I and type II error", in *Encyclopedia of Social Measurement*, K. Kempf-Leonard, Ed., New York: Elsevier, 2005, pp. 883–888, ISBN: 978-0-12-369398-3. DOI: 10.1016/B0-12-369398-5/00110-9 (cited on page 73).

[119] D. Wang, T. Abdelzaher, and L. Kaplan, "Chapter 3 - mathematical foundations of social sensing: An introductory tutorial", in *Social Sensing*, Boston: Morgan Kaufmann, 2015, pp. 21–36, ISBN: 978-0-12-800867-6. DOI: 10.1016/B978-0-12-800867-6.00003-0 (cited on page 74).

[120] M. A. Cruz, H. R. Rocha, M. H. Paiva, M. E. Segatto, E. Camby, and G. Caporossi, "An algorithm for cost optimization of PMU and communication infrastructure in WAMS", *International Journal of Electrical Power & Energy Systems*, vol. 106, pp. 96–104, 2019, ISSN: 0142-0615. DOI: 10.1016/j.ijepes.2018.09.020 (cited on page 76).

[121] A. Benjamin, G. Chartrand, and P. Zhang, *The Fascinating World of Graph Theory*. USA: Princeton University Press, 2015, ISBN: 0691163812 (cited on pages 76, 78).

[122] T. H. Cormen, C. E. Leiserson, R. L. Rivest, and C. Stein, *Introduction to Algorithms, Third Edition*, 3rd. The MIT Press, 2009, ISBN: 0262033844 (cited on page 76).

[123] E. W. Dijkstra, "A note on two problems in connexion with graphs", *Numer. Math.*, vol. 1, no. 1, pp. 269–271, 1959, ISSN: 0029-599X. DOI: 10.1007/BF01386390 (cited on page 76).

[124] G. Sabidussi, "The centrality index of a graph", in *Psychometrika volume*, vol. 31, 1966, pp. 581–603. DOI: 10.1007/BF02289527 (cited on page 76).

[125] W. Kersting, *Distribution System Modeling and Analysis, Third Edition*. Taylor & Francis, 2012, ISBN: 9780429110443. DOI: 10.1201/b11697 (cited on page 77).

[126] J. J. Berman, "Chapter 4 - understanding your data", in *Data Simplification*, Boston: Morgan Kaufmann, 2016, pp. 135–187, ISBN: 978-0-12-803781-2. DOI: 10.1016/B978-0-12-803781-2.00004-7 (cited on page 79).

[127] P. Schober, C. Boer, and L. A. Schwarte, "Correlation coefficients: Appropriate use and interpretation", *Anesthesia & Analgesia*, vol. 126, no. 5, pp. 1763–1768, May 2018. DOI: 10.1213/ANE.0000000000002864 (cited on page 80).

[128] B. Zeng, W. Zhang, P. Hu, J. Sun, and D. Gong, "Synergetic renewable generation allocation and 5G base station placement for decarbonizing development of power distribution system: A multi-objective interval evolutionary optimization approach", *Applied Energy*, vol. 351, p. 121 831, 2023, ISSN: 0306-2619. DOI: 10.1016/j.apenergy.2023.121831 (cited on pages 82, 97, 110).

[129] IEC, "Electrical relays - part 3: Single input energizing quantity measuring relays with dependent or independent time", *International Electrotechnical Commission (IEC)*, 1989 (cited on pages 84, 89).

[130] *Energisa*, https://www.energisa.com.br, Accessed: August 25, 2019 (cited on page 88).

[131] *INMET - national institute of meteorology*, https://portal.inmet.gov.br, Accessed: August 25, 2019 (cited on page 88).

[132] A. C. Rueda-Medina, J. F. Franco, M. J. Rider, A. Padilha-Feltrin, and R. Romero, "A mixed-integer linear programming approach for optimal type, size and allocation of distributed generation in radial distribution systems", *Electric Power Systems Research*, vol. 97, pp. 133–143, 2013, ISSN: 0378-7796. DOI: 10.1016/j.epsr.2012.12.009 (cited on pages 90, 101, 115).

[133] W. H. Kersting, "Radial distribution test feeders", in *2001 IEEE Power Engineering Society Winter Meeting. Conference Proceedings*, vol. 2, 2001, 908–912 vol.2. DOI: 10.1109/PESW.2001.916993 (cited on page 90).

[134] Eaton, *Electrical and industrial: Power management solutions*, https://www.eaton.com/, Accessed: July 09, 2023, 2018 (cited on page 92).

[135] M. A. Mendes, M. C. Vargas, D. S. L. Simonetti, and O. E. Batista, "Load currents behavior in distribution feeders dominated by photovoltaic distributed generation", *Electric Power Systems Research*, vol. 201, p. 107 532, 2021, ISSN: 0378-7796. DOI: https://doi.org/10.1016/j.epsr.2021.107532 (cited on page 95).

[136] P. P. R. Priya, S. Baskar, S. T. Selvi, and C. K. Babulal, "Optimal allocation of distributed generation using evolutionary multi-objective optimization", *Journal of Electrical Engineering & Technology*, Oct. 2022. DOI: 10.1007/s42835-022-01269-y (cited on page 96).

[137] H. A. Taha, M. H. Alham, and H. K. M. Youssef, "Multi-objective optimization for optimal allocation and coordination of wind and solar DGs, BESSs and capacitors in presence of demand response", *IEEE Access*, vol. 10, pp. 16 225–16 241, 2022. DOI: 10.1109/ACCESS.2022.3149135 (cited on pages 101, 115, 129, 130).

[138] N.-A. Masood, A. Jawad, K. T. Ahmed, S. R. Islam, and M. A. Islam, "Optimal capacitor placement in northern region of bangladesh transmission network for voltage profile improvement", *Energy Reports*, vol. 9, pp. 1896–1909, 2023, ISSN: 2352-4847. DOI: 10.1016/j.egyr.2023.01.020 (cited on page 108).

[139] F. Capitanescu, L. F. Ochoa, H. Margossian, and N. D. Hatziargyriou, "Assessing the potential of network reconfiguration to improve distributed generation hosting capacity in active distribution systems", *IEEE Transactions on Power Systems*, vol. 30, no. 1, pp. 346–356, 2015. DOI: 10.1109/TPWRS.2014.2320895 (cited on pages 111, 115, 127).

[140] J. Qiao, Y. Mi, J. Shen, D. Xia, D. Li, and P. Wang, "Active and reactive power coordination optimization for active distribution network considering mobile energy storage system and dynamic network reconfiguration", *Electric Power Systems Research*, vol. 238, p. 111 080, 2025, ISSN: 0378-7796. DOI: 10.1016/j.epsr.2024.111080 (cited on pages 111, 127).

[141] K. Qian, C. Zhou, M. Allan, and Y. Yuan, "Modeling of load demand due to EV battery charging in distribution systems", *IEEE Transactions on Power Systems*, vol. 26, no. 2, pp. 802–810, 2011. DOI: 10.1109/TPWRS.2010.2057456 (cited on pages 113, 114).

[142] S. Faridimehr, S. Venkatachalam, and R. B. Chinnam, "A stochastic programming approach for electric vehicle charging network design", *IEEE Transactions on Intelligent Transportation Systems*, vol. 20, no. 5, pp. 1870–1882, 2019. DOI: 10.1109/TITS.2018.2841391 (cited on page 114).

[143] G. Battapothula, C. Yammani, and S. Maheswarapu, "Multi-objective simultaneous optimal planning of electrical vehicle fast charging stations and DGs in distribution system", *Journal of Modern Power Systems and Clean Energy*, vol. 7, no. 4, pp. 923–934, 2019. DOI: 10.1007/s40565-018-0493-2 (cited on page 115).

[144] P. Sadeghi-Barzani, A. Rajabi-Ghahnavieh, and H. Kazemi-Karegar, "Optimal fast charging station placing and sizing", *Applied Energy*, vol. 125, pp. 289–299, 2014, ISSN: 0306-2619. DOI: 10.1016/j.apenergy.2014.03.077 (cited on page 115).

[145] S. F. Santos, M. Gough, D. Z. Fitiwi, J. Pogeira, M. Shafie-khah, and J. P. S. Catalão, "Dynamic distribution system reconfiguration considering distributed renewable energy sources and energy storage systems", *IEEE Systems Journal*, vol. 16, no. 3, pp. 3723–3733, 2022. DOI: 10.1109/JSYST.2021.3135716 (cited on page 115).